

## **Appendix 37**

---

# **Meadowbank 2018 Groundwater Monitoring Program Report**

---



## **MEADOWBANK GOLD PROJECT**

# **Groundwater Monitoring Plan**

In Accordance with Water License 2AM-MEA1526

Prepared by:  
Agnico Eagle Mines Limited – Meadowbank Division

Version 9  
March 2019

---

## EXECUTIVE SUMMARY

This Groundwater Monitoring Plan presents the historic of groundwater monitoring at Meadowbank mine since 2003 and the extensive groundwater monitoring campaign achieved on site in 2018. Moreover, this document reviews methodology and best practices for drilling, well installation and groundwater sampling, especially in the arctic climate.

The annual monitoring plan is a requirement for the Meadowbank Type A Water License No. 2AM-MEA1526 and is a continuation of previous Monitoring Plans.

The following activities were fulfilled in 2018:

- Four new monitoring wells were installed in 2018 from May 29 to June 4, 2018 following technical advice and field services from an experts firm in the field of hydrogeology and geochemistry to improve the data collected for water quality model updates. The new monitoring wells were implemented considering the current state of knowledge and the monitoring wells were installed in talik;
- The 2018 groundwater monitoring program included the following eleven (11) monitoring stations, specifically: five (5) groundwater observation wells (MW-IPD-01 (s), MW-IPD-01 (d), MW-IPD-07, MW-IPD-09 and MW-16-01), three (3) dike seepages, one (1) pit sump, one (1) Storm management pond sump, and one (1) reclaim water.
- Two groundwater sampling programs from July 5 to July 12, 2018 and September 6 to September 13, 2018 using low-flow sampling techniques for licensing requirements; with duplicate, field blanks, and transport blanks.

Groundwater chemistry data is used to predict the quality of water accumulating in open pits, and to determine any effects of mining on groundwater quality, particularly with respect to tailings deposition.

Groundwater sampling is carried out twice annually. Analytical parameters will comply as per Schedule 1, Table 1, Group 2 of the Meadowbank Water License. Quality Assurance/Quality Control procedures will be implemented during each sampling event.

A groundwater monitoring report will be submitted by Agnico Eagle Mines Limited to the Nunavut Water Board (NWB) and Nunavut Impact Review Board (NIRB) with each Annual Report. The annual report can be found in Appendix A on this management plan. The report will include all data from the previous year's results as well as a historical record (Appendix B), dates and methods of sampling, and an assessment of the data obtained with particular regards to salinity parameters and indicators of tailings reclaim water movement, with respect to total cyanide and dissolved copper.

---

## **IMPLEMENTATION SCHEDULE**

This Plan will be implemented immediately (2019) subject to any modifications proposed by the NWB as a result of the review and approval process.

## **DISTRIBUTION LIST**

AGNICO EAGLE – Geology Superintendent

AGNICO EAGLE – Engineering Superintendent

AGNICO EAGLE – Geotechnical Engineer

AGNICO EAGLE – Environment Superintendent

AGNICO EAGLE – Environment General Supervisor

AGNICO EAGLE – Environmental Coordinator

AGNICO EAGLE – Environmental Technician

### DOCUMENT CONTROL

Version	Date (YMD)	Section	Revision
1	08/08/08		Comprehensive plan for Meadowbank Project
2	09/03/31	all	Comprehensive update of plan to include 2008 well installations
3	11/12/14		Update Executive Summary; insert Figure 1; update Table 1; addition of information on wells created in 2011; include well installation section;
4	14/01		Update Executive Summary; update Section 1.2 to reflect current wells; add Section 3.3 and 3.4 (seep and production drill hole sampling methods); update Section 5 (additional reporting on tailings-related parameters)
5	15/04	1.3 and 3.3 2.3	Sampling of pit wall seeps discontinued. Sampling of Goose Pit sump added. Updated with installation information for new well.
6	15/09	4.1 and 4.2	Updated list of analyse parameters. QAQC Section to include Trip and Field Blank Remove Goose Pit sump as monitoring station
7	17/03	Section 1.5, 3, 5 and 6	Add Section 5 and 6 and modify section 1.5 and 3
8	17/11	all	Comprehensive update
9	19/03	all	Comprehensive update and add 2018 groundwater monitoring report

Version 9

Prepared By: Environmental Department

Approved By:   
Robin Allard  
Environmental General Supervisor

## TABLE OF CONTENTS

<b>1</b>	<b>INTRODUCTION.....</b>	<b>1</b>
1.1	Purpose of Groundwater Monitoring .....	1
1.2	Tailing storage facility expansion at meadowbank.....	2
1.3	Future groundwater monitoring program adapted for in-pit deposition at meadowbank.....	2
<b>2</b>	<b>GROUNDWATER MONITORING PROGRAM.....</b>	<b>3</b>
2.1	Groundwater monitoring program 2003-2018 .....	3
2.2	Groundwater monitoring program achieved in 2018 .....	5
2.3	Monitoring stations and sampling methodologies 2018 .....	6
2.3.1	Monitoring well .....	6
2.3.1.1	MW-16-01.....	6
2.3.1.2	MW-08-02.....	7
2.3.2	Dike seepage .....	7
2.3.3	Wall seepage .....	8
2.3.4	Pit sump .....	8
2.3.5	Deep Lake.....	8
2.3.6	Geotechnical investigation holes .....	8
2.4	Physicochemical and Geochemical parameters .....	9
2.4.1	Groundwater parameters required by the water license.....	9
2.4.2	Additional parameters.....	9
2.5	Quality control on sampling and analysis.....	10
2.5.1	Handling.....	10
2.5.2	Duplicates, field and trip blank.....	10
<b>3</b>	<b>ADAPTED GW MONITORING PROGRAM FOR IPD.....</b>	<b>11</b>
<b>4</b>	<b>DRILLING, WELLS INSTALLATION AND GW SAMPLING IN DEEP PERMAFROST ENVIRONMENT: CHALLENGES AND SOLUTIONS FOR BEST PRACTICES.....</b>	<b>13</b>
<b>5</b>	<b>KEY POINTS AND RECOMMENDATIONS.....</b>	<b>18</b>
<b>6</b>	<b>REPORTING .....</b>	<b>20</b>
<b>7</b>	<b>REFERENCE .....</b>	<b>21</b>

### LIST OF TABLES

Table 1: Samples collected in 2018.....	6
Table 2: Protocol review for drilling and well design in permafrost setting.....	13
Table 3: Protocol review for sampling representative groundwater in permafrost setting .....	16

### LIST OF APPENDICES

Appendix A – 2018 Groundwater Monitoring Report
Appendix B – 2003 - 2018 Historical Data

## **1 INTRODUCTION**

---

The annual monitoring plan is a requirement for Meadowbank Type A Water License No. 2AM-MEA1526.

This document is the 9<sup>th</sup> version of the Groundwater Monitoring Plan for Meadowbank Mine. This version presents an update of the groundwater monitoring program described in Version 8 (November 2017).

This version relates the historic of groundwater monitoring at Meadowbank mine since 2003, presents the extensive groundwater monitoring campaign achieved on site in 2018. Moreover, this document reviews methodology and best practices for drilling, well installation and groundwater sampling, especially in the arctic climate.

### **1.1 PURPOSE OF GROUNDWATER MONITORING**

Groundwater data is used as a tool to predict the chemistry of water accumulating in open pits and to determine any effects of mining on groundwater quality, particularly with respect to tailings deposition activities. To this end, groundwater monitoring wells have been installed to sample groundwater in open talik areas, where unfrozen ground extends beneath large lakes. No groundwater monitoring wells is installed at the Vault Deposit, as the Vault Pit is developed in an area of permafrost.

Groundwater monitoring has traditionally been conducted using installed monitoring wells, but difficulties in obtaining representative samples by this method prompted the investigation of alternative methods from 2013 to 2016 based on technical advices from firms of experts. Nevertheless, groundwater samples are still collected in operable monitoring wells.

In 2017, the whole groundwater monitoring program was revisited, as suggested by Environment and Climate Change Canada (ECCC), to improve the data collected for water quality model updates. Due to sustained difficulties in maintaining and sampling monitoring wells, Agnico Eagle received technical advice and field services from a firm of experts, to optimize low-flow sampling techniques as well as further sampling improvements and pursued opportunities for sampling groundwater from alternative methods as well as the existing wells. An extensive monitoring program campaign took place in 2017 to collect representative samples across the mine site to understand the groundwater background geochemistry and the potential interaction between groundwater and surface water especially in relation to tailing migration. The groundwater investigation was repeated in 2018 with the addition of four new monitoring wells (See Appendix A of the 2018 Groundwater monitoring for wells location MW-IPD-01 (s), MW-IPD-01 (d), MW-IPD-07, MW-IPD-09).



The next phase for 2019 is to prepare a groundwater program that will ensure groundwater flow comprehension and groundwater sample integrity as well as a successful 2019 sampling campaign.

## **1.2 TAILING STORAGE FACILITY EXPANSION AT MEADOWBANK**

Since 2015, Agnico Eagle is working on diverse options to accommodate additional tailings storage facility at Meadowbank. After a Multi-Account Assessment (MAA), the In-Pit Tailings Deposition (IPD) was selected as the preferred option to store tailings waste produced from Whale Tail Mine in addition to its current tailings storage facilities (TSF). IDP demonstrated superior performance capacities in the following categories: health and safety, quality of life, water, air, capital cost, technology, natural hazards, and adaptability (SNC-Lavalin, 2016; 2017a).

To ensure the environment protection and evaluate potential risks for tailing migration into groundwater, a feasibility study was conducted by SNC-Lavalin professionals in 2016-2017 (SNC-Lavalin, 2017a). The feasibility study included a complementary characterization of the geological structures and permafrost extent on site and the development of a detailed hydrogeological numerical 3D model. The numerical simulations were designed to represent the worst-case scenarios in terms of contaminant transport within the aquifers. Therefore, a groundwater monitoring program can be designed in relation to the groundwater flow and contaminant transport simulation results.

## **1.3 FUTURE GROUNDWATER MONITORING PROGRAM ADAPTED FOR IN-PIT DEPOSITION AT MEADOWBANK**

Meadowbank groundwater monitoring program will be adapted to IDP. After regulators' approval, IPD could begin in Q2 2019. IPD would start in Goose Pit, already mine out, followed by an alternate filling of Portage Pit A and Pit E (SNC-Lavalin, 2017a).

Future groundwater monitoring program will continue to be adapted for IPD at Meadowbank. The installation of four (4) new groundwater monitoring wells in 2018 was proposed at strategic locations, based on groundwater numerical simulation results and 2017 borehole data. Moreover, methods to obtain representative groundwater samples and improve well designs under arctic climate continue to be investigated. The groundwater monitoring program will be updated as the project progresses. New information from the hydrogeological numerical model and from hydrogeological field data will be integrated throughout.

## **2 GROUNDWATER MONITORING PROGRAM**

---

### **2.1 GROUNDWATER MONITORING PROGRAM 2003-2018**

Groundwater data is used as a tool to predict the chemistry of water accumulating in open pits, and to determine any effects of mining on groundwater quality particularly with respect to tailings deposition activities. Important components surveyed are chloride concentrations, salinity and Total Dissolved Solid (TDS) calculated via conductivity measurements. Copper and Cyanide are also monitored to trace potential effects of mining operations on groundwater quality. To this end, groundwater monitoring wells have been installed to sample groundwater in open talik areas, where unfrozen ground extends beneath large lakes. No groundwater monitoring wells are installed at the Vault Deposit, as the Vault Pit is developed in an area of permafrost.

Groundwater samples have traditionally been collected in monitoring wells. From 2003 to 2016, fourteen (14) monitoring wells were installed at Meadowbank mine. No groundwater well was installed in 2017. Throughout the years, a total of 34 groundwater samples and 21 duplicates were collected from these sampling wells. However, most of the monitoring wells became inoperable due to the challenging arctic conditions and permafrost environment at Meadowbank, and to this day, only one well remain operable.

In 2017, an extensive groundwater sampling program took place. The program aimed to improve the characterization of the baseline groundwater chemistry, identify potential sources of contaminants at the mine site, and identify potential interaction between surface and groundwater. The program included:

- Review of the sampling methodologies and the historical groundwater quality data;
- Testing and maintenance of the sampling equipment;
- Collection of surface and groundwater samples at specific locations and;
- Data compilation and basic interpretation of groundwater quality.

Well installation and representative groundwater collection have been a major challenge under arctic conditions in permafrost environment. Some of the challenges were:

- Well damaged by frost action;
- Heat traces malfunctioning, therefore ice bridges forming in well annulus;
- Well damaged during site operations;

- Well obstructed with development material, once again due to frost action.

Despite multiple attempts to overcome these challenges, the collection of representative groundwater sampled was unsuccessful for most problematic wells. For example, saline solution was used to melt ice bridges formed in well annulus. The concentration of saline solution required to unplug the well could not be purged afterwards, the groundwater flow was not sufficient and the amount of time that would have been required to purge the well unrealistic under permafrost conditions.

Since well installation and representative groundwater samples collection has been a tremendous challenge at Meadowbank, alternative methods to obtain representative groundwater samples were investigated from 2013 to 2016 (see 2012 Groundwater Monitoring Report and recommendations by Golder Associates). Alternative groundwater monitoring stations investigated includes: pit wall seepages, production drill holes, pit sumps, horizontal wells installed into pit walls, and temporary wells for pit dewatering.

From 2013 to 2016, six (6) groundwater samples were collected from horizontal wells installed in Pit E southeastern wall, one (1) sample from a temporary well for pit dewatering, two (2) samples from pit sumps during exploitation and one (1) production borehole.

Although production and preshear drill holes with sufficient flow rates only occurred on occasion, when sufficient groundwater flow was encountered, sampling was achieved. Moreover, a sample was collected from a temporary dewatering well (6 inches in diameter, 65 meters depth), installed in Pit E from July to August 2016, to reduce water table and ensure pit slope stability. Prior 2016, seepage from pit walls, commonly occurring at different locations, has indicated surface water rather than groundwater flow.

In 2017, only two (2) wells remain operable for groundwater sampling. Aside from the wells, none of the previous monitoring stations were available for sampling in 2017. Due to the difficulties encountered in maintaining and sampling monitoring wells, Agnico Eagle contracted experts to obtain technical advice on optimizing low-flow sampling techniques. Moreover, further sampling improvements and pursued opportunities for sampling groundwater from alternative sources as well as the existing wells were carried out. An extensive monitoring program campaign took place in 2017 to collect representative samples across the mine site to understand the groundwater background geochemistry and the potential interaction between groundwater and surface water especially in relation to tailing migration.

In 2018, only one (1) well (MW-16-01) from previous well installed remain operable and four (4) new wells were installed for groundwater sampling. Aside from the wells, only station for reclaim water and dike seepage remain available from 2017 campaign. Due to the difficulties encountered in maintaining and sampling monitoring wells, Agnico Eagle continue to contracted experts to obtain technical advice on optimizing low-flow sampling techniques and get further sampling improvements and pursued opportunities for sampling groundwater

from alternative sources as well as the existing wells. An extensive monitoring program campaign took place in 2018 to collect representative samples across the mine site to understand the groundwater background geochemistry and the potential interaction between groundwater and surface water especially in relation to tailing migration. Groundwater collected in 2018 from the four (4) newly installed well fits within the natural groundwater category established on 2017 results and can be use as threshold values to monitor groundwater quality in the future.

The locations of each former and existing groundwater wells and other types of groundwater monitoring stations are provided in Appendix A of the 2018 Groundwater Monitoring report.

## **2.2 GROUNDWATER MONITORING PROGRAM ACHIEVED IN 2018**

Two field visits were completed by a SNC-Lavalin professional in the course of summer 2018. The objective of this first site visit was to provide on-site professional support to Agnico Eagle field technicians during the drilling and the installation of four new monitoring wells. The objective of the subsequent visits was to provide on-site professional support to Agnico Eagle field technicians for the installation of dedicated sampling material into four new monitoring wells and to collect surface water and groundwater samples twice in 2018. A photographic report is presented on Appendix C of the 2018 Groundwater Monitoring (Appendix A), showing the well installation. State of the art sampling techniques were performed and each sampling station, which were selected based on its contribution to the global understanding of groundwater quality. Twenty-one (21) water samples were collected in the vicinity of Goose Pit, Portage Pit. The groundwater monitoring program 2018 aimed to:

- Achieve two groundwater sampling programs from July 5 to July 12, 2018 and September 6 to September 13, 2018 using low-flow sampling techniques for licensing requirements; and
- Compile and interpret the water quality data collected to document the potential interaction between surface water and groundwater, especially in relation to tailing migration.
- Improve the density and spatial distribution of groundwater monitoring stations and get representative samples;
- Achieve and repeat a complete groundwater sampling program as well as low-flow sampling techniques for licensing requirements;
- Collect groundwater chemical data required to understand the potential interaction between groundwater and surface water, especially in relation to tailing migration;
- Emit recommendations to improve the groundwater sampling program in the future.

Table 1 summarized the sample collected during the two site visits. In total, the 2018 groundwater monitoring program included the following eleven (11) monitoring stations, specifically: five (5) groundwater observation wells (MW-IPD-01 (s), MW-IPD-01 (d), MW-IPD-07, MW-IPD-09 and MW-16-01), three (3) dike seepages, one (1) pit sump, one (1) Storm management pond sump, and one (1) reclaim water. A map illustrating the locations for each water sample is presented in Appendix A of the 2018 Groundwater Monitoring (Appendix A). The next section explains the context of each sampling station.

**Table 1: Samples collected in 2018**

Sample name	Type	Screens depth (m)	Pump depth (m)	July	September
MW-IPD-01 (s)	Groundwater well	51-69	60	X	x
MW-IPD-01 (d)	Groundwater well	163-181	175	X	x
MW-IPD-07	Groundwater well	42-50	40	X	x
MW-IPD-09	Groundwater well	62-80	70	X	x
MW-16-01	Groundwater well	89-101	95	X	x
ST-S-5	Dike seepage	-	-	X	x
ST-21	Reclaim water	-	-	x	x
ST8-North	Dike seepage	-	-	x	x
ST8-South	Dike seepage	-	-	x	x
BG-Lagoon	Sump	-	-	x	x
SMP (Storm management pond)	Sump	-	-	x	

## 2.3 MONITORING STATIONS AND SAMPLING METHODOLOGIES 2018

### 2.3.1 Monitoring well

In 2018, only one wells was operable from previous year and four (4) news well installed in 2018. Installation details for operational monitoring wells are provided in Appendix A below. Details for all other decommissioned wells are presented in the Groundwater Monitoring Report related to the year of installation. Formation of thick ice bridges in the annular space challenged the sampling of wells MW-08-02 in 2017 and was not sampled in 2018. Therefore, sampling protocols were different for the two wells and methodologies are described below.

#### 2.3.1.1 MW-16-01

A portable double valve sampling pump (DVP) was installed permanently at approximately 95 meters down for the well so that the pump is installed in front of the screened interval. The well was purged to remove standing water inside the well and to induce a fresh groundwater flow from the rock formation by activating the DVP. The pump is activated by pushing compressed air into a ¼ inch Low Density Polyethylene (LDPE) tubing attached to the DVP. The in-situ physicochemical parameters are measured with a PCStestr 35 Oakton Probe that was calibrated prior usage. Purged water quality is monitored for pH, electrical conductivity, temperature, water clarity and colour (visual observation) during this operation. A minimum of 3 well volumes (volume of water between the in-well packer and bottom of

screened interval) are to be removed prior sampling or until the monitored parameters stabilize (values remaining within 10% for three consecutive readings).

Groundwater sampling was carried out immediately after well purging with low-flow techniques. Groundwater samples were collected in clean, laboratory-supplied containers. Groundwater was sampled following quality control procedure on sampling and analysis described in section 2.5 and detailed in Appendix G of the 2018 Groundwater Monitoring Appendix A).

#### **2.3.1.2 MW-08-02**

Well MW-08-02, installed 191 m below ground, has an ice bridge from 30 m to 150 m below ground. The ice blocking the well annulus was melted using a steamer and clean lake water. It took about 4 hours to melt 120 m of ice from the well. Following this procedure, the well remains free of ice for a maximum of 24 hours. To not waste any expensive equipment, the well was purged using compressed air push through a tube lowered 150 m down the well for another 4 hours. Then, the well was allowed to recover for 12 hours to a static water level before sampling. Afterwards, a 200 mL clean bailer was lowered 160 m below ground to retrieve a representative groundwater sample just above the screen interval. Groundwater sampling was carried out immediately after purging reading the in-situ parameters and sampling was carried out as mentioned in the previous section.

After interpreting the geochemical data, it can be stated that there is too much variability in some of the major elements to pursue the sampling of this well as is. Until the well can be free of ice for a period longer than 24 hours, to ensure a proper purge, there is no point trying to retrieve a groundwater samples from this well since it is never going to be truly representative of groundwater by using this methodology (steaming the well). This well was not sample in 2018.

#### **2.3.2 Dike seepage**

The name "dike seepage" as a monitoring station applies to samples collected from dewatering wells (ST-8 North and ST-8 South), installed at the bedrock surface (6 m depth), to control dike seepages. It also includes sumps created naturally by dike seepage (ST-S-5) or sump found between dikes near rock stockpiles (BG Lagoon). In most cases, samples are collected through a tap connected to a dewatering pump.

These sampling stations can be monitored though time, contribute to the understanding of groundwater quality at the mine and can be added to the long term groundwater monitoring program.

### **2.3.3 Wall seepage**

The name "wall seepage" as a monitoring station applies to groundwater collected on pit walls where water comes directly through the bedrock and where a small ¼ diameter LDPE tubing can be inserted into small fracture to prevent the sample to be in contact with the atmosphere. The groundwater runs through the tubing by gravity and physicochemical parameters are recorded and standard sampling procedures are followed.

These sampling stations can be monitored through time, contribute to the understanding of groundwater quality at the mine and can be added to the long term groundwater monitoring program until the pit will be decommissioned. No wall seepages were sampled in 2018.

### **2.3.4 Pit sump**

The name "Pit sump" as a monitoring station applies to groundwater collected at the bottom of a pit when groundwater filled a cavity during exploitation. After interpreting the geochemical data, it can be stated that there is too much ambiguity of the provenance of some elements found in these analysis to pursue the sampling of this well as is. Excavated ground is reworked and a lot of mine operations occur around the sumps such as drilling, blasting, and excavating. Moreover, the exact location of the sampling can never be reproduced year after year. Since an interesting groundwater sample could derive from the pit bottom, a good alternative would be to install a temporary well about 10 m from the sump that could be sample for groundwater.

### **2.3.5 Deep Lake**

The name "Deep Lake" as a monitoring station applies to water collected near lake bottom at its deepest point. Water was collected through a small ¼ inch diameter LDPE tubing, connected to a peristaltic pump. These samples were collected to verify the quality of groundwater at lake's bottom. Also, it aims to compare the different water geochemistry signatures originating from an open talik and a close talik, and later to compare the data with the ones collected on site. These stations were monitored only once in 2017.

### **2.3.6 Geotechnical investigation holes**

Field campaigns in summer 2017 at Meadowbank included drilling of new boreholes susceptible to encounter groundwater. Attempt was made to collect a groundwater sample at borehole IPD-17-06. Although geotechnical holes are made under controlled conditions when compared to production holes, the inside diameter of metal casing are filled with grease, water is dirty and full of particles. After interpreting the physicochemical parameters for groundwater coming from geotechnical holes, and geochemical data from production holes and preshear holes, it can be stated that these holes are not a proper environment to retrieve representative groundwater samples. No further investigation were conducted in 2018.

## 2.4 PHYSICOCHEMICAL AND GEOCHEMICAL PARAMETERS

### 2.4.1 Groundwater parameters required by the water license

For each samples, field parameters are recorded (pH, turbidity, salinity and electrical conductivity). Analytical parameters included the following (per Schedule 1, Table 1, Group 2 of the Meadowbank Water License):

Total and Dissolved Metals: aluminum, antimony, arsenic, boron, barium, beryllium, cadmium, copper, chromium, iron, lithium, manganese, mercury, molybdenum, nickel, lead, selenium, tin, strontium, titanium, thallium, uranium, vanadium and zinc.

Nutrients: Ammonia-nitrogen, total kjeldahl nitrogen, nitrate nitrogen, nitrite-nitrogen, ortho-phosphate, total phosphorous, total organic carbon, total dissolved organic carbon and reactive silica.

Conventional Parameters: bicarbonate alkalinity, chloride, carbonate alkalinity, conductivity, hardness, calcium, potassium, magnesium, sodium, sulphate, pH, total alkalinity, TDS, and TSS, turbidity.

Total cyanide and Free cyanide. If total cyanide is detected above 0.05 mg/L at a monitoring station in receiving environment; further analysis of Weak Acid Dissociable Cyanide (CN WAD) will be triggered.

### 2.4.2 Additional parameters

Each groundwater sample has a distinctive signature on the basis of its dissolved concentrations of chemical constituents. Geochemical interpretation of groundwater data can be very useful to support a conceptual model by improving the understanding of groundwater movements and processes along pathways as water composition varies. It can also help identify zones where surface water and groundwater continually interact or only during permafrost thawing.

The geochemical composition of groundwater is defined by its main anions ( $\text{HCO}_3^-$ ,  $\text{SO}_4^{2-}$ ,  $\text{Cl}^-$ ) and its main cations ( $\text{Ca}^{2+}$ ,  $\text{Na}^+$ ,  $\text{Mg}^{2+}$   $\text{K}^+$ ). Mass balance calculations for main ions dissolved in groundwater are a mandatory reliability check for any geochemical analysis (Hounslow, 1995). Mass balance calculations are useful to gain a first insight into water chemistry. From these calculations, groundwater chemical composition can be represented in Piper and Stiff diagrams, which facilitate its interpretation.

For the reasons presented above, additional parameters were also analyses: dissolved calcium, dissolved potassium, dissolved magnesium, dissolved sodium, fluorides, bromides, and ammonium-nitrogen. The following physicochemical in-situ parameters were also recorded on site: Oxydo-reduction Potential (ORP) and Dissolved Oxygen (DO).



## **2.5 QUALITY CONTROL ON SAMPLING AND ANALYSIS**

### **2.5.1 Handling**

The following procedures will be followed to provide data quality control:

- Measurement of field parameters at selected intervals until stable readings (within 10% of each other);
- Minimization of the exposure of the sampled water to the atmosphere;
- Use of compressed gas to evacuate water for sample collection;
- In-situ measurement of sensitive chemical parameters (pH, electrical conductivity, dissolved oxygen, alkalinity), where applicable;
- Abiding by sample preservation methods (refrigeration and use of preservatives where needed), and specified holding times; and
- Filtering for dissolved metal analysis with a 0.45 microns filter on site.

### **2.5.2 Duplicates, field and trip blank**

A duplicate sample will be collected for one monitoring well per sampling event, and submitted as a blind duplicate to the analytical laboratory. When both results are higher than five times the method detection limit (MDL), the relative percent difference (RPD) will be calculated as:

$$\text{RPD} = \text{absolute difference in concentration} / \text{average concentration} \times 100$$

USEPA (1994) indicates that an RPD of 20% or less is acceptable. Where one or both results are less than five times the MDL, a margin of +/- MDL is acceptable.

One field and one trip blank will also be collected at each sampling campaign.

### **3 ADAPTED GW MONITORING PROGRAM FOR IPD**

---

Since 2015, Agnico Eagle is seeking options to increase Meadowbank's total tailing storage capacity to accommodate the mining of Whale Tail ore deposit. After a Multi-Account Assessment (MAA), the In-Pit Tailings Deposition (IPD) was selected as the preferred option to store tailings waste produced from Whale Tail Mine in addition to its current TSF (SNC-Lavalin, 2016; 2017a).

After regulators' approval, IPD could begin in Q2 2019. IPD would start in Goose Pit, already mined out, and followed by an alternate filling of Portage Pit A and Pit E (SNC-Lavalin, 2017a).

To ensure the environment protection and evaluate potential risks for tailing migration into groundwater, a feasibility study was conducted by SNC-Lavalin professionals in 2016-2017 (SNC-Lavalin, 2017a). The feasibility study included a complementary characterization of the geological structures and permafrost extent on site and the development of a detailed hydrogeological numerical 3D model. The groundwater numerical model aimed at representing the geological and hydrogeological conditions found at the mine site at the end of deposition to reproduce the groundwater flow and contaminant transport in talik zones located throughout the permafrost environment. The numerical simulations were designed to represent the worst-case scenarios in terms of contaminant transport within the aquifers. Therefore, a groundwater monitoring program can be designed in relation to the groundwater flow and contaminant transport simulation results.

Moreover, extensive physical and chemical laboratory analyses were performed on the Whale Tail's tailings that will be deposited to verify their properties and their potential for acid rock drainage (ARD) and release of chemicals (Golder, 2017). Finally, the new Meadowbank groundwater monitoring program will be adapted to monitor the groundwater quality in the vicinity of pit shells with considerations of IPD operations.

Future groundwater monitoring program will be adapted for in-pit deposition at Meadowbank. Four new groundwater monitoring wells was installed at strategic locations based on groundwater numerical simulation results and 2018. Well screen interval was defined based in 2017 borehole data. Moreover, methods to obtain representative groundwater samples and improve well designs under arctic climate continue to be investigated. The groundwater monitoring program will be updated as the project progresses. New information from the hydrogeological numerical model and from hydrogeological field data will be integrated throughout.

Groundwater samples will be collected from the new wells at least once prior the pit deposition. The groundwater data will represent background geochemistry data prior to in-pit tailings deposition. Finally, the groundwater sampling program will be performed twice

annually using on-site monitoring wells and other monitoring stations. One sample per sampling event will be collected in duplicate and submitted blind (using different reference numbers) to the analytical laboratory. One transport blank and field blank will also be collected each year. Specific details on sampling methodologies in monitoring wells are provided on Appendix G of the 2018 Groundwater Monitoring (Appendix A).

#### 4 DRILLING, WELLS INSTALLATION AND GW SAMPLING IN DEEP PERMAFROST ENVIRONMENT: CHALLENGES AND SOLUTIONS FOR BEST PRACTICES

The first objective of this section is to review the challenges encounter while drilling and for the design and operation of groundwater monitoring well in deep permafrost environment. Based on current knowledge, the second objective is to propose better practices to successfully install long-lasting monitoring wells and retrieve representative groundwater samples at the Meadowbank mine site. Two tables synthetizing the information from different sources are presented. Table 2 documents the challenges encounter while drilling and installing wells. Some tested methods to resolve the enumerated problems are listed and promising solutions that could be attempt in the future are presented. Table 3 documents the challenges encounter during groundwater sampling.

Table 2: Protocol review for drilling and well design in permafrost setting

<b>Borehole drilling and well design challenges</b>	<b>Tested methodology</b>	<b>Innovative solution (What could be done)</b>
<u><b>Drilling operation in permafrost.</b></u>	<ul style="list-style-type: none"> <li>• Advance the boreholes with standard HQ (Golder 2008 a)</li> <li>• Use heated water for drilling fluid (Golder 2008 a)</li> <li>• The fluid remaining in the borehole should have a target temperature of 60°C as water near boiling may freeze more quickly (Statler et al. 2010)</li> <li>• Borehole instrumentation should be on site and ready for installation once drilling is complete (Statler et al. 2010)</li> <li>• Drilling should proceed more slowly, providing the rock surrounding the borehole to warm up and allow a maximum time for installation of bottom hole assembly (Statler et al. 2010)</li> <li>• A bottom hole assembly is 15 m long and is used to isolate the bottom of the hole to allow sampling and monitoring (Statler et al. 2010) (includes pneumatic packer inflated with N<sub>2</sub> head over propylene glycol, a</li> </ul>	<p><u><b>Define permafrost and talik location prior or while drilling</b></u></p> <p>Temperature gauging should be conducted and logged during drilling operation. This information is key decision parameter for heat tracing cable length and elevation of purge and sampling pumps (Franz Environmental Inc. 2009)</p> <p>Pressure, salinity parameters should be taking in consideration to define talik/permafrost zones</p>

	<p>U tube sampling system with a sample reservoir and a temperature sensor line (Freifeld et al. 2008)</p> <ul style="list-style-type: none"> <li>• Vertical well have less chances of failure. Inclination must be defined accordingly.</li> <li>• When installing bottom hole assembly, the sampling lines and heat tape should be wrapped with insulation to help prevent freezing</li> <li>• Heat tape should be installed with a safety factor i.e. if the highest thermal conductivity expected is 4 W/mK, plan 10 W/mK (Statler et al. 2010)</li> <li>• Heating cables must be attached on the downward side of the well (Franz 2009).</li> </ul>	
<p><b><u>Breakage of well pipes.</u></b> Freezing of the standing water exposed to permafrost in the well causing breakage of well pipes or obstruction within the pipes</p>	<p>Use steel instead of PVC. PVC centralizers were used to keep the well centered with boring but PVC centralizer may fail.</p> <p>Using two inflatable packers; one with the borehole annulus and another with the well pipe, to prevent talik water to rise in the permafrost section (Golder 2008).</p> <p>Inflate packers according to their purpose, note status of packers year after year to follow the same procedure and minimize damage potential (Franz 2009).</p>	<p>Use centralizer made of another material than PVC, the objective is to keep the well riser in the center of the borehole and prevent that the riser pipe assembly bends (Franz 2009).</p>
<p><b><u>Packer failure.</u></b> Water bypass packers due to cold temperature-induced contraction of packer, loss of inflation</p>	<p>Ensure enough fuel in the generator so it can run continuously during purging so that the heating cable work all the time and both inside and outside packers should be inflated.</p>	
<p><b><u>Material damage through shipping.</u></b> Stainless steel</p>	<p>Material shipped to the site must be properly package and should arrived and be inspected well ahead of the time the material is needed to be used (Franz</p>	

<p>tubing damage during shipping, cause leakage through casing</p>	<p>2009).</p>	
<p><b><u>Well installation.</u></b></p> <p>Well installed from 2003 through 2014 failed for various reasons</p>	<p>Install pre-pack bentonite wells (Meeting minute on lessons learned at Meadowbank 2016)</p> <p>1-1/2" screen is installed in the hole with a 1-1/2 pipe. Prepack bentonite is installed above the screen to create the bentonite plug. Heat trace is tightly taped around the 1-1/2" pipe during to installation to avoid the heat trace to touch each other and create a shortcut. Metal casing is installed and anchored in the bedrock in order to protect the well from material movement. No more grouting is used to fill the space between the casing and the pipe as it didn't prevent the hole MW-11-01 from collapsing.</p> <p>Packer was used in the past to replace the bentonite</p> <p>Proper well inclination should be considered for well installation and in the case of an inline well, heating cables must be attached on the downward side of the well (Franz 2009).</p>	<p>Verify if using U-sampler methodology with borehole assembly would be better over this</p>

**Table 3: Protocol review for sampling representative groundwater in permafrost setting**

<b>GW sampling challenges</b>	<b>Tested methodology</b>	<b>Innovative solution (What should be done)</b>
<p><b><u>Unrepresentative groundwater sample because of cross contamination.</u></b></p> <p>Groundwater sample contaminated by borehole drilling or well operation</p> <p>Mixing between resident groundwater and brines/drill fluid used for drilling restricts a proper interpretation of groundwater chemistry</p> <p>Potential contamination through borehole operations (drill bit, drill cuttings, packers), sampling equipment, sampling environment or during sample transportation</p>		<p>Contamination of samples with drilling brine should be minimized</p> <p>Use a tracer and analyses salinity of drill fluid. Tracer such as sodium fluorescein (Henkemans 2016) or perfluorocarbon tracer (PFT) with drill fluid (Piffner et al. 2008) to define the amount of contamination from drilling fluid from sampled groundwater.</p> <p>At the end of the borehole, block the drill string and perform a "wet" pull to remove as much drill water as possible from the borehole before it froze to the rock surface (Piffner et al. 2008).</p> <p>Perform a "wet" pull following borehole drilling to remove as much drilling fluid as possible. To further clean the hole use a bailer (Statler et al. 2010; Piffner et al. 2008).</p> <p>Use a sampling system such as: U-Tube (Freifeld 2009) or Thermos bottle concept (Sutphin et al. 2006).</p> <p>Minimize contamination with proper sampling equipment i.e. cleaned pump, sanitized equipment dedicated to borehole, test equipment for contamination, use blank sample and transport blank to verify a potential contamination. Field samples must be immediately preserved using appropriate methods to retain competency for subsequent geochemical analyses (Wilkins et</p>

		al. 2014).
<p><b><u>Ice bridge formation within wells.</u></b> Borehole ice formation freezing of the standing water exposed to permafrost in the well also preclude the collection of more than one set of fluid samples from a given borehole due to post drilling formation.</p>	<p>Heat tracer cables penetrating the permafrost zone were attached to the outside of the well pipe and were activated at the sample collection time.</p> <p>Ensure generator run continuously to energized heat cables. Use a downhole camera if necessary to inspect well damage before proceeding to groundwater sampling.</p>	
<p><b><u>Difficulties encountered while well purging and sampling</u></b></p> <p>Melted the nylon line of the DVP pump system used to remove water from the well annulus above the casing packers</p> <p>Inoperable pump in the borehole annulus, therefore packers are of no use. Heat cable (energized to keep the well from freezing)</p>	<p>Required activation of the heating cables to melt the ice in the well prior sampling</p> <p>Use stainless steel tubing connected to the DVD pump rather than nylon</p>	<p>Temperature gauging should be conducted and logged during drilling operation. This will allow defining depth of permafrost and talik water location. This information is key decision parameter for heat tracing cable length and elevation of purge and sampling pumps (Franz Environmental Inc. 2009)</p> <p>Pump should be located within unfrozen water at all times is a key factor in avoiding problems due to freezing groundwater during purging/sampling (Franz 2009)</p>
<p>Line of the U-tube sampling system froze</p>	<p>Use an insulated hose encompassing both the sampling lines and the heat trace cable would have prevented the freezing (Statler et al. 2010; Friefeld et al. 2008).</p>	



## 5 KEY POINTS AND RECOMMENDATIONS

---

- An extensive groundwater monitoring campaign was achieved on site in 2018
- In total, the 2018 groundwater monitoring program included the following eleven (11) monitoring stations, specifically: five (5) groundwater observation wells (MW-IPD-01 (s), MW-IPD-01 (d), MW-IPD-07, MW-IPD-09 and MW-16-01), , three (3) dike seepages, one (1) pit sump, one (1) Storm management pond sump, and one (1) reclaim water.
- Please refer to Section 5.1 of Appendix A below for a complete review of the recommendation to improve groundwater flow comprehension and groundwater sample integrity, for future drilling and monitoring well installation and for future groundwater monitoring.
- No new groundwater are planned to be installed in 2019. The groundwater monitoring program will be updated as the project progresses. New information from the hydrogeological numerical model and from hydrogeological field data will be integrated throughout. Moreover, methods to obtain representative groundwater samples and improve well designs under arctic climate continue to be investigated.
- For the next field investigation, water used by the laboratory to fill the blank samples should be analyzed for the same parameters than the monitoring samples itself. If water used for the blank samples is clean (free of all parameters), then a source of contamination during transport should be identified by Agnico Eagle regarding the following parameters: carbon, nitrogen, cyanide, sulfate, etc. Transport containers should be cleaned and selected accordingly. Moreover, transport blank should be kept in a refrigerator that is not used to store samples;
- Only a few studies are available on deep permafrost environment. In most study, permafrost is defined by the temperature isotherm zero. However, pressure and salinity will influence the actual freezing point of water and therefore the presence or the absence of ice (Stotler et al. 2010; van Everdigen 1976). Pressure, salinity and the visual absence of ice in cores should be considered in the search for talik zones instead of just relying on temperature data.
- Important to define properly talik zones not only based on temperature gradient. Pressure and salinity will influence freezing temperature and the definition of permafrost/talik zone.
- Drilling methodology is the basis to a proper setting form representative groundwater sampling (many procedures have to be followed).
- Groundwater sample contamination can come from many sources, it is important to minimize and prevent the effect of sample contamination as much as possible (avoid

drill/brine fluid, purge well as much as possible, clean purging and sampling equipment before use, installed well properly to avoid leakage of cross-contamination of fluid).

- There is always a percentage of drill fluid left in the rock formation, so it is relevant to use a tracer to define the percentage of contamination (Piffner et al. 2008). Brine and drill fluid get pushed into fractures and former drill fluid stays in the rock formation and risk to contaminate groundwater samples. This would lead to erroneous groundwater salinity and TDS concentrations. What is suggested is that fresh water be used during the drilling. Cross-contamination between layers can occur as brine water from drilling won't freeze as readily as fresh water, heated fresh water would form an icy zone around the borehole and could be removed during the melting and purging procedures of the monitoring well. Some suggestions include the use of tracer with drilling fluid to define the degree of contamination of a groundwater sample, the usage of a U-sampler known for high purity samples for real-time and laboratory analysis, and a rigorous assessment of sample contamination including subsampling of material in contact with the borehole, drilling lubricant, drill cuttings, tools used for groundwater sampling, etc. The collection of blank samples during well and sampling operation is recommended.

- Agnico Eagle will make effort to put in place or use the innovative solutions and best practices when possible to improve the groundwater well installation and sampling program.

- Agnico Eagle will seek new opportunities from forthcoming field campaigns at Meadowbank Mine to collect representative groundwater samples at new locations.

## 6 REPORTING

---

An annual groundwater monitoring report presented in Appendix A will be submitted by Agnico Eagle Mines Limited to the NWB and NIRB with the Meadowbank Annual Report of the following year. This report will include the following information:

- Installation logs for any new monitoring wells;
- Location in UTM coordinates of all groundwater monitoring locations;
- Description of the working condition of the existing wells;
- Date of groundwater sampling;
- Details of sampling methods;
- Analytical results including: field data, laboratory analytical data and QA/QC information;
- Comparative assessment of data obtained to date to input values used in the Water Quality Model for the site (relevant salinity parameters); and
- Comparative assessment of parameters indicative of mine impacts to groundwater, with particular regard to tailings (total cyanide and dissolved copper);
- Actions taken regarding recommendations for the groundwater sampling program.

A historical trending from 2003 to 2018 is also provided in Appendix B.

## 7 REFERENCE

---


- Franz T. (2009) Peer Review of Monitoring Well designs to Minimize the Effects of permafrost Damage at Agnico Eagle's Meadowbank Mine in Nunavut. Franz Environmental Inc.
- Freifeld B., Perkins E., Underschultz J., Boreham C. (2009) The U-tube sampling methodology and real-time analysis of geofluids. URL: <http://escholarship.org/uc/item/4jc2m4g9>
- Freifeld B.M., Chan E, Onstott T.C., Pratt L.M., Johnson A., Stotler R., Holden B., Frape S. Pfiffner S.M., DiFurio S., Ruskeeniemi T., and Neill I. (2008) Deployment of a Deep Borehole Observatory at the High Lake Project Site, Nunavut, Canada. NINTH INTERNATIONAL CONFERENCE ON PERMAFROST (28 June - 3 July 2008) Fairbanks, Alaska, USA
- Henkemans E. (2016) Geochemical Characterization of Groundwaters, Surface Waters and Water-Rock Interaction in an Area of Continuous Permafrost Adjacent to the Greenland Ice Sheet, Kangerlussuaq, Southwest Greenland. Ph.D. Thesis, Waterloo University, 308 p.
- Hounslow AW (1995) Water Quality Data: analysis and interpretation. CRC Press, Florida
- Golder, 2007. Meadowbank Gold Project. 2006 Baseline Ground Water Monitoring. August 16, 2007.
- Golder (2008a). Technical Memorandum: 2008 Groundwater Monitoring Well Design DRAFT for Client Review Only. May 23, 2008.
- Golder (2008b). Technical Memorandum: 2008 Groundwater Monitoring Plan Meadowbank Gold Project. August 1, 2008.
- Golder (2009a). 2008 Groundwater Quality Monitoring Program, Meadowbank Mine. January 14, 2009.
- Golder (2009b). 2009 Groundwater Quality Monitoring Program, Meadowbank Mine. October 29, 2009.
- Golder, 2017. Whale Tail Pit Project, Laboratory Testing on Tailings. October 16th. Project no.: 001-1775467-MTA-Rev B.
- Pfiffner S.M., Onstott T.C., Ruskeeniemi T., Talikka M., Bakermans C., McGown D., Chan E., Johnson A., Phelps T.J., Le Puil M., Difurio S.A., Pratt L.M., Stotler R., Frape S. Telling J., Sherwood B.L., Neill I., and Zerbin B. (2008) Challenges for Coring Deep Permafrost on Earth and Mars ASTROBIOLOGY Volume 8, Number 3 © Mary Ann Liebert, Inc. DOI: 10.1089/ast.2007.0159
- SNC-Lavalin, 2016. Multiple Account Analysis for the tailings facility extension project. Version A00, Oct.24. Ref.: 637215-5000-4GER-0001.
- SNC-Lavalin, 2017c. TSFE Final Report. Version A00, January 30rd, Ref.: 637215-6000-4GER-0001.

- SNC-Lavalin, 2017a (unreleased). TSFE - In-Pit Deposition - Prefeasibility Study. Final Report. Version BPB, unreleased, Ref.: 637215-7000-40ER-0001.
- Stotler R.L., Frape S.K., Freifeld B.M., Holden B., Onstott T.C., Ruskeeniemi T, and Chan E. (2010) Hydrogeology, chemical and microbial activity measurement through deep permafrost. Groundwater. DOI: DOI: 10.1111/j.1745-6584.2010.00724.x
- Stotler R.L., Frape S.K., Ruskeeniemi T, Ahonen L., Onstott T.C., and Hobbs M.Y. (2009) Hydrogeochemistry of groundwaters in and below the base of thick permafrost at Lupin, Nunavut, Canada. *Journal of Hydrology* 373: 80–95.
- Stotler R.L. (2008) Evolution of Canadian Shield Groundwaters and Gases: Influence of Deep Permafrost. PH.D. Thesis. Waterloo University, 265 p.
- Sutphin J.D., Atkinson L.C., and Mahoney J.J., (2016) MONITORING AND SAMPLING OF GROUNDWATER BENEATH DEEP PERMAFROST Sea to Sky Geotechnique 2006 59th Canadian Geotechnical Conference and 7th Joint CGS and IAH-CNC, Vancouver B.C., 1613-1618.
- Wilkins MJ, Daly R.A., Mouser P.J., Trexler R., Sharma S., Cole D.R., Wrighton K.C., Biddle J.F., Denis E.H., Fredrickson J.K., Kieft T.L., Onstott T.C., Peterson L., Pfiffner S.M., Phelps T.J. and Schrenk M.O. (2014) Trends and future challenges in sampling the deep terrestrial biosphere. *Frontiers in Microbiology*, perspective article. DOI: 10.3389/fmicb.2014.00481

**APPENDIX A**

**2018 Groundwater Factual Report**

---

 <b>SNC • LAVALIN</b>	<b>TECHNICAL NOTE</b> <b>2018 Groundwater Monitoring</b>	Prepared by : Laurie Tremblay Reviewed by : Denis Vachon		
		Rev.	Date	Page
	645182-3000-4EER-0001	00	2018-12-17	i

**Title of document:**                    **2018 GROUNDWATER MONITORING**

**Client:**                                    **AGNICO EAGLE MINES LIMITED**


**Project:**                                 **GROUNDWATER MONITORING**

*Prepared by :*            Laurie Tremblay, P. Geo. (OGQ 2107),  
 Ph.D. \_\_\_\_\_

*Reviewed by:*            Denis Vachon, Water Specialist . \_\_\_\_\_

*Approved by :*            Dominic Tremblay, P..Eng. (OIQ  
 133511), M.A.Sc. \_\_\_\_\_

---

 <b>SNC • LAVALIN</b>	<b>TECHNICAL NOTE</b> <b>2018 Groundwater Monitoring</b>	Prepared by : Laurie Tremblay Reviewed by : Denis Vachon		
	645182-3000-4EER-0001	Rev.	Date	Page
		00	2018-12-17	ii

### REVISION INDEX

Revision				Pages Revised	Remarks
#	Prep.	App.	Date		
PA	L.T.	D.T.	27-11-2018	All	Issued for internal review
PB	L.T.	D.T.	24-10-2018		Issued for client review
00	L.T.	D.T.	17-12-2018	All	Issued for final review


### NOTICE TO READER

This document contains the expression of the professional opinion of SNC-Lavalin Inc. (“SNC-Lavalin”) as to the matters set out herein, using its professional judgment and reasonable care. It is to be read in the context of the agreement dated May 16th 2018 (the “Agreement”) between SNC-Lavalin and Agnico Eagle Mines Limited (the “Client”) and the methodology, procedures and techniques used, SNC-Lavalin’s assumptions, and the circumstances and constraints under which its mandate was performed. This document is written solely for the purpose stated in the Agreement, and for the sole and exclusive benefit of the Client, whose remedies are limited to those set out in the Agreement. This document is meant to be read as a whole, and sections or parts thereof should thus not be read or relied upon out of context.

SNC-Lavalin has, in preparing estimates, as the case may be, followed accepted methodology and procedures, and exercised due care consistent with the intended level of accuracy, using its professional judgment and reasonable care, and is thus of the opinion that there is a high probability that actual values will be consistent with the estimate(s). Unless expressly stated otherwise, assumptions, data and information supplied by, or gathered from other sources (including the Client, other consultants, testing laboratories and equipment suppliers, etc.) upon which SNC-Lavalin’s opinion as set out herein are based have not been verified by SNC-Lavalin; SNC-Lavalin makes no representation as to its accuracy and disclaims all liability with respect thereto.

To the extent permitted by law, SNC-Lavalin disclaims any liability to the Client and to third parties in respect of the publication, reference, quoting, or distribution of this report or any of its contents to and reliance thereon by any third party.




 <b>SNC • LAVALIN</b>	<b>TECHNICAL NOTE</b> 2018 Groundwater Monitoring	Prepared by : Laurie Tremblay		
		Reviewed by : Denis Vachon		
	645182-3000-4EER-0001	Rev.	Date	Page
	00	2018-12-17	iii	

## TABLE DES MATIÈRES

<b>1.0</b>	<b>INTRODUCTION.....</b>	<b>1</b>
1.1	Background .....	1
<b>2.0</b>	<b>FIRST SITE VISIT –MONITORING WELLS INSTALLATION (MAY 29 TO JUNE 4, 2018).....</b>	<b>2</b>
2.1	Objectives .....	2
2.2	Monitoring Wells Installations.....	2
	2.2.1 Monitoring Wells Installation Summary.....	3
	2.2.2 Summary of SNC-Lavalin Professional activities carried out on-site.....	3
<b>3.0</b>	<b>SECOND AND THIRD SITE VISIT – WELL SAMPLING .....</b>	<b>4</b>
3.1	Objectives .....	4
3.2	Methodology.....	4
	3.2.1 Monitoring Wells Development Methodology .....	4
	3.2.2 Groundwater Sampling Methodology .....	4
3.3	Analytical program .....	5
	3.3.1 Quality Assurance / Quality Control (QA/QC) .....	6
3.4	Analytical Results and Preliminary Interpretation.....	6
	3.4.1 Quality Assurance / Quality Control (QA/QC).....	7
	3.4.2 Water Quality Results and Criteria .....	8
	3.4.3 Stiff Diagrams .....	9
	3.4.4 Interpretation.....	10
<b>4.0</b>	<b>SUMMARY AND CONCLUSIONS : .....</b>	<b>12</b>
<b>5.0</b>	<b>RECOMMENDATIONS.....</b>	<b>12</b>
5.1	Recommendations .....	13
	5.1.1 Recommendations to improve groundwater flow comprehension and groundwater sample integrity.....	13
	5.1.2 Recommendations for future drilling and monitoring well installation:.....	13
	5.1.3 Recommendations for future groundwater monitoring: .....	14

### Liste de figures

Figure 3-1: Dissolved Calcium concentrations vs pH.....	11
Figure 3-2: Sulfate concentration vs dissolved calcium and magnesium concentrations .....	11


 <b>SNC • LAVALIN</b>	<b>TECHNICAL NOTE</b> 2018 Groundwater Monitoring	Prepared by : Laurie Tremblay Reviewed by : Denis Vachon		
		Rev.	Date	Page
	645182-3000-4EER-0001	00	2018-12-17	iv

### Liste de tableaux

Table 2-1: 2018 Groundwater Monitoring Well Details .....	2
Table 3-1: Samples collected .....	5
Table 3-2 : Parameters exceeding the quality criteria for the duplicate samples.....	8
Table 3-3 : Samples and Parameters exceeding Criteria (three times TPL concentration).....	9

### Liste des annexes

APPENDIX A:	WATER SAMPLING STATIONS LOCATION MAP
APPENDIX B:	WELL SKETCHES BY AGNICO EAGLE – (ELECTRONIC FILE)
APPENDIX C:	PHOTOGRAPHIC REPORT
APPENDIX D:	COMPARATIVE TABLE AND RECOMMENDATIONS
APPENDIX E:	LITTERATURE
APPENDIX F:	PURGING OPERATIONS BY AGNICO EAGLE – (ELECTRONIC FILE)
APPENDIX G:	GROUNWATER SAMPLING PROCEDURES
APPENDIX H:	TEMPLATE SHEET FOR GROUNDWATER SAMPLING
APPENDIX I:	GEOCHEMICAL DATA – (ELECTRONIC FILE)
APPENDIX J:	STIFF DIAGRAMS

 <b>SNC • LAVALIN</b>	<b>TECHNICAL NOTE</b> <b>2018 Groundwater Monitoring</b>	Prepared by : Laurie Tremblay		
		Reviewed by : Denis Vachon		
	645182-3000-4EER-0001	Rev.	Date	Page
	00	2018-12-17	1	

## 1.0 INTRODUCTION

This factual report provides a summary for the 2018 groundwater monitoring program carried out at the Meadowbank Mine (Meadowbank). The report includes a description of the monitoring wells installation, a description of the surface water and groundwater sampling and a presentation of the water quality results. SNC-Lavalin professional offered its technical services to support Agnico Eagle Mines Limited (Agnico Eagle) with the following:

- › Observe the installation of four new monitoring wells from May 29 to June 4, 2018;
- › Achieve two groundwater sampling programs from July 5 to July 12, 2018 and September 6 to September 13, 2018 using low-flow sampling techniques for licensing requirements; and
- › Compile and interpret the water quality data collected to document the potential interaction between surface water and groundwater, especially in relation to tailing migration.

### 1.1 Background


At Meadowbank, groundwater quality investigation is used to predict the chemistry of water accumulating in open pits and to assess any effects of mining on groundwater quality, particularly with respect to tailings deposition activities.

From 2003 to 2016, 14 groundwater monitoring wells have been installed to characterize the groundwater. Throughout these years, 34 groundwater samples and 21 duplicates were collected from these wells. However, most of the monitoring wells became inoperable due to the challenging arctic condition and permafrost environment at Meadowbank, and to this day, only one well remain operable.

From 2013 to 2016, alternative methods were investigated to collect groundwater samples including pit wall seepages, production drill holes, pit sumps, horizontal wells installed into pit walls, and temporary wells for dewatering. In total, six groundwater samples were collected from horizontal wells installed in pit E walls, one sample from a temporary dewatering well, two samples from pit sumps during pit exploitation and one sample from production borehole.

Despite efforts to overcome multiple challenges related to collect groundwater sample under arctic conditions and permafrost environment at Meadowbank, groundwater historical chemistry data seem unrepresentative of the real conditions. Conclusions from the historical groundwater quality data review are:

- › De-icing salt and calcium chloride brine used to prevent the boreholes from freezing after drilling operation remains in groundwater for years despite intensive purging of wells after installation. When those products are used in boreholes without a dye tracer, it becomes impossible to establish background conditions of groundwater chemistry, despite extensive purging of the wells. Salinity, concentration of calcium and chloride dissolved in groundwater fluctuate from multiple order of magnitude throughout the years and show no logical trend;
- › The sampling methodology used to retrieve groundwater samples induce the sample to be either diluted (sample not collected in front of the well screen) or charged with parameters that come from fine particulates found in dirty water (sediment in suspension in a sample from sumps and horizontal well can induce false results because groundwater samples are collected in bottle with preservatives but are not filtered in the field before adding the water to the bottles with preservatives); and
- › Important chemical parameters to establish background chemistry were missing from the data set (major ions dissolve in groundwater).

 <b>SNC • LAVALIN</b>	<b>TECHNICAL NOTE</b> <b>2018 Groundwater Monitoring</b>	Prepared by : Laurie Tremblay Reviewed by : Denis Vachon		
	645182-3000-4EER-0001	Rev.	Date	Page
		00	2018-12-17	2

In 2017, an extensive groundwater sampling program took place. The program aimed to improve the characterization of the baseline groundwater chemistry, identify potential sources of contaminants at the mine site, and identify potential interaction between surface and groundwater. The program included:

- › Review of the sampling methodologies and the historical groundwater quality data;
- › Testing and maintenance of the sampling equipment;
- › Collection of surface and groundwater samples at specific locations and;
- › Data compilation and basic interpretation of groundwater quality.

The groundwater investigation was repeated in 2018 with the addition of four new monitoring wells. However, access to the pit was limited and groundwater seepage from pit walls could not be sampled this year.

The locations of each former and currently operable groundwater wells and other groundwater monitoring stations are provided in Appendix A.

## 2.0 FIRST SITE VISIT –MONITORING WELLS INSTALLATION (MAY 29 TO JUNE 4, 2018)

### 2.1 Objectives

The objective of this first site visit was to provide on-site professional support to Agnico Eagle field technicians during the drilling and the installation of four new monitoring wells. Prior to the site visit, recommendations in relation with the drilling and installation of the new monitoring wells were provided in the following documents:

1. Groundwater Monitoring Plan Version 7 March 2017;
2. Groundwater Monitoring Plan Version 8 January 2018;
3. Recommendations\_monitoringwell\_2018 sent in by email with the object; Monitoring well construction and installation sent on 2017-12-11 (15:56); and
4. Follow up: December 18, 2017, discussion on Monitoring well construction and installation sent on 2017-12-22 (15:42).


### 2.2 Monitoring Wells Installations

Four new monitoring wells were installed in boreholes drilled by Forage Orbit Garant (Orbit). The boreholes were cored vertically with a nominal diameter of 96 mm (HQ). Agnico Eagle employees provided the monitoring well equipment and helped with the monitoring wells installation. Detailed information on the boreholes including collar coordinates and installations details are presented in Table 2-1.

**Table 2-1: 2018 Groundwater Monitoring Well Details**

Well Identification	Easting (m)	Northing (m)	Screen Interval (m)	Heat Trace Cables Interval (m)	Bentonite Seal Interval (m)
MW-IPD-01 (s)	639240.3	7214249.9	51.0 – 69.0	-5.1 – 34.9	44.0 – 50.1
MW-IPD-01 (d)	639240.0	7214245.0	163.0 – 181.0	2.0 – 42.0	155.6 – 161.7
MW-IPD-07	638859.6	7212597.2	42.0 – 50.0	-5.0 – 35.0	37.4 – 40.5
MW-IPD-09	639065.2	7213024.5	62.0 – 80.0	-3.2 – 36.4	55.0 – 61.1

Figures in Appendix B (excel spreadsheet made by Agnico Eagle) provide installation details for the four monitoring wells installed in 2018. SNC-Lavalin field observations showing each step of the installation are presented in a photographic report in Appendix C. A table comparing the recommendations previously made for monitoring well

 <b>SNC • LAVALIN</b>	<b>TECHNICAL NOTE</b> <b>2018 Groundwater Monitoring</b>	Prepared by : Laurie Tremblay		
		Reviewed by : Denis Vachon		
	645182-3000-4EER-0001	Rev.	Date	Page
	00	2018-12-17	3	


installation with the activities carried out on site is available in Appendix D. The last column of the table lists the corrective measures to be taken. The next sections provided a summary of the activities carried out during the installation.

### 2.2.1 Monitoring Wells Installation Summary

- › Boreholes drilling took place from May 25 to June 4 and monitoring wells installation was from May 28 to June 4;
- › Monitoring well equipment was inspected at the mine site prior to the drilling operation to guarantee pipes integrity;
- › Monitoring wells were installed at strategic location in relation to future In-Pit-Disposal;
- › Based on the monitoring well depth, drilling operation lasted between 1 and 4 days;
- › Based on the monitoring well depth, the monitoring wells installation lasted between 1.5 and 4 hours;
- › Rock cores were collected in each borehole for the entire well depth;
- › Lake water and environmentally safe drilling additives (DD2000) were used as drilling fluid. As recommended, no other additives, such as de-icing salt or calcium chloride that could impact the water chemistry, were used during drilling or installation;
- › Well screens were sealed with prepack bentonite composed of a 2-inch (50.8 mm) diameter stainless steel (S.S.) pipe and bentonite sleeve (outside diameter (O.D.) between 63.5 and 76.2 mm (2-1/2 to 3 in);
- › Modified foam bridges (88.9 mm (3-1/2 in) O.D.) on a 0.76 m (2.5 ft) long 2-inch (50.8 mm) diameter S.S. pipe were installed between the monitoring well screens and the bentonite sleeve to prevent the bentonite to seep downwards in the monitoring well screen interval;
- › Prior to the installation, monitoring well screens and pipes with threads aligned on the same side were numbered in the sequence that they had to be lowered. During this step, S.S. centralizers were installed on every third pipe (centralizer spacing of 9.14 m (30 ft)); and
- › Heat trace cables were installed outside of every monitoring well pipes up to a depth of 40 m to cover the projected permafrost interval.

### 2.2.2 Summary of SNC-Lavalin Professional activities carried out on-site

- › Inspection and measurements of monitoring well material;
- › Professional support throughout monitoring well installations;
- › Verification and inventory of groundwater purging and sampling equipment;
- › Installation and testing of dedicated monitoring well head; and
- › Pit walls overview for groundwater seepage under winter/spring conditions.

 <b>SNC • LAVALIN</b>	<b>TECHNICAL NOTE</b> <b>2018 Groundwater Monitoring</b>	Prepared by : Laurie Tremblay Reviewed by : Denis Vachon		
	645182-3000-4EER-0001	Rev.	Date	Page
		00	2018-12-17	4

## 3.0 SECOND AND THIRD SITE VISIT – WELL SAMPLING

### 3.1 Objectives

The objective of the subsequent visits was to provide on-site professional support to Agnico Eagle field technicians for the installation of dedicated sampling material into four new monitoring wells and to collect surface water and groundwater samples twice in 2018.

### 3.2 Methodology

In 2018, surface water and groundwater sampling campaigns were carried out twice from July 5 to July 12, 2018 and September 6 to September 13, 2018.

The principal activities carried out are listed below:

- › Development of monitoring wells was performed by Agnico Eagle staff prior to the arrival of a SNC-Lavalin professional (between June 21 and June 28, 2018);
- › Installation of the monitoring well heads, and dedicated pumps and tubing in each monitoring well (between July 6 and July 8, 2018);
- › Groundwater sampling in monitoring wells (pit wall seepages were not sampled due to safety issues);
- › Surface water sampling (only at specific location); and
- › Pit walls overview for groundwater seepage under summer conditions.


#### 3.2.1 Monitoring Wells Development Methodology

Due to the drilling method employed, large amount of warm water was introduced into the borehole. The warm water was added to the borehole to prevent ice bridges during or after the drilling operations. After borehole completion and prior to the well installation, borehole development (removal of the rock cutting and the water added) was not possible because of the type of drilling rig available on site. Therefore, the four new monitoring wells were developed after the installation of the groundwater monitoring well. The development was done by Agnico Eagle staff at the end of June 2018, approximately one week before groundwater sampling was performed.

The monitoring wells were purged by Agnico Eagle staff using an air compressor fitted on 60 m long HDPE Waterra tubing with a diameter of ½ inch. The Waterra tubing was introduced into the borehole and water was airlifted outside the boreholes with compressed air. Purge operation was monitored by Agnico Eagle staff and groundwater physicochemical parameters were recorded along with approximate volumes of groundwater removed from the monitoring well (Excel spreadsheet in Appendix F). During monitoring wells purging, turbidity was very high, especially for the shallow monitoring wells, and the other physicochemical parameters fluctuated and did not stabilize. Therefore, the monitoring well purging was performed to remove as much water as possible.

#### 3.2.2 Groundwater Sampling Methodology

Surface water and groundwater sampling were performed by an Agnico Eagle field technician and an SNC-Lavalin professional. Prior to carry out the groundwater sampling program, the groundwater sampling methodologies were reviewed; the equipment was tested, cleaned and adapted when required by the SNC-Lavalin professional. In total five dedicated monitoring well heads, Solinst double valve pump, and tubing were installed on each currently operable monitoring well. The specific information about each monitoring well can be found within the groundwater sampling protocol presented in Appendix G. A template sheet to monitor all the important information while groundwater sampling is provided in Appendix H. Table 3-1 lists the samples collected in July and September 2018. The location of each station is shown on the map presented in Appendix A.

 <b>SNC • LAVALIN</b>	<b>TECHNICAL NOTE</b> <b>2018 Groundwater Monitoring</b>	Prepared by : Laurie Tremblay Reviewed by : Denis Vachon		
	645182-3000-4EER-0001	Rev.	Date	Page
		00	2018-12-17	5

Water samples from the following stations were collected directly from a tap inside a small pumping building: ST-8 North, ST-8 South ST-S-5, and ST-21. The stations ST-8 North and ST-8 South are both shallow 6 m groundwater dewatering wells. While samples ST-S-5 and ST-21 are surface water. Sample station BG-Lagoon and Storm management pond (SMP) were collected from the shore with a clean measuring cup and transferred directly to sampling bottles.

**Table 3-1: Samples collected**

Sample name	Type	Screens depth (m)	Pump depth (m)	July	September
MW-IPD-01 (s)	Groundwater well	51-69	60	X	x
MW-IPD-01 (d)	Groundwater well	163-181	175	X	x
MW-IPD-07	Groundwater well	42-50	40	X	x
MW-IPD-09	Groundwater well	62-80	70	X	x
MW-16-01	Groundwater well	89-101	95	X	x
ST-S-5	Dike seepage	-	-	X	x
ST-21	Reclaim water	-	-	x	x
ST8-North	Dike seepage	-	-	x	x
ST8-South	Dike seepage	-	-	x	x
BG-Lagoon	Sump	-	-	x	x
SMP (Storm management pond)	Sump	-	-	x	

At each monitoring well location, new and clean Low Density Polyethylene (LDPE) tubing was used for each sample. For dissolved metals analysis purpose, the water was passed through a 0.45 microns filter and kept in bottles containing preservatives to minimize any possible chemical alteration during transport to the laboratory. Groundwater and surface water samples were collected in clean, laboratory-supplied containers. Duplicates samples and transport blanks were used for quality control. Water bottles were preserved onsite at 4°C and were transported to the lab within 24 h with its transport blank. For the sampling campaign taking place in June 2018, groundwater from each monitoring well was collected with a duplicate. Two samples were collected from each new monitoring well to evaluate the disturbance induced by purging the wells only a week prior sampling activities.


At the completion of the surface water and groundwater sampling program, water quality data were compiled and a basic interpretation of the chemical results was completed.

### 3.3 Analytical program

Prior to water sample collection, the following in situ physicochemical parameters were recorded: pH, turbidity, salinity and electrical conductivity, oxydoreduction potential (ORP) and dissolved oxygen (DO). In situ parameters were recorded via a flow-through cell for most samples with an YSI® Pro, Hanna or Eureka probe.

Analytical parameters included the following parameters with respect of the Meadowbank Water License (Schedule 1, Table 1, Group 2):

- › Total and Dissolved metals: aluminum, antimony, arsenic, boron, barium, beryllium, cadmium, copper, chromium, iron, lithium, manganese, mercury, molybdenum, nickel, lead, selenium, tin, strontium, titanium, thallium, uranium, vanadium and zinc.
- › Nutrients: Ammonia-nitrogen, total kjeldahl nitrogen, nitrate-nitrogen, nitrite-nitrogen, ortho-phosphate, total phosphorous, total organic carbon, total dissolved organic carbon and reactive silica.

 <b>SNC • LAVALIN</b>	<b>TECHNICAL NOTE</b> <b>2018 Groundwater Monitoring</b>	Prepared by : Laurie Tremblay Reviewed by : Denis Vachon		
	645182-3000-4EER-0001	Rev.	Date	Page
		00	2018-12-17	6

- › Conventional Parameters: bicarbonate alkalinity, chloride, carbonate alkalinity, conductivity, hardness, calcium, potassium, magnesium, sodium, sulphate, pH, total alkalinity, total dissolved solids (TDS), total suspended solids (TSS) and turbidity.
- › Total cyanide, free cyanide and Weak Acid Dissociable Cyanide (CN WAD).
- › Additional analyses were performed to calculate mass balance reliability check on each analysis and include: dissolved calcium, dissolved potassium, dissolved magnesium, dissolved sodium, fluoride, bromide and ammonium-nitrogen.

### 3.3.1 Quality Assurance / Quality Control (QA/QC)

Prior data interpretation, some verification was completed to assess potential sample contamination during collection, shipping and analysis. Five field duplicates, one field blank blanks, and one transport blanks were sampled in 2018.

Field duplicates assure a quality control and assess if two water samples collected from the same sampling station using identical sampling procedure have reproducible analytical results. Duplicates 2018 results were verified with the same method as referenced in Agnico Eagle Groundwater Report 2016. This USEPA (1994)<sup>1</sup> method can be applied when both concentrations are higher than five times the method detection limit (MDL). Then, the relative percent difference (RPD) of those duplicates is calculated as following:

$$RPD = \frac{\text{maximum concentration} - \text{minimum concentration}}{\text{average concentration}} \times 100$$

USEPA (1994) indicates that an RPD of 20% or less is acceptable. If one or both concentrations are less than five times the MDL, a margin of +/- MDL is acceptable. For example, poor RPD results could indicate inappropriate field practice such as: unclean sampling bottles, poor sampling methodology, and inefficient monitoring well purge.

Field blanks and transport blanks and sample bottles filled with deionize water. Field blanks are open in the filed while sampling. Transport blanks are shipped to the laboratory together with the collected samples to assess any potential sample contamination during shipping. Contamination could be due to a leaky bottle containing preservative during transport, contact between highly and low contaminated water bottles or just due to an unfit container.


### 3.4 Analytical Results and Preliminary Interpretation

Each groundwater sample has a distinctive signature defined by its dissolved concentrations of chemical constituents. The interpretation of groundwater chemistry data contributes to improve the understanding of groundwater flow, contaminants migration and transformation processes along pathways as water composition varies. It can also help to identify zones where surface water and groundwater interact and define if the interaction is continuous or is only during permafrost thawing.

---

<sup>1</sup> USEPA, 1994. USEPA Contract Laboratory Program National Functional Guidelines for Inorganic Data Review. Office of Emergency and Remedial Response, U.S. Environmental Protection Agency, Washington, DC, February 1994.



 <b>SNC • LAVALIN</b>	<b>TECHNICAL NOTE</b> <b>2018 Groundwater Monitoring</b>	Prepared by : Laurie Tremblay Reviewed by : Denis Vachon		
	645182-3000-4EER-0001	Rev.	Date	Page
		00	2018-12-17	7

Water chemical results are presented in Appendix I. The following sections present the preliminary interpretation of water quality result and include:


- › Result for Quality Assurance / Quality Control (QA/QC):
  - Verification of duplicates for sample integrity and reproducibility;
  - Verification of field blank for potential contamination in the field while sampling;
  - Verification of transport blanks for potential contamination during sample transport;
- › Water chemical results and criteria; and
- › Stiff diagrams and graphical interpretation.

### 3.4.1 Quality Assurance / Quality Control (QA/QC)

Results show that all water sample duplicates have RPD values within 20% range or concentrations within 5xMDL, for most parameters demonstrating that the sampling methodology and operations were appropriate. The parameters that did not meet this requirement are listed for each duplicate sample in Table 3-2.

As mentioned in the section 3.2.1, the water turbidity was very high following the monitoring well purge and could be an explanation for the discrepancy with the duplicate samples, especially for the month of July.

Analytical results for the transport blank are also presented in Appendix I and show small concentrations for the following parameters: alkalinity, total dissolved solid, reactive silica, and potassium.

 <b>SNC • LAVALIN</b>	<b>TECHNICAL NOTE</b> <b>2018 Groundwater Monitoring</b>		Prepared by : Laurie Tremblay Reviewed by : Denis Vachon		
	645182-3000-4EER-0001		Rev.	Date	Page
			00	2018-12-17	8

**Table 3-2 : Parameters exceeding the quality criteria for the duplicate samples**

Duplicates Sample ID	LDR	Units	MW-IPD-01 (S)	MW-IPD-01 (D)	MW-IPD-07	MW-IPD-09	MW-IPD-01-(D)
Sampling Date			July 08	July 08	July 08	July 08	September 09
Alkalinity (CaCO <sub>3</sub> )	2	mg CaCO <sub>3</sub> /L	x				
Bicarbonate Alkalinity (HCO <sub>3</sub> <sup>-</sup> )	2	mg CaCO <sub>3</sub> /L	x				
Hardness (CaCO <sub>3</sub> )	1	mg CaCO <sub>3</sub> /L		x	x	x	
Total Organic Carbon	0.2	mg/L			x		
Total Suspended Solids	1	mg/L		x		x	
Dissolved Calcium (Ca)	0.03	mg/L				x	
Dissolved Copper (Cu)	0.0005	mg/L					x
Dissolved Manganese (Mn)	0.0005	mg/L			x	x	
Dissolved Molybdenum (Mo)	0.0005	mg/L			x		
Dissolved Nickel (Ni)	0.0005	mg/L		x			
Dissolved Potassium (K)	0.05	mg/L				x	
Dissolved Sodium (Na)	0.05	mg/L				x	
Dissolved Zinc (Zn)	0.001	mg/L					x
Total Aluminium (Al)	0.006	mg/L	x	x		x	x
Total Arsenic (As)	0.0005	mg/L		x		x	
Total Baryum (Ba)	0.0005	mg/L		x			
Total Calcium (Ca)	0.03	mg/L		x	x	x	
Total Iron (Fe)	0.01	mg/L		x		x	
Total Magnesium (Mg)	0.02	mg/L		x	x	x	
Total Manganese (Mn)	0.0005	mg/L		x		x	
Total Nickel (Ni)	0.0005	mg/L				x	
Total Potassium (K)	0.05	mg/L		x		x	
Total Sodium (Na)	0.05	mg/L		x	x	x	
Total Ammonia Nitrogen (NH <sub>4</sub> <sup>+</sup> and NH <sub>3</sub> )	0.01	mg N/L			x		

### 3.4.2 Water Quality Results and Criteria

Water analytical results were compared to the criteria listed in Agnico Eagle Groundwater Report 2016 to 2018. Parameters exceed the criteria when they are three times the concentrations of Third Portage Lake (TPL) fresh water. Analytical results are found in Appendix I (Excel spreadsheet) and concentrations exceeding these criteria are highlighted in bold format. Table 3-3 also shows the sampling stations and parameters that are exceeding criteria.

**Table 3-3 : Samples and Parameters exceeding Criteria (three times TPL concentration)**

Station name	Alkalinity	TSS <sup>a)</sup>	Total Copper	Total Mercury	Total Ammonia Nitrogen
MW-IPD-01 (s)	X	X			
MW-IPD-01 (d)	X				
MW-IPD-07	X	X			
MW-IPD-09	X				
MW-16-01	X	X			
ST-S-5	X				X
ST-8-North	X	X			
ST-8-South	X			X	
BG Lagoon	X				
ST-21 South	X	X	X		X
SWMP	X	X			

a) TSS =Total suspended sediment

Exceeding parameters (copper, total mercury, total ammonia nitrogen) are related to the reclaim water signature. Aside from reclaim water sample, high concentrations above TPL background is found at monitoring station ST-S-5 for ammonia nitrogen.


Provincial criteria (Quebec) and Federal criteria for groundwater quality and resurgence in surface water are also listed in the Appendix I table as a reference. However, since many water samples are considered to be surface water instead of groundwater, the results were not compared to these groundwater criteria.

### 3.4.3 Stiff Diagrams

The geochemical composition of groundwater is defined by dissolved main anions ( $\text{HCO}_3^-$ ,  $\text{SO}_4^{2-}$ ,  $\text{Cl}^-$ ) and main cations ( $\text{Ca}^{2+}$ ,  $\text{Na}^+$ ,  $\text{Mg}^{2+}$ ,  $\text{K}^+$ ). Mass balance calculation (expressed in meq/L) is the difference between main anions and cations dissolved in groundwater and were performed with the free software "Diagramme"<sup>2</sup>. The calculations are a mandatory reliability verification for any geochemical analysis (Hounslow, 1995)<sup>2</sup> and are useful to gain a first insight into water chemistry. The calculations results are presented on a Stiff diagram in Appendix J. The left side of the Stiff Diagram represents the major cation concentrations (sodium + potassium, calcium and magnesium), while the right side represents the major anions (chloride, bicarbonate + carbonate and sulfate + nitrate). Each side of the diagram should be equivalent, meaning that both concentrations (in meq/l) of cations and anions should within 5% difference.

<sup>2</sup> <http://www.lha.univ-avignon.fr/LHA-Logiciels.htm>

<sup>2</sup> Hounslow, A. (1995) Water Quality Data: Analysis and Interpretation. CRC Press, Boca Raton.

 <b>SNC • LAVALIN</b>	<b>TECHNICAL NOTE</b> <b>2018 Groundwater Monitoring</b>	Prepared by : Laurie Tremblay		
		Reviewed by : Denis Vachon		
		Rev.	Date	Page
	645182-3000-4EER-0001	00	2018-12-17	10

Samples with the least charged water (natural groundwater) were presented on a scale of 0 to 5 meq/l on Figure 1 of Appendix J, while the samples with the higher concentrations were presented on Figure 2, on a scale of 0 to 50 meq/l. Stiff diagrams were used to support comparison between the sampling period and the sampling locations nearby mining activities.

#### 3.4.4 Interpretation

Results for 2018 samples (displayed in color) were plotted along with 2017 values (displayed in light grey) on two graphs (see Figure 3-1 and Figure 3-2). In 2017, these graphs showed some major chemical components and demonstrated the chemical signature and evolution of water.

Reclaim water sampling station named ST-21-South, was identified in 2017 as the main source of elevated components found in water and is illustrated by black cross on both graphs (Figure 3-1 and Figure 3-2). In 2017, from Figure 3-2, three potential groups were interpreted:

- 1) Samples containing reclaim water signature;
- 2) Sample containing a potential signature from waste rock NAG stockpiles (further investigation would be required); and
- 3) Natural surface water and groundwater signature.

In 2018, ST-S-5 shows higher concentration than the one found in ST-21-South. However, these two locations are still the main source for sulfate and calcium, as demonstrated in 2017. Reclaim water signature can still be detected in the groundwater from well MW-16-01.

However, compared to the 2017 results, there is no apparent trending between the 2018 results. This year, there are only two categories of water distinguishable: Reclaim associated water (ST-21, ST-S-5, and MW-16-01) and natural background water. There is no geochemical trending or linkage between the two categories.

In 2017, the diluted signal of reclaim water could be identified along flow path (shown by grey dots on the graph) from alternative sampling stations such as pit wall seepage, there is no apparent linkage between Reclaim water signature, surface water and groundwater samples collected in 2018.


In 2017, alternative sampling station, geographically positioned along flow paths, allowed to identify dilution trends from the reclaim water source (shown by grey dots on the graph). In 2018, the groundwater collected from the four newly installed well fits within the natural groundwater category and can be used as threshold values to monitor groundwater quality in the future.

**Figure 3-1: Dissolved Calcium concentrations vs pH**

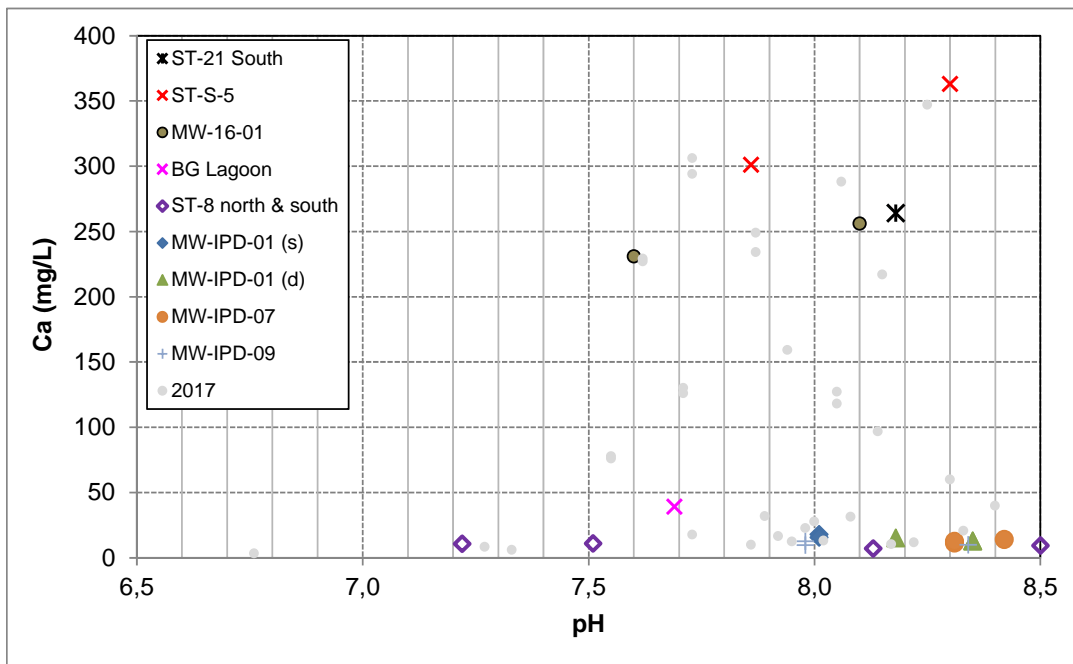
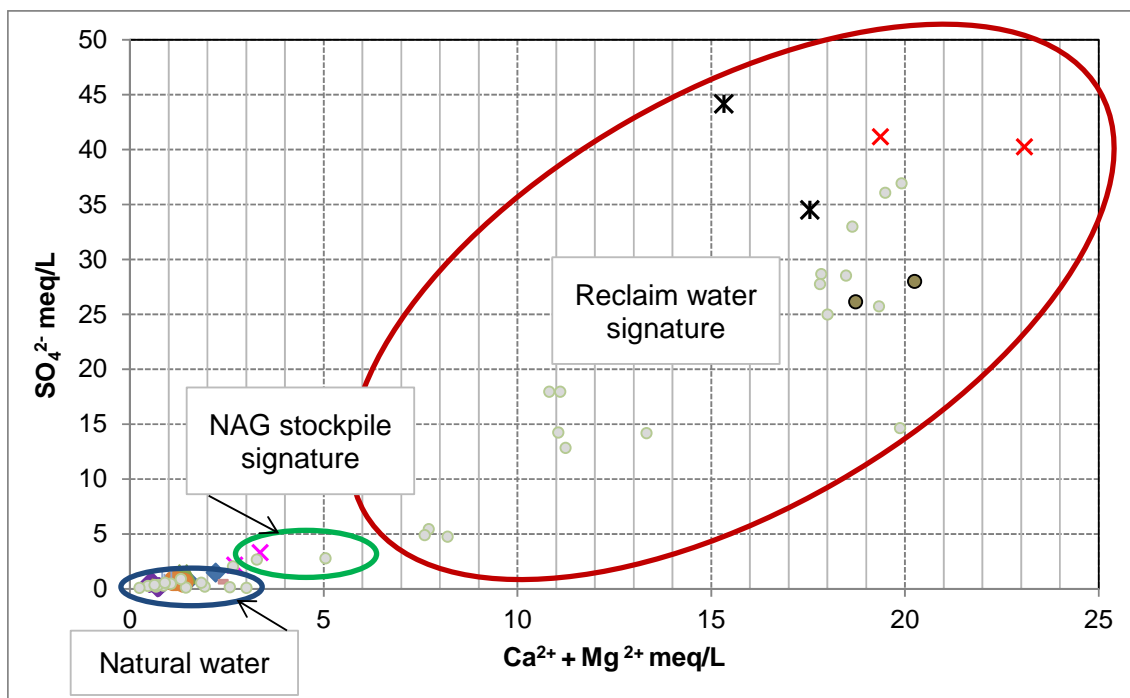


**Figure 3-2: Sulfate concentration vs dissolved calcium and magnesium concentrations**



 <b>SNC • LAVALIN</b>	<b>TECHNICAL NOTE</b> <b>2018 Groundwater Monitoring</b>	Prepared by : Laurie Tremblay Reviewed by : Denis Vachon		
	645182-3000-4EER-0001	Rev.	Date	Page
		00	2018-12-17	12


## 4.0 SUMMARY AND CONCLUSION :

After the completion of three site visits in 2018, the active participation of SNC-Lavalin professionals to the Meadowbank groundwater field sampling program review, elaboration and interpretation, led to the following conclusions:

- › Four monitoring wells were installed to complete the monitoring network. The new monitoring wells were implemented considering the current state of knowledge and the monitoring wells were installed in talik areas (see recommendations and monitoring well design from Appendix D);
- › Heat traces cables were installed along the monitoring well pipes within the permafrost zones;
- › State of the art sampling techniques were performed and each sampling station was selected based on its contribution to the global understanding of groundwater quality, sampling procedures are available in Appendix G and a Template sheet to record the information is provided in Appendix H;
- › A double valve pump, tubing and a well head were dedicated to each monitoring well;
- › Equipment was inspected, replaced or calibrated when required and cleaned to prevent any contamination during sampling operations;
- › Low flow technique with nitrogen was used for groundwater sampling;
- › Groundwater was filtered on site with 0.45 microns filters for dissolved metal analysis;
- › Duplicate, field and transport blanks were collected (5% of total samples);
- › To be able to compare data within the dataset, all stations were sampled during the same week of the same month in 2017 and 2018. A long-term groundwater monitoring network was established.
- › Purging the water from the wells a few days before the first sampling event of the season induced a lot of sediments in suspension in groundwater and explains the variabilities for many parameters for the duplicate samples in July. Since the well will settle in the future;
- › Interpretation of 2018 geochemical data aims to provide a global portrait of groundwater quality at the mine site and its potential linkage to surface water of mining activities;
- › Reclaim water in South Cell is a source of sulfate, chloride, sodium, potassium, calcium, manganese, and other traces elements for surface and groundwater on the site and can be traced at ST-S-5, MW-16-01; and
- › Groundwater collected in 2018 from the four (4) newly installed well fits within the natural groundwater category established on 2017 results and can be use as threshold values to monitor groundwater quality in the future.

## 5.0 RECOMMENDATIONS

Based on a review of the analytical results obtained prior 2017, participation to the field sampling campaigns in 2017 and 2018 by SNC-Lavalin professional (two site visits in 2017 and three site visit in 2018) , the following recommendations are made:

 <b>SNC • LAVALIN</b>	<b>TECHNICAL NOTE</b> <b>2018 Groundwater Monitoring</b>	Prepared by : Laurie Tremblay		
		Reviewed by : Denis Vachon		
	645182-3000-4EER-0001	Rev.	Date	Page
	00	2018-12-17	13	


## 5.1 Recommendations

### 5.1.1 Recommendations to improve groundwater flow comprehension and groundwater sample integrity

- › Carry out logging of drill rock core for basic geology, lithological contacts, fracture types, joint description (aperture, spacing, infilling, alteration). It is suggested to log the rock cores with a hydrogeological point of view as shown in Mayer et al. (2014) and Gupta and Singhal, Chapter 2 (2010) presented in Appendix Ea and Eb;
- › Display on the same log the following information:
  - Thermistor profile;
  - Geological description;
  - Geomechanical description; and
  - Well installation details.
- › Verify the sealing integrity of each monitoring well with a dye tracer as the prepack bentonite sleeves installed in the new wells had smaller diameter (63.5-76.2 mm O.D.) than the one suggested (88.9 mm O.D.). Sealing integrity test is recommended to verify the proper sealing of each MW screen from water coming from overburden or upper bedrock levels. The sealing integrity test can be performed after collection of the first sample by adding a dye tracer between the casing and the S.S. pipe. If no dye tracer appears while pumping the MW, seal integrity will be confirmed. Volume and concentration of dye tracer to be added must be calculated by a professional;
- › Add to well sketch all the specific measurements for the well material installed (ex. , well riser inside and outside diameters, bentonite sleeve diameter)
- › Add to well sketch the duration of the borehole drilling, notes on difficulties encounter during drilling (rock alteration and brittle intervals making drilling difficult) and well installation duration (Appendix B).

### 5.1.2 Recommendations for future drilling and monitoring well installation:

- › Quantity of drilling fluid or additive added (water) in the borehole during or after drilling should be noted;
- › Drilling fluid sample needs to be collected and sent to the lab for chemistry analysis;
- › A dye tracer needs to be added to the drilling fluid while additives are used in the drilling fluid (DD2000);
- › If a dye tracer is used, the concentration during drilling needs to be constant as possible and closely monitor. Good record should be kept of the monitoring;
- › Appropriate tools and clams need to be used for the well-piping installation, to avoid damaging the pipes;
- › HWT flush joint casings have to be installed above ground level so that water coming from the surface cannot enter the annulus space;
- › Uses stainless steel collars to fix extra equipment to the well, especially below the bentonite section (do not use tape). Use ASTM approved material for groundwater wells only;
- › Uses a longer foam bridge (the same length as the riser pipe length 0.76 m) and with a diameter appropriate for the borehole diameter.
- › Uses prepack bentonite sleeves adjusted for the well diameter and use prepack made of bentonite pellets instead of powder.


 <b>SNC • LAVALIN</b>	<b>TECHNICAL NOTE</b> <b>2018 Groundwater Monitoring</b>	Prepared by : Laurie Tremblay		
		Reviewed by : Denis Vachon		
	645182-3000-4EER-0001	Rev.	Date	Page
	00	2018-12-17	14	

- › Carry out extensive development operations prior to the well installation to remove all the drilling fluid. During the monitoring well development, record the following field physicochemical parameters until you have 3 consecutive readings that are (every 15 min for the first hour and then every flush):
  - pH is within 0.1 or 0.2 of a standard unit;
  - Temperature is within 0.2 °C or 3%;
  - Specific conductance is within 5% for values equal to or less than 100 microsiemens and 3% for values greater than 100 microsiemens;
  - DO (dissolved oxygen) is within 10%;
  - Eh/ORP (oxidoreduction potential) is within 10 millivolts; and
  - Turbidity is within 10% for values greater than 1 NTU but less than 100 NTU;


### 5.1.3 Recommendations for future groundwater monitoring:

- › The dedicated double valve pump located in well MW-IPD-07 has to be reinstalled at depth 52 m below ground level to be within the screen interval of the monitoring well. The pump was installed higher in June 2018 due to the high turbidity found in the well during that time ;
- › All five well heads mounted on a PVC tube installed on the each original metal well riser pipe above ground have to be solidified so they do not slip along the original metal well pipe;
- › Same sampling methodologies have to be used at each station and Agnico Eagle staff needs to be trained accordingly to be familiar with the technical equipment;
- › Appropriate and calibrated probes have to be used to measure salinity and TDS. Currently, the value given by the probe is just a calculation from the conductivity measurements;
- › Appropriate and calibrated probes have to be used to measure all physicochemical parameters and a flow through cell should be used to avoid contact with ambient air;
- › For the next field investigation, water used by the laboratory to fill the blank samples should be analyzed for the same parameters than the monitoring samples itself. If water used for the blank samples is cleaned (free of all parameters), then a source of contamination during transport should be identified by Agnico Eagle regarding the following parameters: carbon, nitrogen, cyanide, sulfate, etc. Transport containers should be cleaned and selected accordingly. Moreover, transport blank should be kept in a refrigerator that is not used to store samples;
- › Groundwater major dissolved ions Ca, Na, Mg, K, Cl, SO<sub>4</sub>, and HCO<sub>3</sub> must be analyzed and ionic balance can be calculated to establish if a sample is representative. Therefore, a few parameters should be added to the list to complete the monitoring program and certify data quality. For example, analysis of some isotopes would support the comprehension of groundwater migration along flow paths and the origin of those chemical components;
- › Alkalinity concentrations (HCO<sub>3</sub> and CO<sub>3</sub> values) are measured at the lab from bottle that has no preservative. It is recommended to measure alkalinity directly on the site as no external processes could alter the sample (contact with ambient air, storage in a refrigerator and transportation to the lab); and
- › List of material to be purchased by Agnico Eagle to pursue groundwater monitoring:
  - Backup control unit for the double valve pump (black box);
  - 2 pairs of vice-grips to clamp on tubing on Solinst pumps;

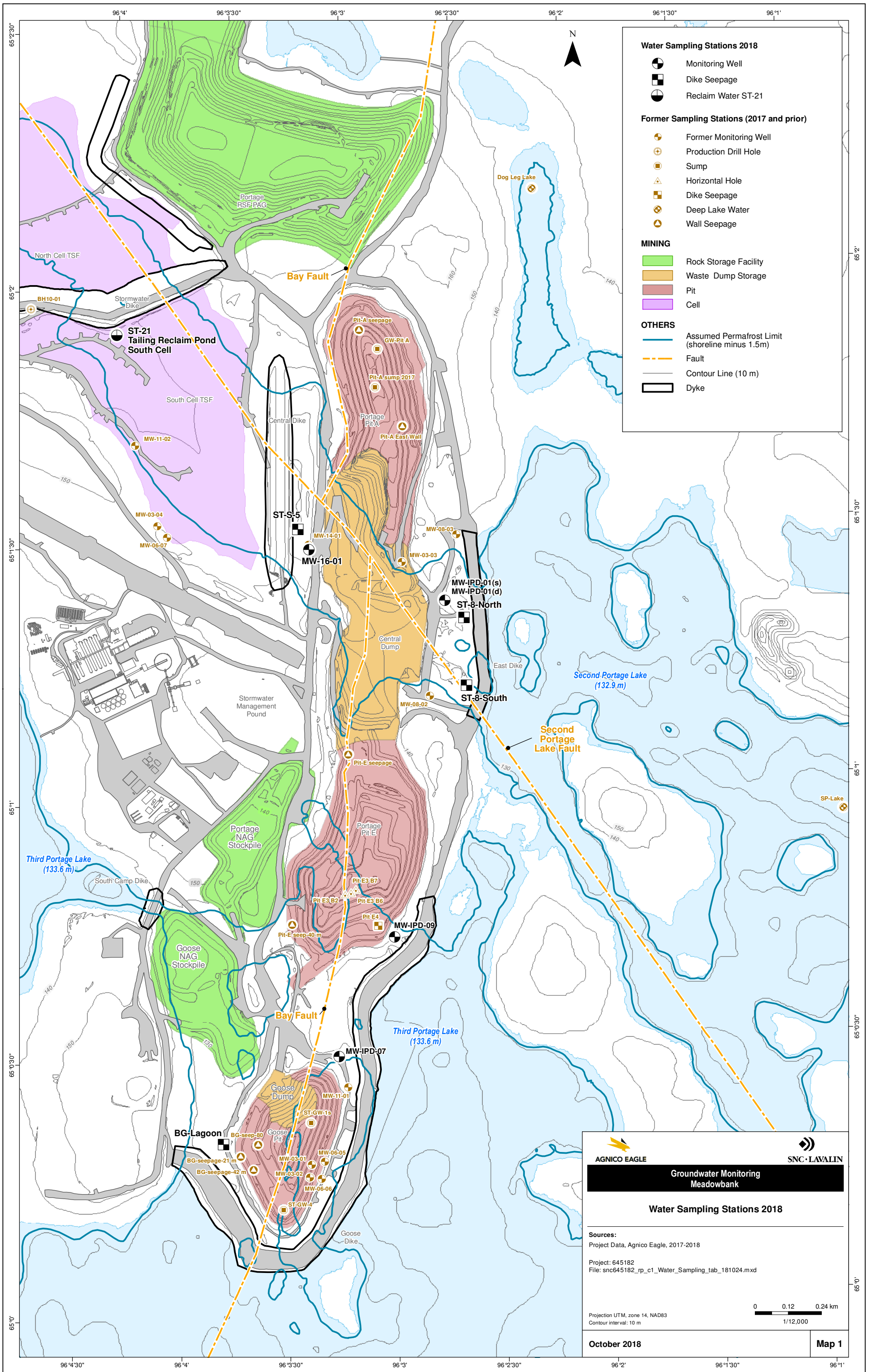


 <b>SNC • LAVALIN</b>	<b>TECHNICAL NOTE</b> 2018 Groundwater Monitoring	Prepared by : Laurie Tremblay Reviewed by : Denis Vachon		
		Rev.	Date	Page
	645182-3000-4EER-0001	00	2018-12-17	15

- 2 adapted gas regulators for the nitrogen tanks;
- A 1 1/8 wrench to tight the regulator on the nitrogen tank; and
- Multi parameter probe with a flow through cell.

 <b>SNC • LAVALIN</b>	<b>TECHNICAL NOTE</b> 2018 Groundwater Monitoring	Prepared by : Laurie Tremblay Reviewed by : Denis Vachon		
		Rev.	Date	Page
	645182-3000-4EER-0001	00	2018-12-17	16

## APPENDIX A: WATER SAMPLING STATIONS LOCATION MAP



**Water Sampling Stations 2018**

- Monitoring Well
- Dike Seepage
- Reclaim Water ST-21

**Former Sampling Stations (2017 and prior)**

- Former Monitoring Well
- Production Drill Hole
- Sump
- Horizontal Hole
- Dike Seepage
- Deep Lake Water
- Wall Seepage

**MINING**

- Rock Storage Facility
- Waste Dump Storage
- Pit
- Cell

**OTHERS**

- Assumed Permafrost Limit (shoreline minus 1.5m)
- Fault
- Contour Line (10 m)
- Dyke

**AGNICO EAGLE** **SNC-LAVALIN**

**Groundwater Monitoring Meadowbank**

**Water Sampling Stations 2018**


**Sources:**  
Project Data, Agnico Eagle, 2017-2018

Project: 645182  
File: snc645182\_rp\_c1\_Water\_Sampling\_tab\_181024.mxd


Projection UTM, zone 14, NAD83  
Contour interval: 10 m

0 0.12 0.24 km  
1/12,000

**October 2018** **Map 1**

 <b>SNC • LAVALIN</b>	<b>TECHNICAL NOTE</b> 2018 Groundwater Monitoring	Prepared by : Laurie Tremblay Reviewed by : Denis Vachon		
		Rev.	Date	Page
	645182-3000-4EER-0001	00	2018-12-17	17

**APPENDIX B: WELL SKETCHES BY  
 AGNICO EAGLE –  
 (ELECTRONIC FILE)**

 <b>SNC • LAVALIN</b>	<b>TECHNICAL NOTE</b> 2018 Groundwater Monitoring	Prepared by : Laurie Tremblay Reviewed by : Denis Vachon		
		Rev.	Date	Page
	645182-3000-4EER-0001	00	2018-12-17	18

## APPENDIX C: PHOTOGRAPHIC REPORT



## P1: ORDERING AND RECEIVING EQUIPMENT FOR WELL INSTALLATION

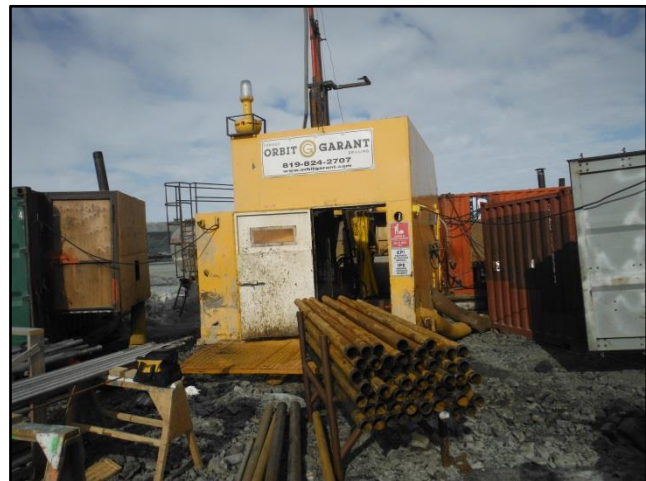


Based on information received by M. Collard, (Agnico Eagle field technician and assigned to drilling supervision and monitoring well installation), all well riser pipes were inspected prior to drilling. Damaged threads on riser pipes were reworked and identified with pink and green color. These riser pipes were left aside and utilized as backup material if necessary.

## P2-P3: DRILLING OPERATIONS



Drilling installation at monitoring well MW-IDP-09.



Drilling installation at monitoring well MW-IDP-01(d).

Drilling installation at monitoring well MW-IDP-01(d). The overburden was drilled with a HWT casing (101,6 mm I.D) anchored into the bedrock before resuming the borehole with a nominal diameter of 96 mm (HQ). Drilling operation lasted between 1 and 4 days for each borehole.



 <b>SNC • LAVALIN</b>	<b>PHOTOGRAPHIC REPORT</b> 2018 Groundwater Monitoring	Prepared by : Laurie Tremblay		
		Reviewed by : Denis Vachon		
	645182-3000-4EER-0001	Rev.	Date	Page
		PA	2018-12-12	2

### P4-P8: DRILLING & CORING



Rock cores were drilled at the four new monitoring well sites. Rock cores were recovered for the entire vertical borehole length. The four pictures show the various stratigraphy and fractures types found across the boreholes.

Fractures and discontinuities are amongst the most important features for the comprehension of groundwater flow paths. Any indication in cores on how continuous a fracture plane is should be recorded. Features such as joints, fractures, joint filling and other discontinuity parameters should be recorded (Appendix 3a and 3b). Cores logging should be carried out accordingly.

### P9: DRILLING & CORING




The front bedrock core sample shows a fracture infilled with calcite material.

The back bedrock core sample shows alteration, fractures and veins.

Such features should be described in order to identify potential water bearing apertures.



 <b>SNC • LAVALIN</b>	<b>PHOTOGRAPHIC REPORT</b> 2018 Groundwater Monitoring	Prepared by : Laurie Tremblay		
		Reviewed by : Denis Vachon		
	645182-3000-4EER-0001	Rev.	Date	Page
		PA	2018-12-12	3

**P9-P10: HWT (101.6 mm (4 in) I.D.) FLUSH JOINT CASING INSTALLED IN OVERBURDEN**



The two pictures show a monitoring well installation and a HWT casing. HWT casing was installed through the overburden into the bedrock to prevent the borehole from collapsing. On the right picture, the HWT casing stops below the ground level. HWT casing have to extend above ground level as on the left picture, to prevent surface water to enter the annulus space between the casing and the well.

**P11-P12: WELL SCREEN AND BOTTOM TREAD PLUG**



Prior to each monitoring well installation, well screens were inspected, prepared and numbered and set in their order of installation. The bottom plug was installed on the first screen (slot aperture is 0.254 mm (0.010 in)). Pipe centralizers were installed every three length of pipes (9.14 m (30 feet)).





**P13-P16: FOAM BRIDGE ON A RISER**




The pictures show a stainless steel riser pipe with a foam bridge. The foam bridge (88.9 mm (3-1/2 in) O.D.) on a 0,76 m (2,5 ft) long 2-inch (50.8 mm) diameter S.S. pipe was installed between the monitoring well screens and the bentonite sleeves to prevent the bentonite to seep downwards in the monitoring well screen interval. The foam bridge is 101.6 mm (4 in) long. Since the foam bridge risked to be damaged during installation, the Agnico Eagle technician added tape over the foam at monitoring well MW-IPD-01 (s).

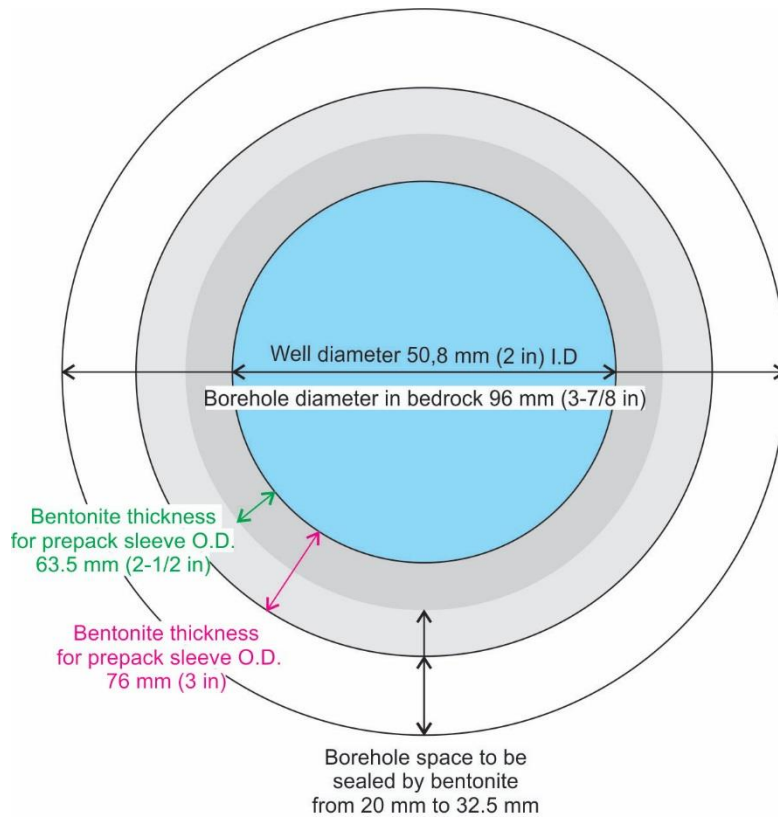


The picture shows a prepack bentonite on a well riser pipe 50.8 mm (2 in) I.D. fitted above the foam bridge. For additional protection, the Agnico Eagle field technician added a geomembrane around the foam bridge. Holes were made on both side of the geomembrane to allow water to in the well to run through while the pipes were lowered into the borehole. This was done for monitoring well installations MW-IDP-01d, MW-IDP-07 and MW-IDP-09.



 <b>SNC • LAVALIN</b>	<b>PHOTOGRAPHIC REPORT</b> 2018 Groundwater Monitoring	Prepared by : Laurie Tremblay		
		Reviewed by : Denis Vachon		
645182-3000-4EER-0001		Rev.	Date	Page
		PA	2018-12-12	5

### P17-P18: BENTONITE PREPACK VERIFICATION



The left drawing shows a scaled cross-section of the material installed in the borehole at the bentonite prepack level in the borehole (refer to Appendix 1 for monitoring well installation sketches). The right picture shows the prepack bentonite sleeve.

Prepack bentonite sections have the purpose to seal the annulus space between the borehole and the well riser pipe to isolate the well screens (refer to Appendix 1 for monitoring well installation sketches).

To verify the bentonite seal integrity, a dye tracer test is suggested. The dye tracer test can be conducted by adding a known volume and concentration of dye tracer in the monitoring well annulus (between the HWT casing and the well casing). If colored water is pumped out of the well while sampling, it could be concluded that the prepack bentonite is sealing the well screen properly.



**P19-P20: WELL RISER VERIFICATION**



2 " to 1-1/2 " connector

Above the bentonite sections, well risers pipe have a diameter of 38.1 mm (1-1/2 in) I.D.. The smaller diameter riser pipes were required to accommodate the heat trace cables installed within permafrost zone (0-40 m from ground level).

A connector is added to fit the 2 in (O.D.) riser pipe with the 1-1/2 in riser pipes.

Before installation, all well riser pipes were numbered and centralizers were installed at every three pipes.

Before the installation, ice stuck in the fitting of the well riser pipes was melted and all the pipes were verified a last time to ensure proper installation.





### P21-P22: WELL SCREEN INSTALLATION



A pipe clamp was used to hold the heavy well equipment while additional riser pipes were added and screwed on. However, the pipe clamp slightly compressed the pipes. For further well installations, adapted tools (clamps) are proposed to prevent permanent damage to well equipment.





**SNC • LAVALIN**

**PHOTOGRAPHIC REPORT**  
**2018 Groundwater Monitoring**

645182-3000-4EER-0001

Prepared by : Laurie Tremblay

Reviewed by : Denis Vachon

Rev.

Date

Page

PA

2018-12-12

8

**P23-P24: BENTONITE PREPACK INSTALLATION**



Driller assistant was standing below the drill head, in the pit, to orientate the riser pipes into the borehole.

Foam bridge and bentonite prepack installations.

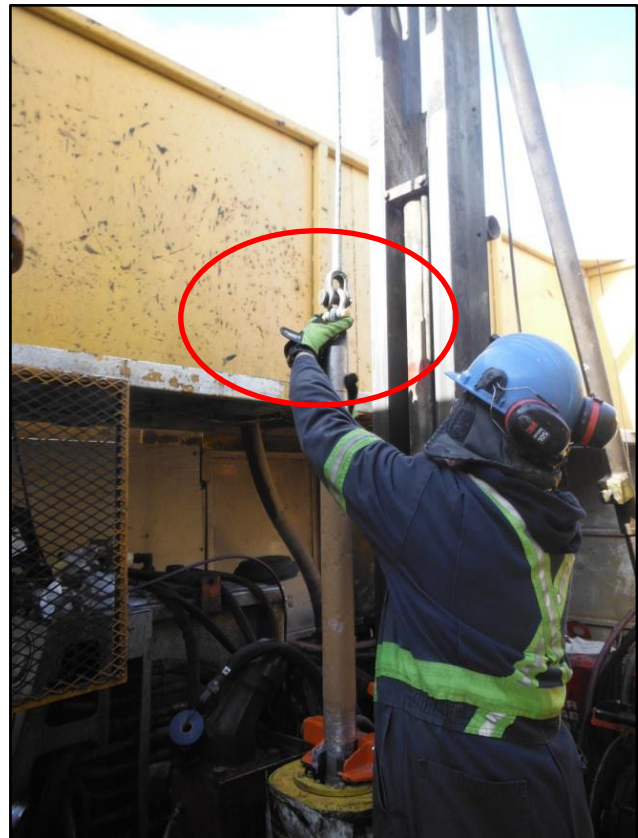




**P25-P26: PREPACK BENTONITE INSTALLATION**



A steel hoisting plug was screwed onto the well riser to lower down the monitoring well material into the borehole.





**SNC • LAVALIN**

**PHOTOGRAPHIC REPORT**  
**2018 Groundwater Monitoring**

645182-3000-4EER-0001

Prepared by : Laurie Tremblay

Reviewed by : Denis Vachon

Rev.

Date

Page

PA

2018-12-12

10

**P27-P28: WELL RISER PIPE INSTALLATION**

After the bentonite sleeves were installed, a crossover connector was added to fit 1-1/2 in (I.D.) well riser pipes. A centralizer was installed on the first riser pipe.



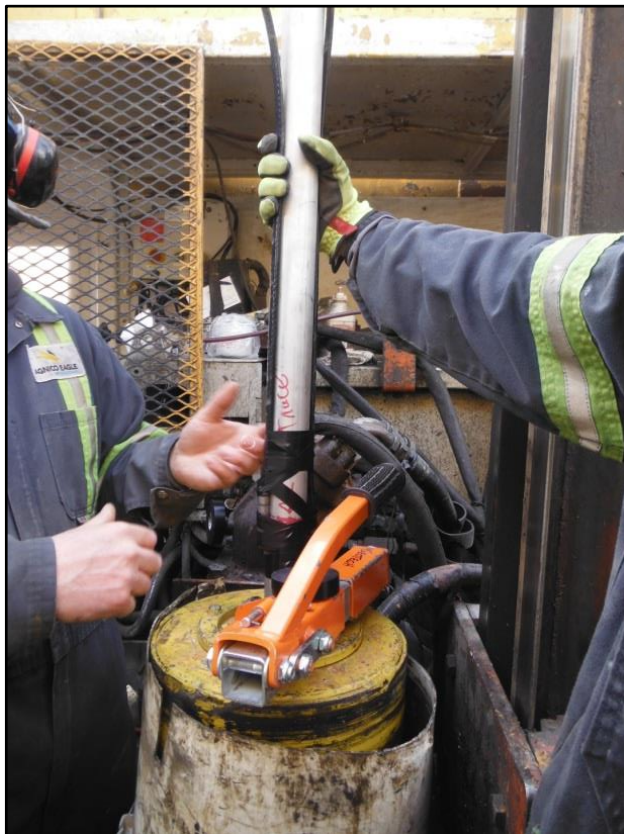
2 in to 1-1/2 in pipe  
Size crossover  
connector



**P29-P32: HEAT TRACE INSTALLATION**



Heat trace cables were installed around the 38.1 mm (1-1/2 in) I.D. well riser pipes. Heat trace cables are taped along the well riser pipes and installed meticulously around well centralizers. Heat trace cables are installed within the permafrost intervals to prevent ice bridges to form in the monitoring well.





 <b>SNC • LAVALIN</b>	<b>PHOTOGRAPHIC REPORT</b> 2018 Groundwater Monitoring		Prepared by : Laurie Tremblay	
	645182-3000-4EER-0001		Reviewed by : Denis Vachon	
	Rev.	Date	Page	
	PA	2018-12-12	12	

### P33-P35: WELL SET UP



The two pictures show a monitoring well installation and HWT casing anchor in bedrock. The left picture shows MW-IDP-07 well installed on June 2, 2018. On the right, MW-IDP-01(s) well was installed on May 28, 2018 the day before SNC professional arrival. The monitoring well installation of MW-IDP-01(s) took three hours. At MW-IDP-01s, a sea can was installed and heat trace cables were connected to an electrical panel. Heat trace cables were functional and the sea can was installed.



Heat trace cables are connected to a permanent electrical box for MW-IDP-01s and MW-IDP-01d. For MW-IDP-07 and MW-IDP-09, heat trace cables are connected temporarily on a light tower, working with fuel generator.





### P36-P37: WELL HEAD INSTALLATION AND TESTING



One well head was installed and tested at MW-16-01. The dedicated well head and pump set up are aiming to ease groundwater sampling and prevent groundwater sample cross-contamination.


All fittings were tested to verify no material was missing in prevision of the next groundwater sampling campaign planned for July 5<sup>th</sup> to 13<sup>th</sup> 2018.

Heat trace cables were installed below the well head to avoid melting of the well head. It is important to drain the water line properly, for the portion of the well not covered by heat trace cable, to avoid any water freezing and line damage.



Once the well head is closed, all sampling material is protected again cross-contamination (dust, grease, etc.) and is ready for the next sampling event.



 <b>SNC • LAVALIN</b>	<b>PHOTOGRAPHIC REPORT</b> 2018 Groundwater Monitoring	Prepared by : Laurie Tremblay Reviewed by : Denis Vachon		
		Rev.	Date	Page
645182-3000-4EER-0001		PA	2018-12-12	14


**P38-P39: WINTER INVESTIGATION OF PIT WALL SEEPAGE**



Goose Pit view looking southwest. All wall faces show frozen ice sheets at seepage areas.

View of Portage Pit E, looking west. In comparison to Goose Pit, Portage Pit E water on wall is not frozen. It will be interesting to continue sampling these Pit E walls during the next campaign, as this area was not accessible last year.




 <b>SNC • LAVALIN</b>	<b>TECHNICAL NOTE</b> 2018 Groundwater Monitoring	Prepared by : Laurie Tremblay Reviewed by : Denis Vachon		
		Rev.	Date	Page
	645182-3000-4EER-0001	00	2018-12-17	19

## APPENDIX D: COMPARATIVE TABLE AND RECOMMENDATIONS

Recommendations prior field work (made in 2017-2018)	Agnico Eagle drilling and well installation - spring 2018	Recommended corrective measures	Photo (Appendix C)
<b>Ordering and receiving equipment for well installation</b>			
Use stainless steel pipes. Purchase extra material to account for damaged or lost equipment. Use centralizer made of stainless steel.	Stainless steel pipes and centralizers were ordered as well as extra material in case of material failure or damage during shipping.	Order material ahead of time to be able to replace or return material if required.	-
Material shipped to the site must be properly packaged and inspected upon arrival. Monitoring well material made of stainless steel must be inspected for cracks and damaged threads.	All material was inspected under the supervision of Jerome Collard, an Agnico Eagle field technician. Some of the stainless steel pipes were damaged at the thread interface, the damaged pipes were identified with spray paint and machined on site to be functional.	Inspect bentonite sleeves for proper O.D. diameter and verify that the annulus space in the sleeve is free. Bentonite sleeves are packed in boxes with brown paper put on both sides to protect it. The paper may enter and remain stuck in the annulus space. A lot of brown paper pieces were found in well MW-IPD-01 (s) during purging operations.	P1
<b>Drilling operation</b>			
It was proposed that the borehole drilling for new monitoring well installations were going to be done by destructive drilling.	Rock cores were collected for the entire length of each borehole	Fractures and discontinuities are amongst the most important features for the comprehension of main groundwater flow paths. Any indication in cores about how continuous a fracture plane is should be recorded. Features such as joints, fractures, joint filling and other discontinuity parameters should be recorded (Appendix 3a and 3b). Cores should be logged from a hydrogeological point of view to target main groundwater flow zone.	P2-P8
Install a HWT flush joint casing 101.6 mm (4 in) I.D. while drilling the overburden material and anchored the casing into the bedrock located below the overburden.	A flush joint casing was installed in overburden and was anchored into the bedrock.	Flush joint casings have to extend above ground level to prevent surface water entering the annulus space between the casing and the well.	P9-P10
Temperature gauging should be conducted and logged during the drilling operation. This information is key decision parameters for heat tracing cable length and elevation of purge and sampling pumps. (Franz Environmental Inc. 2009);  Pressure and salinity parameters should be taken into consideration to define talik/permafrost zones.	Permafrost zones and monitoring well design were defined from a previous geotechnical study: SNC-Lavalin (2017) Hydrogeological Field Investigation for the in-pit tailings deposition, November 16, 2017. Available thermistor data were also used to selected screen depth interval.	There was some uncertainty regarding fractures and permeability along MW-IDP-09 borehole. The selected intervals for the well screens were not based on a packer test. Agnico Eagle had to confirm the depth to an important permeable fracture with Tetratex (specific details on North channel interception (30-40 m approx.). Well screens were installed from 60 to 80 m for this well, without any confirmation.  Proceed with a rock cores logging to verify main fracture/discontinuity along the borehole. This will allow a better understanding of groundwater flow at the MW location and precise potential flow paths.	-
Vertical well have less chances of failure. Inclination must be defined accordingly.	All boreholes were drilled at 90°	None	-
At the end of the borehole, block the drill string and perform a wet pull to remove as much drill water as possible from the borehole before it freezes to the rock surface (Pfiffner et al. 2008).	Warm water was circulated continuously through the borehole until the drill was ready for well installations. It was not possible to purge the well after drilling with the drill installation available.	Record water quantity added to the borehole and use a dye tracer with drill fluid	-
Tracer such as sodium fluorescein (Henkemans 2016) or perfluorocarbon tracer (PFT) should be added to the drilling fluid (Pfiffner et al. 2008) to identify if all drilling fluid was flushed during well purging operations. Quantity of solution added to the borehole during drilling or after should be noted. Quantity of water added during drilling should also be noted.	No solid salt was added to the borehole as recommended. However, drill fluid DD2000 was used. No tracer was used in the solution, quantity of drilling mud and water are unknown.	Perform an extensive purge at each well to remove all drilling fluids. Recording in situ parameters (ORP, conductivity, temperature, DO, pH) with a multiparameter probe while purging may help to determine if the purged water is representative of the groundwater at the well screen interval.  For future reference, use a dye tracer at a known concentration and quantities when drilling mud is added to water so that it will be easier to make sure all drilling fluid is removed before sampling the well.	-
<b>Well design and installation</b>			
Use one bottom tread plug made of stainless steel for each well	Done	None	P11-P12
Use well screen made of stainless steel 10 feet long with slot 0,010 x 6 at the exception of x 3 for Well MW-IDP-07	Done	None	P11-P12
Use a foam bridge on a well riser pipe above the well screens and below the prepack bentonite	Modifications were made to the foam bridge. Tape was added to monitoring well MW-IPD-01 (s) and a geomembrane was added over the foam at monitoring wells MW-IPD-01 (d), MW-IPD-07 and MW-IPD-09.	Use a foam bridge made for the entire riser length 0,762 m with diameters matching the borehole. (Use stainless steel collars to fix equipment on well risers located in the screens interval. As groundwater quality can be impacted by glue and tape material. Use only ASTM material not to impact groundwater quality.	P13-P16

3-1/2" Prepack bentonite section on 2" well riser pipe	Smaller 2-1/2" Prepack bentonite sections have been installed	Monitoring wells integrity will need to be tested to make sure that the bentonite seal prevents the water from the surface to infiltrate the screen area of the monitoring well. This can be done by adding a dye tracer between the HWT flush joint casing and the well casing. If colored water is coming up while sampling, the seal is not isolating the well screens properly.	P17-P18
2" stainless steel risers	Well risers pipe have 1-1/2 in diameter to accommodate space for the heat lines that are installed in the permafrost zones.	None	P19-P20
Have all monitoring well material ready prior to the monitoring well installation. Install monitoring well as soon as the borehole is completed	All material was prepared ahead of time, all parts were numbered and verified	Planned to have the proper equipment for well installations which would be adapted for the weight of the material inserted into the borehole. Requirements would be: 1) equipment that ensures well material integrity; 2) that does not cause a risk for the workers installing the well. This should be planned in advance first to prevent injuries and second so that no material is lost into the borehole or damaged during installation.  Only a clamp was available to hold the heavy well equipment down the borehole while the risers were added and screwed on to the next. The clamp compressed the pipe permanently which is a risk for the long-term well integrity.	P21-P28
Heat trace cables should be used in the permafrost interval and above prepack bentonite. Therefore, prepack bentonite has to be installed in the talik zones. Ensure that heat cables can be energized at all time, have a backup generator in case of failure.	Heat trace cables were installed at a depth of 40 m for every monitoring well. They are covering the permafrost interval and are working.	At MW-IDP-01d site, the heat trace cables end 2 m below the ground surface. The electrical cables will have to be verified in winter time to make sure that they are working under frost action (0-2 m).	P29-P35
Dedicated well head for sampling. Dedicated systems aim to ease groundwater sampling and avoid cross-contamination.	One dedicated well head was installed and tested.	None	P36-P37
Identify pit wall seepage areas (not frozen) during winter investigation to select future sampling sites on pit walls	n/a	None	P38-P39

 <b>SNC • LAVALIN</b>	<b>TECHNICAL NOTE</b> 2018 Groundwater Monitoring	Prepared by : Laurie Tremblay Reviewed by : Denis Vachon		
	645182-3000-4EER-0001	Rev.	Date	Page
		00	2018-12-17	20

## APPENDIX E: LITERATURE



# Application of statistical approaches to analyze geological, geotechnical and hydrogeological data at a fractured-rock mine site in Northern Canada

J. M. Mayer · D. M. Allen · H. D. Gibson ·  
D. C. Mackie

**Abstract** Mine site characterization often results in the acquisition of geological, geotechnical and hydrogeological data sets that are used in the mine design process but are rarely co-evaluated. For a study site in northern Canada, bivariate and multivariate (hierarchical) statistical techniques are used to evaluate empirical hydraulic conductivity estimation methods based on traditional rock mass characterisation schemes, as well as to assess the regional hydrogeological conceptual model. Bivariate techniques demonstrate that standard geotechnical measures of fracturing are poor indicators of the hydraulic potential of a rock mass at the study site. Additionally, rock-mass-permeability schemes which rely on these measures are shown to be poor predictors of hydraulic conductivity in untested areas. Multivariate techniques employing hierarchical cluster analysis of both geotechnical and geological data sets are able to identify general trends in the data. Specifically, the geological cluster analysis demonstrated spatial relationship between intrusive contacts and increased hydraulic conductivity. This suggests promise in the use of clustering methods in identifying new trends during the early stages of hydrogeological characterization.

**Keywords** Fractured rocks · Hydraulic testing · Geotechnical data · Statistical modeling · Canada

## Introduction

Groundwater can have a detrimental effect on slope/tunnel stability, increasing operating costs of both open pit and

underground mining operations (Wyllie and Mah 2004; Beale 2009). Its presence can affect the design of excavations in two important ways. First, fluid pressure within discontinuities and pore spaces reduces the effective stress leading to a reduction in shear strength (Piteau 1970). Second, depending on the groundwater conditions, inflows can occur that may lead to specific water-management requirements within excavations. Excessive inflow or high water tables may result in a loss of access to part or all of the mine, increased costs associated with blasting, wear and tear on equipment, inefficient hauling, and unsafe working conditions. Fluid pressure and saturation state may, however, be controlled by an effective dewatering/depressurization plan (Sperling 1990; Sperling et al. 1992; White et al. 2004; Rodriguez et al. 2008). If these plans are designed effectively, they may also allow for steeper pit walls leading to long-term cost savings. However, these plans can have relatively high initial capital costs, require operator commitment to be implemented effectively, and can require significant lead time to allow for proper drainage. As a result, early characterization of the hydrogeological system and identification of characteristics that may influence stability are important for proper slope design and the design of effective dewatering and depressurization systems.

Characterization of the hydrogeological regime at most hard-rock (metamorphic and igneous) mine sites is commonly characterized by fracture-controlled groundwater flow, with complex flow dynamics owing to the presence of discrete fractures, fracture and fault zones, and a low permeability rock matrix (Fetter 1994; Caine et al. 1996; Singhal and Gupta 2010). Hydraulic properties of the rock mass are found to vary in relation to the complex interplay between in-situ stress, rock matrix properties and fracture characteristics, including aperture, density, persistence, orientation, interconnectivity, fill, and roughness (Snow 1970; Witherspoon et al. 1980; Lee and Farmer 1993; Zimmerman and Bodvarsson 1996). Targeted evaluation of hydraulic properties through traditional hydraulic testing methods (e.g. pumping, injection and/or slug testing) are cost prohibitive during the early stages of mine site characterization (Bellin et al. 2011). Thus, the use of empirical methods, which can

Received: 19 September 2013 / Accepted: 3 April 2014

© Springer-Verlag Berlin Heidelberg 2014

J. M. Mayer (✉) · D. M. Allen · H. D. Gibson  
Department of Earth Sciences,  
Simon Fraser University, Burnaby, BC, Canada V5A 1S6  
e-mail: jmm6@sfu.ca

D. C. Mackie  
SRK Consulting (Canada) Inc., Vancouver, BC, Canada V6E 3X2



estimate hydraulic properties from qualitative rock-mass-characterization schemes remain enticing, due to lower costs compared to traditional methods (Gates 1997; Hsu et al. 2011).

The use of empirical methods is a common practice in the geotechnical community, with borehole logging typically conducted to characterize the block shape and size, as well as the fracture surface conditions. This is done through the use of a series of categorical descriptors using systems such as the geological strength index (GSI) or rock mass rating (RMR) (Bieniawski 1973; Hoek et al. 2002). The end result is an estimation of the rock mass strength characteristics based on degree and type of fracturing. Since, hydrogeological studies are typically piggy-backed on geotechnical investigations to reduce exploration costs, cross correlation between data sets can provide additional insights into the role of fracturing on fluid flow (Bellin et al. 2011).

The purpose of this study is twofold: First, an evaluation of empirical hydraulic conductivity estimation methods based on traditional rock-mass-characterization schemes is explored through bivariate and multivariate (hierarchical) statistical techniques. Second, the study attempts to integrate the geological, geotechnical and hydrogeological data to assess the regional hydrogeological conceptual model for a northern mine site. To the authors' knowledge, this is a novel approach to hydrogeological characterization at a mine site. Finally, recommendations are provided to improve current rock-mass-characterization schemes.

## Study site

Data for this study were collected at an undisclosed mine site located in Canada (Fig. 1). The geology of the site is characterized as a greenstone-hosted, quartz-carbonate vein, lode-gold deposit. Mineralization trends are hosted within regional antiformal and synformal folds, formed during syn- to post-peak metamorphism. Gold mineralization is considered coeval with quartz vein emplacement within the hinge zones of the regional folds. The site is cross-cut by a series of post-peak metamorphic diabase dykes with contact metamorphic haloes extending up to 20 m into the country rock. Late stage localized brittle faulting and regional shearing are observed throughout the region, with faults generally displaying dips of greater than 70°.

The general groundwater conceptual model for the site is considered unique to northern regions due to the presence of permafrost in the near surface. Frozen ground acts as an impermeable layer which restricts recharge, discharge and movement of groundwater, limiting the volume of unconsolidated material and bedrock in which groundwater may be stored (Williams 1970). Permafrost varies locally in thickness, areal extent and temperature as a result of variations in the thermal properties of the host material, climate, topography, geothermal gradient, vegetation, geology and hydrogeology. Research conducted in

unconsolidated units of the Arctic Coastal Plain and its surrounding areas has shown that the permafrost extends to depths as great as 610 m, preventing the downward percolation of groundwater from snowmelt (Williams and van Everdingen 1973). However, even in the most northern climates, permafrost is not spatially continuous. Instead, zones of unfrozen ground, referred to as taliks, may exist that have small areal extent and persist from year to year (Yershov 1996). Taliks are typically located beneath lakes and may be either open, in that they penetrate the whole permafrost stratum, or closed and isolated from the lower groundwater system. The hydrogeology of the site is generally controlled by the presence of these taliks and is considered a low flux, lake-dominated flow system, with the highest hydraulic conductivities found within the taliks (Fig. 2).

The level of the water table is found to be controlled regionally by the locations of various lakes, which are frozen over for approximately half the year. Low hydraulic conductivity and low gradients throughout the region indicate that the overall groundwater flux is minimal. Groundwater recharge is also considered minimal and assumed not to fluctuate significantly throughout the year. This is due to the taliks providing the only direct recharge routes for groundwater flow and minimal fluctuations in annual lake levels.

## Methodology

### Hydrogeological data collection

Hydraulic conductivity data were collected using a packer-isolation, injection testing methodology. Tests were conducted synchronously with active drilling and guided by onsite hydrogeologists specifying test zone intervals during the drilling process. Intervals were selected to facilitate a random sampling of various geological features including, stratigraphic units, lithologic contacts and faults. While an attempt was made to test as many zones as possible, the limited number of samples means that some features were likely missed during the characterization. Although this is not ideal, it is common during such characterization studies, given the limited budget. Testing was conducted by first pulling back drill rods and exposing desired intervals. Next, a single hydraulic packer was used to seal the desired test interval below the drill rods.

Test zones varied between 6.0 and 108.0 m, with an average length of 48.6 m. Depths varied between 12.5 m below ground surface (mbgs) and 489.0 mbgs with an average depth of 175.5 mbgs. Boreholes were inclined between approx. 60 and 80°; however, presented depths have been converted to mbgs. Boreholes were HQ-sized diamond drill rods (hole size = 96 mm). Borehole geophysics was not conducted on any of the tested boreholes. Tests were conducted both in summer and winter, with summer testing near lake boundaries and winter testing underneath the lakes since winter drilling could be carried out from atop the ice.

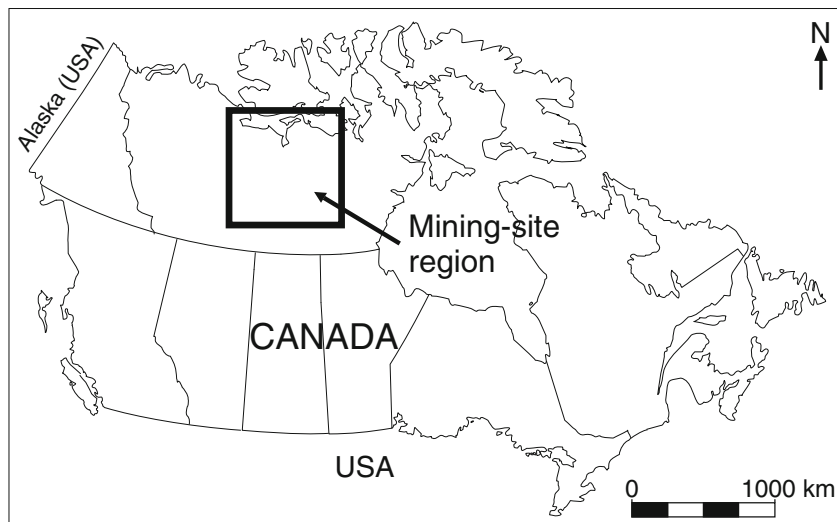


**Fig. 1** General location of mining region under study

Injection testing was conducted using the five-step Lugeon testing methodology, which is analogous to a step test (Lugeon 1933). The method involves injecting water in a series of fixed “steps” into a test zone at a specific pressures and recording the resulting flow rates once steady-state conditions have been achieved. The data collected from the Lugeon test were analyzed using the Thiem method (Singhal and Gupta 2010). A total of 43 hydraulic tests were analyzed using this method. The number of tests within each borehole varied between 1 and 5, with a total of 16 holes tested.

### Rock mass parameters

Rock-mass-classification systems have gained widespread use in geotechnical design studies, providing a powerful aid in estimating rock mass strength values (Terzaghi 1946; Lauffer 1958; Deere et al. 1967; Wickham et al. 1972; Bieniawski 1973; Barton et al. 1974). At the study

site, the modified rock mass rating (MRMR) system was used for rock mass classification (Laubscher 1975; Laubscher and Taylor 1978; Laubscher 1990; Laubscher and Jakubec 2001; Jakubec and Esterhuizen 2007). The system involves first estimating in-situ rock mass rating (RMR) values, based on current subsurface conditions, then modifying results to MRMR values based on projected future mining conditions. The current study focused on unmodified RMR values for statistical analysis, as they best reflect the current in-situ conditions under which hydraulic testing was conducted.

Unmodified RMR values range between 0 and 100 and are composed of three components: intact rock strength, fracture spacing and joint condition. Logging is conducted on a domain basis, with core visually subdivided into a series of zones with similar geomechanical characteristics. The intact rock strength (IRS) component is a measure of the uniaxial compressive strength. This parameter was largely ignored because intact rock strength is assumed to

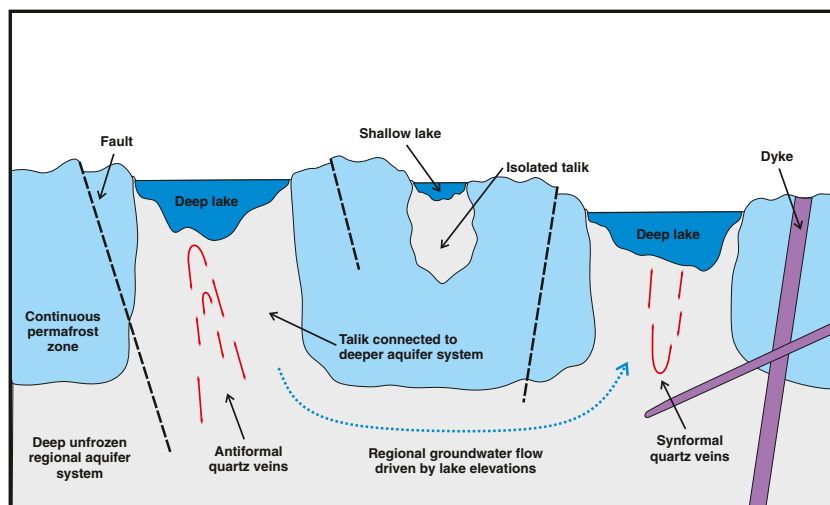


**Fig. 2** Generic, schematic regional hydrogeological conceptual model for groundwater flow at the northern Canadian mine sites

have little effect on the overall groundwater flow when compared to parameters describing the fracture state.

The fracture spacing component is a measure of the distance between all non-cemented, natural discontinuities within the rock mass. Laubscher (1990) presented two techniques to assess the effects of fracture spacing. In the first approach, fracture spacing is assessed using the rock quality designation (RQD) and fracture spacing separately. The alternative technique is to assess the relative fracture frequencies per meter of each individual fracture set. Data at the mine site were collected using the former of these two approaches.

RQD is a core recovery technique commonly employed within the mining industry, which assesses the percentage of core recovered that is bounded by discontinuities and greater than 100 mm in length compared to the total length of recovered core. The index has been in use since the mid-1960s as a measure of the rock quality (Deere and Deere 1988). The parameter is typically used in combination with either the number of joint sets (Q system) or the joint spacing (MRMR system) to estimate block size. The usefulness of block size estimation techniques in the geotechnical literature cannot be understated, as most rock-mass-classification schemes and/or failure criterion either directly or indirectly rely on block size in the determination of rock mass strength (Deere et al. 1967; Bieniawski 1973; Barton et al. 1974; Laubscher and Taylor 1978; Laubscher and Jakubec 2001; Hoek et al. 2002; Palmstrom 2005).

Fracture spacing ratings are assigned by taking into consideration the distance between all non-cemented discontinuities and the number of discontinuity sets. Fractures are considered to be any discontinuity which fully cross-cuts the borehole and may include joints, fissures, fractures, cracks, or natural breaks. The separation of mechanical and natural breaks is an important part of the overall assessment procedure as the extensive disturbance from the drilling process and core handling procedures can easily double the number of breaks within a length of drill core. If this is not taken into consideration, fracture frequencies could grossly overestimate the in-situ conditions. Bedded and/or foliated rocks are particularly prone to this, with core breaking at the surface during the inspection of the core. A hard cap of one fracture per 2.5 cm or 40 fractures per meter is typically used, as this represents the highest fracture frequency allowed in the Laubscher MRMR method. In addition, a maximum of three discontinuity sets are considered, as the method assumes that any other minor sets merely modify the shape of the block, but do not change its overall size (Laubscher 1990).

In addition to block size considerations, the Laubscher MRMR system also takes into account fracture fractional properties, through the characterization of large- and small-scale waviness, wall alteration, fill and in some cases the presence and/or absence of water along discontinuity surfaces (Laubscher 1990). The common integration of hydrogeological models or pore pressure distributions into geomechanical models has limited the usefulness of water content parameters in most rock classification systems. In addition, water content

observations can be difficult to collect or subjective when using diamond drill sampling techniques. As such, the water content parameter is typically not recorded at most mine sites, including the one used in this study. Instead, the study focused on the effects of fracture roughness and fill on rock mass permeability. For a full description of the fracture conditions parameters used in this study refer to Laubscher (1990) or Laubscher and Jakubec (2001).

In addition to the standard parameters collected for calculation of the Laubscher RMR values, additional data were collected including micro-defect intensity and presence or absence of major structures. The micro-defect intensity is defined as the intensity of alteration of the rock masses, which results in a reduction of the overall rock mass strength. Values are assigned between 0 and 3, with a value of 0 indicating un-altered rock and 3 indicating heavily altered rock. Major structures are defined as any significant feature in the core that the geotechnician determines would cause a considerable decrease in the strength of the rock mass. Major structures are further broken down into four categories, namely: broken, gouge, fractured and sheared zones.

The geotechnical logging procedure described above was carried out for all hydraulic test intervals used in this study. Data were collected using 3-m long split-tube coring techniques (triple tubes), with the exception of two boreholes, where double-tube core barrels were used. Data collection was conducted by on-site geotechnicians at the drill rigs while core was still in split tubes. The data later underwent quality assurance and quality-control checks though a visual assessment of borehole photographs to ensure that collected data matched drill core. Geotechnical parameters presented herein are averaged results across the packer test intervals. Table 1 shows a summary of the various rock mass characteristics measured in this study.

### **Permafrost-related parameter–borehole distance from lakes**

The general hydrogeological conceptual model proposes the existence of a thick permafrost zone with isolated unfrozen taliks beneath the regional lakes. Talik margins are here assumed to be near vertical, with frozen-unfrozen boundaries forming along the edges of regional lakes (Fig. 2). Based on this conceptual model, permafrost zones are assumed to be impermeable. Conceptually, isolated pockets of unfrozen ground can occur within permafrost due to brine concentration through freezing processes; however, this has not been found in tested areas of the study site (Gosink and Baker 1990).

While the conceptual model includes impermeable conditions within permafrost zones, thawing around active boreholes due to drilling processes are likely to cause a small permeable halo to form around test intervals, although the size of such a halo is uncertain, but likely of limited extent. As a result, hydraulic testing within permafrost zones is likely to show a low permeability, as opposed to impermeable conditions, when applying the Lugeon method.

**Table 1** Summary of rock mass parameters used in this study

Geotechnical parameter	Description
Rock quality designation (RQD)	The RQD was developed by Deere (1967) as a qualitative measure of the percentage of “good” quality rock within a borehole. The parameter is defined as “the percentage of intact core pieces longer than 100 mm in the total length of core”
Fracture frequency	The fracture frequency is defined as the number of discontinuities per meter which fully cross-cuts the borehole. Discontinuities included in this measurement include any joints, fissures, fractures, cracks, or natural breaks
Fracture sets	Fracture sets are defined as a group of fractures within a single borehole run which share a similar alpha angle. The alpha angle is the minimum angle between the maximum dip vector of the discontinuity and the core axis. As per the Laubscher MRMR system, a maximum of three fracture sets are recorded (Laubscher 1990)
Micro-deformational intensity	Micro-deformational intensity is a qualitative measure of the degree of alteration within the drill run that causes a reduction in the strength of the rock matrix. Values vary between 0 (unaltered) and 3 (heavily deformed)
Fracture roughness	Fracture roughness at the drill core scale is a measure of the unevenness of the fracture surfaces and tends to indicate the degree of movement that may have occurred along the fracture plane. Roughness data were collected using the International Society for Rock Mechanics scale, which varies roughness values between 1 and 9 (Barton 1978). The fracture roughness values were used in the statistical analysis by subdividing fractures into stepped, undulating and planar surfaces prior to comparisons with hydraulic conductivity estimates
Fracture fill	Fracture fill is an indication of the degree of alteration, buildup of precipitates, or gouge along fracture surfaces. Data were subdivided into four fill categories based on geotechnical logs, namely; unfilled fractures, non-softening filled fractures, softening fractures, and gouge filled fractures. ‘Softening’ filled fractures refer to soft deposits that can be chipped off of the fracture surfaces with a finger nail (e.g. clays, gypsum or fine micas), whereas, ‘non-softening’ deposits indicate harder material (e.g. calcite or quartz)

Based on the conceptual model, a spatial relationship should exist between hydraulic conductivity and borehole location relative to lake margins, with low hydraulic conductivity observed near lake boundaries. In order to test this hypothesis, the distances between test zones and lake boundaries were calculated using easting and northing locations for the midpoint of each packer test and 1:50,000 scale shapefiles of regional water bodies imported from the Natural Resources Canada online file directory (NRCAN 2011). Euclidean distance between packer tests and lake boundaries were then calculated within the software package ArcGIS (ESRI 2011).

### Permeability classification schemes

Two permeability classification schemes are explored within this study, which have been proposed to empirically estimate rock mass permeability, namely, the hydro-potential (HP) scheme of Gates (1997) and the “HC-system” of Hsu et al. (2011). These schemes attempt to rate the relative permeability of an interval of core using a simplified rock-mass-rating system. Both systems were designed for use in sedimentary rock environments, and have not been validated for other rock types. Nevertheless, given that there are few such methods, it was felt worthwhile to test the applicability of such systems in our case study.

#### HP scheme

The HP scheme proposed by Gates (1997) is based on the Q-system for geotechnical classification by Barton et al. (1974), with both systems using a similar empirical formulation. The system is based on six

parameters, which are used to define the degree of fracturing, fracture surface conditions and saturation state of the fractures. Using these parameters an HP rating is calculated by:

$$HP_{\text{rating}} = \frac{RQD}{J_n} \times \frac{J_r}{J_k \times J_{af}} \times J_w \quad (1)$$

where RQD is the rock quality designation,  $J_n$  is the fracture number,  $J_k$  is the fracture hydraulic conductivity,  $J_{af}$  is the fracture aperture and  $J_w$  is the joint water content. It should be noted that although  $J_k$  is referred to as the fracture hydraulic conductivity, the parameter is used to describe the joint infill material.

The HP scheme was originally designed to estimate rock mass hydraulic properties using outcrop data, with aperture ( $J_{af}$ ) and fracture saturation ( $J_w$ ) measured directly from the scanlines. However, for the purposes of this study, neither aperture nor fracture saturation data were available due to an inability to collect these parameters during drilling and recovery activities. As a result, a value of 1.0 was given to each of the parameters in final  $HP_{\text{rating}}$  calculations. The use of constant values should not have a significant effect on the final results, as the statistics are based on a rank-order analysis, and are therefore unaffected as the data ordering remains unchanged.

#### HC-system

An alternative to the HP scheme was devised by Hsu et al. (2011), which relies on the rock quality designation (RQD), depth, gouge content and lithology to estimate

rock mass hydraulic conductivity. Ratings for the proposed system are calculated from:

$$HC_{\text{rating}} = (1 - \text{RQD}) \times \text{DI} \times (1 - \text{GCD}) \times \text{LPI} \quad (2)$$

where RQD is the rock quality designation, DI is the depth index, GCD is the gouge content designation and LPI is the lithology permeability index. Within this system, the depth index is calculated from:

$$\text{DI} = 1 - \frac{L_c}{L_t} \quad (3)$$

where  $L_c$  is the depth to the midpoint of the hydraulic test, and  $L_t$  is the total length of the borehole. The gouge content designation is calculated from:

$$\text{GCD} = \frac{R_g}{R_t - R_s} \quad (4)$$

where  $R_g$  is the total length of gouge content,  $R_t$  is the total length of the drill run, and  $R_s$  is the total length of solid core. The lithology permeability index is a rock type specific constant used to describe the matrix permeability.

### Statistical analysis

In contrast to conventional empirically based groundwater studies, this section outlines a methodology for a statistical approach to groundwater conceptual model development. Two main statistical approaches were employed, namely bivariate analysis and multivariate (hierarchical) cluster analysis. The methods were used to determine the relationships between the various rock mass properties and hydraulic conductivity. Table 1 lists the various parameters that were analyzed. A summary of the statistical techniques is provided in Table 2.

#### Bivariate analysis

Prior to bivariate analyses, normality tests were conducted on the geotechnical parameters in order to determine if parametric or non-parametric statistical methods should be used. Normality testing was conducted using the Shapiro-Wilk's Test (Shapiro and Wilk 1965). Based on the results of the analysis, the null hypothesis, that a sample originates from a normally distributed population, was rejected for all geotechnical parameters.

As a result, Spearman's rank order correlation was used to quantify the association between the various geotechnical parameters and hydraulic conductivity. It is a non-parametric technique for measuring the statistical dependence between two variables (Spearman 1904). The method assesses how well the relationship between two variables can be described using a monotonic function.

The Spearman correlation coefficient or Spearman's rho ( $r_s$ ) is calculated by:

$$r_s = 1 - \frac{6 \sum D^2}{n(n^2 - 1)} \quad (5)$$

where  $D$  is the difference between ranks of corresponding observations and  $n$  is the number of paired observations. Similar to the Pearson's product-moment correlation, Spearman correlation coefficients of +1 and -1 are obtained when each variable is a perfect function of the other (Pearson 1896). The advantages of the technique over the Pearson's product-moment correlation is that variables do not need to follow a normal distribution, the method is not very sensitive to outliers, and it is applicable to data collected on ordinal, interval or ratio scales. In addition to the correlation coefficient, standard hypothesis testing was conducted, which tested the null hypothesis that the ranks of one variable do not covary with ranks of the other variable (McDonald 2009). Hypothesis testing was conducted using the Hammer et al. (2001) software PAST. A significance level ( $p$ -value) of 0.05 was used throughout the study. Bivariate analyses were conducted within semi-log space with hydraulic conductivity on a logarithmic scale and rock mass parameters on an arithmetic scale.

#### Un-paired group analysis

The Mann-Whitney test was used to compare tests conducted in permafrost and talik zones. The method is a non-parametric test, which assesses a null hypothesis that two data sets originate from the same population (Hammer 2011). The test involves the calculation of the U statistic:

$$U = n_1 n_2 + \frac{n_1(n_1 + 1)}{2} - T_1 \quad (6)$$

where  $n_1$  and  $n_2$  are the number of data points in the first and second sample groups, and  $T_1$  is sum of ranks of the first sample set. The U statistic varies between zero and the product of the sample size of the two data sets. Following calculation of the U statistic, results were used to test the null hypothesis against a significance level ( $p$ -value) of 0.05 within the software package PAST (Hammer et al. 2001)

#### Hierarchical cluster analysis

Cluster analysis groups similar observations within a data set (Jain et al. 1999; Jain 2010). The algorithms for conducting a cluster analysis are broadly classified into two primary groups: (1) hierarchical or agglomerative methods, and (2) partitioning methods (Kaufman and Rousseeuw 1990). For the purposes of this study,

**Table 2** Summary of statistical techniques

Statistical technique	Description
Shapiro-Wilk's test	Normality test, conducted to determine if a sample set originates from a population with a normal (Gaussian) distribution
Spearman's rank order correlation	Non-parametric measure of the correlation between two data sets, using a rank-order analysis. Values vary between -1 (strong negative correlation) and +1 (strong positive)
Mann-Whitney test	Test used to assess if two sample sets originate from the same population
Hierarchical cluster analysis	Subdivides a data set into a series of clusters based on the similarity between sample points. Used to identify board trends in the data sets

hierarchical methods were chosen as they do not require the user to pre-define a set number of clusters.

Hierarchical clustering methods work by first starting with  $n$  clusters, where  $n$  equals the number of observations (Jambu and Lebeaux 1983). Next, clusters are grouped by merging the two closest clusters based on the relative distances between them; these Euclidean distances can be thought of as the amount of separation between observations within a multi-parameter space (StatSoft 2007). The process is repeated, with each stage merging the next closest pair of clusters, until all the observations are grouped within a single cluster. Amalgamation of the clusters was done using Ward's (1963) method, which clusters observations to minimize within-group variance; this is done by minimizing the sum of squares of any two groups (Hammer 2011). The final product of the technique is a dendrogram, which is used to visually identify clusters and shows the progressive relationship among observations at increasing distances (Jain and Dubes 1988). Distances are normalized to values between 0 and 1 to give a percentage of similarity.

In this study, clusters were used to identify associations between the hydraulic conductivity and various parameters. Two cluster analyses were performed. The first (geotechnical cluster analysis) included hydraulic conductivity measurements and four key parameters assumed to influence these measurements: fracture frequency, number of major structures, depth of hydraulic test and distance from lakes.

The second cluster analysis (Geological Cluster Analysis) considered geological logs for the boreholes. The logs consisted of a simplified categorization scheme, with units categorized into broad geological categories. The first step in the cluster analysis involved converting the geological data from a nominal to binary scale needed for the cluster analysis. The conversion was done by creating a variable for each of the geologic units and assigning either a value of 1 or 0 depending on whether the particular geological unit is present (1) or not (0) within the packer test interval. Following data conversion, the cluster analysis was conducted using the geological and hydrogeological data.

All cluster analyses were conducted using the TIBCO Spotfire S+ software package (TIBCO 2010). Prior to inputting the parameters, data were normalized using a z-score transformation, in order to reduce excessive weighting of variables due to differences in measurement scales (Jain and Dubes 1988). Interpretation of the cluster analysis results was aided by summary statistics for the various clusters and box plots in order to determine which parameters were controlling the clustering algorithm.

## Results

This section provides a summary of the statistical techniques applied to the study site. Techniques were applied to a total of 43 packer tests conducted within 16 boreholes. Hydraulic conductivity estimates were found to vary between  $4.8 \times 10^{-11}$  and  $2.4 \times 10^{-7}$  m/s, with a geometric mean of  $1.6 \times 10^{-9}$  m/s. Analysis of test interval size indicates that it does not have a significant influence on the results (regression coefficient = -0.29). Depth of the test interval shows a similar trend with a correlation coefficient of -0.28. Bivariate analyses are conducted using spatially averaged data (e.g. hydraulic conductivity, RQD, etc.), as geotechnical data are commonly collected in this manner at mine sites.

### Bivariate analysis

#### General geotechnical parameters

The results of the Spearman analysis indicate a weak to non-existent correlation between the hydraulic conductivity and commonly collected geotechnical parameters: RQD, fracture frequency, number of fracture sets and micro-deformational intensity (Fig. 3). The strongest relationship is observed with fracture frequency; however, the correlation is weak with a Spearman coefficient of 0.33. The results are consistent with other studies, suggesting that other parameters, e.g. aperture, may have more control on the hydraulic conductivity (Romm 1966; Hamm et al. 2007; Singhal and Gupta 2010).

The overall poor correlation between the fracture frequency and hydraulic conductivity may be the result of the inability to distinguish transmissive and non-transmissive fractures. Morin et al. (1997) showed only approximately 18 % of fractures within a fractured rock aquifer is associated with fluid flow. The implication for this study is that the frequency of transmissive fractures is likely only a small percentage of the total fracture frequency, with the ratio of transmissive to total fractures likely varying between test zones.

#### Fracture roughness

Regression analysis of fracture roughness data indicates that no statistically significant correlation exists with either the stepped or undulating fractures. However, a weak positive correlation is found between the planar fractures and hydraulic conductivity (Table 3). The higher

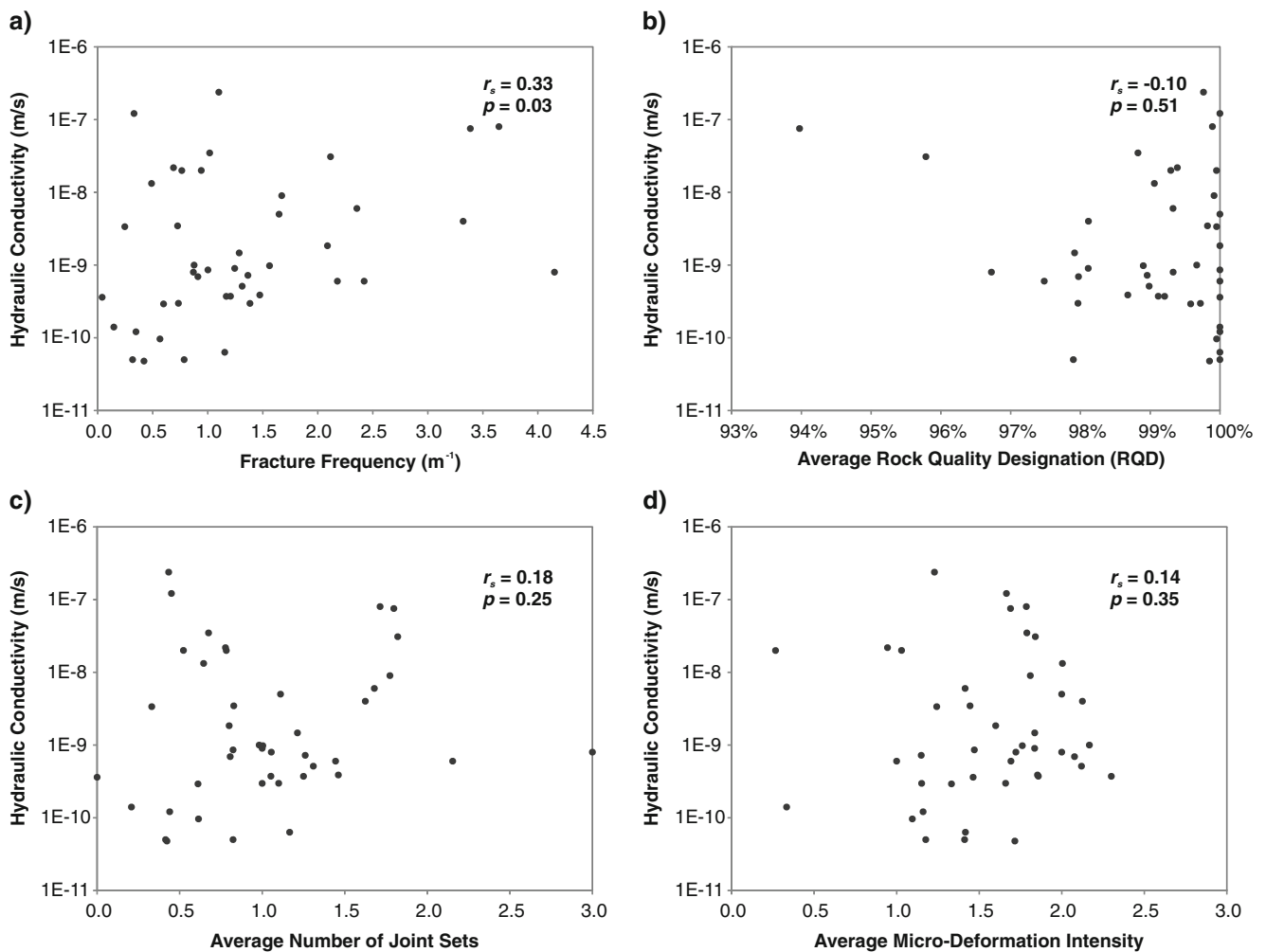


Fig. 3 Bivariate analysis of general geotechnical parameters

correlation coefficients calculated for the planar fracture surfaces compared to the stepped and undulating fracture surfaces indicate that fluid flow is likely restricted along fractures with rough surfaces and is more easily facilitated along smooth walled fractures. In concept, this is likely due to flow within fractures with rougher surfaces either being forced to flow in a more channelized manner, or exhibiting more turbulent behaviour (Romm 1966; Singhal and Gupta 2010).

#### Fracture fill

Regression analysis of fracture fill conditions indicates a weak to moderate, statistically significant correlation between unfilled fractures and hydraulic conductivity (Table 4). This is consistent with other studies which have observed a positive correlation between unfilled

fractures and increased hydraulic conductivity (Banks et al. 1992, 1994). The same correlation is not observed between the other fill categories.

#### Distance from lakes

Mann-Whitney analysis of the data sets from talik and permafrost zones suggests that the two groups originate from independent populations ( $p$ -value=0.01). This is consistent with the conceptual model, which predicts lower hydraulic conductivities beyond lake boundaries. However, further exploration of the data indicates that tests performed within the assumed permafrost regions cluster in areas of low fracture frequencies (Fig. 4). Therefore, the observed low hydraulic conductivity values may actually reflect a lack of permeable fractures within the test zones. This trend of lower fracture frequencies

Table 3 Spearman rank-order results for fracture roughness

Parameter	$r_s$	$p$ -value
Stepped fracture frequency ( $m^{-1}$ )	0.26	0.09
Undulating fracture frequency ( $m^{-1}$ )	0.14	0.93
Planar fracture frequency ( $m^{-1}$ )	0.40	0.01

**Table 4** Spearman rank-order results for fracture fill

Parameter	$r_s$	$p$ -value
Stained and unstained fracture frequency ( $m^{-1}$ )	0.41	0.01
Non-softening fracture frequency ( $m^{-1}$ )	-0.11	0.50
Softening fracture frequency ( $m^{-1}$ )	-0.05	0.75
Gouge filled fracture frequency ( $m^{-1}$ )	0.11	0.50

away from the regional lakes may reflect a regional trend of reduced fracture development away from emplaced ore bodies, as deposits are located beneath the regional lakes.

#### Rock-mass-permeability schemes

The HC-system and HP value rock-mass-categorization schemes were designed to estimate hydraulic conductivity values using in-situ rock properties (Gates 1997; Hsu et al. 2011). However, regression analysis from this study showed no statistically significant correlations between the HC-system and hydraulic conductivity, while the HP scheme only showed a minor statistically significant correlation (Fig. 5). These results are not altogether surprising given the poor correlation between RQD and hydraulic conductivity mentioned previously, which is used by both systems as an indicator of the degree of fracturing. Moreover, both systems assume that all fractures contribute equally to the overall hydraulic properties of the rock mass, and fail to explicitly distinguish between the frequencies of permeable and impermeable fractures. Finally, both systems assume average values for fracture properties, i.e. fill, roughness, etc., instead of exploring the influence of individual fractures.

### Hierarchical cluster analysis

#### Geotechnical cluster analysis

Clusters were identified using hierarchical cluster analysis (Fig. 6a), based on a percent of similarity of 45 %.

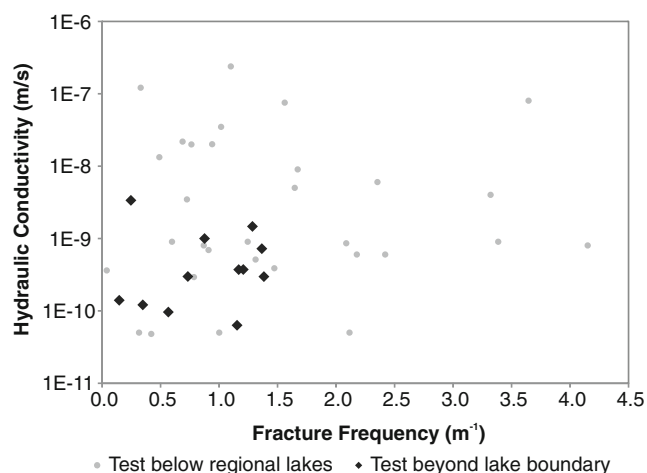


**Fig. 4** Tests conducted below and beyond lake boundaries. Tests conducted beyond lake boundaries are found to coincide with low fracture frequencies

Summary statistics for the identified clusters are presented in Fig. 6b. Clusters A and B are both associated with tests conducted in the talik zones, with sub-clustering relating to the degree of fracturing and depth of testing. Differences between the clusters are due mainly to variability in the number of major structures, with low to moderate major structure frequencies observed in cluster B and none observed in cluster A. The large variability in hydraulic conductivity observed in clusters A and B make it difficult to associate particular studied parameters with higher permeabilities. However, the similarity between the clusters suggests that the presence or absence of major structures does not limit the possible range in hydraulic conductivity.

Cluster C remains an independent outlier and is associated with the highest number of major structures per meter, suggesting that the test was likely conducted within or near a fault zone. The presence of gouge within drill core and low hydraulic conductivity suggests that, if a fault is present, it may be acting as a barrier to groundwater flow. The final cluster (D) is associated with packer tests conducted within permafrost zones, and displays an overall lower average hydraulic conductivity than preceding clusters.

Although the geotechnical cluster analysis was able to identify a number of parameters that can together relate to hydraulic conductivity, no new significant associations were found in the data that were not already evident from the bivariate analysis. For example, although data points that are located a considerable distance from regional lakes are found to cluster with the lower hydraulic conductivities, this observation had been noted previously. Therefore, although the geotechnical cluster analysis helps to confirm the results of bivariate analysis, it does not appear to provide new information.

#### Geological cluster analysis

Figure 7a shows the results of the cluster analysis conducted using the geological logs for the boreholes. The first large cluster (A) is associated with the mafic volcanic (MV), deformation zone (DZ), and late mafic intrusion (MI) units. Hydraulic conductivities vary between  $1 \times 10^{-10}$  and  $8 \times 10^{-8}$   $m/s$ , with a geometric mean of  $8 \times 10^{-10}$   $m/s$  (Fig. 7b). The cluster can be further subdivided into three subsets. Hydraulic conductivities within clusters  $A_2$  and  $A_3$  generally display below average values, suggesting lower permeability within deformation zones and mafic intrusion units. In comparison, cluster  $A_1$  displays the largest degree of variability, indicating that



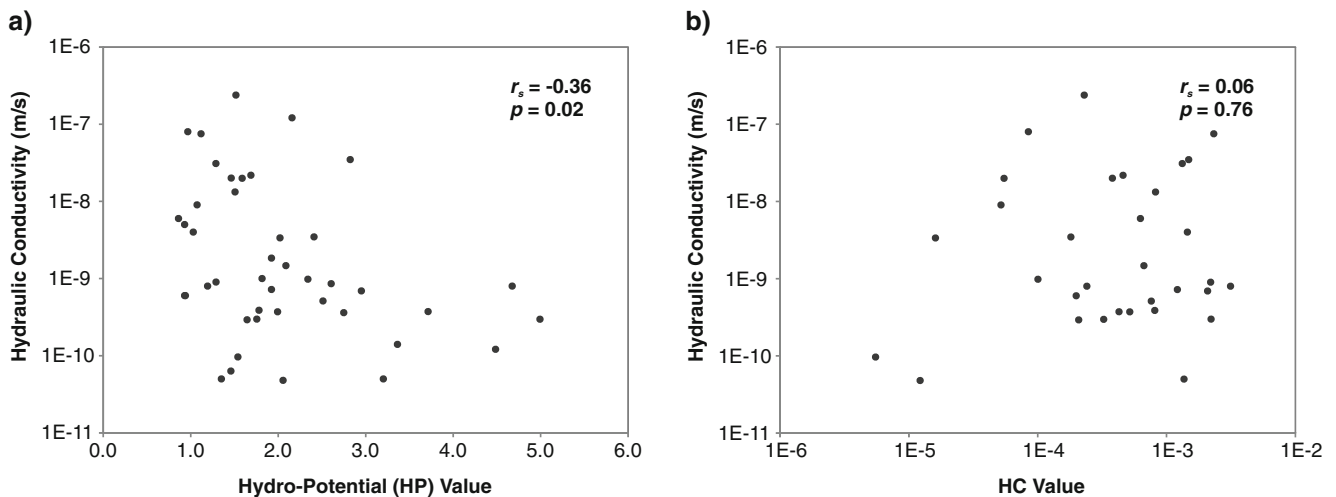


**Fig. 5** Relationship between rock-mass-permeability-classification schemes and hydraulic conductivity data: **a** HP value and **b** HC value

the presence or absence of mafic volcanic is a poor indicator of overall permeability.

Cluster B is associated with tests conducted along the boundary of the diabase dykes (DD) and MV. The hydraulic conductivity within the cluster displays a bimodal distribution, with clusters B<sub>1</sub> and B<sub>2</sub> having geometric means of  $4 \times 10^{-8}$  and  $3 \times 10^{-10}$  m/s, respectively (Fig. 7b). The differences between the two clusters are the result of differences in the permafrost conditions, as all tests within B1 occurred beneath regional lakes.

Cluster (C) is associated primarily with the interbedded volcanic and sedimentary rock (VS) units. However, other lithologic units, including the epidote-bearing gabbro (EG), quartz vein (VN), intermediate volcanic (IV), and interbedded argillite and sandstone (WA), are also present. This cluster has the lowest geometric mean hydraulic conductivity at  $5 \times 10^{-10}$  m/s, and ranges between  $5 \times 10^{-11}$  to  $3 \times 10^{-9}$  m/s (Fig. 7b). Sub-clustering within C is based on the presence or absence of the interbedded wacke and argillite unit (WA).

The presence of both the MV and interbedded volcanic and sedimentary rock (VS) units defines cluster (D), although other units are also present. In general, hydraulic conductivities within this cluster are moderate for the site, with a geometric mean of  $2 \times 10^{-9}$  m/s and a range of  $4 \times 10^{-10}$  to  $9 \times 10^{-9}$  m/s (Fig. 7b). Subdivision of the unit into sub-units contributes little to the overall understanding of the site as each of the sub-sets display similar values.

Finally, cluster (E) is defined primarily by tests performed within the interbedded wacke and argillite (WA), argillite and siltstone (SAi), and wacke and sandstone (WS) units. Hydraulic conductivity values vary between  $5 \times 10^{-11}$  and  $8 \times 10^{-8}$  m/s, with geometric mean value of  $2 \times 10^{-9}$  m/s (Fig. 7b). The cluster can be further subdivided into two subsets based on the presence (E<sub>1</sub>) or absence (E<sub>2</sub>) of the quartz vein (VN) unit, with veined units displaying a higher hydraulic conductivity of  $1 \times 10^{-8}$  m/s compared to  $4 \times 10^{-10}$  m/s.

Based on the results of the geological cluster analysis, two main trends are identified. First, a large amount of

variability exists within the MV unit, with hydraulic conductivity values ranging between  $5 \times 10^{-11}$  and  $8 \times 10^{-8}$  m/s (cluster A). Second, packer tests which straddle VN and DD boundaries are associated with higher hydraulic conductivities (sub-clusters B<sub>1</sub>, B<sub>2</sub> and E<sub>2</sub>).

## Discussion

### Usefulness of geotechnical data in hydrogeological characterization

The primary goal of the study was to assess the usefulness of cross-correlation between hydrogeological and geotechnical data sets. The initial assumption of the study was that groundwater is controlled by the fracture network, with high hydraulic conductivity features controlling the groundwater flow system within a low permeability matrix. However, the Spearman rank order correlation analysis showed only limited, statistically significant correlations between the fracture properties and hydraulic conductivity. The majority of fracture properties (i.e. fracture frequency, rock quality designation, etc.) were found to have no statistically significant correlations with hydraulic conductivity. This lack of statistical significance may be due to the small sample sizes; however, it raises the question that if groundwater flow is conceptualized as fracture-dominated in hard rock settings, why is there such a lack of evidence demonstrating this dependency? Traditional fracture network studies have generated discrete fracture networks (DFNs) which assume that most, if not all, fractures transmit fluid (Surrette and Allen 2008). However, if this were the case, a stronger statistical correlation between general fracture frequency and hydraulic conductivity would have been expected. Instead, statistically significant correlations were only observed when fractures were broken down into sub-categories. In one regard, these results are consistent with flow impeller studies which have shown that fracture flow into boreholes is limited to a small number of fractures (Morin et al. 1997). However, this raises a major question in the mine water industry, namely, given the limited number of transmissive fractures,

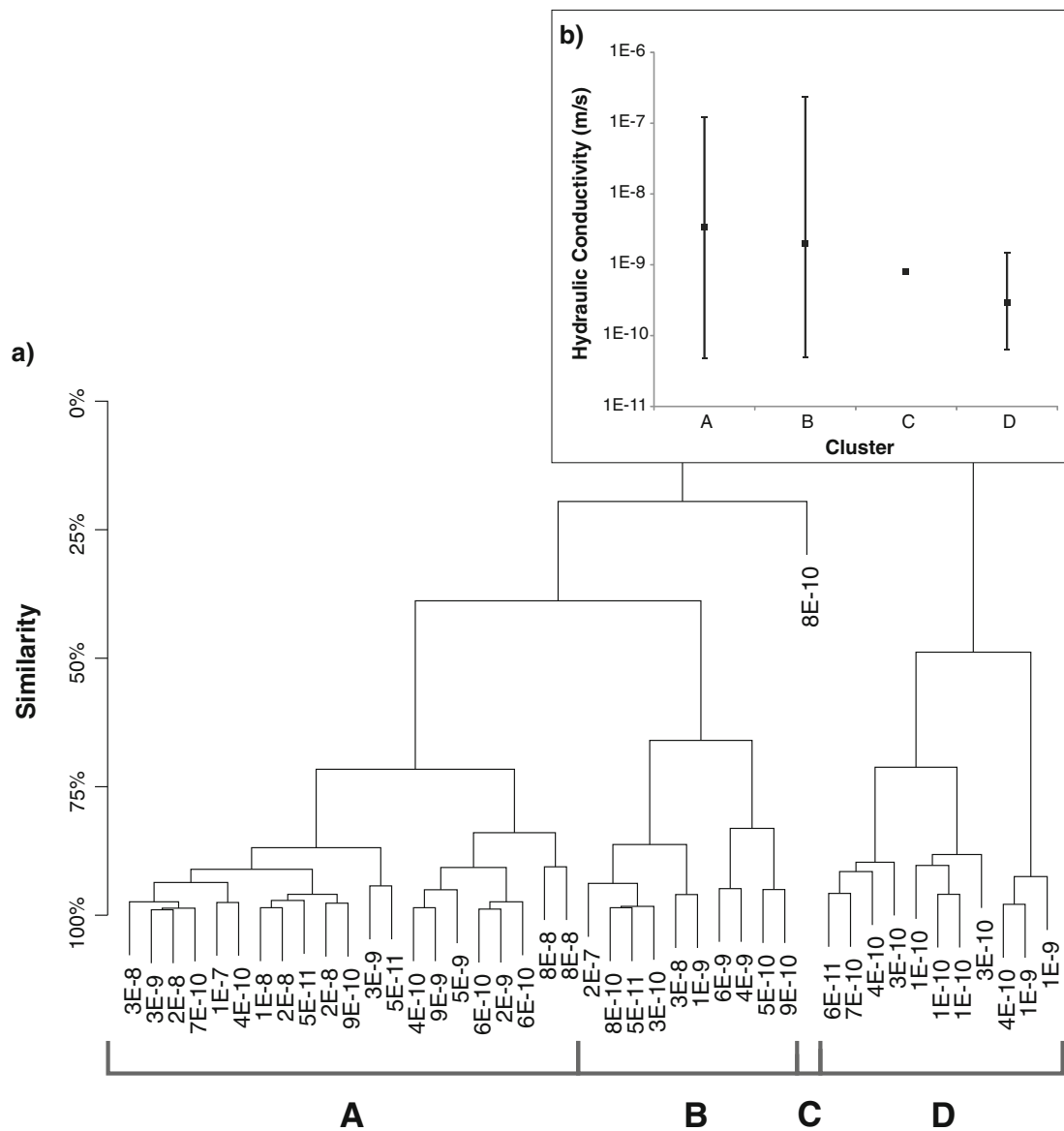


**Fig. 6** a Hierarchical cluster analysis results for select geotechnical parameters (values are hydraulic conductivity results in m/s). b Hydraulic conductivity summary for sub-clusters, geometric mean (*squares*), minimum and maximum (*bars*)

how can borehole logging techniques be adjusted to better understand subsurface fluid flow?

Traditional geotechnical logging practices attempt to characterize the block shape and size through a series of categorical descriptors of the drill core. For example, the commonly employed Hoek-Brown failure criterion currently relies on the geological strength index (GSI; Hoek et al. 2002). This parameter is a quantitative representation of the block shape and fracture conditions that compose a rock mass. The problem with this representation from a hydrogeological perspective is that instead of collecting detailed data on individual fractures, rock mass data are collected with the idea of estimating average block shapes and internal friction coefficients. If future data are to be collected with hydrogeological needs in mind then a shift needs to occur in the way data are logged. A few rock mass permeability classification schemes have been

proposed, including the HP and HC schemes (Gates 1997; Hsu et al. 2011). However, results from this research demonstrated that both systems are limited in their ability to predict hydraulic conductivity values from rock mass properties (Fig. 5). This limitation can be attributed to the selection of input parameters used in the formulation of both systems. This includes the over-reliance of RQD as an indication of the fracture state, despite its limitations in closely and widely spaced fracture systems (Palmstrom 2005). In addition, both systems assume that all fractures contribute equally to groundwater flow, despite this and other research indicating that flow is heterogeneously distributed within the fracture network (Banks et al. 1992, 1994).

The HP scheme is further limited by the fact that it was designed for use with outcrop data. As a result, the system relies on the use of fracture aperture and water content

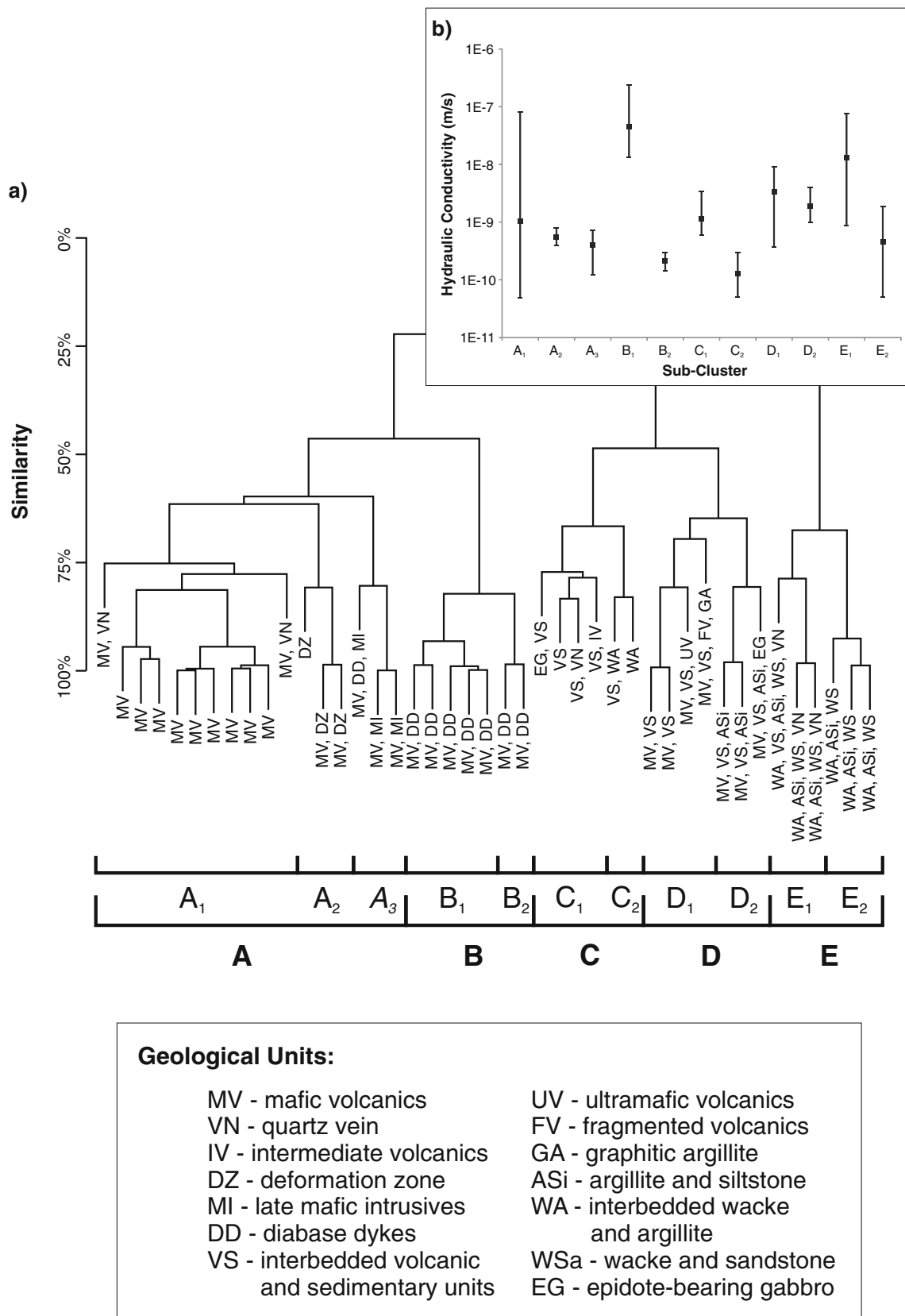


**Fig. 7** a) Hierarchical cluster analysis results for geological units. b) Hydraulic conductivity summary for sub-clusters, geometric mean (squares), minimum and maximum (bars)

parameters which are difficult to collect using traditional borehole techniques. In the case of the water content parameter, it was originally designed to indicate the amount of seepage observed at the outcrop from a given fracture set. However, due to active borehole flushing techniques during diamond drilling, it is nearly impossible to assess the degree of seepage using the original scheme devised by Gates (1997). This scheme could, however, be revised to consider factors such as the degree of staining and/or fluid alteration along joint surfaces, to give a similar indication of fluid flow, provided future projects wish to use the scheme for rock mass classification.

In the case of the fracture aperture parameter, used in the HP scheme, the variable is currently difficult to collect given modern diamond drilling techniques and collection methodologies. As a result, any use of the scheme requires a constant value to be used. However, with further development and increased use of televiwer technology it is likely that this parameter will be collected on a more regular basis at mine sites. Although televiwer aperture readings can be dubious due to in-situ rock mass disturbance around boreholes, the collected information is still likely better than the alternative of having no information. Incorporation of this parameter into the HP scheme should also be altered to better reflect the non-linear dependency between hydraulic conductivity and aperture, as described by the cubic law (Witherspoon et al. 1980).

Additional limitations also exist within the HC-system, as it fails to take into consideration variations in fracture conditions by only considering a total gouge content within a given test interval. While the gouge content is surely an important factor, other types of fracture fill can play an important role in fluid flow. This was outlined in the bivariate analysis by the increases in correlation coefficients with unfilled and planar fractures compared to total fracture frequencies. In addition, secondary fracture features such as persistence and aperture undoubtedly play an important role in the overall fluid flow characteristics and need to be taken into consideration in any rock mass permeability scheme.

Although both the HC and HP schemes present a formal methodology for the classification of rock mass properties and estimation of fluid flow characteristics, both methods are limited in their ability to empirically estimate hydraulic conductivity values. The bivariate analyses presented in this study have shown the limitations of the methodologies when applied to rock masses not originally considered when these techniques were first formulated. Instead, a new system needs to be developed which takes into consideration the shortcomings of these methods, and presents a formal methodology for rock mass classification within a hydrogeological framework. Although this is beyond the scope of this research, a number of propositions are put forth, upon which any new rock mass permeability classification scheme could be based.

First, on-site detailed descriptions of joint surface conditions should be conducted by personnel familiar with hydrogeological characterization, with the aim of identifying possible flow conduits. Data from this research

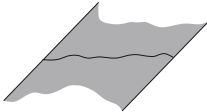
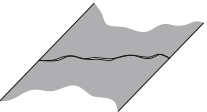
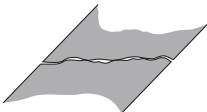
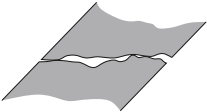
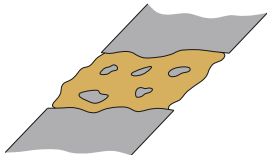
has confirmed results from previous researchers (Banks et al. 1992, 1994; Morin et al. 1997; Sausse and Genter 2005) that fracture flow is not homogeneously distributed throughout the fracture network, but instead occurs preferentially along a small number of discrete features. Therefore, it is important for any rock-mass-permeability scheme to have a way of classifying fractures based on their likelihood of fluid transmission. This should involve detailing the degree of staining/infill on any given fracture, as well as looking at the “freshness” of the fracture surface or how weathered the surface appears. This identification should be conducted by qualified personnel to ensure consistency across, as well as between sites.

Second, an indication of how continuous the core is across a fracture plane should be recorded; such an indicator would represent how well two pieces of core match-up across a given fracture plane (Fig. 8). Where the core continuity across the plane is high, it can be assumed that the in-situ fracture likely has a low aperture and, hence, poor ability to transmit fluid, whereas a poor core continuity would indicate a higher in-situ aperture. Although this is a qualitative approach and not a direct measure of aperture, it is likely to be the best method of estimation using traditional borehole collection methods. The advent of increased televiwer use in the mining industry may make this parameter obsolete; however, until such time, a core continuity factor should be implemented in rock characterization studies. As a result, it is proposed that any scheme should collect these data in a similar fashion to that shown in Fig. 8.

Finally, a far more detailed means of describing fault zone characteristics in relation to fluid flow properties is required. The presence of barrier and/or conduit type faults is often very important for mining activity, as faults either act as major inflow centers or compartmentalize and restrict dewatering efforts and can lead to high pore pressure gradients (Caine et al. 1996; Goodwin et al. 1999; Faulkner et al. 2010). Characterization efforts are further burdened by the difficulty in identifying faults during active drilling, landing packer testing equipment within the specified zone and orientation issues associated with explicitly testing either core and/or damage zones (Anderson 2006; Benedek et al. 2009). For these reasons, it is important to develop a characterization scheme which can be used by the hydrogeological, geotechnical and structural geology communities, which collects the necessary information for hydrogeologists to make educated approximations of fault zone characteristics so they can be categorized as either barrier and/or conduit type features. For this to happen, a synergy needs to evolve between these three communities, with all parties involved understanding the requirements and limitations of the other disciplines.

### **Assessment of the hydrogeological conceptual model**

The second goal of the study was to advance the understanding of the hydrogeological conceptual model

ID	Description	Figure
Fully Connected	Fracture is fully connected along borehole trace with no observable aperture / gap between fracture planes	
Minor Non-Continuity	Fracture displays minor non-continuity along borehole trace (<1 mm)	
Moderate Non-Continuity	Fracture displays moderate non-continuity along borehole trace (1 - 3 mm)	
Major Non-Continuity	Fracture displays major non-continuity along borehole trace (3 - 10 mm)	
Displaced	Fracture planes fully displaced with either rubble and/or gouge between surfaces (>10 mm)	

**Fig. 8** Proposed categorization scheme for core continuity

at the study site using a statistical approach. Such an approach differs from traditional site characterization methods which are empirically based. While the approach did not change the general overarching conceptual model, it did refine it and provide additional evidence for a number of its characteristics. First, the approach demonstrated a relationship between hydraulic conductivity and distance from lake boundaries in both the bivariate and cluster analysis, suggesting that the presence or absence of permafrost is an important factor effecting groundwater flow. The bivariate analysis indicated that the association may be complicated by the additional observed relationship of low fracture frequencies away from ore bodies; however, later thermistor string installations have confirmed freezing conditions exist beyond lake boundaries confirming initial permafrost conceptual models. Given this association, future inflow predictions will need to take into consideration the presence of permafrost, as well as the possibility for higher than predicted hydraulic conductivities, due to sub-surface thaw near mine installations.

The second major advance in conceptual model understanding was achieved through the geological cluster analysis. Prior to the study, no direct relationship had been observed between hydraulic conductivity and lithology. However, results from the cluster analyses suggest an association between higher than average hydraulic conductivities and intrusive contacts. The first of these intrusive contacts, diabase dykes, were observed to be associated with a zone of increased vug development within bounding mafic units, suggesting increased porosity and likely increased permeability along contacts. These results suggest that dykes are functioning as a conduit-barrier type feature (Caine et al. 1996), which could limit dewatering/depressurization efforts due to compartmentalization effects (Beale 2009).

The second intrusive contact identified in the cluster analysis to be associated with high hydraulic conductivity was the quartz vein unit. Quartz veins at the site are known to be associated with central anticlinal/synclinal structures. Given the increased propensity of extensional features within the anticlinal/synclinal hinge zones and

brittle nature of the quartz material itself, it is possible that increase flow rates are due to increased fracturing in, and around, quartz vein material. However, without further testing, the exact location of higher permeability structures is uncertain, and the association between higher hydraulic conductivity values and quartz veining is considered speculative.

Finally, the analysis technique was unable to attribute general flow characteristics to the regional faults; with the geotechnical cluster analysis unable to differentiate significant variations between tests conducted in the presence or absence of major structures. This inability in identifying trends is partially due to limitations in the data set, as most faults have only a single hydraulic conductivity estimate, which makes the extrapolation of results to overall fault behaviour questionable. In addition, the heterogeneous nature of faulting makes it difficult to determine if tests reflect either core and/or damage zone hydraulic conductivities.

## Conclusions

This study employed a holistic approach to hydrogeological characterization which incorporated hydrogeological, geotechnical and geological data. The study tested both bivariate and multivariate statistical techniques to explore the cross-correlations between the data sets, and aimed to assess the conceptual groundwater flow model for a northern mine site. The results of the study demonstrate that:

- Standard geotechnical measures of the degree of fractures, such as the RQD, are poor indicators of the hydraulic conductivity potential of a rock mass at the study site. None of the standard geotechnical parameters tested were found to have a Spearman correlation coefficient greater than 0.33.
- Although correlations were weak, and unable to be used for prediction, a stronger correlation with hydraulic conductivity was observed between unfilled and smooth fractures compared to filled and rough fractures. This suggests preferential fluid flow within the fracture network, which is consistent with other researchers (Morin et al. 1997; Banks et al. 1992, 1994).
- Evaluation of the HC-system and HP value rock-mass-permeability systems showed limited to no statistically significant correlations between either system and hydraulic conductivity at the study site. These results suggest that caution should be used when applying the designed systems at other sites, as estimated hydraulic conductivity values may not be representative of actual in-situ conditions.
- Comparisons between the geotechnical and hydrogeological data sets using hierarchical cluster analysis showed no new trends that had not already been previously noted in the bivariate analysis. This suggests that while cluster analysis may be useful

during early stages of trend analysis, it is limited in identifying new trends after a site has been previously characterized.

- Hierarchical cluster analysis between the geological and hydrogeological data sets was able to identify a number of general trends, including an association between quartz veining and diabase dyke contacts with higher than average hydraulic conductivities.

**Acknowledgements** This research was supported by Simon Fraser University through an Undergraduate Summer Research Award to John Mayer, and the Natural Sciences and Engineering Research Council of Canada through Discovery Grants held by Diana Allen and Dan Gibson. The authors also acknowledge SRK Consulting Ltd. for provision of the data, and Dan Mackie for his review of earlier drafts of this paper. The authors also thank the associate editor and the three anonymous reviewers for their helpful comments.

## References

- Anderson EI (2006) Analytical solutions for flow to a well through a fault. *Adv Water Resour* 29:1790–1803
- Banks D, Solbjørg ML, Rohr-Torp E (1992) Permeability of fracture zones in a Precambrian granite. *Q J Eng Geol* 25:377–388
- Banks D, Rohr-Torp E, Skarphagen H (1994) Groundwater resource in hard rock: experiences from the Hvaler study, southeastern Norway. *Appl Hydrogeol* 2:33–42
- Barton N (1978) Suggested methods for the quantitative description of discontinuities in rock masses. *Int J Rock Mech Min Sci Geomech Abstr* 15:319–368
- Barton N, Lien R, Lunde J (1974) Engineering classification of rock masses for the design of tunnel support. *Rock Mech* 6:189–236
- Beale G (2009) Hydrogeological model. In: Read J, Stacey P (eds) *Guidelines for open pit slope design*. CSIRO, Collingwood, Australia, pp 141–200
- Bellin J, Mohr P, Rex A (2011) Integrated geotechnical-hydrogeological field programs in open-pit mining—a win-win situation? In: Eberhard E, Stead D (eds) *Slope stability 2011*. Proceedings of the International Symposium on Slope Stability in Open Pit Mining and Civil Engineering, Vancouver, Canada, September 18–21, p 10
- Benedek K, Bóthi Z, Mező G et al (2009) Compartmented flow at the Bataapáti site in Hungary. *Hydrogeol J* 17:1219–1232
- Bieniawski Z (1973) Engineering classification of jointed rock masses. *Trans S Afr Inst Civ Eng* 15:335–344
- Caine JS, Evans JP, Forster CB (1996) Fault zone architecture and permeability structure. *Geology* 11:1025–1028
- Deere DU, Deere DW (1988) The rock quality designation (RQD) index in practice. In: Kirkaldie L (ed) *Rock classification systems for engineering purposes*. ASTM, Philadelphia, PA, pp 91–101
- Deere DU, Hendron AJ, Patton FD, Cording EJ (1967) Design of surface and near-surface construction in rock. In: Fairhurst C (ed) *Failure and breakage of rock—eighth symposium on rock mechanics—1967*, Society of Mining Engineers of AIME, New York, pp 237–302. <http://www.onemine.org/search/summary.cfm/Design-Of-Surface-And-NearSurface-Construction-In-Rock?d=174A9CE20480751F4F63C474CD800A9E502BBE33C08F195B90ABB48709F7278331300>
- ESRI (Environmental Systems Research Institute) (2011) *ArcMap 9.2*. ESRI, Redlands, CA
- Faulkner DR, Jackson CAL, Lunn RJ et al (2010) A review of recent developments concerning the structure, mechanics and fluid flow properties of fault zones. *J Struct Geol* 32:1557–1575
- Fetter C (1994) *Applied hydrogeology*, 4th edn. Prentice Hall, Upper Saddle River, NJ, 598 pp

- Gates WC (1997) The hydro-potential (HP) value; a rock classification technique for evaluation of the ground-water potential in fractured bedrock. *Environ Eng Geosci* 2:251–267
- Goodwin LB, Mozley PS, Moore JS et al (1999) Introduction. In: Haneberg WC, Mozley PS, Moore JS et al (eds) *Faults and subsurface fluid flow in the shallow crust*. American Geophysics Union, Washington, DC, pp 1–5
- Gosink JP, Baker GC (1990) Salt fingering in subsea permafrost: some stability and energy considerations. *J Geophys Res* 95:9575–9583
- Hamm S, Kim M, Cheong J et al (2007) Relationship between hydraulic conductivity and fracture properties estimated from packer tests and borehole data in a fractured granite. *Eng Geol* 92:73–87
- Hammer O (2011) PAST: paleontological statistics. Reference Manager, University of Oslo, Oslo, Norway, 284 pp
- Hammer Ø, Harper DA, Ryan PD (2001) PAST: paleontological statistics software package for education and data analysis. *Palaeontol Electron* 4:1–9
- Hoek E, Carranza-Torres C, Corkum B (2002) Hoek-Brown failure criterion–2002 edition. In: Hammah R (ed) *NARMS-TAC 2002*. Proceedings of the 5th North American Rock Mechanics Symposium and the 17th Tunnelling Association of Canada Conference, Society of Mining Engineers of AIME, New York, pp 267–273. [http://books.google.ca/books/about/NARMS\\_TAC\\_2002.html?id=J8rzAAAAMAAJ&redir\\_esc=y](http://books.google.ca/books/about/NARMS_TAC_2002.html?id=J8rzAAAAMAAJ&redir_esc=y) or <https://www.rocsience.com/hoek/references/H2002.pdf>
- Hsu S, Lo H, Chi S et al (2011) Rock mass hydraulic conductivity estimated by two empirical models. In: Dikinya O (ed) *Developments in hydraulic conductivity research*. InTech, New York, pp 134–158
- Jain AK (2010) Data clustering: 50 years beyond K-means. *Pattern Recogn Lett* 31:651–666
- Jain AK, Dubes RC (1988) *Algorithms for clustering data*. Prentice Hall, Englewood Cliffs, NJ, 320 pp
- Jain AK, Murty MN, Flynn PJ (1999) Data clustering: a review. *ACM Comput Surv* 31:264–323
- Jakubec J, Esterhuizen GS (2007) Use of the mining rock mass rating (MRMR) classification: industry experience. In: Mark C, Pakalnis R, Tuchman RJ (eds) *Proceedings International Workshop on Rock Mass Classification in Underground Mining*, vol. 9498. National Institute for Occupational Safety and Health Information Circular (IC), Vancouver, BC, pp 413–421. <http://stacks.cdc.gov/view/cdc/8482>
- Jambu M, Lebeaux MO (1983) *Cluster analysis and data analysis*. North-Holland, New York, 898 pp
- Kaufman L, Rousseeuw PJ (1990) *Finding groups in data: an introduction to cluster analysis*. Wiley, New York, 342 p
- Laubscher D (1975) Class distinction in rock masses. *Coal Gold Base Min S Afr* 23:37–50
- Laubscher D (1990) A geomechanics classification system for the rating of rock mass in mine design. *J S Afr Inst Metall* 90:257–273
- Laubscher D, Jakubec J (2001) The MRMR rock mass classification for jointed rock masses. In: Hustrulid WA, Bullock RL (eds) *Underground mining methods: engineering fundamentals and international case studies*, Society of Mining Metallurgy and Exploration, SMME, pp 475–481. <http://www.amazon.ca/Underground-Mining-Methods-Fundamentals-International/dp/0873351932>
- Laubscher D, Taylor H (1978) The importance of geomechanics classification of jointed rock masses in mining operations In: Bieniawski ZT (ed) *Proc Symp Exploration Rock Eng*, vol 1. Balkema, Cape Town, pp 119–128
- Lauffer H (1958) *Gebirgsklassifizierung für den stollenbau [Rock mass classification for tunneling]*. *Geol Bauwes* 24:46–51
- Lee C, Farmer IW (1993) *Fluid flow in discontinuous rocks*. Chapman and Hall, London, 169 pp
- Lugeon M (1933) *Barrages et géologie [Dams and geology]*. Dunoid, Paris, 138 pp
- McDonald JH (2009) *Handbook of biological statistics*, 2nd edn. Sparky House, Baltimore, MD, 313 pp
- Morin RH, Carleton GB, Poirier S (1997) *Fractured-aquifer hydrogeology from geophysical logs: the Passaic Formation*, New Jersey. *Ground Water* 35:328–339
- NRCAN (2011) *GeoGratis 1:50000*. Available <http://geogratis.cgdi.gc.ca/>. Accessed 3 March 2011
- Palmstrom A (2005) Measurements of and correlations between block size and rock quality designation (RQD). *Tunn Undergr Space Technol* 20:363–377
- Pearson K (1896) *Mathematical contributions to the theory of evolution. III. Regression, heredity and panmixia*. *Philos Trans R Soc Lond A* 187:253–318
- Piteau DR (1970) Geological factors significant to the stability of slopes cut in rock. In: Van Rensburg PWJ (ed) *Proc Symp Plan Open Pit Min*, Johannesburg, Balkema, Cape Town, pp 33–53
- Rodriguez R, Aunzo Z, Kote J, Gumo S (2008) Depressurization as a strategy for mining ore bodies with an active geothermal system. *Proceedings of the Thirty-Third Workshop on Geothermal Reservoir Engineering*, Stanford, California, January 28–30, p 5 [https://pangea.stanford.edu/ERE/db/IGAstandard/record\\_detail.php?id=5283](https://pangea.stanford.edu/ERE/db/IGAstandard/record_detail.php?id=5283)
- Romm ES (1966) *Flow characteristics of fractured rocks (in Russian)*. Nedra, Moscow, 283 pp
- Sausse J, Genter A (2005) Types of permeable fractures in granite. *Petrophysical Properties of Crystalline Rocks*. Geological Society, London, Special Publications, vol. 240, pp 1–14 <http://sp.lyellcollection.org/content/240/1/1.short#cite-by>
- Shapiro SS, Wilk MB (1965) An analysis of variance test for normality (complete samples). *Biometrika* 52:591–611
- Singhal B, Gupta RP (2010) *Applied hydrogeology of fractured rocks*, 2nd edn. Springer, New York, 408 pp
- Snow DT (1970) The frequency and apertures of fractures in rock. *Int J Rock Mech Min Sci Geomech Abstr* 7:23–40
- Spearman C (1904) The proof and measurement of association between two things. *Am J Psychol* 15:72–101
- Sperling T (1990) *Risk-cost-benefit framework for the design of dewatering systems in open pit mines*. PhD Thesis, University of British Columbia, Vancouver, Canada, 319 pp
- Sperling T, Freeze RA, Massmann J et al (1992) Hydrogeological decision analysis: 3. application to design of a ground-water control system at an open pit mine. *Ground Water* 30:376–389
- StatSoft I (2007) *Electronic statistics textbook*. StatSoft, Tulsa, USA. Available <http://www.statsoft.com/textbook/>. Accessed 1 February 2011
- Surette M, Allen DM (2008) Quantifying heterogeneity in fractured sedimentary rock using a hydrostructural domain approach. *Geol Soc Am Bull* 120:225–237
- Terzaghi KC (1946) *Introduction to tunnel supports*. In: Proctor RV, White TL (eds) *Rock tunneling with steel supports: with an introduction to Tunnel Geology, Commercial Shearing and Stamping Company, Youngstown, USA*, pp 17–99 <http://www.amazon.com/TUNNELING-SUPPORTS-introduction-Tunnel-Geology/dp/B000PS32N4>
- TIBCO (2010) *Spotfire S+ (version 8.2)*, Somerville, USA, <https://docs.tibco.com/products/tibco-spotfire-s-8-2-0>
- Ward JH Jr (1963) Hierarchical grouping to optimize an objective function. *J Am Stat Assoc* 58:236–244
- White SP, Ashley L, Bixley PF et al (2004) Modeling the dewatering and depressurization of the Lihir open-pit gold mine, Papua New Guinea. *Geothermics* 33:443–456
- Wickham GE, Tiedemann HR, Skinner EH (1972) Support determinations based on geologic predictions. In: Lane KS, Garfield LA (eds) *Proc N Am Rapid Excav Tunnelling*, Chicago. *Soc Min Eng Am Inst Min Metall Petrol Eng*, New York, pp 43–64
- Williams JR (1970) *Groundwater in the permafrost regions of Alaska*. <http://pubs.usgs.gov/pp/0696/report.pdf>
- Williams JR, Van Everdingen R (1973) *Groundwater investigations in permafrost regions of North America: a review*. *Permafrost North American Contribution 2nd International Permafrost Conference*, National Academy of Sciences, Washington, DC, Yakutsk, USST. <http://books.google.ca/books?hl=en&lr=&id=M4SvF9Qax7EC&oi=fnd&pg=PA435&dq=Groundwater+investigations+in+permafrost+regions+of+North+>

- [America:+a+review&ots=gqCyiLzGSO&sig=ntyc8xbfcm0nkE  
CaKHwSPjwmvo#v=onepage&q=Groundwater%  
20investigations%20in%20permafrost%20regions%20of%  
20North%20America%3A%20a%20review&f=false](#)
- Witherspoon P, Wang J, Iwai K et al (1980) Validity of cubic law for fluid flow in a deformable rock fracture. *Water Resour Res* 16:1016–1024
- Wyllie DC, Mah CW (2004) *Rock slope engineering: civil and mining*, 4th edn. Taylor and Francis, New York, 431 pp
- Yershov ED (1996) *General geocryology*. Cambridge University Press, Cambridge, UK, 585 pp
- Zimmerman RW, Bodvarsson GS (1996) Hydraulic conductivity of rock fractures. *Transp Porous Media* 23:1–30



## 2.1 Introduction

From the hydrogeological point of view, fractures and discontinuities are amongst the most important of geological structures. Most rocks possess fractures and other discontinuities (Fig. 2.1) which facilitate storage and movement of fluids through them. On the other hand, some discontinuities, e.g. faults and dykes may also act as barriers to water flow. Porosity, permeability and groundwater flow characteristics of fractured rocks, particularly their quantitative aspects, are rather poorly understood. Main flow paths in fractured rocks are along joints, fractures, shear zones, faults and other discontinuities.

There is a great need to understand hydraulic characteristics of such rocks, in view of: (a) groundwater development, to meet local needs; and (b) as depositories for nuclear and other toxic wastes.

There could be multiple discontinuities in fractured rocks along which groundwater flow takes place. A number of factors including stress, temperature, roughness, fracture geometry and intersection etc. control the groundwater flow through fractures. For example, fracture aperture and flow rate are directly interrelated; non-parallelism of walls and wall roughness lead to friction losses; hydraulic conductivity through fractures is inversely related to normal stresses and depth, as normal stress tends to close the fractures and reduce the hydraulic conductivity.

It has also been noted that fracture permeability reduces with increasing temperature. As temperature increases with depth, thermal expansion in rocks takes place which leads to reduction in fracture aperture and corresponding decrease in permeability. Further the permeability is also affected by cementation, filling, age and weathering (see Chap. 8).

Parallel fractures impart a strong anisotropy to the rock mass. On the other hand, greater number of more interconnected fractures tends to reduce anisotropy. Further, larger fracture lengths, greater fracture density and larger aperture increase hydraulic conductivity.

Therefore, summarily, for hydrogeological studies, it is extremely important to understand and describe the structure of the rock-mass and quantify the pattern and nature of its discontinuities (van Golf-Racht 1982; Sharp 1993; Lee and Farmer 1993; de Marsily 1986).

## 2.2 Discontinuities—Types, Genetic Relations and Significance

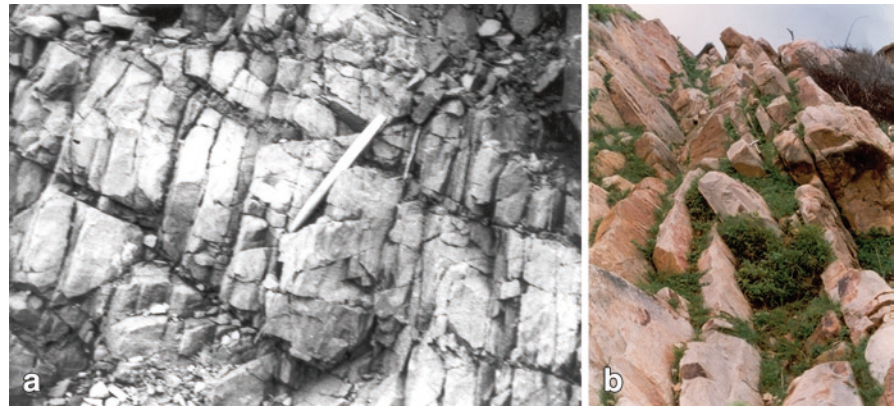
Discontinuity is a collective term used here to include joints, fractures, bedding planes, rock cleavage, foliation, shear zones, faults and other contacts etc. In this discussion using a genetic approach, we group discontinuities into the following categories:

1. Bedding plane
2. Foliation including cleavage
3. Fractures (joints)
4. Faults and shear zones, and
5. Other geological discontinuities.

### 2.2.1 Bedding Plane

Primary bedding and compositional layers in sedimentary rocks form the bedding plane. Usually, it is the most significant discontinuity surface in all sedimentary rocks such as sandstones, (Fig. 2.1b) siltstones, shales etc., except in some massive sandstones or

**Fig. 2.1** Examples of fractured rocks; **a** Metamorphic rocks (meta-argillites) in Khetri Copper Belt, India. Several sets of fractures including shear planes are developed; some of the fractures possess infillings. **b** Sandstones of Vindhyan Group, India; bedding planes constitute the dominant discontinuity surfaces. (Photograph (b) courtesy of A.K. Jindal)



limestones. Bedding plane can be readily identified in the field owing to mineralogical-compositional-textural layering.

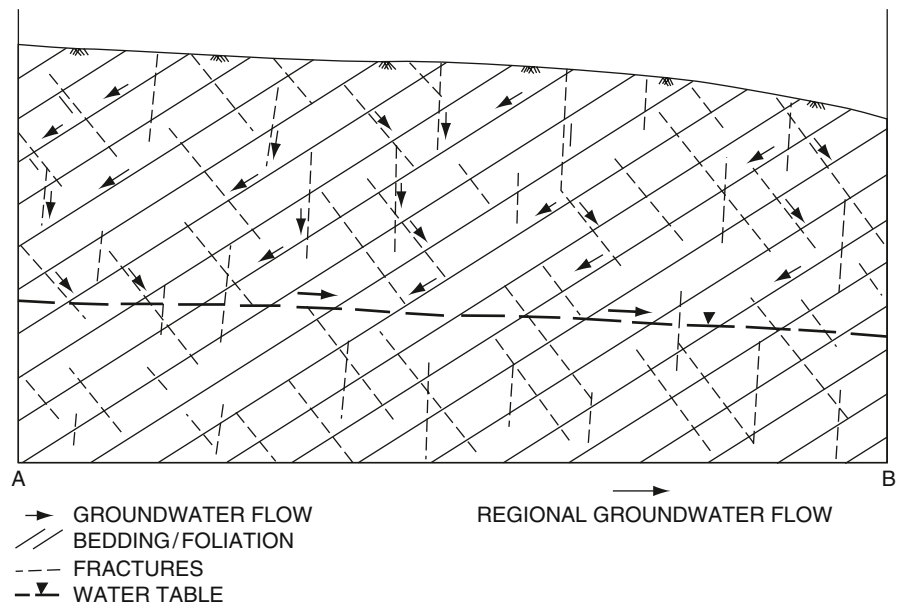
Bedding plane, being the most important discontinuity, imparts anisotropy and has a profound influence on groundwater flow in the vadose zone. The groundwater flow is by-and-large down-dip (Fig. 2.2).

Folds are flexures in rocks formed due to warping of rocks. Although a wide variety of folds are distinguished, the two basic types are anticlines (limbs dipping away from each other) and synclines (limbs dipping towards each other). Folding leads to change or reversal in dip directions of beds, and this affects groundwater flow. Further, folding is accompanied by fracturing of rocks. In an anticline, the crest undergoes higher tensional stresses and hence develops open

tensile fractures, which may constitute better sites for groundwater development.

### 2.2.2 Foliation

Foliation is the property of rocks, whereby they break along approximately parallel surfaces. The term is restricted to the planes of secondary origin occurring in metamorphic rocks. Foliation develops due to parallel-planar alignment of platy mineral grains at right angles to the direction of stress, which imparts fissility. The parallel alignment takes place as a result of recrystallisation during regional dynamothermal metamorphism, a widespread and common phenomenon



in crystalline rocks. *Rock cleavage* is almost a synonymous term. It is also used for planes of secondary origin along which the rock has a tendency to break in near-parallel surfaces. Some terms are used for specific metamorphic rocks. Thus, the term *slaty cleavage* is used for rock cleavage in slates; *schistosity* is used for schists and *gneissosity* for gneisses. Foliation planes may or may not be parallel to bedding. Foliation that is parallel to the bedding is often referred to as bedding foliation. Fracture cleavage is produced by closely-spaced jointing. In many schistose rocks, shear cleavages are developed due to closely spaced shear-slip planes, known as slip-cleavage. In a folded region, the foliation often developed parallel to the axial plane of folds is called the axial plane foliation.

Foliation in metamorphic rocks has a profound influence on groundwater movement, possessing quite the same role as bedding in the sedimentary rocks, both being the most significant discontinuities in the respective rock categories (e.g. see Fig. 2.2).

### 2.2.3 Fractures and Joints

#### 2.2.3.1 Introduction and Terminology

Fractures, also called joints, are the planes along which stress has caused partial loss of cohesion in the rock. It is a relatively smooth planar surface representing a plane of weakness (discontinuity) in the rock. Conventionally, a fracture or joint is defined as a plane where there is hardly any visible movement parallel to the surface of the fracture; otherwise, it is classified as a fault. In practice, however, a precise distinction may be difficult, as at times within one set of fractures, some planes may show a little displacement whereas others may not exhibit any movement. Slight movement at right angles to the fracture surface will produce an open fracture, which may remain unfilled or may get subsequently filled by secondary minerals or rock fragments.

‘Fracture zones’ are zones of closely-spaced and highly interconnected discrete fractures. They may be quite extensive (length > several kilometres) and may even vary laterally in hydraulic properties.

Fracture-discontinuities are classified and described in several ways using a variety of nomenclature, such as: joints, fracture, fault, shear, gash, fissure, vein etc.

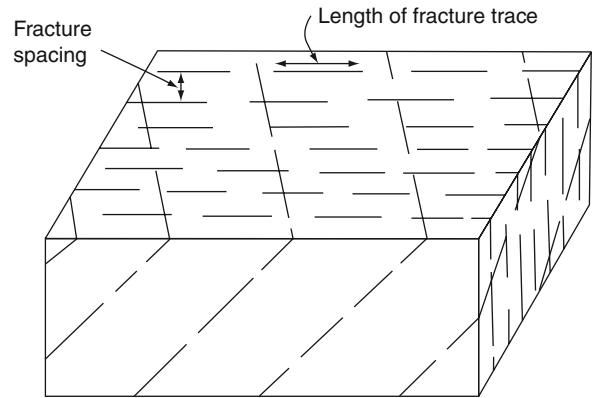


**Fig. 2.3** Two sets of fractures are schematically shown in the block. An individual fracture has limited spatial extent and is discontinuous in its own plane. Fracture spacing and fracture trace length are indicated for one set

Generally, the term fracture is used synonymously with joint, implying a planar crack or break in rock without any displacement. The terms fault and shears are used for failure planes exhibiting displacement, parallel to the fracture surfaces. Gash is a small-scale open tension fracture that occurs at an angle to a fault. Fissure is a more extensive open tensile fracture. A filled-fissure is called a vein.

An individual fracture has a limited spatial extent and is discontinuous in its own plane (Fig. 2.3). On any outcrop, fractures have a certain trace lengths and fracture spacings. By mutual intersection, the various fracture sets may form interconnected continuous network, provided that the lengths of the joints in the different sets are much greater than the spacings between them (see Fig. 2.18). The interconnectivity of fractures leads to greater hydraulic conductivity.

#### 2.2.3.2 Causes of Fracturing

Although fractures are extremely common and widespread in rocks, geologically they are still not well-enough studied (Price and Cosgrove 1990). Complex processes are believed to be involved in the origin of fractures, which are related to geological history of the area. Fractures are created by stresses which may have diverse origin, such as: (a) tectonic stresses related to the deformation of rocks; (b) residual stresses due to events that happened long before the fracturing; (c) contraction due to shrinkage because of cooling of magma or dessication of sediments; (d) surficial

movements such as landslides or movement of glaciers; (e) erosional unloading of deep-seated rocks; and (f) weathering, in which dilation may lead to irregular extension cracks and dissolution may cause widening of cavities, cracks etc.

### 2.2.3.3 Types of Fractures

Firstly, fractures may be identified into two broad types: (a) systematic, which are planar, and more regular in distribution; and (b) non-systematic, which are irregular and curved (Fig. 2.4). The non-systematic fractures meet but do not cross other fractures and joints, are curved in plan and terminate at bedding surface. They are minor features of dilational type and develop in the weathering zone. Curvilinear pattern is their general characteristic. Parallel systematic fractures are treated as a set of fractures.

*Geometric classification*—Considering the geometric relationship with bedding/foliation, the systematic fractures or joints are classified into several types. Strike joints are those that strike parallel to the strike of the bedding/foliation of the rock. In dip joints, the strike direction of joints runs parallel to the dip direction of the rock. Oblique or diagonal joints strike at an angle to the strike of the rocks. Bedding joints are essentially parallel to the bedding plane of the associated sedimentary rock.

Depending upon their extent of development, fractures may be classified into two types: first-order and second-order. First-order fractures cut through several layers of rocks; second-order fractures are limited to a single rock layer. Further, depending upon the strike trend of fractures with respect to the regional fold axis, fractures are designated as longitudinal (paral-

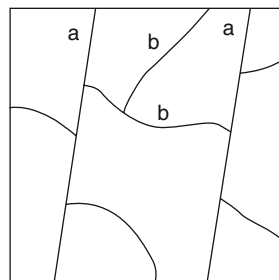
lel), transverse (perpendicular) or oblique ones (see Fig. 2.7 later).

*Genetic classification*—Genetically, the systematic fractures can be classified into three types:

1. *Shear fractures*, which may (or may not) exhibit shear displacement and are co-genetically developed in conjugate sets with a dihedral angle  $2i > 45^\circ$ .
2. *Dilational fractures*, which are of tensile origin, commonly, developed perpendicular to the bedding plane, and are open fractures with no evidence of shear movement.
3. *Hybrid fractures*, which exhibit features of both shear and dilational origin. They may occur in conjugate sets with a dihedral angle  $2i < 45^\circ$ . They are open (extension!), may be partly filled with veins, and may also exhibit some shear displacement.

The physical stress conditions under which these three types of fractures develop are illustrated by the Mohr diagram in Fig. 2.5. The curve ABC is a Mohr envelope. The stress circles touching the Mohr envelope at A, B and C points indicate different failure conditions of the rock. In condition 'A', the principal maximum compressive stress is negative, i.e. extensional, and therefore it leads to a dilational failure. In condition, 'C', a typical conjugate shear failure takes place, such that the dihedral angle  $2i > 45^\circ$ . 'B' represents a condition that there is a positive maximum principal compressive stress and a negative minimum principal compressive stress, i.e. the effective normal stress perpendicular to the fracture plane is negative (extensional). This can be attributed to high fluid pressure conditions at depth. Hence, there is a tendency for such shear fractures to open and also get filled with minerals. Typically, in such hybrid shear-extension fractures, the dihedral angle is  $2i < 45^\circ$ .

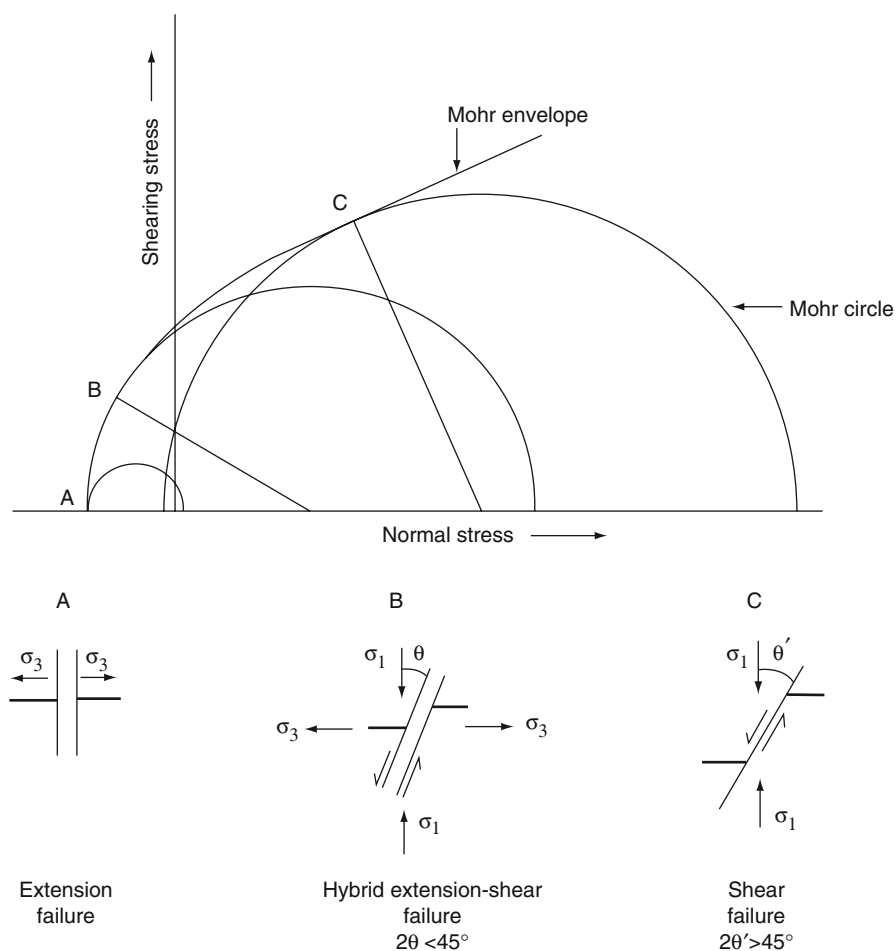
Conjugate shear fractures developing at greater depths are of ductile nature and possess a large  $2i$  ( $\sim 90^\circ$ ). On the other hand, conjugate brittle shears develop at a shallower depth and possess a smaller  $2i$  ( $\sim 60^\circ$ ). Further, brittle deformation causes derivative shears of several orders to form successively deviating trends, which cause a spread in the trends of conjugate shears (Ruhland 1973). The process of shearing is also accompanied by tensile deformation. Thus, brittle deformation may produce fractures of different magnitude and direction in successive orders. In a rock mass fractured by three orders of brittle deformation, tensile



a : Systematic fractures  
b : Non-systematic fractures

**Fig. 2.4** Systematic and non-systematic types of fractures

**Fig. 2.5** Basic genetic types of fractures: *A* extension fracture; *B* hybrid extension-shear fracture; *C* shear fracture. The Mohr diagram indicates the stress conditions for these failures.  $\sigma_1$  and  $\sigma_3$  are the maximum and minimum principal compressive stresses respectively



fracturing may spread over a range of about  $75^\circ$  and shear fracturing over a range of nearly  $135^\circ$  (Fig. 2.6).

#### 2.2.3.4 Discrimination Between Shear and Extension Fractures

The rheological principles indicate that there is no sharp categorization between extension and shear fractures. In fact, all gradations from one category to the other take place. However, from hydrogeological point of view, it is important to distinguish between shear and extension joints as dilational joints are more open and possess greater hydraulic conductivity than shear joints. Discrimination between shear and tension joints may be difficult, particularly in complexly deformed areas. However, the following features may help in their discrimination:

1. Shear joints may exhibit displacement parallel to the plane of the joints, which is absent in the case of extension joints.
2. Shear joints commonly occur in conjugate sets which may be indicated by a statistical analysis.
3. In field, slickensides and other criteria of relative movement may be observed in the case of shear joints.
4. Generally, extension joints are open and shear joints are tight.
5. The orientation of the joints with respect to the bedding/foliation and or fold-axis can provide information on shear vs. tensile origin of fractures, as shear joints occur in oblique conjugate sets whereas extension joints occur as longitudinal and transverse joints forming an orthogonal pair (Fig. 2.7).
6. The cumulative trend diagram of fractures may also provide information on the related stress field,

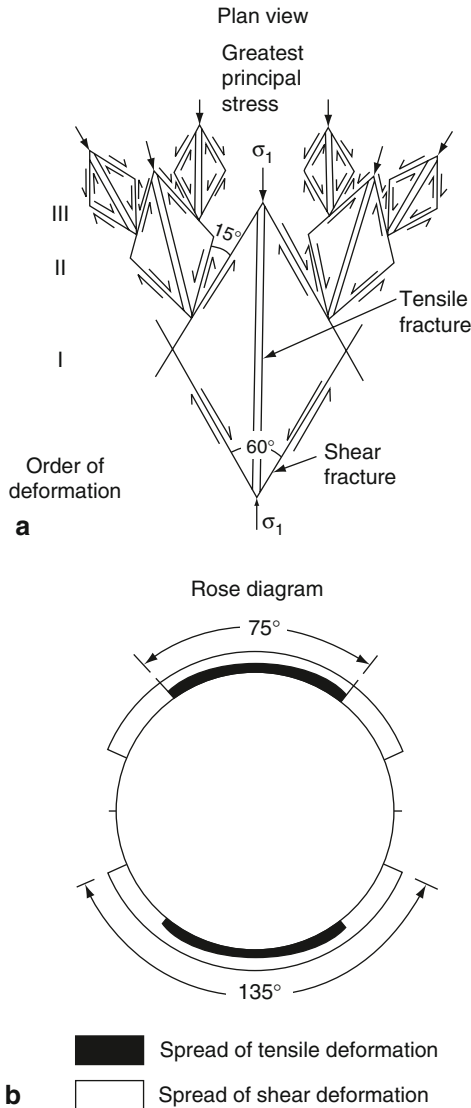


**Fig. 2.6** Scheme of brittle deformation of a homogeneous rock mass. The rose diagram illustrates the ranges of orientations of tensile and shear fractures due to three orders of deformation. (After Ruhland 1973)

and therefore the likely trends of shear and extension fractures; the maximum principal compressive stress bisects the dihedral angle of conjugate shear fractures and is parallel to the tensile fracture.

A field example of large-scale tensional and shear fractures extending for several kilometres is given in Fig. 2.8 where tensional fractures appear as wide open and shear joints are characterized by relative displacements.

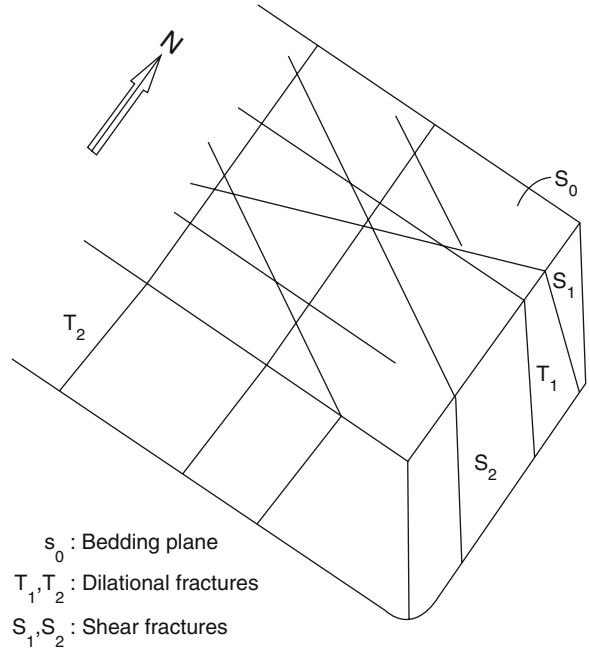


**Fig. 2.7** Development of four sets of fractures in the case of simple dipping strata (see also Fig. 2.9)

### 2.2.3.5 Orientation of Fractures vis-à-vis Regional Structure

Ideally, in the case of simple-dipping strata, four sets of fractures (systematic) develop (Fig. 2.7).  $S_1$  and  $S_2$  form a conjugate set of shear fractures and  $T_1$  and  $T_2$  are extension fractures. All these fractures are perpendicular to the bedding plane and contain the intermediate principal compressive stress  $\sigma_2$ .

Figure 2.9 shows a simplified ideal relationship between fractures and folds.  $\sigma_1$  is the maximum principal compressive stress perpendicular to the fold-axis (b). A conjugate set of oblique trending right-lateral and left-lateral shear fractures develops. There are two sets of extension fractures, one longitudinal and the other transverse to the fold-axis, both being mutually orthogonal.

During folding, bending of a bed causes extension on the convex side and compression on the concave side (Fig. 2.10). This results in extension fractures and normal faults on the crests of anticlines. Less commonly, thrust faults also develop in the inner areas of compression.

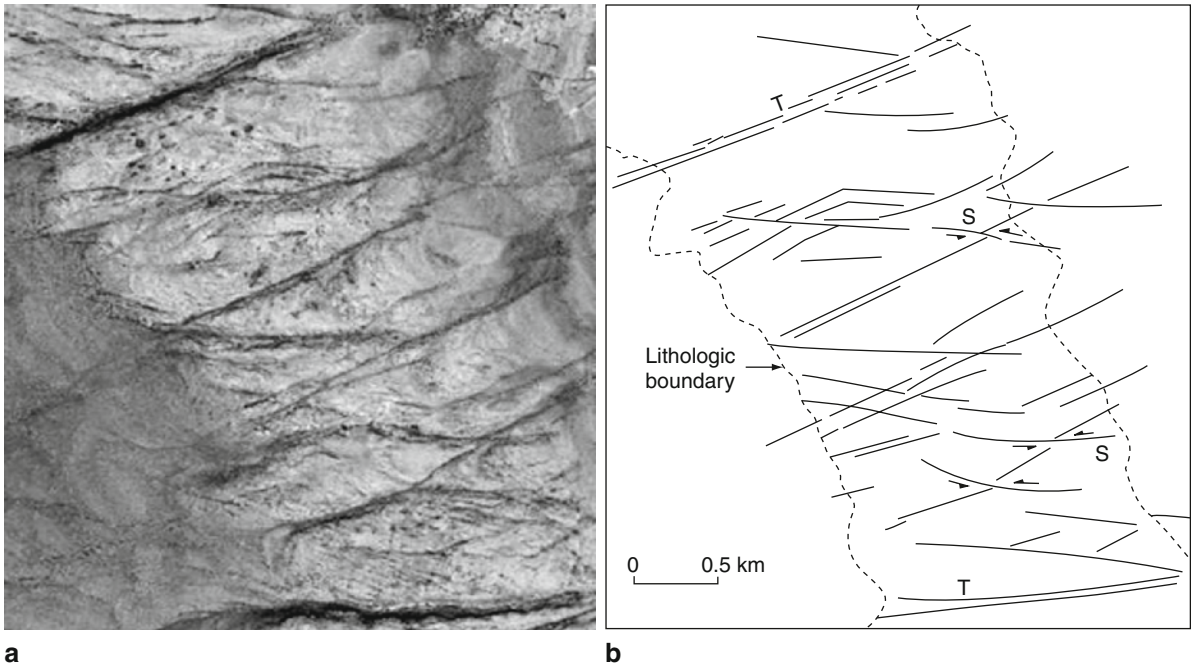


**Fig. 2.8** **a** Example of large-scale tensional and shear fractures extending for several kilometres in a part of the Precambrian Cuddapah basin, India; black-and-white image generated from GoogleEarth. **b** Interpretation map of the above image; fractures

marked *T* are wide open tensional fractures that are vegetated implying groundwater seepage, *S* are shear fractures exhibiting lateral relative displacement at places

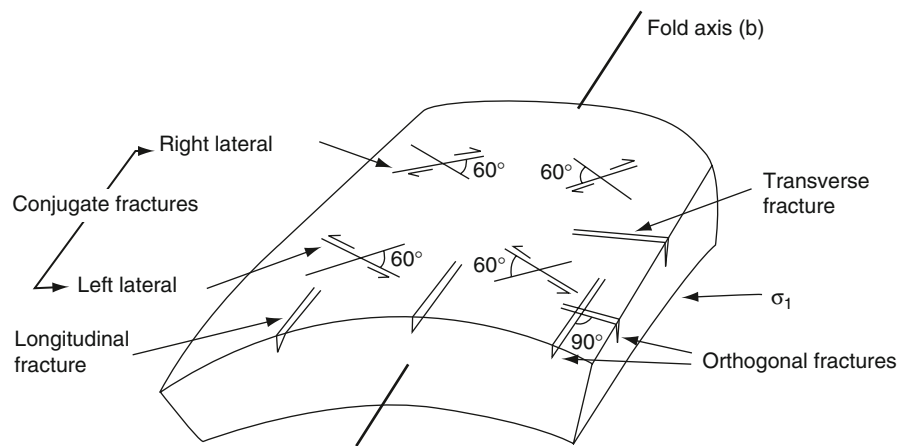
**2.2.3.6 Other Types of Fractures**

*Sheeting joints:* These joints are generally flat, somewhat curved and nearly parallel to the topographic surface, often developed in granitoid rocks. They are closely developed near to the surface, and their spacing

increases with depth. They are generated due to release of overburden stress.

*Columnar joints:* Joints of this type are tension fractures generated due to shrinkage in rocks. Shrinkage may occur due to cooling or dessication. Igneous rocks contract on cooling. Mud and silt shrink because of

**Fig. 2.9** Ideal relationship between major joint sets in a folded bed. There are two sets of conjugate shear fractures and two sets of mutually orthogonal dilational fractures. All the fractures are shown vertical



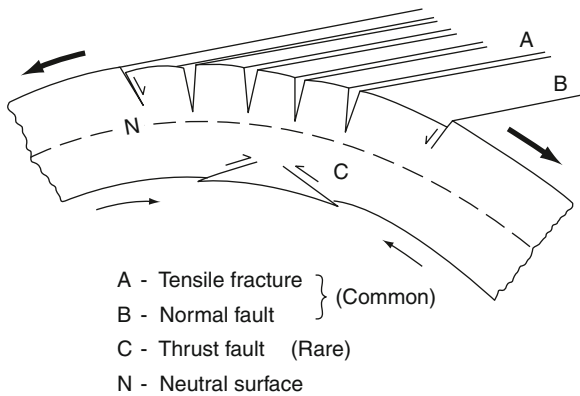


**Fig. 2.10** Development of extensional fractures and normal faults on the crest and the upper axial zone of an anticline. Thrust faults may also develop, occasionally, in the inner area of compression

dessication. As a result, polygonal and columnar joints develop. The columns are generally a few centimetres to a metre in diameter, and several metres long (high). Frequently, the columns are four, five or six sided in shape (see Fig. 14.5).

## 2.2.4 Faults and Shear Zones

Rupture and shear movement due to stresses leads to faulting. The stress in rocks is mostly a result of mountain building tectonic activity. From a hydrogeological point of view, faults and shear zones constitute very important types of discontinuities in rocks. Faults are planes and zones of rupture along which the opposite walls have moved past each other, parallel to the surface of rupture. The orientation of a fault plane is defined in terms of strike and dip, as that of any other plane in structural geology. Faults vary in dimension from a few millimetres long with minor displacement to several hundred kilometres in strike lengths with movement of several tens of kilometres.

### 2.2.4.1 Terminology

In describing faults, a range of terminology is used; only some of the more important terms are introduced

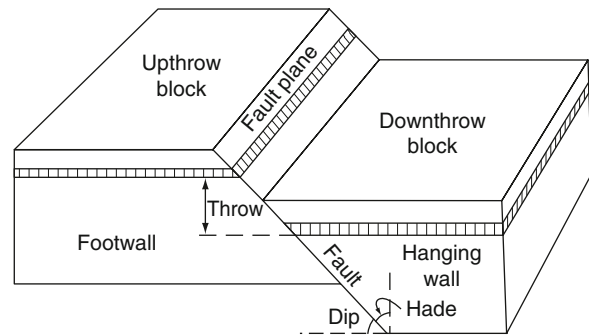


**Fig. 2.11** Common terms used in describing a fault

here (see e.g. Billings 1972; Price and Cosgrove 1990). The fault block above the dipping fault plane is called *hanging wall*; the block below the faults plane is called *footwall* (Fig. 2.11). The angle which a fault plane makes with the vertical plane parallel to the strike of the fault is called *hade*; it is complement of the dip. In many instances the displacement is distributed through a zone, called the fault zone, which may be a few centimetres to hundreds of metres wide. Faults may exhibit simple translational or rotational movements. Slip is the relative displacement as measured on the fault surface. Strike-slip and dip-slip are the displacements along the strike direction and dip direction respectively on the fault plane. *Throw* is the vertical displacement caused by the fault. The blocks which have moved up and down are called *upthrow* and *downthrow blocks*, respectively.

Shear zones are generally filled with broken and crushed rocks, which may be embedded in clay matrix. Shear zones tend to be more extensive and continuous than joints.

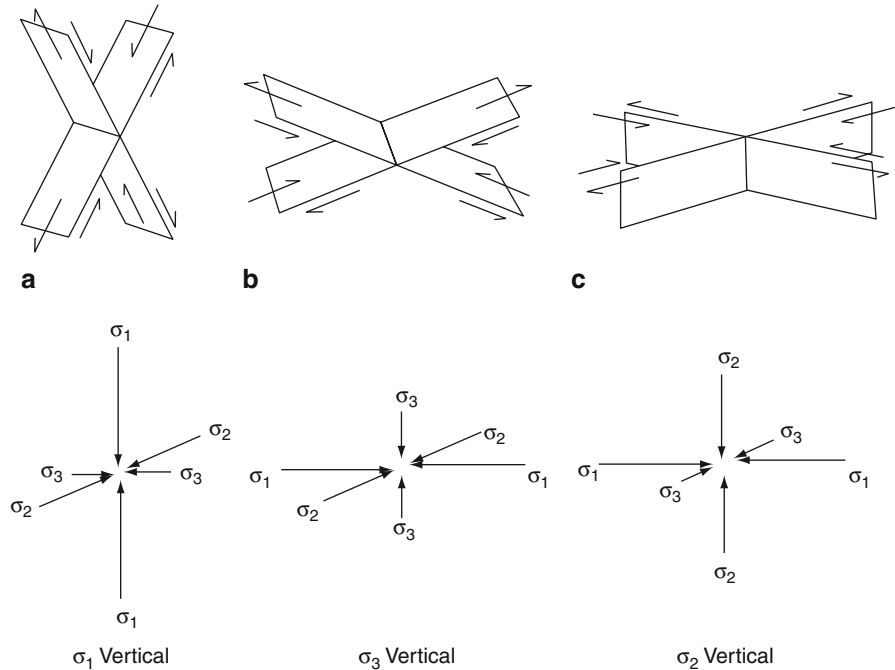
### 2.2.4.2 Classification

Faults are classified in various ways in the literature. Some classifications are based on geometrical relations between the fault plane and country rocks. Genetically, faults are classified into three types: (a) normal, (b) reverse and (c) strike-slip. They are related to the stress conditions (Fig. 2.12).

In the case of a normal fault, hanging wall moves relatively downward. Normal faults are generally high-angle faults caused when  $\sigma_1$  is vertical. Reverse faults are generally low-angle (gently dipping) faults



**Fig. 2.12** The basic genetic types of faults: **a** normal, **b** reverse and **c** strike-slip. Orientations of principal compressive stresses are also shown



caused when  $\sigma_3$  is vertical. It is characterised by the relative upward movement of the hanging wall. Strike faults are vertical faults marked by movement only in the strike direction of the fault. These are caused when  $\sigma_2$  is vertical.

### 2.2.4.3 Recognition of Faults in the Field

A number of criteria are used to decipher the presence of faults, though in a specific case only some of the features may be present. Some of the more important criteria include: (a) displacement of key beds; (b) truncation of beds and structures; (c) repetition and omission of strata; (d) presence of features indicating movement on fault surface such as slickensides, mylonite, breccia, gouge, grooving etc; (e) evidence of mineralisation, silicification, along fault zones; (f) physiographic features such as fault scarps, offset ridges, etc; (g) alignment such as springs alignment, pond alignment, vegetation alignment, rectilinearity of a stream; (h) indication of sudden anomalous changes in river course, such as knick points, offset of streams, anomalous or closed meanders etc.; (i) erosional features such as triangular facets, unpaired terraces etc.

Investigations for faults may be made in outcrops, road cuttings, mines or other excavations, where smaller faults could often be directly observed. A larger fault, on the other hand, may be identified on stratigraphic and physiographic evidences, and particularly on remote sensing images, as only small segments of the fault may be exposed in field, and the feature may be largely covered under soil, debris or vegetation (see Sect. 4.8.11).

### 2.2.4.4 Effect of Faults on Groundwater Regime

Faults may affect groundwater regime in numerous ways, some of the more important being the following:

1. It is well known that faults may have such effects as truncation, displacement, repetition or omission of beds. In this light, the distribution and occurrence of aquifers may be affected by faults as locally an aquifer unit may get displaced/truncated/omitted (Fig. 2.13a, b).
2. A fault may bring impervious rock against an aquifer, which would affect groundwater flow and distribution (Fig. 2.13a).

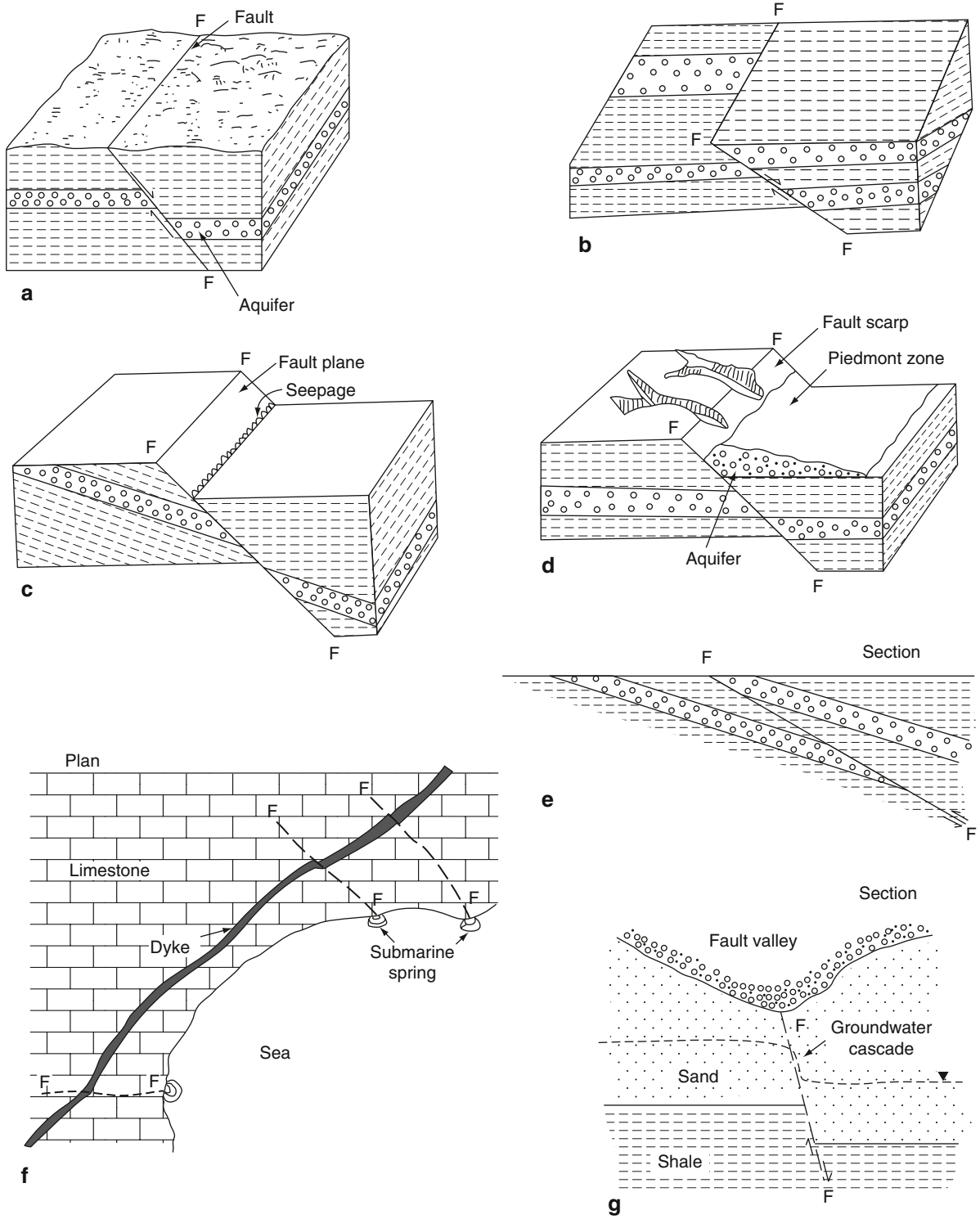


**Fig.2.13** Effects of faults on aquifers (for details see text)

3. Truncation of an aquifer by a fault may lead to seepage and formation of a spring line along the fault (Fig. 2.13c).
4. A fault may lead to a scarp; intensive erosion of the upthrow block and deposition of extensive piedmonts on the downthrow block may follow; the piedmont deposits may serve as good aquifers (Fig. 2.13d).
5. An aquifer may get repeated in a borehole due to thrust faulting; further it may also get re-exposed on the surface for recharge (Fig. 2.13e).
6. Vertical dykes, veins etc. which generally act as barriers to groundwater flow, may be breached by faults and this may produce local channel-ways across the barrier (Fig. 2.13f).
7. A fault may lead to a groundwater cascade (Fig. 2.13g).
8. Faults create linear zones of higher secondary porosity; these zones may act as preferred channels of groundwater flow, leading to recharge/discharge.
9. A fault may lead to inter-basinal subsurface flow.
10. A fault zone, when silicified, may act as a barrier for groundwater flow.

Figures 2.14 and 2.15 give field examples of extensive faults with strike length of kilometres, showing displacements of beds and marked by preferential alignment of vegetation indicating groundwater seepage.

### 2.2.5 Other Geological Discontinuities

In addition to the above structural features, there could be other geological boundaries such as unconformities and intrusive contacts which may act as discontinuities.

Unconformity is a surface of erosion and nondeposition separating overlying younger strata from the underlying older rocks. Conglomerate beds and palaeosols usually occur along the unconformity surface which often forms good aquifers. An unconformity implies that a hydrogeological unit may get laterally pinched out and spatially replaced by another unit (Fig. 2.16).

Intrusive contacts are other geological boundaries of significance in the context of hydrogeology. Intrusive bodies occur in a variety of shapes and sizes, such



**Fig. 2.14** Faults displacing the sedimentary layers of sandstones and shales (Vindhyan Super Group, near Chhattaigarh, India). The terrain has a semi-arid climate. Note the preferential growth of vegetation along fault zones related to the seepage of groundwater. Sedimentary layering is also marked by vegetation banding. Black-and-white image from GoogleEarth

as batholiths, dykes, sills etc. Their relation with the host rocks could be concordant, transgressive, or discordant. The igneous plutonic bodies crystallize under high pressure and temperature; they are devoid of primary porosity. Therefore, hydrogeological characters

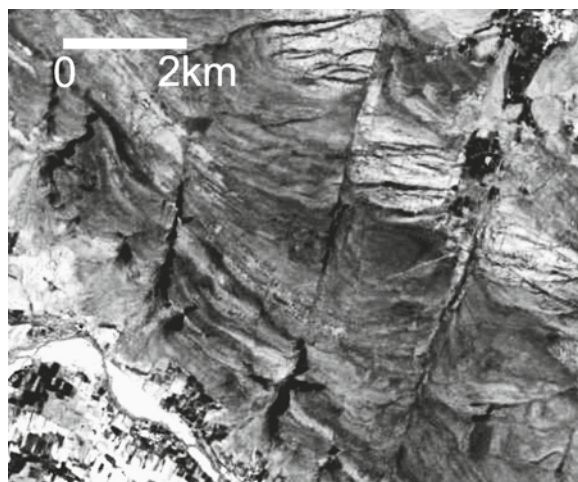


**Fig. 2.15** Large-scale parallel faults running for several kilometres displacing the sedimentary layers of Cuddapah basin, India. Note the vegetation alignment along the southern parts of fault zones related to the seepage of groundwater. Black-and-white image from GoogleEarth

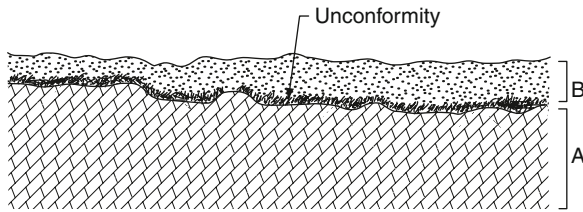


**Fig. 2.16** Development of an aquifer along an unconformity between two impervious beds A and B

of the host rocks and intrusive rocks may be vastly different from each other. Hence, igneous contacts act as regional boundaries from a hydrogeological point of view.

## 2.3 Fracture Characterization and Measurements

A fractured rock mass can be considered to be made up of three basic components: (a) fracture network, (b) matrix block and (c) infillings along the fractures, if present (see Fig. 2.1). A single fracture or discontinuity plane is characterised by its orientation, genetic nature (shear/tensile), persistence and aperture etc. Several fracture planes of the same type create a fracture set. They have certain spacing (frequency). Several intersecting intercommunicating fracture sets create a fracture network which facilitates fluid flow. Thus, it is extremely important to characterize discon-

tinuities and make their measurements, for a meaningful application. The various important parameters are summarised in Table 2.1.

The concept of Representative Elementary Volume (REV) is very important and may be introduced here. REV is the minimum rock mass volume which has the hydraulic and or mechanical properties similar to those of the rock mass. For mechanical properties, a sample size of a few cubic meters may be sufficient for approaching a REV; however, in case of hydraulic flow, REV may be substantially larger, and in some cases, it may not even exist due to strong anisotropy and spatial variability of rock characters.

### 2.3.1 Number of Sets

Several sets of discontinuities are often developed in a rock mass, three to four sets being most common. Number of sets of discontinuities in a exposure can be statistically determined by contouring the pole-plots (see Fig. 2.18). Relevant data as orientation, spacing, length, aperture etc. has to be collected for each set of discontinuity.

### 2.3.2 Orientation

Orientation is the parameter to define a single fracture plane in space, using angular relationships, as for any

**Table 2.1** Parameters for discontinuity characterization

Parameter	Description
1. Number of sets	Number of sets of discontinuities present in the network
2. Orientation	Attitude of discontinuity present in the network
3. Spacing	Perpendicular distance between adjacent discontinuities of the same set
4. Persistence	Trace length of the discontinuity seen in exposure
5. Density	
– linear	Number of fractures per unit length
– areal	Cumulative length of fractures per unit area of exposure
– volumetric	Cumulative fractured surface area per unit bulk rock volume
6. Fracture area and shape	Area of fractured surface and its shape
7. Volumetric fracture count	Number of fractures per cubic metre of rock volume
8. Matrix block unit	Block size and shape resulting from the fracture network
9. Connectivity	Intersection and termination characteristics of fractures
10. Aperture	Perpendicular distance between the adjacent rock-walls of a discontinuity, the space being air or water-filled
11. Asperity	Projections of the wall-rock along the discontinuity surface
12. Wall coatings and infillings	Solid materials occurring as wall coatings and filling along the discontinuity surface

geological planar surface. It is defined in terms of dip direction (angle with respect to north) and dip amount (angle with horizontal). The orientation is expressed in terms of a pair of numbers, such as  $25^\circ/\text{N } 330^\circ$ , implying a plane dipping at  $25^\circ$  in the direction  $330^\circ$  measured clock-wise from the north. In field, inaccuracies often creep-in the measurements, and therefore statistical analysis is desirable.

*Rose diagram* is a method of displaying the relative statistical prevalence of various directional trends, e.g. strike direction of fractures, lineaments etc. It can be prepared for parameters such as number or length, i.e. number of joints direction-wise, or length of joints direction-wise. Frequently, the directions are grouped in  $10^\circ$  interval. Frequency in a group-interval is represented along the radial axis, the length of petals becoming a measure of relative dominance of the trend. The strike petals possess a mirror image about the centre of the rosette. Data on the magnitude of dip cannot be incorporated in the rosette, and may however be shown outside the circumference (Fig. 2.17). *Histogram plot* is another way to represent the relative prevalence of the trends.

*Spherical projection:* For representing orientation of geological planar surfaces, the method of stereographic equal-area projection is frequently employed, as it accurately shows the spatial distribution of data. Basic concepts on great-circle plots and  $\pi$ -pole plots to represent planes can be found in any standard text on structural geology (e.g. Billings 1972; Price and Cosgrove 1990). The method of plotting pole has a relative advantage over the great-circle method in that clusters of poles and their relative concentrations can be readily ascertained

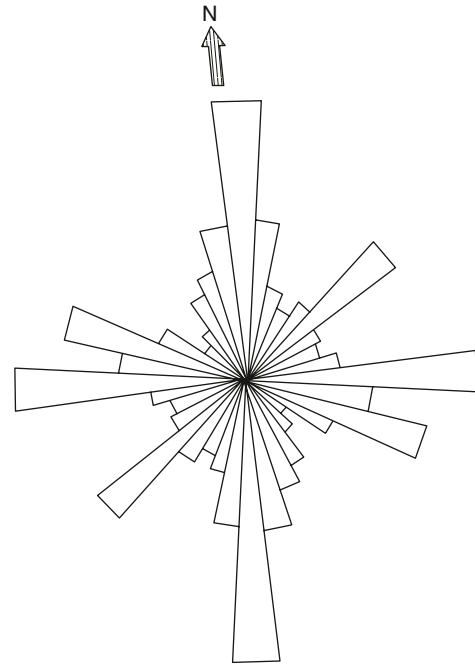


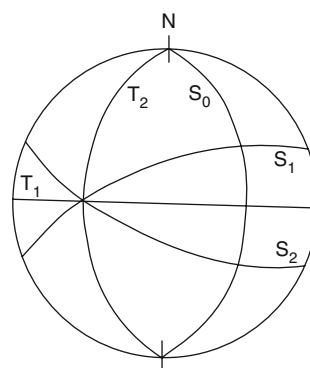
**Fig. 2.17** Rose diagram of strike trends of discontinuities showing their relative prevalence

on such plots by contouring. Schmidts-net is often used for density contouring to provide information on highest concentration, i.e. the most dominant fracture plane. Figure 2.18 gives an example.

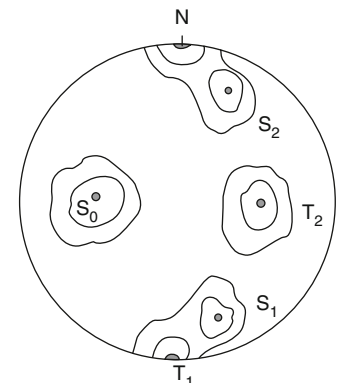
It may be important to find the over-all effect of various discontinuities. The mean direction of a group of poles can be represented by a simple vector-sum of all the constituting poles, following Fisher distribution. Similarly a resultant vector can be calculated

Sr. No.	Surface	Strike	Dip direction	Dip amount
1	$S_0$	N - S	E	$45^\circ$
2	$T_1$	E - W	Vertical	—
3	$T_2$	N - S	W	$45^\circ$
4	$S_1$	N $68^\circ$ - N $248^\circ$	N $338^\circ$	$80^\circ$
5	$S_2$	N $112^\circ$ - N $292^\circ$	N $202^\circ$	$80^\circ$

**a** Fracture orientation data



**b** Great circle diagram



**c**  $\pi$ -Pole diagram

**Fig. 2.18** a Orientation data of discontinuities.  $S_0$  is bedding plane,  $T_1$  and  $T_2$  are tensile fractures and  $S_1$  and  $S_2$  are shear fractures. Their great-circle and  $\pi$ -pole diagrams are shown in figures (b) and (c) respectively

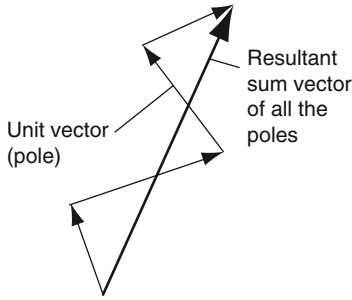


**Fig. 2.19** Principle of determining the mean pole direction as the resultant vector sum of all the vectors (poles), following Fisher method

by summing all the clusters, to give a net directional effect of all the sets of discontinuities (Fig. 2.19).

It may be mentioned here that only selected and not all of the discontinuities present may play a significant role in fluid movement in the rock mass. Therefore, selection and data integration ought to be done judiciously. Further, Sharp (1993) gave a more useful concept for integration of discontinuity trend, frequency and aperture data to make hydraulic zonation maps (see Sect. 7.2.5).

### 2.3.3 Spacing (Interval)

Systematic joints are roughly equidistant and possess parallelism, and therefore, the parameter statistical

spacing has significance. It describes the average (or modal) perpendicular distance between two adjacent discontinuities of the same set. It has a profound influence on rock mass permeability and groundwater flow. Fracture spacing is reciprocal of the fracture frequency or linear fracture density. It also controls fracture intensity and matrix block size.

Fracture separation ( $f_s$ ) is related to lithology and thickness of the bed ( $b$ ), and is given as (Price and Cosgrove 1990):

$$f_s = Y \cdot b \tag{2.1}$$

where  $Y$  is a constant related to lithology. Modelling and theoretical approaches also show that fracture spacing and bed thickness should have a linear relationship, for a given lithologic material.

By spreading a tape in any convenient direction on an outcrop face, average apparent spacing ( $f_{sa}$ ) between fractures of a set can be measured. This measurement has to be corrected for angular distortion ( $\theta$ ) to give the value of true fracture interval, perpendicular to the fracture orientation. The correction angle ( $\theta$ ) equals the angle between the direction of tape alignment and the pole to the fracture plane, and can be easily computed using a stereographic net (Fig. 2.20). The true fracture spacing ( $f_s$ ) can be obtained from the measured fracture spacing ( $f_{sa}$ ) as:

$$f_s = f_{sa} \cdot \cos \theta \tag{2.2}$$

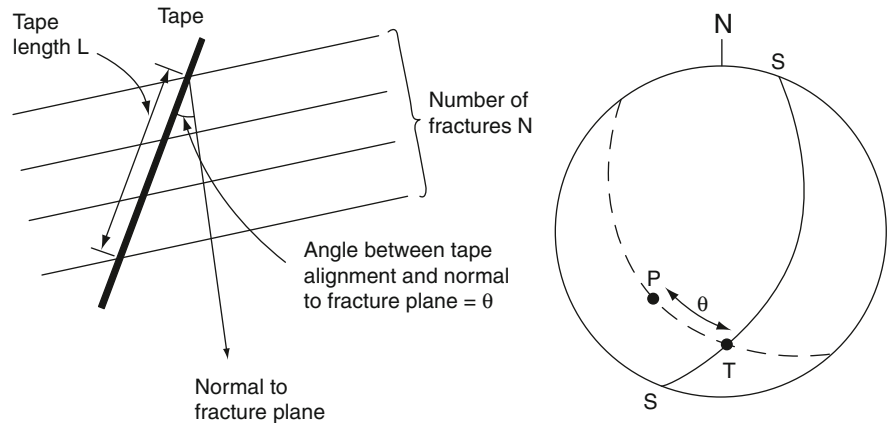


**Fig. 2.20** Spacing of fractures and computation of true fracture spacing. **a** Measurements in field for apparent fracture spacing. **b** Angle of correction, i.e. the angle between the line of tape alignment and pole to the fracture plane, computed by stereographic method

Apparent fracture spacing =  $L / N = dm$   
 True fracture spacing =  $dm \cos \theta$

**a**

- S-S = Great – circle of the outcrop face orientation
- T = Tape alignment
- P = Pole to the fracture plane
- b**  $\theta$  = Correction angle

Further, it has been reported that fairly reliable estimates of fracture spacing can also be given by the P-wave velocity using seismic refraction techniques (see Sect. 5.6).

### 2.3.4 Persistence (Fracture Length)

Fracture persistence or length is a measure of the extent of development of discontinuity surface (Fig. 2.21). This carries the notion of size and controls the degree of fracturing. It is a crude measure of the penetration length of a fracture in a rock mass. Fracture trace length is also related to fractured surface area. As some of the discontinuities are more persistent and continuous than others, it becomes a very important parameter in controlling groundwater flow.

Persistence is rather difficult to quantify, as it would differ in the dip and strike directions. It can be measured by observing the discontinuity trace length in an exposure, in both dip and strike directions.

The observed trace length may be only an apparent value of the true trace length due to various types of bias creeping in the data during measurements in exposures, drifts, excavations, benches etc. For example, the biases could be like: (a) inability to recognize fracture traces shorter than a certain threshold length will lead to a bias (truncation of the histogram); (b) inability to measure full length of the traces owing to incomplete exposures in drift-walls, excavations etc. will lead to recording of censored length data; (c) the observed length of fracture trace depends on the relative orientation between the fracture plane and the exposure face; (d) in the sampling area or scanline, a stronger discontinuity is more likely to appear than a weaker one. Considering such aspects, methods for estimating the true trace length are discussed by a few workers (e.g. Pahl 1981; Laslett 1982; Chiles and de Marsily 1993).

### 2.3.5 Fracture Density

Fracture density is measured for each set of fracture set separately and corresponds to the degree of rock fracturing. It can be described in three ways: linear, areal and volumetric, depending upon whether the measurement/computation corresponds to length (1D), area (2D) or volume (3D) aspect, respectively.

1. Linear fracture density (1D fracture density,  $d_1$ ) is the average number of fractures of a particular set, per unit length measured in a direction perpendicular to the fracture plane. It equals fracture frequency ( $F_f$ ) and is the reciprocal of fracture spacing.
2. Areal fracture density (2D fracture density,  $d_2$ ) is a way to quantify persistence of the discontinuity. It is the average fractured length (of traces) per unit area on a planar surface.
3. Volumetric fracture density (3D fracture density,  $d_3$ ) is the average fractured surface area per unit rock volume, created by all the fractures of a given set.

All types of fracture densities,  $d_1$ ,  $d_2$ , and  $d_3$  have the same dimension ( $L^{-1}$ ). The volumetric density ( $d_3$ ) is independent of direction and is a static parameter, like porosity. On the other hand, areal and linear densities are directional parameters and have bearing on fluid flow.

Both  $d_1$  and  $d_2$  depend on the orientation of the fractures vis-à-vis that of the scanline/exposure face. However,  $d_3$  is independent of direction and can be estimated from a survey with boreholes or scanlines, with the help of proper weighting of the observed fractures (Chiles and de Marsily 1993). For computing the correct weighting factors, consider first the case of a borehole or a scanline survey (Fig. 2.22). The surveyed straight line can be considered as a cylinder of length  $L$  with a small section  $p$ , as in the case of a borehole. If  $n$  fractures intersect the survey line and  $i_i$  is the acute angle made by the  $i$ th fracture plane with the borehole, then the fracture surface within the

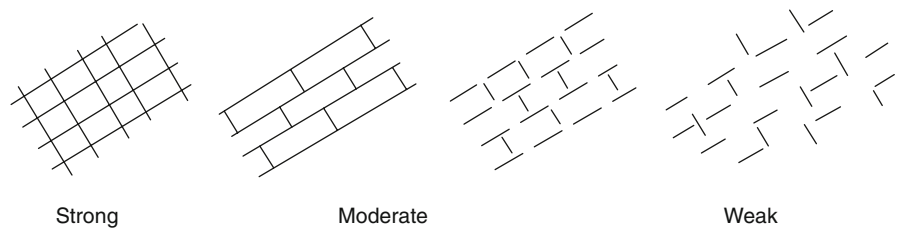


**Fig. 2.21** Influence of persistence of discontinuity on the degree of fracturing and interconnectivity

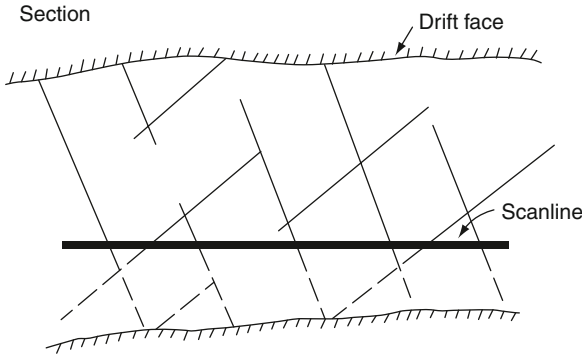


**Fig. 2.22** Scanline method of discontinuity survey

cylinder is  $p/\sin i_i$ , for the  $i$ th fracture. Hence, 3D fracture density  $d_3$  is:

$$d_3 = \frac{1}{L \cdot p} \sum_{i=1}^n \frac{p}{\sin \theta_i} = \frac{1}{L} \sum_{i=1}^n \frac{1}{\sin \theta_i} \quad (2.3)$$

Thus, the weighting factor is related to the acute angle between the fracture plane and the scanline.

Similarly, considering the case of an areal survey, the exposure can be considered as a layer of area  $S$  and a small thickness  $e$ . Within the surveyed rectangle, if  $n$  fractures are traced on the exposure (Fig. 2.23), and  $i$ th fracture has a trace length  $l_i$  and makes an angle  $i_i$  with the exposure plane, then the fractured surface area for the  $i$ th fracture is  $e \cdot l_i / \sin i_i$ . Hence, 3D fracture density is:

$$d_3 = \frac{1}{S \cdot e} \left( \sum_{i=1}^n \frac{e \cdot l_i}{\sin \theta_i} \right) = \frac{1}{S} \left( \sum_{i=1}^n \frac{l_i}{\sin \theta_i} \right) \quad (2.4)$$

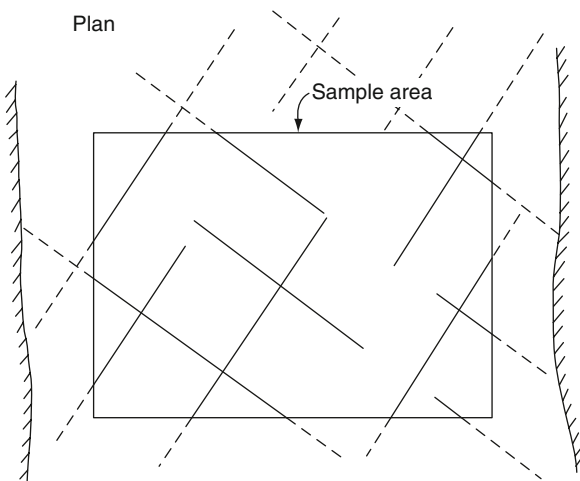


**Fig. 2.23** Areal method of discontinuity survey

Thus, the weighting factor is related to acute angle and fracture trace length. If all the fractures have the same trace length, then  $l$  is constant. For parallel fractures,  $i_i$  can be replaced by  $i$ . For example, in an area in Bundelkhand granites (India), the 3D fracture density was computed using the scanline method at 64 observation sites. It is observed that  $d_3$  in the area varies generally from about  $6 \text{ m}^{-1}$  to  $21 \text{ m}^{-1}$ , whereas there are smaller pockets of higher values of  $d_3$ , of the order of  $31 \text{ m}^{-1}$ . The variation in  $d_3$  across the study area is shown in Fig. 2.24, where the magnitude of  $d_3$  is plotted as a circle of appropriate radius.

With simplifications and assumptions,  $d_1$ ,  $d_2$  and  $d_3$  can be interrelated; if fracture orientations are purely random, then (Chiles and de Marsily 1993):

$$d_1 = 1/2 \cdot d_3 \quad (2.5)$$

$$d_2 = \pi/2 \cdot d_3 \quad (2.6)$$

### 2.3.6 Fracture Area and Shape

Fracture area can be estimated from the strike trace length and dip trace length, assuming that the fractured surface has a certain regular shape, e.g. circular, square, elliptical, rectangular or polygonal. Out of these the case of circular discs is the simplest. Disc diameter  $D$  can be related to fracture surface area  $A$  as:

$$A = (\pi/4) \cdot (D^2 + S_D^2) \quad (2.7)$$

where  $S_D$  is the standard deviation of disc diameter distribution. Statistical aspects on the bearing of fracture shape on area estimation are discussed by a few workers (e.g. Lee and Farmer 1993). The 3D density of disc centres  $\tau$ , average disc surface area  $A$  and the 3D fracturation density  $d_3$  are interrelated as:

$$d_3 = \tau \times A \quad (2.8)$$

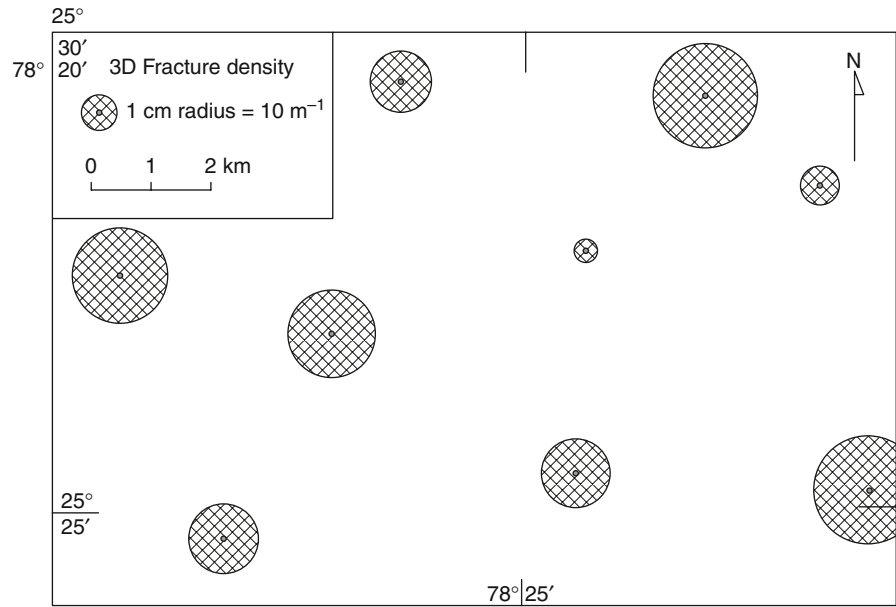
### 2.3.7 Volumetric Fracture Count

Volumetric fracture count ( $V_f$ ) is the total number of fractures per cubic meter ( $\text{m}^3$ ) of rock volume and is determined from the mean fracture spacing as:

$$V_f = 1/f_{s1} + 1/f_{s2} + 1/f_{s3} \cdots + 1/f_{si} \quad (2.9)$$



**Fig. 2.24** Map showing variation in 3D fracture density in a part of Bundelkhand granites, Central India



where  $f_{si}$  is the mean fracture spacing of the  $i$ th fracture set in metres. This also carries the notion of fracture intensity which is defined as the number of discontinuities per unit length, measured along a line, area or volume. Volumetric fracture count has a direct bearing on the size of matrix blocks and the representative elementary volume (REV).

### 2.3.8 Matrix Block Unit

The rock block bounded by fracture network is called matrix block unit. Each matrix block unit can be considered to be hydrogeologically separated from the adjacent block. The shape of the matrix block unit could be prismatic, cubical or tabular, as governed by the orientation of fractures and their distribution (Fig. 2.25). For example, predominantly vertical fractures produce columnar and parallelepiped blocks (e.g. columnar joints in basalts); dominantly horizontal joints lead to plates and sheets (e.g. sheeting joints in granitoid rocks). These features impart hydraulic anisotropy to the geologic unit.

Consider an ideal case where beds are horizontal and fractures only vertical. It is known that fracture spacing and bed thickness are directly related (Eq. 2.1). It follows that a particular lithology has a tendency to develop block units of a certain shape, the block unit volume being dependent upon the bed thickness.

Block size is also related to the volumetric fracture count  $V_f$ . The maximum number of matrix blocks  $N_{bmax}$  can be expressed as (Kazi and Sen 1985):

$$N_{bmax} = \left( \frac{V_f}{3} + 1 \right)^3 \quad (2.10)$$

Fractal concepts are also used to define fragmented rocks. It is found that for fragmented materials including rocks, there is a size-frequency relationship of the form:

$$N(r) \propto (r^{-D}) \quad (2.11)$$

where  $N(r)$  is the number of fragments with a characteristic linear dimension greater than ( $r$ ) and  $D$  is the

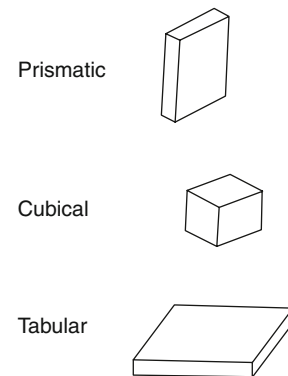


**Fig. 2.25** Shape of matrix block units: prismatic, cubical and tabular

fractal dimension. It is believed that in future, fractal dimensions could be very useful in defining rock mass characteristics (e.g. Mojtabai et al. 1989; Ghosh 1990).

### 2.3.9 Fracture Connectivity

Discontinuities may exhibit differing termination and connectivity characteristics (Fig. 2.26a). Intersection of discontinuities is important as groundwater flow takes place through multiple fractures. Greater continuous inter-communication among the fracture network is provided by a higher degree of fracturing. Fracture connectivity increases with increasing fracture length and fracture density, as the chance of fracture intersection increases.

For evaluating connectivity it is necessary to study how the fractures terminate. Barton et al. (1987) classified fractures into three categories: abutting, crossing, and blind. The fractures of blind type do not intersect other fractures and remain unconnected. Laubach (1992) suggested that in many cases fracture connectivity may be gradual and that many fractures earlier classified as abutting, were really diffuse (interfingering type). He grouped fracture terminations into blind, diffuse and connected (which includes abutting). The data can be plotted in a ternary diagram to represent the bulk condition of fracture intersection in the rock mass (Fig. 2.26b). As an example, it is shown in the figure that most the joints in Bundelkhand granites (BG) are of connected type.

### 2.3.10 Rock Quality Designation (RQD)

RQD is a semi-quantitative measure of fracture density which can be estimated from core recovery data.

RQD is defined as the ratio of the recovered core more than 4 in. (about 10 cm) long and of good quality to the total drilled length and is expressed as a percentage. Although RQD is mainly used in assessing the geomechanical properties of rocks, it is also considered to be an important parameter in assessing relative permeability.

### 2.3.11 Aperture

Aperture is the perpendicular distance separating the adjacent rockwalls of an open discontinuity, in which the intervening space is air or water-filled. Aperture may vary from very tight to wide. Commonly, subsurface rock masses have small apertures. Tensile stress may lead to larger apertures or open fractures. Often shear fractures have much lower aperture values than the tensile fractures.

Aperture may increase by dissolution, erosion etc. particularly in the weathered zone. It may decrease with depth due to lithostatic pressure, and there fracture wall compression strength is an important parameter governing aperture as lithostatic pressure tends to close the fracture opening. Table 2.2 gives aperture ranges as usually classified in rock mechanics.

Fracture aperture can be measured by various methods which include feeler gauge, fluorescent dyes, impression packer, tracer test, hydraulic test etc. Readers may refer to Indraratna and Rajnith (2001) for details of various methods used for measurement of fracture aperture. Often, measurement of aperture in surface exposures is made with a vernier caliper or gauge and the measured opening is termed as the mechanical aperture. In the laboratory, fracture aperture can be estimated by impregnating rock samples

**Fig. 2.26** Fracture connectivity. **a** Different types of fracture terminations: *B* blind; *C* crossing; *D* diffusely connected. **b** Ternary diagram of fracture terminations (After Laubach 1992); the point *BG* corresponds to data from Bundelkhand granites indicating high degree of fracture interconnectivity

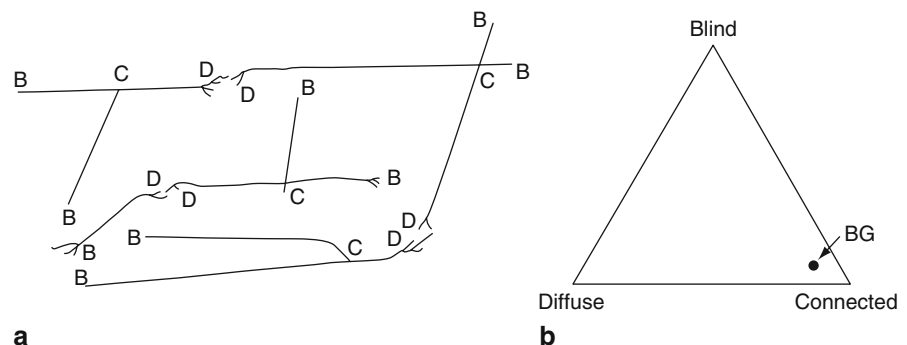


**Table 2.2** Aperture classification by size. (After Barton 1973)

Aperture (mm)	Term
<0.1	Very tight
0.1–0.25	Tight
0.25–0.50	Partly open
0.50–2.50	Open
2.50–10.0	Moderately wide
>10.0	Wide

with dyes or resin and by studying the thin sections under the microscope. This method can even be used in soft sediments viz. clay till (Klint and Rosenbem 2001). Lerner and Stelle (2001) have suggested two field techniques to estimate the in-situ spatial variation of fracture aperture: one is the conventional slug hydraulic testing using packers and in the second technique NAPL (sunflower oil) is injected into isolated fractures in a borehole.

The term ‘equivalent aperture’ is introduced to account for the variation in fracture which can be estimated from tracer test and hydraulic tests. The terms ‘tracer aperture’ and ‘hydraulic aperture’ are introduced by Tsang (1999) depending on the method of estimation. The hydraulic aperture is estimated from hydraulic tests based on the Cubic Law:

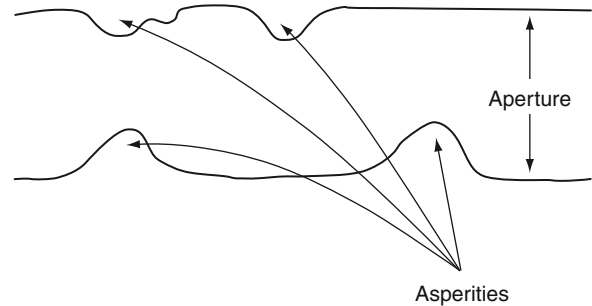
$$T_f \propto a^3 \quad (2.12)$$

where  $a$  is the fracture aperture and  $T_f$  is the transmissivity of the formation (also see Sect. 7.2.1).

The data on discontinuity sets with corresponding apertures is to be recorded. Asperities affect the aperture size and also render its measurement difficult in field. Therefore, when considering fluid flow, apertures are defined in terms of flow properties, as volumetric flow rate is governed by the cube of aperture. Aperture can be integrated with fracture density to give an integrated function representative of hydraulic conductivity (see Sect. 7.2.5).

### 2.3.12 Asperity

Fracture walls are not flat parallel smooth surfaces but contain irregularities, called asperities (Fig. 2.27). The asperity reduces fluid flow and leads to a local channelling effect of preferential flow. This reduces the

**Fig. 2.27** Asperities in fracture walls

effective porosity and makes flow velocities irregular. Observations on asperities should be made for each type of fracture surface and measurement made. Mean height of asperities together with Reynolds number  $Re$  has a direct influence on flow regime, i.e. laminar vs. turbulent flow (Sect. 7.1.1).

### 2.3.13 Wall Coatings and Infillings

It is the solid material occurring between the adjacent walls of a discontinuity, e.g. clay, fault gouge, breccia, chert, calcite, etc. Filling material could be homogeneous or heterogeneous, and could partly or completely fill the discontinuity. The material may have variable permeability, depending upon mineralogy, grain size, width etc. The net effect of wall coatings and infillings is a reduced aperture.

## 2.4 Methods of Field Investigations

Methods of field investigations can be classified into two broad types (Jouanna 1993): 2D and 3D (Table 2.3). The 2D methods are based on observations made at rock surface, at surface or subsurface levels. They include scanline surveys, borehole surveys, and different types of areal surveys (Fig. 2.28). These methods give an idea of the hydrogeological properties at and around the site of observation.

The 3D methods are aimed at gathering information on the bulk volumetric properties involving inner structure of the fractured rock mass. There can be direct or indirect 3D methods. Brief descriptions of the various 2D and 3D methods are given below.

**Table 2.3** Methods of field investigations

1.	2D Methods—Based on rock surface observations on lithology, structure, fractures, and their characteristics; made at surface or subsurface levels
1.1	Scanline surveys
1.2	Areal surveys—on outcrops, pits, trenches, adits, drift etc. including terrestrial geophotogrammetry and remote sensing
1.3	Borehole surveys—including drilling, study of oriented cores, borehole logging, dipmeter, borehole cameras and formation microscanner methods
2.	3D Method—Investigations aimed at bulk volumetric properties of rock mass in 3D
2.1	Hydraulic well tests
2.2	Hydrochemical methods
2.3	Geophysical methods including seismic, electrical, EM, gravity, magnetic and georadar

### 2.4.1 Scanline Surveys

Scanline surveys involve direct observation of rock features along a line on the rock surface, e.g. on an outcrop, drift face, excavation, adit etc. (Fig. 2.22). Scanlines are usually horizontal; however, vertical scanlines are preferred where fractures are mostly horizontal. Data on fractures obtained by sampling techniques such as along scanline (and also borehole) are strongly biased towards the fractures oriented perpendicular to the scanline/core and needs to be corrected for sampling bias by applying correction (Terzaghi 1965).

A suitable rock exposure or face is selected. A sample scanline is marked on the face, and its orientation (rake on the face) is recorded. Fractures intersecting the line are collected. Each fracture is represented by its trace which can be measured. Observations are made for various parameters, like: location of the fracture trace intersection with the scanline; orientation of the fracture and angle made with the scanline; termination type if seen and connectivity; alternatively, whether the

fracture extends beyond the top of face/batter; fracture type and other relevant fracture characteristics.

### 2.4.2 Areal Surveys

Areal surveys can be treated as extension of the scanline surveys. They are used for surveying fracture characteristics on a rock surface area, e.g. on an outcrop, drift face, adit, tunnel etc. (Fig. 2.23). In field, an area is first demarcated on a rock surface for observation and statistical sampling. Detailed observations on fracture characteristics are made within the marked area where all the fractures data are collected.

Direct observations and field mapping at natural rock outcrops is an old established technique. Weathering, surficial cover, soil, vegetation etc. influence the accessibility and visibility of good outcrops. Excavations, pits and trenches are made to expose the fresh rocks at shallow depth for visual inspection. Subsurface direct observation can be made in adits and tun-

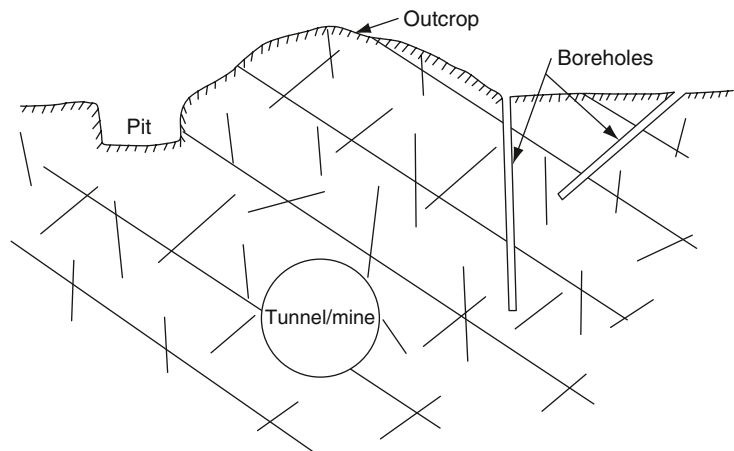


**Fig. 2.28** The various 2D methods of field investigations

nels. Geological maps of rock faces exposed can be prepared and fracture characteristics measured.

Remote sensing includes study of photographs and images acquired from aerial and space platforms. This technique can give valuable information on geology, structure, fractures, lineaments etc. and forms an important mapping tool (Chap. 4). Further, stereo-photographs of rocks exposed in outcrops, scarps, excavations, etc. can be taken from a ground-based (terrestrial) platform. These stereo pairs can be studied and measurements of fracture characteristics can be done in laboratory.

### 2.4.3 Borehole Surveys

These are the only tools for direct observations of rock surface and features occurring at depth. A number of methods are available. As drilling is expensive, optimum combination of methods is employed for getting maximum information from drilling. In the case of vertical and sub-vertical fractures, inclined bores are preferred to intercept a number of such fractures. Study of drill cores, particularly oriented drill cores provides data on orientation of structures, fractures, their apertures as well as infillings. Further, borehole walls can be studied in several ways. Geophysical well logging is a standard technique, including electrical, caliper, radioactivity, magnetic logging etc. These give information on lithology and structure. Borehole televiewer provides images of the borehole walls with joints and fractures. Dipmeter and formation microscanner help measure orientation of structural features at depth in-situ (for drilling and well observation techniques, see Chap. 5).

It may be mentioned here again that data on fractures obtained by sampling techniques such as along scanline and borehole are strongly biased towards the fractures oriented perpendicular to the core/scanline and needs to be corrected for sampling bias by applying a correction (Terzaghi 1965).

### 2.4.4 3D Methods

As mentioned above, 3D methods are aimed to provide information on bulk volumetric properties of

the fractured rock mass. These methods include hydraulic well tests, hydrochemical methods and geophysical techniques. The hydraulic well tests comprise pumping tests of various configurations and types, and give bulk volumetric assessment. Slug tests will give a first hand dependable information about the hydraulic conductivity at much lower costs than pumping tests (see Chap. 9). In hydrochemical methods various types of geochemical tracer studies and solute transport studies are carried out for bulk volumetric hydrogeological characterization (see Sect. 10.3). Further, a number of geophysical methods are used such as seismic, electrical, EM, gravity, magnetic and georadar. They are briefly described in Chap. 5 from a hydrogeological investigation point of view.

#### Summary

Most rocks possess fractures, broadly termed as discontinuities here, which facilitate storage and movement of fluids through the medium. The discontinuities may be formed by planar surfaces such as bedding plane, foliation, fractures, faults shear zones etc. The common systematic fractures are of three main genetic origins: extensional, shear and hybrid. Faults can cause truncation or repetition of aquifers and may lead to formation of springs and interbasinal subsurface flow. Discontinuities are characterized in terms of a number of parameters such as orientation, spacing, persistence, fracture and shape, connectivity, aperture coatings etc., and these data may be collected from field surveys by scanline method or areal surveys or in borehole observations.

### Further Reading

- Billings MP (1972) Structural Geology. 3rd ed., Prentice Hall, New Delhi, 606 p.
- Lee CH, Farmer I (1993) Fluid Flow in Discontinuous Rocks. Chapman and Hall, London, 169 p.
- Marshak S, Mitra G (2006) Basic Methods of Structural Geology. 2nd ed., Prentice Hall, New Jersey, 446 p.
- van Golf-Racht TD (1982) Fundamentals of Fractured Reservoir Engineering. Elsevier, Amsterdam, 710 p.




<http://www.springer.com/978-90-481-8798-0>

Applied Hydrogeology of Fractured Rocks  
Second Edition


Singhal †, B.B.S.; Gupta, R.P.

2010, XIX, 408 p., Hardcover

ISBN: 978-90-481-8798-0


 <b>SNC • LAVALIN</b>	<b>TECHNICAL NOTE</b> 2018 Groundwater Monitoring	Prepared by : Laurie Tremblay Reviewed by : Denis Vachon		
		Rev.	Date	Page
	645182-3000-4EER-0001	00	2018-12-17	21

## APPENDIX F: PURGING OPERATIONS BY AGNICO EAGLE – (ELECTRONIC FILE)

 <b>SNC • LAVALIN</b>	<b>TECHNICAL NOTE</b> 2018 Groundwater Monitoring	Prepared by : Laurie Tremblay Reviewed by : Denis Vachon		
	645182-3000-4EER-0001	Rev.	Date	Page
	00	2018-12-17	22	

## APPENDIX G: GROUNWATER SAMPLING PROCEDURES



 <b>SNC • LAVALIN</b>	<b>SAMPLING PROCEDURE</b> <b>2018 Groundwater Monitoring</b>		Prepared by : Laurie Tremblay	
	645182-3000-4EER-0001		Reviewed by : Denis Vachon	
	Rev.	Date	Page	
	PA	2018-12-12	1	

**Purpose:**

- › Conduct a groundwater (GW) monitoring program to investigate mining impacts on local GW. This is in accordance with both Meadowbank NWB and NIRB permits.
- › Standardize methodologies

**Groundwater Sampling SOP:**

GW sampling consists of measuring field parameters and collecting GW samples within the designated bottles, twice a year, at the same period of the year (early July and early September).

**Wells to sample:**

Well name	x	y	Screens depth (m)	Pump depth (m)
MW-16-01	638750.9	7214427.3	89-101	95
MW-IPD-01 (s)	639240.3	7214249.9	51-69	60
MW-IPD-01 (d)	639240.0	7214245.0	163-181	175
MW-IPD-07	638859.6	7212597.2	42-50	40
MW-IPD-09	639065.2	7213024.5	62-80	70


**A week before sampling check for:**

- Heat trace cables functionality (can't be check at MW-IPD-01 (d) since heat trace cables start 2 m below ground, so the lines won't feel warm);
- Make sure the light tower generator are running at MW-IPD-07 and MW-IPD-09
- Make sure the nitrogen tanks are in place and secured



Light tower generator at MW-IPD-07 and MW-IPD-09 to keep the heat trace cables working



 <b>SNC • LAVALIN</b>	<b>SAMPLING PROCEDURE</b> 2018 Groundwater Monitoring		Prepared by : Laurie Tremblay Reviewed by : Denis Vachon		
	645182-3000-4EER-0001		Rev.	Date	Page
			PA	2018-12-12	2

**Material required for sampling:**


- Nitrogen tanks (JDE number 134720) already installed at each sampling station
- Solinst double valve pump (already in the monitoring well), two spare pumps are in the cooler
- Nitrogen regulator
- Solinst Control unit 464 ECU 250 psi
- Black drive line and supply line
- Clean pails
- Graduated measuring cups
- Calibrated multi-parameter probe and a flow through cell (to prevent the water sample to be in contact with oxygen): temperature, specific conductivity, pH, oxydoreduction potential, dissolved oxygen, total dissolved solid, salinity, turbidity;
- Water level probe
- Sampling bottles (see list below)
- Syringe and adapted 0,45 micron filters
- Nitrile gloves
- Permanent marker

**Sampling bottle check list:**

- 1 \* 1 L clear plastic bottle with no preservative
- 1 \* 250 ml clear plastic bottle with no preservative
- 1 \* 125 ml clear plastic bottle with H<sub>2</sub>SO<sub>4</sub>
- 2 \* 125 ml clear plastic bottle with nitric acid (HNO<sub>3</sub>)
- 1 \* 125 ml clear plastic bottle with NaOH
- 1 \* 125 ml clear plastic bottle with NaOH - SGS laboratory bottle
- 1 \* 125 ml clear plastic bottle with HCl

Well name	Pressure left in the nitrogen tank	Gas used for each sampling even	Comment
	psi	psi	
MW-IDP-01s	1600	200	-
MW-IDP-01d	200	800	Need a new nitrogen tank
MW-IDP-07	2200	150	-
MW-IDP-09	2000	150	-
MW-16-01	1000	500	Need a new nitrogen tank soon



 <b>SNC • LAVALIN</b>	<b>SAMPLING PROCEDURE</b> <b>2018 Groundwater Monitoring</b>	Prepared by : Laurie Tremblay		
		Reviewed by : Denis Vachon		
	645182-3000-4EER-0001	Rev.	Date	Page
		PA	2018-12-12	3

### Sampling procedures

#### Prior sampling the water in the monitoring well

- 1- Remove well head cap
- 2- Remove the red plug on well head
- 3- Lower the small water level probe into the hole where the red cap was located and measure the water level from the well head hole level
- 4- Place the ¼ inch waterra line on the well head



Well name	Water level at plastic well head level	HWT casing above ground level	Well casing above ground level	casing above ground level with PVC and well head addition
	m	m	m	m
MW-IDP-01 (s)	18,19	0,17	0,29	0,75
MW-IDP-01 (d)	18,07	0,00	0,28	0,35
MW-IDP-07	1,79	0,06	0,19	0,45
MW-IDP-09	2,36	0,00	0,26	0,45
MW-16-01	5,30	0,17	?	0,745

#### Setting up the nitrogen tank and the gas line

- 5- Screw on the nitrogen regulator on the nitrogen tank and tighten lightly with a 1 1/8in wrench ((ideally not an adjustable wrench since it will damage the bolt)
- 6- Connect the supply line into the regulator to "air in" on the control box
- 7- Connect the drive line from the air out on the control box to the well head





This end goes into the nitrogen



Manual Control Button

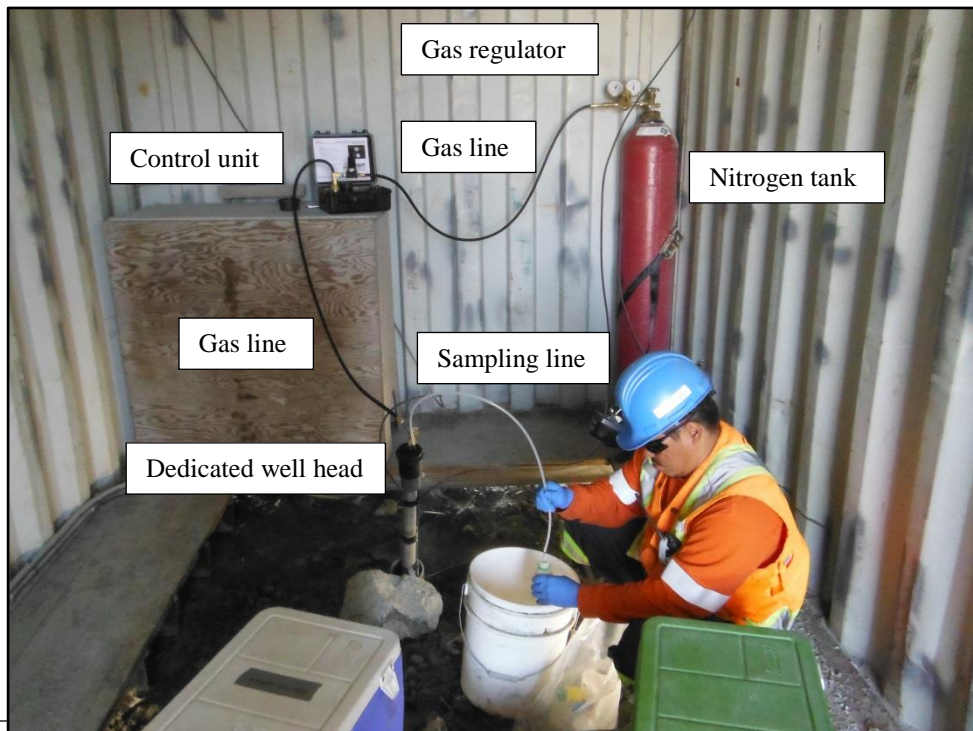
Air Out

Air In

Regulator

Pressure Gauge

Battery Enclosure



Gas regulator

Control unit

Gas line


Nitrogen tank

Gas line

Sampling line

Dedicated well head




 <b>SNC • LAVALIN</b>	<b>SAMPLING PROCEDURE</b> <b>2018 Groundwater Monitoring</b>		Prepared by : Laurie Tremblay	
			Reviewed by : Denis Vachon	
		Rev.	Date	Page
645182-3000-4EER-0001		PA	2018-12-12	5

- 8- **Open** to its maximum position (turning towards the left side) the handle/valve located on the gas pressure regulator at the maximum (the close position would send the maximum nitrogen pressure to the air line and we want to avoid that). The valve should feel loose, not tighten;
- 9- **Slowly open** (1/4 turn to the left) the valve located on the nitrogen tank. You should be able to read the pressure left in the nitrogen tank on the pressure gage located on the right side of the regulator;
- 10- **Slowly closed** (a tiny bit, less than 1/8 turn to the right) the valve located on the gas pressure regulator until the gauge on the left side indicated 150 psi. **NEVER EXCEED 250 psi** or you are going to blow up the controller box.
- 11- On the control box press RUN than select the menu on AUTO mode for Preset Flow Rate.
- 12- This should take 1 minute before the water is flowing.



Well name	Pressure set on control unit box (flow rate set to medium)	Flow setting on controller unit	GW flow rate measured while pumping	Comments
	psi		mL/min	
MW-IDP-01s	50	medium	100	
MW-IDP-01d	110	medium	50	
MW-IDP-07	40	medium	200	Rate too fast, water level was decreasing
MW-IDP-09	50	high	165	
MW-16-01	50	high	100	



 <b>SNC • LAVALIN</b>	<b>SAMPLING PROCEDURE</b> <b>2018 Groundwater Monitoring</b>	Prepared by : Laurie Tremblay		
		Reviewed by : Denis Vachon		
		Rev.	Date	Page
	645182-3000-4EER-0001	PA	2018-12-12	6

- 13- While the water is purging from the monitoring well measure the flow rate with a measuring cup and a timer. The ideal flow rate is equal or below 100 ml/min. Keep measuring and recording the water level. If the water level is not stable and diminishes it means that you are pumping the water from the well and not from the bedrock formation and you want to avoid that. You want to keep a flow rate that will keep your water level stable.
- 14- Let it run for 45 minutes, measure and record physicochemical parameters and record every 15 minutes.
- 15- Sample the water from the well when you have more than 3 consecutive readings that are:
- a. pH is within 0.1 or 0.2 of a standard unit;
  - b. temperature is within 0.2 °C or 3%;
  - c. specific conductance is within 5% for values equal to or less than 100 microsiemens and 3% for values greater than 100 microsiemens;
  - d. DO (dissolved oxygen) is within 10%;
  - e. Eh/ORP (oxido-reduction potential) is within 10 millivolts;
  - f. Turbidity is within 10% for values greater than 1 NTU but less than 100 NTU;
- 16- To filter the sample for the dissolved metal analysis, use a larger filter and hold it to ¼ diameter LDPH tubing (respect the flow direction indicated by an arrow) or fill the syringe directly with the water coming out of the ¼ diameter LDPH tubing, install a small filter on the syringe and fill the dissolved metal bottles.
- 17- Remove the filter and fill all the other bottles.
- 18- See instruction to set up personalised drive and vent ranges.

<https://www.solinst.com/products/groundwater-samplers/464-pneumatic-pump-control-units/electronic-control-unit-datasheet/>

### Optimizing Pumping Pressure


To collect a representative sample, especially when monitoring for volatiles, it is important to avoid the drive gas to enter the pump and aerate the sample water during a drive period. This means, you need to carefully calculate the appropriate pumping pressure to be applied. To do so, it is important to measure the depth of the static water level.

The pumping pressure needed is calculated due that it takes about 1 psi of pressure to raise 2.3 ft. of water plus 10 psi for line loss. To calculate the pumping pressure needed in psi, take depth to static level in feet, and multiply by 0.43 psi/ft. (1 psi /2.3 feet = 0.43 psi/ft.). E.g., if depth to static water level is 50 ft., the pumping pressure needed is calculated by the following:

50 ft. to static level x 0.43 psi/ft. + 10 psi = 32 psi needed.

Refer to Solinst Website for more instruction: <https://www.solinst.com/products/groundwater-samplers/408-double-valve-pumps/technical-bulletins/getting-best-quality-samples-double-valve-pump.php>



 <b>SNC • LAVALIN</b>	<b>TECHNICAL NOTE</b> 2018 Groundwater Monitoring	Prepared by : Laurie Tremblay Reviewed by : Denis Vachon		
		Rev.	Date	Page
	645182-3000-4EER-0001	00	2018-12-17	23

## APPENDIX H: TEMPLATE SHEET FOR GROUNDWATER SAMPLING





## Groundwater sampling


**REMINDER :** Stop taking value when 3 samples or within the range listed below

pH is within 0.1 or 0.2	D.O. (dissolved oxygen) is within 10%
Turbidity is within 10 % for values greater than 1 NTU but less than 100 NTU	
Temperatur is within 0.2 °C OR 3 %	Eh/ORP (oxidoreduction potential is within 10 millivolts
Specific conductance is within 5% for values equal to or less than 100 microsiemens and 3% for values greater than 100 microsiemens	

**BOTTLE CHECKLIST**

- 1 \* 1 L clear plastic bottle with no preservative
- 1 \* 250 ml clear plastic bottle with no preservative
- 1 \* 125 ml clear plastic bottle with H2SO4
- 2 \* 125 ml clear plastic bottle with nitric acid (HNO3)
- 1 \* 125 ml clear plastic bottle with NaOH
- 1 \* 125 ml clear plastic bottle with NaOH - SGS laboratory bottle
- 1 \* 125 ml clear plastic bottle with HCl

**Field Notes:** Don't forget to write down the total of volume purged

---




---




---



---

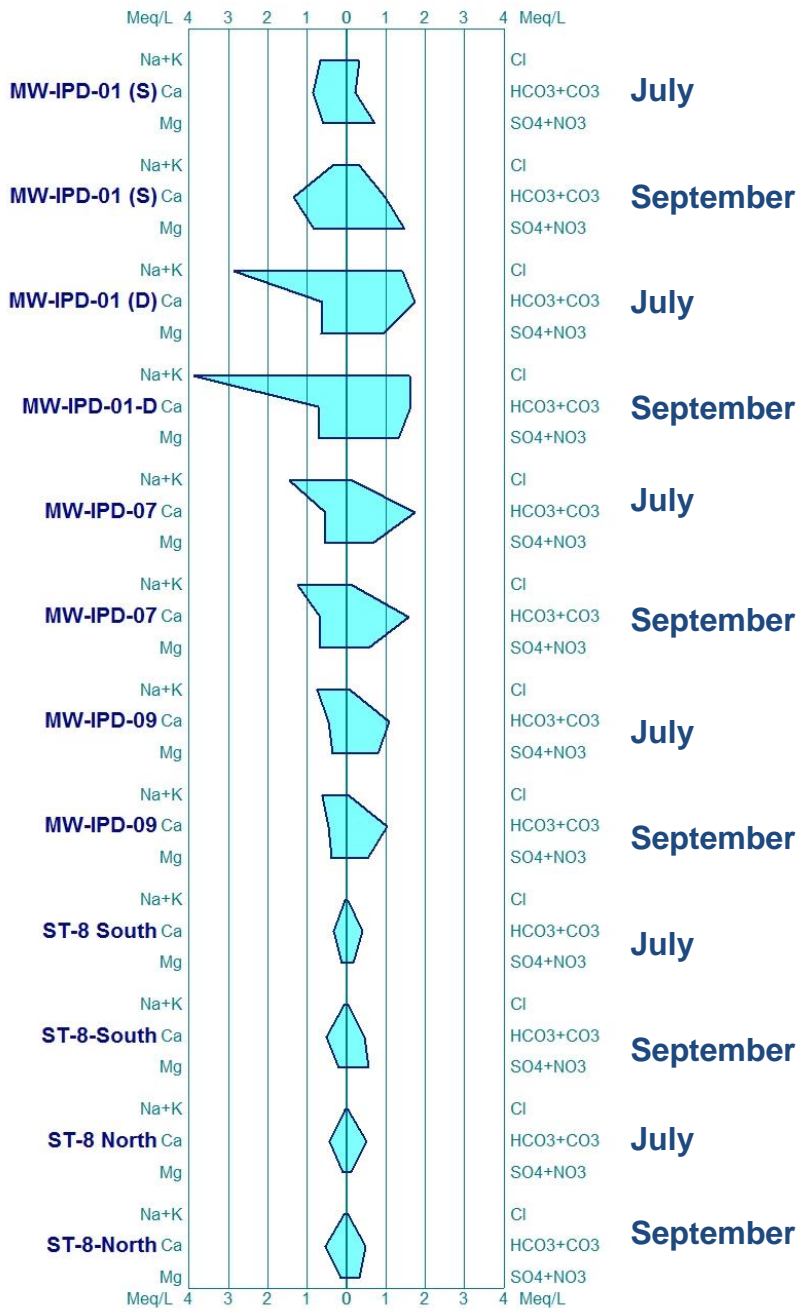
 <b>SNC • LAVALIN</b>	<b>TECHNICAL NOTE</b> 2018 Groundwater Monitoring	Prepared by : Laurie Tremblay Reviewed by : Denis Vachon		
	645182-3000-4EER-0001	Rev.	Date	Page
		00	2018-12-17	24


## APPENDIX I: GEOCHEMICAL DATA – (ELECTRONIC FILE)

 <b>SNC • LAVALIN</b>	<b>TECHNICAL NOTE</b> 2018 Groundwater Monitoring	Prepared by : Laurie Tremblay Reviewed by : Denis Vachon		
	645182-3000-4EER-0001	Rev.	Date	Page
		00	2018-12-17	25

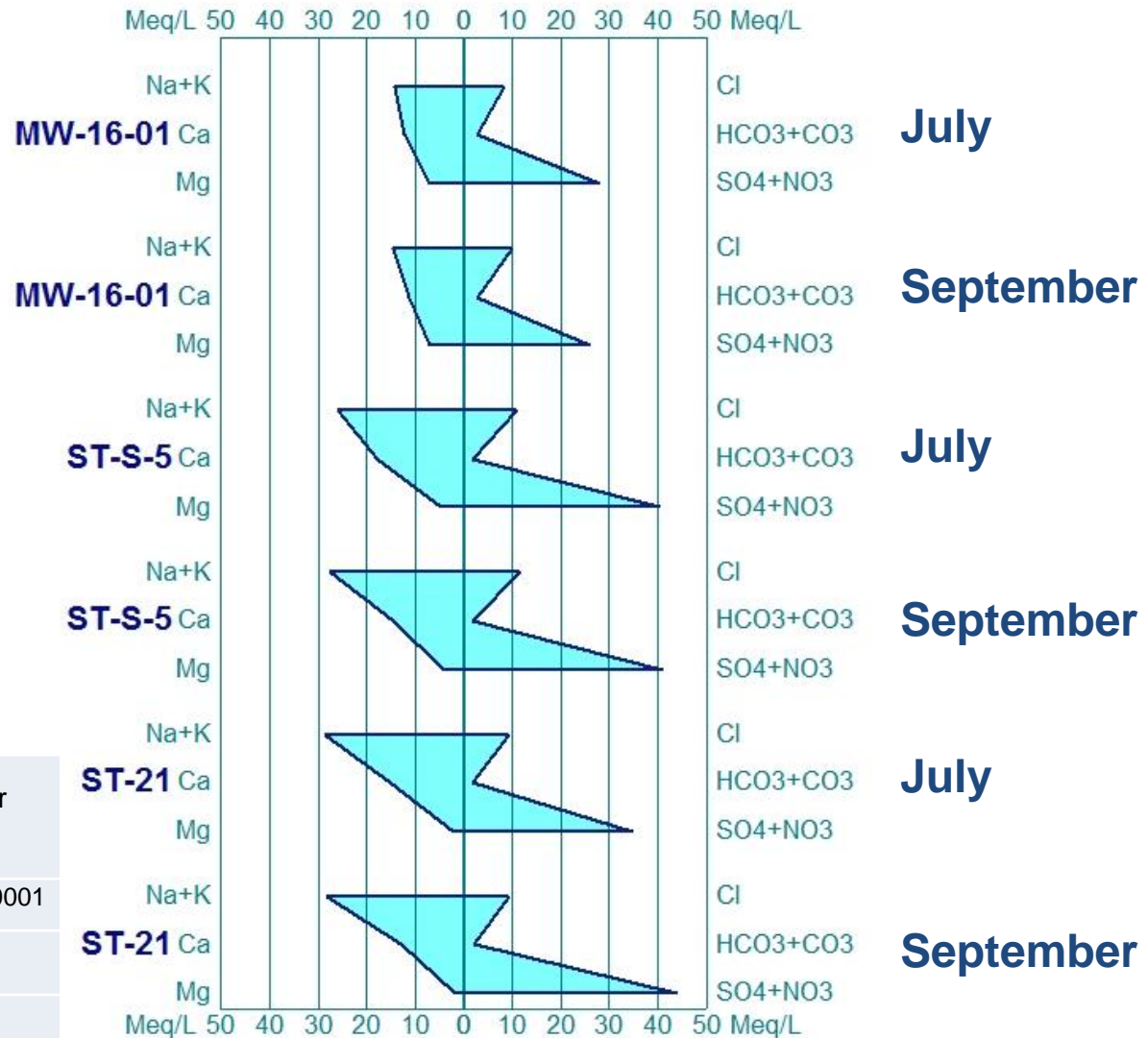
## APPENDIX J: STIFF DIAGRAMS

# Natural groundwater signature (scale 0-5 Meq/L) 2018



 <b>SNC • LAVALIN</b>	2018 Groundwater Monitoring
	645182- 3000- 4E ER-0001
Prepared by : Laurie Tremblay Reviewed by : Denis Vachon	<b>Figure 1</b>
Rev.	Date
PA	2018-12-12

# Water indicating Reclaim water signature (scale 0-50 Meq/L) in 2018



**SNC • LAVALIN**

2018 Groundwater  
Monitoring

645182- 3000- 4E ER-0001

Prepared by : Laurie Tremblay

Reviewed by : Denis Vachon

Figure 2

Rev.

Date

PA

2018-12-12

**APPENDIX B**

**2003 - 2018 Historical Data**

---

---

**TO :** Robin Allard (AEM) **DATE :** April 5<sup>th</sup>, 2019

**C.C. :** Dominic Tremblay, Daniel Meles (SNC)

**FROM :** Guillaume Comeau, Anh-Long Nguyen (SNC) **REF. :** 663133-7000-40ER-0001, ver. A00

**SUBJECT :** Meadowbank Annual Groundwater Quality Report – Historical Groundwater Analytical Results

---

## 1.0 SCOPE OF WORK

SNC-Lavalin was mandated by Agnico Eagle Mines (AEM) to compile the groundwater quality analysis sampled around the pits at Meadowbank and provide a factual analysis of the historical groundwater quality data. The scope of work for this mandate involves the following:

1. Compilation of groundwater and surface water quality data sampled over the years at the Meadowbank site in a single Microsoft Excel file, in a database format;
2. Present historical analytical results for groundwater quality in summary tables for all parameters; and,
3. Produce historical analytical graphs for Chloride, Sulfate, Total Cyanide, Total Copper, Total Iron and Total Arsenic.

The following memorandum presents a summary of the historical groundwater quality trends for selected parameters that were sampled around the pits and provide key factual observations based on the available data.

## 2.0 HISTORICAL DATA

Table 1 summaries the available analytical results for each groundwater sampling station, grouped based on the following site areas:

- South Cell and Central Dike;
- East flat;
- Goose Pit;
- Portage Pit A;
- Portage Pit E.

Historical groundwater quality data starts from 2003. From 2003 to 2016, 14 groundwater monitoring wells were installed to characterize the groundwater (SNC-Lavalin, 2018) in these areas. Throughout the years, a total of 34 groundwater samples and 21 duplicates were collected from these sampling wells.

However, most of the monitoring wells became inoperable due to the challenging arctic condition and permafrost environment at Meadowbank. In 2017, groundwater samples were taken from 4 wells (MW-08-02, MW-16-01,



ST-8-North and ST-8-South) and pit wall seepages. In 2018, four additional monitoring wells (MW-IPD-01(s), MW-IPD-01(d), MW-IPD-07 and MW-IPD-09) were added to the sampling network. To this day, out of the 18 monitoring wells, a total of 8 wells remain operable.

Appendix A presents the location of sampling monitoring wells stations and site areas (SNC-Lavalin, 2018).

Appendix B presents summary tables of the water quality analytical results at these groundwater sampling stations.

**Table 1: Historical groundwater sampling available results**

Site Area / Station ID	Station Type	2003	2004	2005	2006	2007	2008	2009	2010	2011	2012	2013	2014	2015	2016	2017	2018
<b>South Cell / Central Dike</b>		x			x				x	x			x	x	x	x	x
BH-10-01	Temporary borehole								x								
MW-03-04	Monitoring Well	x															
MW-06-07	Monitoring Well				x												
MW-11-02	Monitoring Well									x							
MW-14-01	Monitoring Well											x	x				
MW-16-01	Monitoring Well														x	x	x
<b>East Flat</b>							x	x	x	x	x	x	x	x	x	x	x
MW-08-02	Monitoring Well						x	x	x	x	x	x	x	x	x	x	x
MW-08-03	Monitoring Well						x					x					
ST-8-North	Pumping well															x	x
ST-8-South	Pumping well															x	x
ST-8-discharge	Discharge from PW													x	x	x	x
MW-IPD-01(S)	Monitoring Well																x
MW-IPD-01(D)	Monitoring Well																x
<b>Goose Pit</b>		x	x		x	x	x	x	x	x						x	x
BG-Seep-21m	Pit wall seepage															x	x
BG-Seep-42m	Pit wall seepage															x	x
BG-Seep-80m	Pit wall seepage															x	
MW-03-01	Monitoring Well	x	x		x												
MW-03-02	Monitoring Well	x	x														
MW-06-05	Monitoring Well				x	x	x	x	x								
MW-06-06	Monitoring Well				x												
MW-11-01	Monitoring Well									x							
MW-IPD-07	Monitoring Well																x
<b>Portage Pit A</b>		x	x													x	x
MW-03-03	Monitoring Well	x	x														
Pit-A-Seep-East	Pit wall seepage															x	
Pit-A-Seep-North	Pit wall seepage																x
<b>Portage Pit E</b>														x	x	x	x
Pit E3-B2	Horizontal hole													x			
Pit E3-B6	Horizontal hole													x	x		
Pit E3-B7	Horizontal hole														x		
Pit E4	Pit wall seepage														x		
Pit-E-Seep-North	Pit wall seepage															x	x
Pit-E-Seep-SW	Pit wall seepage															x	
MW-IPD-09	Monitoring Well																x



### 3.0 KEY OBSERVATIONS

#### 3.1 Approach

Historical groundwater quality analytical results, including monitoring wells and pit wall seepages stations (as shown in Table 1) were grouped for each site location. For this study, historical groundwater quality analytical results are presented for the following parameters, which are typically associated with the reclaim water chemical signature:

- Chloride;
- Sulfate;
- Total Cyanide;
- Total Copper;
- Total Iron;
- Total Arsenic.

Maximum average concentrations (MAC) for water discharge to Third Portage Lake, as per Meadowbank Mine Water License (Type A Water License 2AMMEA1525 in July 2015), are found at Table 2 for selected parameters and on the following figures.

**Table 2: Water Licenses discharge criteria**

Analytical Parameter	Unit	Water License Maximum Average Concentration Discharge to Third Portage Lake
Chloride	mg/L	1000
Sulfate	mg/L	Na
Total Cyanide	mg/L	0.5
Total Copper	mg/L	0.1
Total Iron	mg/L	Na
Total Arsenic	mg/L	0.3
Note: na: Not applicable.		

If the case of non-detect parameter, half the value of the laboratory's detection limit is used in the graph.

No analytical results were discarded from the produced graphs. Some results might not be representative of the groundwater quality for different reasons, such as the use of de-icing salts during former monitoring wells installations, purging or sampling methodology, etc. (SNC-Lavalin, 2018).

Note that the water quality data shown on the figures for each site could come from different sampling stations located in the same area.



### 3.2 Chloride

- Total chloride concentrations remain below MAC, but for 3 results.
- High chloride concentrations were found in several monitoring wells before 2014, especially in the Goose Pit area. The cause of these elevated level of chloride could related to the used of de-icing salt and calcium chloride brine solution used to prevent the boreholes of the monitoring well from freezing after drilling operation and remains present in the groundwater for years despite intensive purging of the wells after installation.
- Chloride concentrations at South Cell and Central Dike area show higher values than the other monitoring wells and could be directly related to the reclaim water stored in the South Cell Tailings Storage Facility (TSF).

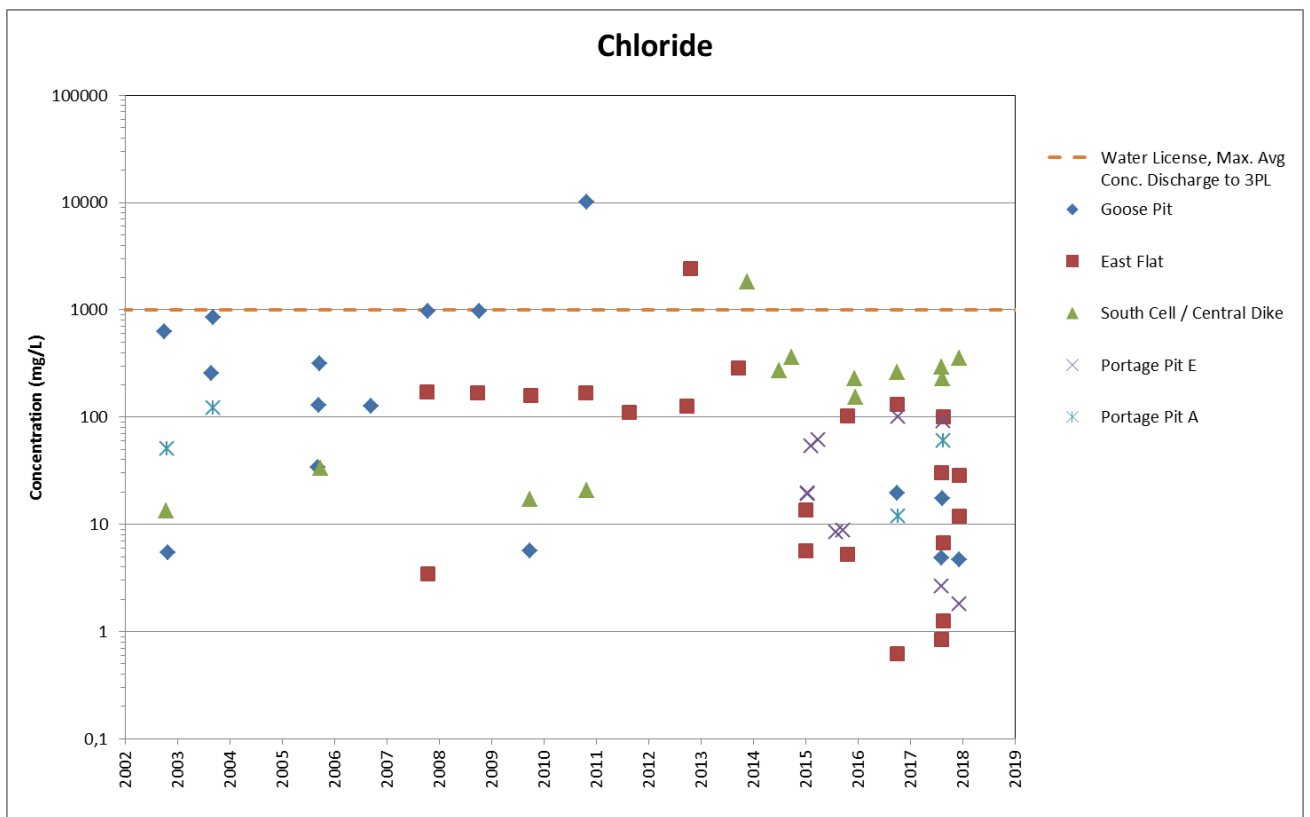
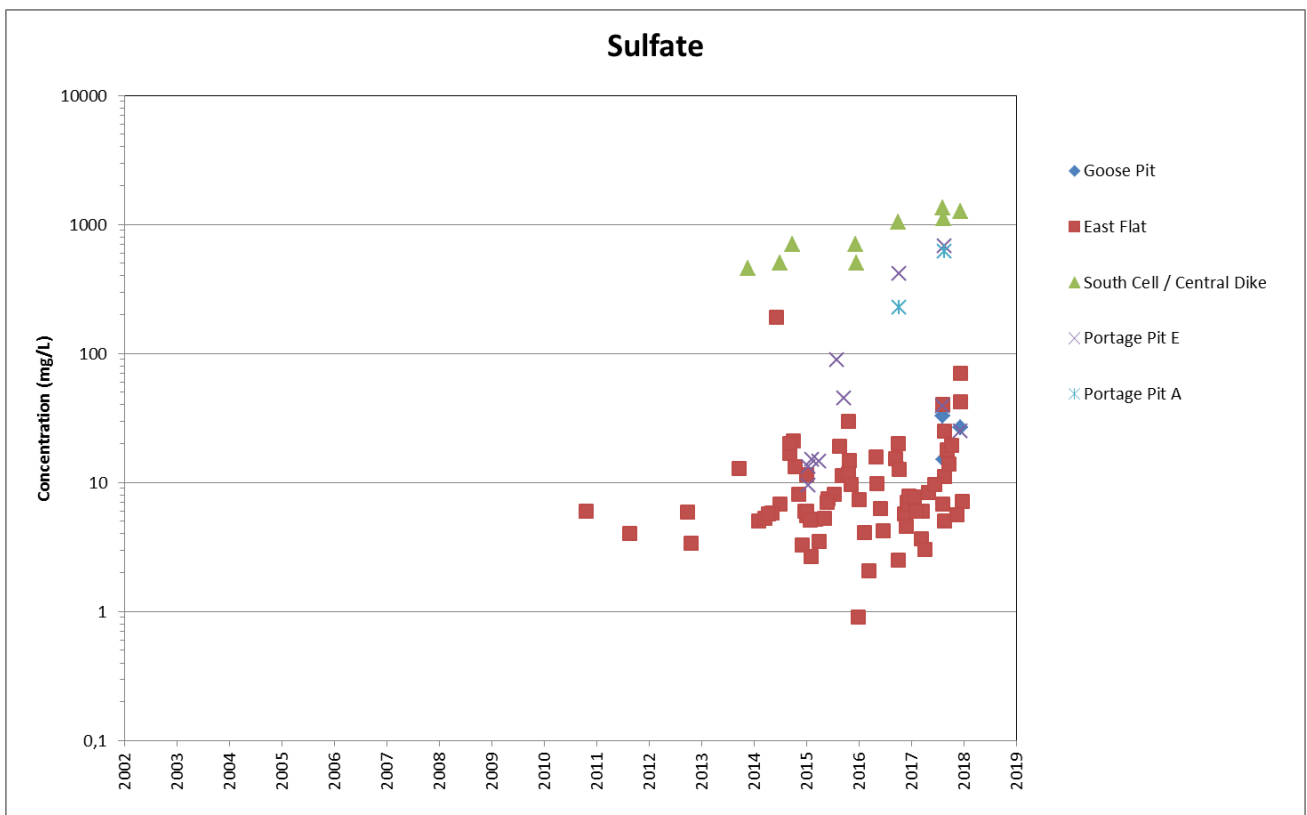


Figure 1: Historical Chloride concentrations in groundwater

### 3.3 Sulfate

- There is no MAC for sulfate concentrations;
- Sulfate concentrations seem to be trending upward since 2014 at South Cell and Central Dike area. The presence of sulfate could be directly related to the reclaim water stored in the South Cell TSF.
- East flat area shows lower sulfate concentrations generally between 2 and 300 mg/L, without clear trend.
- At Portage Pit E, higher sulfate concentrations were found during the latest sampling campaigns, mainly from sampling locations located closer to the reclaim water stored in the South Cell TSF.



**Figure 2: Historical Sulfate concentrations in groundwater**

### 3.4 Total Cyanide

- All historical total cyanide concentrations in groundwater are below MAC criteria;
- Total cyanide concentrations are higher in samples taken around the South Cell and Central Dike area, since the reclaim pond is located nearby;
- No clear trend can be interpreted from these historical concentrations.

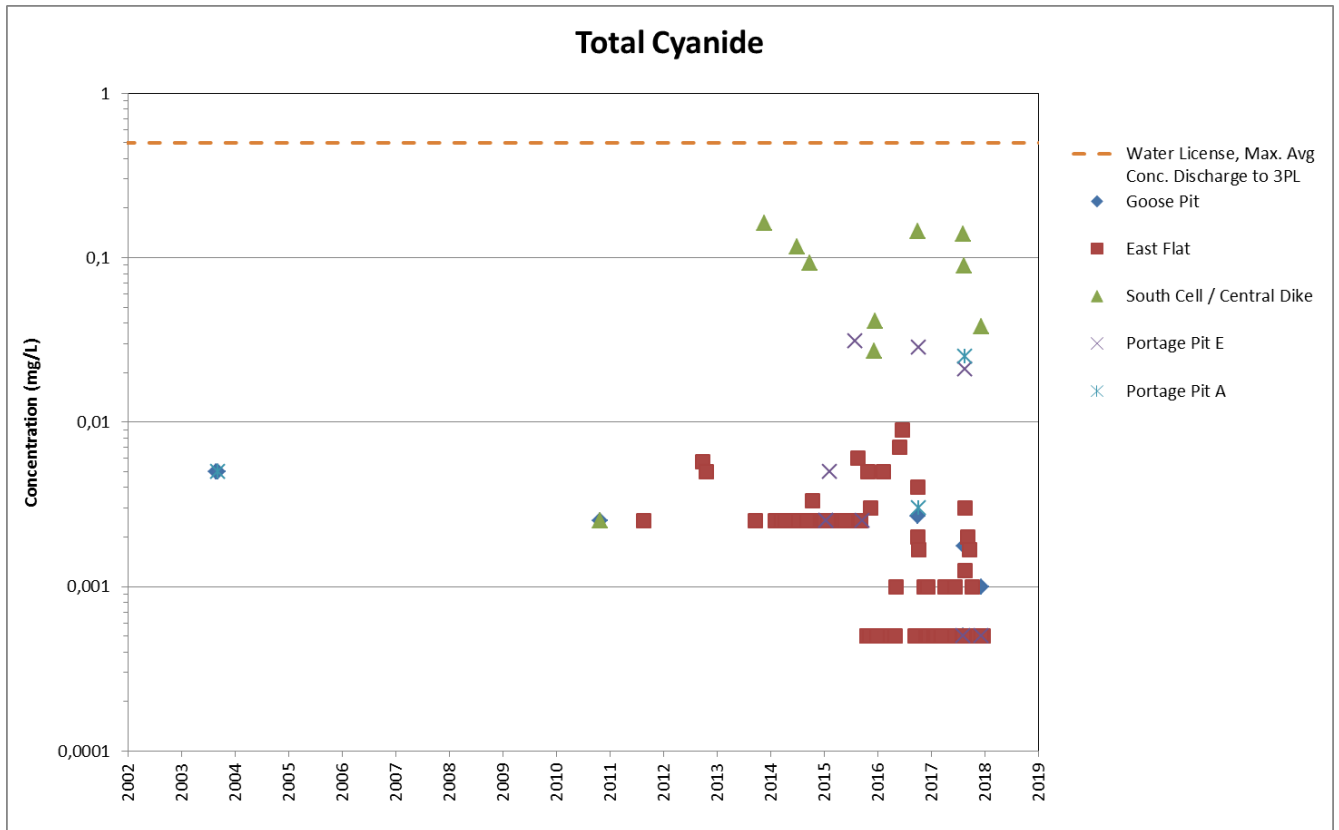


**Figure 3: Historical Total Cyanide concentrations in groundwater**





### 3.6 Total Iron

- There is no MAC for Total Iron concentrations;
- Total iron concentrations in groundwater seem to have increased slightly at South Cell and Central Dike area since 2005 and could be related with the storage of reclaim water in the South Cell TSF.

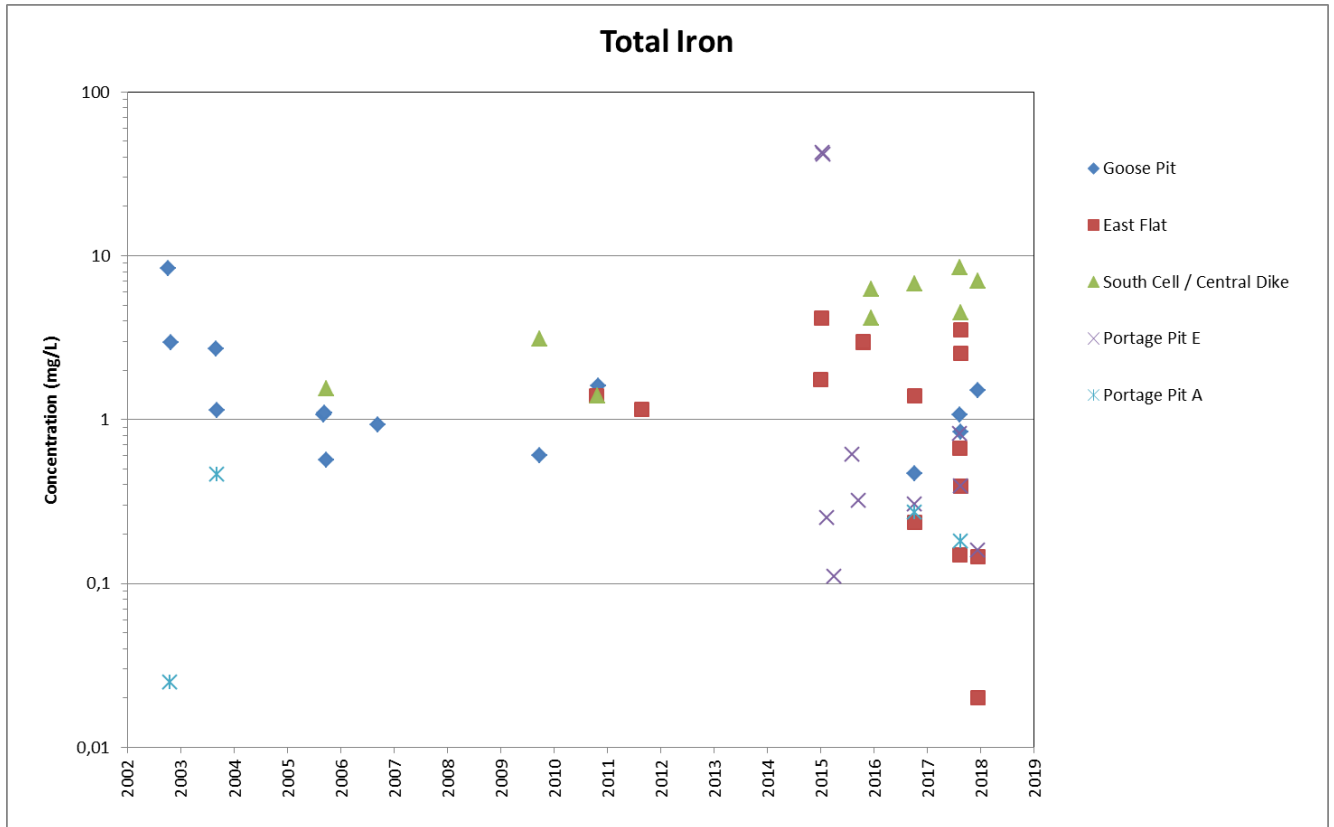
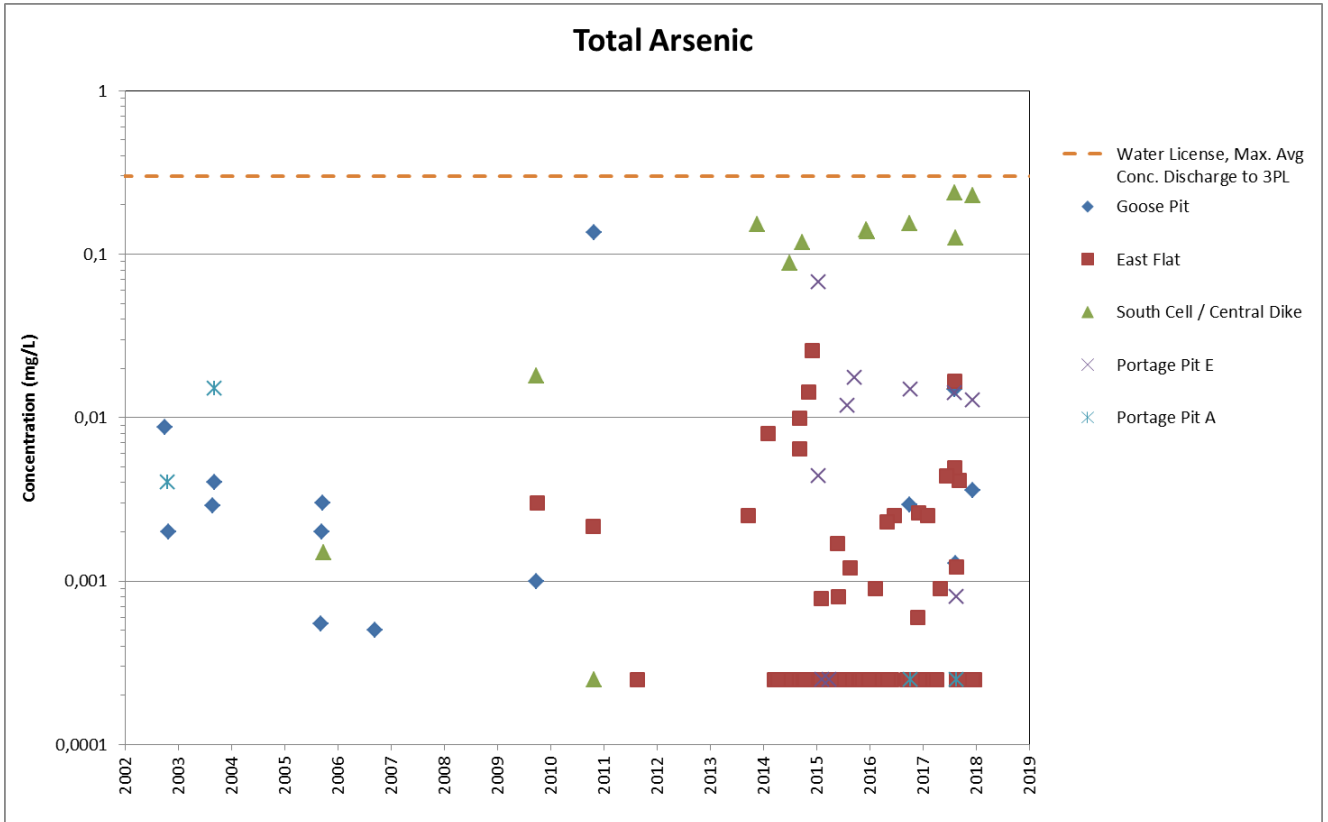


Figure 5: Historical Total Iron concentrations in groundwater

### 3.7 Total Arsenic

- All historical total arsenic concentrations in groundwater are below MAC criteria;
- Total arsenic concentrations at South Cell and Central Dike area are relatively stable since 2013, but are higher when compared to the other samples taken around the pit. This could be due to the presence of reclaim water stored in the South Cell TSF.



**Figure 6: Historical Total Arsenic concentrations in groundwater**

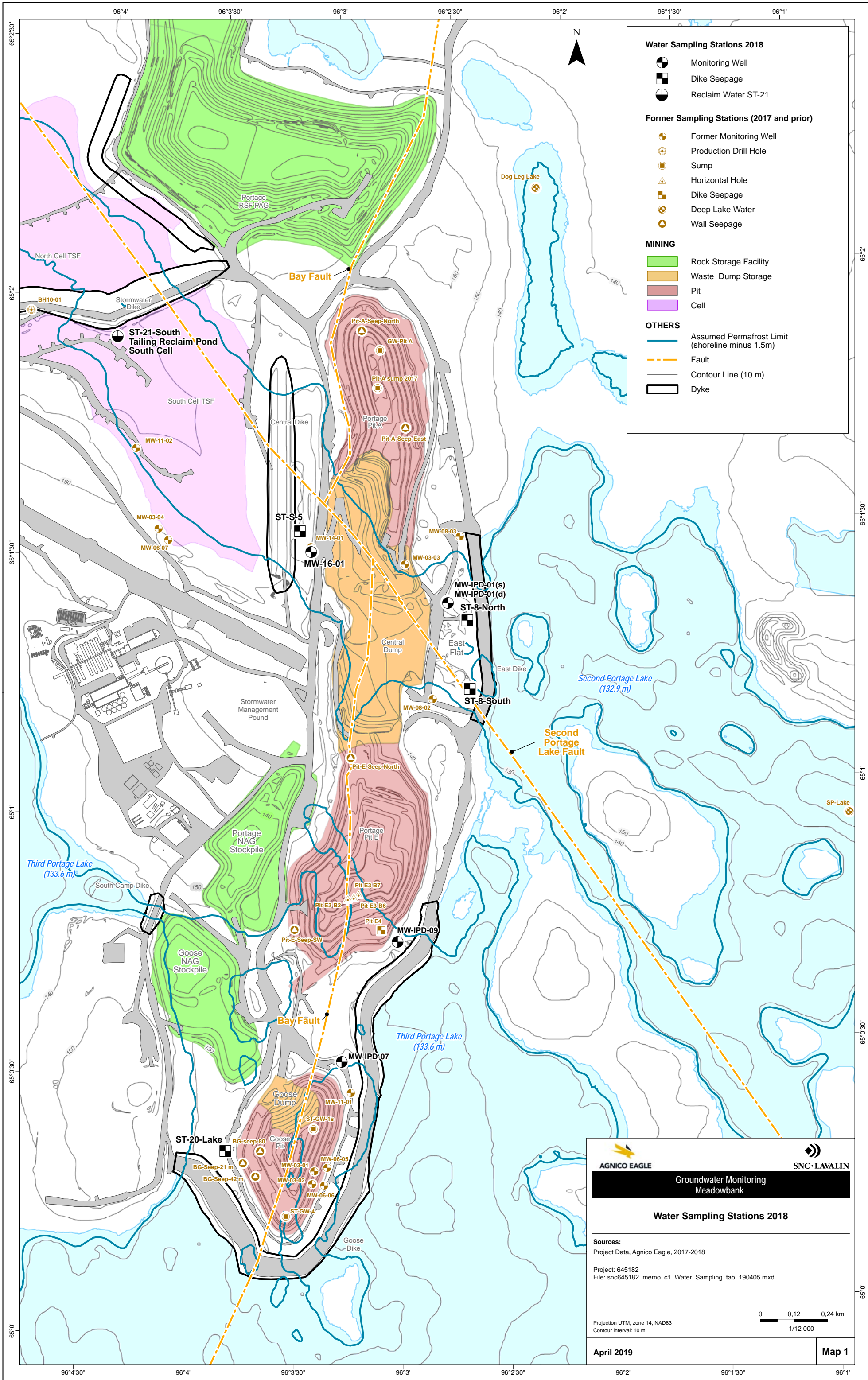
### 4.0 REFERENCES

SNC-Lavalin (2018). 2018 Groundwater Monitoring. Technical Note. 645182-3000-4EER-0001. Rev. 00 2018-12-17.

## **Appendix A: Groundwater Sampling Stations**







**Water Sampling Stations 2018**

- Monitoring Well
- Dike Seepage
- Reclaim Water ST-21

**Former Sampling Stations (2017 and prior)**

- Former Monitoring Well
- Production Drill Hole
- Sump
- Horizontal Hole
- Dike Seepage
- Deep Lake Water
- Wall Seepage

**MINING**

- Rock Storage Facility
- Waste Dump Storage
- Pit
- Cell

**OTHERS**

- Assumed Permafrost Limit (shoreline minus 1.5m)
- Fault
- Contour Line (10 m)
- Dyke

**AGNICO EAGLE** **SNC-LAVALIN**

Groundwater Monitoring  
Meadowbank

**Water Sampling Stations 2018**

**Sources:**  
Project Data, Agnico Eagle, 2017-2018

Project: 645182  
File: snc645182\_memo\_c1\_Water\_Sampling\_tab\_190405.mxd

Projection UTM, zone 14, NAD83  
Contour interval: 10 m

0 0,12 0,24 km  
1/12 000

**April 2019** **Map 1**



## **Appendix B: Groundwater Analytical Results**

---

APPENDIX B - Analytical Results for Groundwater Stations

Site Area Station ID Sampling Date	Unité	Goose Pit						
		BG-Seepage-21m		BG-Seepage-42m		BG-Seepage-80m	MW-03-01	
		2018-07-16	2017-09-03	2018-07-16	2017-09-03	2017-09-03	2006-08-08	2004-08-07
<b>FIELD PARAMETERS</b>								
Temperature	degC	2,5	3	6,2	3,5	7,6	7,7	8
pH	-	7,95	7,86	7,98	7,92	8,33		8,03
Conductivity	µS/cm	87,2	92,7	193,5	168,4	232		2500
Oxygen Reduction Potential	mV	-160,6	-188,2	-156,9	-174,2	-60,7		119
Turbidity	NTU	1,57	3,49	4,79	2,3	2,74		
<b>LABORATORY ANALYSIS</b>								
<b>General</b>								
Total Alkalinity	mg/L	68	61	108	104	97		27,3
Bicarbonate Alkalinity HCO3	mg/L	68	61	108	104	97		33,3
Carbonate Alkalinity CO3	mg/L	<2	<2	<2	<2	<2		<0,5
Reactive silica	mg/L	9,4	7,9	7,8	7,8	4,4		
Sulphate (SO4)	mg/L	21,1	12	9	4,4	25,3		15,9
Hardness (CaCO3)	mg/L	54	46	101	75	95		385,5
Dissolved Organic Carbon	mg/L	3	2,6	4,3	4,2	3,1		
Total Organic Carbon	mg/L	3,2	2,6	4,3	4,2	3,1		
Total Suspended Solids	mg/L	<1	1	1	2	6		13
Total Dissolved Solids	mg/L	106	106	212	194	238		1335
<b>Total Metals</b>								
Total Aluminium	mg/L							
Total Antimony	mg/L	<0,0001	0,0001	<0,0001	<0,0001	0,0006		0,0004
Total Arsenic	mg/L	0,0023	0,0083	<0,0005	<0,0005	<0,0005		0,004
Total Barium	mg/L	0,0215	0,0262	0,0756	0,0742	0,0295		0,301
Total Beryllium	mg/L	<0,0005	<0,0005	<0,0005	<0,0005	<0,0005		<0,0002
Total Bismuth	mg/L							<0,0002
Total Boron	mg/L	<0,01	0,02	0,08	0,07	0,07		2,43
Total Cadmium	mg/L	0,00003	<0,00002	<0,00002	<0,00002	<0,00002		<0,00004
Total Calcium	mg/L	12,5	10,7	23,4	17	21,2		95,4
Total Chrome	mg/L							0,004
Total Cobalt	mg/L							0,0009
Total Copper	mg/L	0,0013	<0,0005	0,0023	<0,0005	0,0058		0,0035
Total Iron	mg/L	0,83	0,76	0,84	0,58	0,07		1,14
Total Lead	mg/L	<0,0003	<0,0003	<0,0003	<0,0003	0,0025		0,0025
Total Lithium	mg/L	<0,005	<0,005	0,012	0,006	0,005		0,04
Total Magnesium	mg/L	5,58	4,79	10,5	7,92	10,4		37,1
Total Manganese	mg/L	0,067	0,0609	0,0733	0,0462	0,0081		0,415
Total Mercury	mg/L	0,00018	0,00027	0,00023	0,00032	0,00002		<0,00002
Total Molybdenum	mg/L	0,0108	0,0103	0,0109	0,0084	0,0101		0,0083
Total Nickel	mg/L	0,0006	<0,0005	0,002	<0,0005	0,0342		0,0045
Total Potassium	mg/L	3,02	2,72	2,71	2,09	4,06		9,13
Total Selenium	mg/L	<0,001	<0,001	0,001	0,001	0,001		<0,0002
Total Silicon	mg/L							5,07
Total Silver	mg/L	<0,0001	<0,0001	<0,0001	<0,0001	<0,0001		0,00028
Total Sodium	mg/L	7,89	7,1	20	17,7	18,9		357
Total Strontium	mg/L	0,151	0,133	0,337	0,286	0,249		1,56
Total Tellurium	mg/L							<0,0002
Total Thallium	mg/L	<0,0008	<0,0008	<0,0008	<0,0008	<0,0008		<0,0002
Total Thorium	mg/L							<0,0001
Total Tin	mg/L	<0,001	<0,001	<0,001	<0,001	<0,001		0,0009
Total Titanium	mg/L	0,01	0,01	0,01	0,01	0,01		0,01
Total Uranium	mg/L	<0,001	<0,001	<0,001	<0,001	0,013		0,0003
Total Vanadium	mg/L	<0,0005	<0,0005	0,001	<0,0005	<0,0005		0,0004
Total Zinc	mg/L	<0,001	<0,001	0,008	0,003	<0,001		0,007
Total Zirconium	mg/L							<0,002
<b>Dissolved Metals</b>								
Dissolved Aluminum	mg/L							
Dissolved Antimony	mg/L	<0,0001	<0,0001	0,0002	<0,0001	0,0006		0,0002
Dissolved Arsenic	mg/L	0,0018	<0,0005	<0,0005	<0,0005	<0,0005		0,0038
Dissolved Barium	mg/L	0,0209	0,0203	0,0746	0,0707	0,0305		0,3
Dissolved Beryllium	mg/L							<0,0002
Dissolved Bismuth	mg/L							<0,0002
Dissolved Boron	mg/L	<0,01	0,01	0,04	0,07	0,07		2,39
Dissolved Cadmium	mg/L	<0,00002	<0,00002	<0,00002	<0,00002	<0,00002		<0,00004
Dissolved Calcium	mg/L	12,4	9,93	22,7	16,4	20,6		94,2
Dissolved Chrome	mg/L	<0,0006	<0,0006	<0,0006	<0,0008	<0,0012		0,0002
Dissolved Cobalt	mg/L							0,0008
Dissolved Copper	mg/L	<0,0005	<0,0005	<0,0005	<0,0005	0,0047		0,0004
Dissolved Iron	mg/L	0,81	0,27	0,69	0,03	<0,01		0,08
Dissolved Lead	mg/L	<0,0003	<0,0003	<0,0003	<0,0003	<0,0003		<0,0002
Dissolved Lithium	mg/L	<0,005	<0,005	0,014	0,005	<0,005		0,033
Dissolved Magnesium	mg/L	5,43	4,49	9,77	7,67	9,94		35,1
Dissolved Manganese	mg/L	0,0729	0,0569	0,0712	0,0458	0,0059		0,381
Dissolved Mercury	mg/L	0,00017	0,00029	0,00029	0,0003	0,00007		<0,00002
Dissolved Molybdenum	mg/L	0,0119	0,011	0,0116	0,0089	0,0104		0,0076
Dissolved Nickel	mg/L	0,0006	0,001	0,002	<0,0005	0,0334		0,0026
Dissolved Phosphorus	mg/L							0,04
Dissolved Potassium	mg/L	3,37	2,58	2,74	2,07	3,92		8,56
Dissolved Selenium	mg/L	<0,001	<0,001	0,001	<0,001	0,001		<0,0002
Dissolved Silicon	mg/L							3,89
Dissolved Silver	mg/L	<0,0001	<0,0001	<0,0001	<0,0001	<0,0001		<0,00005
Dissolved Sodium	mg/L	8,16	6,67	19,8	17,7	18,5		327
Dissolved Strontium	mg/L	0,149	0,138	0,307	0,305	0,248		1,46
Dissolved Tellurium	mg/L							<0,0002
Dissolved Thallium	mg/L	<0,0008	<0,0008	<0,0008	<0,0008	<0,0008		<0,0002
Dissolved Thorium	mg/L							<0,0001
Dissolved Tin	mg/L	<0,001	<0,001	<0,001	<0,001	<0,001		<0,0002
Dissolved Titanium	mg/L	<0,01	<0,01	0,01	0,01	0,01		0,0003
Dissolved Uranium	mg/L	<0,001	<0,001	<0,001	<0,001	0,013		0,0003
Dissolved Vanadium	mg/L	0,0023	<0,0005	0,0007	<0,0005	<0,0005		<0,0002
Dissolved Zinc	mg/L	<0,001	0,002	0,008	<0,001	<0,001		0,002
Dissolved Zirconium	mg/L							<0,002
<b>Anions</b>								
Bromide	mg/L							
Chloride	mg/L	2,9	2,7	32	23	33,3		845
Fluoride	mg/L	1	0,86	1,06	0,93	0,79		0,12
<b>Nutrients</b>								
Ammonium (N-NH4)	mg/L	0,51	0,65	0,34	0,46	<0,05		
Ammonia-Nitrogen (NH3-NH4)	mg/L							
Ammonia (NH3) (non-ionized)	mg/L	0,01	0,02	0,01	<0,01	<0,01		
Nitrate and Nitrite	mg/L							<0,01
Nitrate	mg/L							
Nitrite	mg/L	<0,01	<0,01	0,03	<0,01	<0,01		
Orthophosphate	mg/L	0,52	0,41	0,05	0,15	0,01		
Total Kjeldahl Nitrogen	mg/L	1,46	0,61	0,51	0,38	0,21		0,3
Total Phosphorus	mg/L	0,71	0,52	0,16	0,19	<0,04		0,105
<b>Cyanide</b>								
Total Cyanide	mg/L	<0,001	0,003	0,003	0,002	0,003		<0,01
Free Cyanide	mg/L							<0,1
Weak Acid Dissociable Cyanide	mg/L	<0,001	0,002	<0,001	0,003	0,004		

APPENDIX B - Analytical Results for Groundwater

Site Area		Goose Pit						
Station ID		MW-03-01		MW-06-05				
Sampling Date		2003-09-07	2003-09-07	2009-09-07	2009-09-07	2006-08-08	2006-08-08	2006-08-14
FIELD PARAMETERS	Unité							
Temperature	degC	11,7	11,7	5,4				9,9
pH	-	7,36	7,36	6,97		7,93		7,58
Conductivity	µS/cm	1855	1855	2436		382		538
Oxygen Reduction Potential	mV							
Turbidity	NTU							
<b>LABORATORY ANALYSIS</b>								
<b>General</b>								
Total Alkalinity	mg/L	30	30	15	18			51
Bicarbonate Alkalinity HCO3	mg/L	36,6	36,6					62,2
Carbonate Alkalinity CO3	mg/L	<0,5	<0,5					<0,5
Reactive silica	mg/L							
Sulphate (SO4)	mg/L	15,6	15,8	3,9	3,6	42,8	43,1	51,1
Hardness (CaCO3)	mg/L	290	327,5	450	440	78,95	79,45	149
Dissolved Organic Carbon	mg/L							
Total Organic Carbon	mg/L							
Total Suspended Solids	mg/L							4
Total Dissolved Solids	mg/L	793	793	1900	1900	159	126	348,5
<b>Total Metals</b>								
Total Aluminium	mg/L							
Total Antimony	mg/L	<0,001	<0,001			<0,0002	<0,0002	<0,001
Total Arsenic	mg/L	<0,001	0,017			0,0005	0,0006	0,002
Total Barium	mg/L	0,18	0,2			0,027	0,028	0,052
Total Beryllium	mg/L	<0,001	<0,001			<0,0002	<0,0002	<0,001
Total Bismuth	mg/L	<0,001	<0,001			<0,0002	<0,0002	<0,001
Total Boron	mg/L	0,59	1,07			0,11	0,11	0,27
Total Cadmium	mg/L	0,00024	0,00037			<0,00004	<0,00004	<0,0002
Total Calcium	mg/L	72	87,1			19,1	19,1	33,4
Total Chrome	mg/L	0,049	0,32			0,0017	0,0021	<0,001
Total Cobalt	mg/L	0,004	0,016			0,0005	0,0005	<0,001
Total Copper	mg/L	0,044	0,071			0,0022	0,002	<0,001
Total Iron	mg/L	6,05	10,7			1,02	1,11	1,1
Total Lead	mg/L	0,013	0,03			0,0015	0,0013	<0,001
Total Lithium	mg/L	0,025	0,031			0,0031	0,0032	0,006
Total Magnesium	mg/L	33,2	41,5			8,29	8,2	15,6
Total Manganese	mg/L	0,073	0,72			0,309	0,304	0,93
Total Mercury	mg/L					<0,00002	<0,00002	<0,00002
Total Molybdenum	mg/L	<0,0005	0,011			0,013	0,013	0,012
Total Nickel	mg/L	0,056	0,13			0,002	0,0022	<0,001
Total Potassium	mg/L	7,31	9,1			3,63	3,68	6,1
Total Selenium	mg/L	<0,001	<0,001			<0,0002	<0,0002	<0,001
Total Silicon	mg/L	0,4	4,12			2,31	2,71	2,7
Total Silver	mg/L	0,0064	0,011			<0,00005	<0,00005	<0,00025
Total Sodium	mg/L	22	25			16	15,9	50,5
Total Strontium	mg/L	0,68	0,79			0,119	0,12	0,28
Total Tellurium	mg/L	<0,001	<0,001			<0,0002	<0,0002	<0,001
Total Thallium	mg/L	<0,0001	<0,0001			<0,00002	<0,00002	<0,0001
Total Thorium	mg/L	<0,0005	0,0038			0,0005	0,0006	<0,0005
Total Tin	mg/L	<0,001	0,002			<0,0002	<0,0002	<0,001
Total Titanium	mg/L	0,01	0,22			0,024	0,029	0,006
Total Uranium	mg/L	0,0012	0,0017			0,0006	0,0006	<0,0005
Total Vanadium	mg/L	<0,001	0,029			0,0007	0,0008	<0,001
Total Zinc	mg/L	0,063	0,087			0,005	0,005	<0,005
Total Zirconium	mg/L	<0,001	<0,001			<0,002	<0,002	<0,01
<b>Dissolved Metals</b>								
Dissolved Aluminium	mg/L							
Dissolved Antimony	mg/L	<0,001	<0,001			<0,0002	<0,0002	<0,001
Dissolved Arsenic	mg/L	<0,001	0,003	<0,002	<0,002	0,0005	0,0005	0,003
Dissolved Barium	mg/L	0,12	0,13	0,42	0,39	0,025	0,025	0,051
Dissolved Beryllium	mg/L							
Dissolved Bismuth	mg/L	<0,001	<0,001			<0,0002	<0,0002	<0,001
Dissolved Boron	mg/L	0,53	1,03			0,1	0,1	0,27
Dissolved Cadmium	mg/L	0,00007	0,00012	<0,001	<0,001	<0,00004	<0,00004	<0,0002
Dissolved Calcium	mg/L	65,6	67	100	99	17,6	17,9	33,7
Dissolved Chrome	mg/L	<0,001	<0,001			0,0012	0,0012	<0,001
Dissolved Cobalt	mg/L	0,001	0,001			0,0004	0,0004	<0,001
Dissolved Copper	mg/L	0,002	0,002	<0,003	<0,003	0,0016	0,0016	<0,001
Dissolved Iron	mg/L	<0,05	0,07	<0,1	<0,1	0,84	0,85	0,2
Dissolved Lead	mg/L	<0,001	<0,001	<0,001	0,001	0,0014	0,0012	<0,001
Dissolved Lithium	mg/L	0,017	0,017			0,0028	0,0027	0,005
Dissolved Magnesium	mg/L	23,4	24,3	46	47	7,76	7,92	16,1
Dissolved Manganese	mg/L	0,06	0,28	0,22	0,22	0,286	0,293	0,98
Dissolved Mercury	mg/L			<0,0001	<0,0001	<0,00002	<0,00002	<0,00002
Dissolved Molybdenum	mg/L	<0,0005	0,0057	<0,03	<0,003	0,012	0,012	0,013
Dissolved Nickel	mg/L	0,006	0,005	<0,01	<0,01	0,0019	0,0019	<0,001
Dissolved Phosphorus	mg/L	0,1	0,15			<0,03	<0,03	<0,15
Dissolved Potassium	mg/L	5,71	5,95	11	11	3,27	3,28	6,1
Dissolved Selenium	mg/L	<0,001	<0,001	<0,001	<0,001	<0,0002	<0,0002	<0,001
Dissolved Silicon	mg/L	0,32	3,27			1,96	1,98	2,5
Dissolved Silver	mg/L	<0,0001	<0,0001	<0,0003	<0,0003	<0,00005	<0,00005	<0,00025
Dissolved Sodium	mg/L	20	22	420	430	15	15,6	52,5
Dissolved Strontium	mg/L	0,58	0,59			0,111	0,114	0,29
Dissolved Tellurium	mg/L	<0,001	<0,001			<0,0002	<0,0002	<0,001
Dissolved Thallium	mg/L	<0,0001	<0,0001	<0,01	<0,01	<0,00002	<0,00002	<0,0001
Dissolved Thorium	mg/L	<0,0005	<0,0005			0,0004	0,0004	<0,0005
Dissolved Tin	mg/L	<0,001	<0,001			<0,0002	<0,0002	<0,001
Dissolved Titanium	mg/L	<0,001	<0,001			0,019	0,018	<0,001
Dissolved Uranium	mg/L	0,0006	0,0006			0,0006	0,0006	<0,0005
Dissolved Vanadium	mg/L	<0,001	<0,001			0,0006	0,0006	<0,001
Dissolved Zinc	mg/L	0,006	<0,005	<0,003	<0,003	0,005	0,005	<0,005
Dissolved Zirconium	mg/L	<0,001	<0,001			<0,002	<0,002	<0,01
<b>Anions</b>								
Bromide	mg/L							
Chloride	mg/L	626	621	990	950	34,7	33,7	128
Fluoride	mg/L	<0,05	<0,05	0,1	<0,1	0,16	0,17	0,16
<b>Nutrients</b>								
Ammonium (N-NH4)	mg/L							
Ammonia-Nitrogen (NH3-NH4)	mg/L							
Ammonia (NH3) (non-ionized)	mg/L							
Nitrate and Nitrite	mg/L	<0,01	<0,01	<0,42	<0,42	<0,01	<0,01	
Nitrate	mg/L							
Nitrite	mg/L					0,003	0,004	0,002
Orthophosphate	mg/L							
Total Kjeldahl Nitrogen	mg/L	0,7	0,6			0,3	0,3	
Total Phosphorus	mg/L	0,069	0,075			<0,035	<0,035	<0,15
<b>Cyanide</b>								
Total Cyanide	mg/L							
Free Cyanide	mg/L							
Weak Acid Dissociable Cyanide	mg/L							

APPENDIX B - Analytical Results for Groundwater

FIELD PARAMETERS	Unité	Goose Pit						
		MW-06-05					MW-03-02	
		2007-08-17	2007-08-17	2008-09-15	2008-09-15	2010-08-26	2004-07-31	2004-07-31
Temperature	degC	6,7		1		3,1	12	
pH	-	7,43		6,7		7,13	7,19	
Conductivity	µS/cm	776		2100		340	1104	
Oxygen Reduction Potential	mV						32	
Turbidity	NTU							
<b>LABORATORY ANALYSIS</b>								
<b>General</b>								
Total Alkalinity	mg/L	36,7	36,7	24	33	49	41,6	42,9
Bicarbonate Alkalinity HCO3	mg/L	44,8	44,8			345	50,8	52,4
Carbonate Alkalinity CO3	mg/L	<0,5	<0,5				<0,5	<0,5
Reactive silica	mg/L							
Sulphate (SO4)	mg/L	46,5	46,3	6	5,7	87	38,4	38,2
Hardness (CaCO3)	mg/L	111,5	110,5	310	320	77	310,5	
Dissolved Organic Carbon	mg/L							
Total Organic Carbon	mg/L							
Total Suspended Solids	mg/L	2	3	5	7		96	90
Total Dissolved Solids	mg/L	319	250	1100			499	
<b>Total Metals</b>								
Total Aluminium	mg/L							
Total Antimony	mg/L	<0,001	<0,001				0,0003	
Total Arsenic	mg/L	<0,001	<0,001			<0,002	0,0038	
Total Barium	mg/L	0,053	0,052			<0,03	0,096	
Total Beryllium	mg/L	<0,001	<0,001				<0,0002	
Total Bismuth	mg/L	<0,001	<0,001				<0,0002	
Total Boron	mg/L	0,23	0,23				0,97	
Total Cadmium	mg/L	<0,0002	<0,0002			<0,001	0,00018	
Total Calcium	mg/L	26,1	25,1	73		21	74,7	
Total Chrome	mg/L	<0,001	<0,001				0,008	
Total Cobalt	mg/L	<0,001	<0,001				0,0072	
Total Copper	mg/L	0,001	0,001			<0,003	0,007	
Total Iron	mg/L	0,94	0,93			0,6	4,72	
Total Lead	mg/L	0,001	0,001				0,0035	
Total Lithium	mg/L	<0,005	<0,005				0,021	
Total Magnesium	mg/L	12,4	12,1			6,1	30,7	
Total Manganese	mg/L	0,77	0,75			0,55	0,517	
Total Mercury	mg/L	<0,00002	<0,00002			<0,0001	<0,00002	
Total Molybdenum	mg/L	0,0084	0,0084			<0,03	0,015	
Total Nickel	mg/L	0,001	0,001			<0,01	0,017	
Total Potassium	mg/L	4,7	4,5			2,1	7,8	
Total Selenium	mg/L	<0,001	<0,001			<0,001	<0,0002	
Total Silicon	mg/L	1,4	1,3				13,8	
Total Silver	mg/L	<0,00025	<0,00025			0,0014	0,00067	
Total Sodium	mg/L	39,1	37,5			2,5	91,9	
Total Strontium	mg/L	0,24	0,24				0,759	
Total Tellurium	mg/L	<0,001	<0,001				<0,0002	
Total Thallium	mg/L	<0,0001	<0,0001			<0,01	0,00006	
Total Thorium	mg/L	<0,0005	<0,0005				<0,0001	
Total Tin	mg/L	<0,001	<0,001				0,0003	
Total Titanium	mg/L	0,003	0,003				0,158	
Total Uranium	mg/L	<0,0005	<0,0005				0,002	
Total Vanadium	mg/L	<0,001	<0,001				0,0039	
Total Zinc	mg/L	0,009	0,009			0,009	0,042	
Total Zirconium	mg/L	<0,01	<0,01				<0,002	
<b>Dissolved Metals</b>								
Dissolved Aluminium	mg/L							
Dissolved Antimony	mg/L	<0,001	<0,001				0,0003	
Dissolved Arsenic	mg/L	<0,001	<0,001	0,0001	0,0001	<0,002	0,002	
Dissolved Barium	mg/L	0,048	0,051	0,25	0,25	<0,03	0,086	
Dissolved Beryllium	mg/L							
Dissolved Bismuth	mg/L	<0,001	<0,001				<0,0002	
Dissolved Boron	mg/L	0,2	0,21				0,94	
Dissolved Cadmium	mg/L	<0,0002	<0,0002	0,0002	0,0002	<0,001	0,00016	
Dissolved Calcium	mg/L	24	24,5	73	75	18	73,5	
Dissolved Chrome	mg/L	<0,001	<0,001				0,0004	
Dissolved Cobalt	mg/L	<0,001	<0,001				0,006	
Dissolved Copper	mg/L	<0,001	0,001	0,0015	0,0023	<0,003	0,0014	
Dissolved Iron	mg/L	<0,05	<0,05	0,03	0,03	<0,1	0,05	
Dissolved Lead	mg/L	<0,001	<0,001	0,00021	0,0002	<0,001	<0,0002	
Dissolved Lithium	mg/L	<0,005	<0,005				0,016	
Dissolved Magnesium	mg/L	11,4	11,6	31	32	4,1	30,2	
Dissolved Manganese	mg/L	0,7	0,72	0,43	0,44	0,36	0,492	
Dissolved Mercury	mg/L	<0,00002	<0,00002	<0,00001	<0,00001	<0,0001	<0,02	
Dissolved Molybdenum	mg/L	0,0079	0,0079	0,0082	0,0078	<0,03	0,014	
Dissolved Nickel	mg/L	0,001	0,001	0,0015	0,0015	<0,01	0,012	
Dissolved Phosphorus	mg/L	<0,15	<0,15				<0,03	
Dissolved Potassium	mg/L	4,3	4,4	8,4	8,5	1,5	7,43	
Dissolved Selenium	mg/L	<0,001	<0,001	0,001	0,001	<0,001	<0,0002	
Dissolved Silicon	mg/L	1,2	1,2				5,88	
Dissolved Silver	mg/L	<0,00025	<0,00025	0,0001	0,0001	<0,0003	<0,00005	
Dissolved Sodium	mg/L	34,2	35			1,8	89,5	
Dissolved Strontium	mg/L	0,22	0,22				0,736	
Dissolved Tellurium	mg/L	<0,001	<0,001				<0,0002	
Dissolved Thallium	mg/L	<0,0001	<0,0001	0,002	0,002	<0,01	<0,00002	
Dissolved Thorium	mg/L	<0,0005	<0,0005				<0,0001	
Dissolved Tin	mg/L	<0,001	<0,001				<0,0002	
Dissolved Titanium	mg/L	<0,001	<0,001				0,0008	
Dissolved Uranium	mg/L	<0,0005	<0,0005				0,0013	
Dissolved Vanadium	mg/L	<0,001	<0,001				<0,0002	
Dissolved Zinc	mg/L	<0,005	0,005	0,017	0,014	0,011	0,029	
Dissolved Zirconium	mg/L	<0,01	<0,01				<0,002	
<b>Anions</b>								
Bromide	mg/L							
Chloride	mg/L	126	126	950	980	5,7	251	259
Fluoride	mg/L	0,18	0,18	<0,1	<0,1	0,2	0,6	0,57
<b>Nutrients</b>								
Ammonium (N-NH4)	mg/L							
Ammonia-Nitrogen (NH3-NH4)	mg/L							
Ammonia (NH3) (non-ionized)	mg/L							
Nitrate and Nitrite	mg/L			<0,2	<0,4	0,09	<0,05	<0,05
Nitrate	mg/L							
Nitrite	mg/L	0,002	<0,002	<0,2	<0,4		0,006	0,007
Orthophosphate	mg/L							
Total Kjeldahl Nitrogen	mg/L	<0,2	0,2				0,4	
Total Phosphorus	mg/L	<0,082	<0,085				0,285	0,25
<b>Cyanide</b>								
Total Cyanide	mg/L						<0,01	
Free Cyanide	mg/L						<0,1	
Weak Acid Dissociable Cyanide	mg/L							

APPENDIX B - Analytical Results for Groundw

Site Area Station ID Sampling Date	Unité	Goose Pit					East Flat	
		MW-03-02	MW-06-06		MW-11-01		MW-IPD-07	MW-08-03
		2003-09-28	2006-08-24	2006-08-24	2011-09-29	2011-09-29	2018-07-08	2008-09-14
<b>FIELD PARAMETERS</b>								
Temperature	degC	3,5	12,4					5
pH	-	7,68	7,59		10,3			7,1
Conductivity	µS/cm	660	1306		3999			366
Oxygen Reduction Potential	mV	8,2						
Turbidity	NTU							
<b>LABORATORY ANALYSIS</b>								
<b>General</b>								
Total Alkalinity	mg/L	103	49,9	49,9	23	37	92	60
Bicarbonate Alkalinity HCO3	mg/L	125	60,9	60,9			81	
Carbonate Alkalinity CO3	mg/L	<0,5	<0,5	<0,5			11	
Reactive silica	mg/L						14,22	
Sulphate (SO4)	mg/L	263	65,1	56	29	30	32,8	56
Hardness (CaCO3)	mg/L	303	335,5	331,5	13264	14759	57	180
Dissolved Organic Carbon	mg/L							
Total Organic Carbon	mg/L						1,2	
Total Suspended Solids	mg/L		16	28			97	56
Total Dissolved Solids	mg/L	387	619	678	14840	14620	171	
<b>Total Metals</b>								
Total Aluminium	mg/L							
Total Antimony	mg/L	<0,001	<0,001	<0,001			<0,0001	
Total Arsenic	mg/L	0,002	0,003	0,003	0,128	0,142	0,0138	
Total Barium	mg/L	0,028	0,024	0,024	0,1484	0,1991	0,0066	
Total Beryllium	mg/L	<0,001	<0,001	<0,001			<0,0005	
Total Bismuth	mg/L	<0,001	<0,001	<0,001				
Total Boron	mg/L	0,06	0,36	0,31			0,16	
Total Cadmium	mg/L	<0,0002	<0,0002	<0,0002	<0,00002	0,00009	<0,00002	
Total Calcium	mg/L	68,3	89,3	86,1	5263	5857	11,5	
Total Chrome	mg/L	0,003	<0,001	<0,001			<0,0006	
Total Cobalt	mg/L	0,004	0,002	0,002				
Total Copper	mg/L	0,004	0,001	0,005	0,0237	0,0357	<0,0005	
Total Iron	mg/L	2,96	0,57	0,57	1,3	1,9	1,02	
Total Lead	mg/L	0,002	<0,001	<0,001	<0,0003	0,0031	<0,0003	
Total Lithium	mg/L	0,021	0,029	0,028			0,013	
Total Magnesium	mg/L	35,2	25	24,5	29,9	32,6	7,06	
Total Manganese	mg/L	1,04	0,41	0,43	0,0433	0,05	0,0347	
Total Mercury	mg/L	<0,00002	<0,00002	<0,00002	0,00073	0,00077	<0,00001	
Total Molybdenum	mg/L	0,022	0,0087	0,009	<0,0005	<0,0005	0,0156	
Total Nickel	mg/L	0,008	0,007	0,01	0,2109	0,2269	0,0037	
Total Potassium	mg/L	5,94	6,7	6,5	201	225	2,22	
Total Selenium	mg/L	<0,001	<0,001	<0,001	0,564	0,594	<0,001	
Total Silicon	mg/L	10,7	4,7	4,6				
Total Silver	mg/L	<0,0001	<0,00025	<0,00025	0,0123	0,0146	<0,0001	
Total Sodium	mg/L	6,81	59	55,9	344	550	26,7	
Total Strontium	mg/L	0,26	0,75	0,72			0,135	
Total Tellurium	mg/L	<0,001	<0,001	<0,001				
Total Thallium	mg/L	<0,0001	<0,0001	<0,0001	<0,005	<0,005	<0,0008	
Total Thorium	mg/L	0,0007	<0,0005	<0,0005				
Total Tin	mg/L	<0,001	<0,001	<0,001			<0,001	
Total Titanium	mg/L	0,063	0,005	0,005			<0,01	
Total Uranium	mg/L	0,0084	0,0018	0,0018			0,002	
Total Vanadium	mg/L	0,002	0,002	0,002			0,0012	
Total Zinc	mg/L	0,014	<0,005	<0,005	0,038	0,091	0,008	
Total Zirconium	mg/L	<0,001	<0,01	<0,01				
<b>Dissolved Metals</b>								
Dissolved Aluminum	mg/L							
Dissolved Antimony	mg/L	<0,001	<0,001	<0,001			<0,0001	
Dissolved Arsenic	mg/L	0,002	0,002	0,002	0,137	0,13	0,0131	0,001
Dissolved Barium	mg/L	0,023	0,018	0,019	0,13	0,136	<0,0005	0,033
Dissolved Beryllium	mg/L							
Dissolved Bismuth	mg/L	<0,001	<0,001	<0,001				
Dissolved Boron	mg/L	0,06	0,37	0,44			0,2	
Dissolved Cadmium	mg/L	<0,0002	<0,0002	<0,0002	<0,005	<0,005	<0,00002	0,0002
Dissolved Calcium	mg/L	63,1	87,1	85,3	5136	5099	12,7	46
Dissolved Chrome	mg/L	0,001	<0,001	<0,001			<0,0006	
Dissolved Cobalt	mg/L	0,004	<0,001	<0,001				
Dissolved Copper	mg/L	0,004	0,001	<0,001	0,021	0,015	<0,0005	0,003
Dissolved Iron	mg/L	1,91	<0,05	<0,05	1,3	0,97	0,01	0,03
Dissolved Lead	mg/L	0,001	<0,001	<0,001	<0,005	<0,005	<0,0003	0,00056
Dissolved Lithium	mg/L	0,019	0,028	0,025			0,008	
Dissolved Magnesium	mg/L	32,1	24	23,6	22,5	25,8	6,79	17
Dissolved Manganese	mg/L	0,96	0,006	0,003	0,029	0,029	0,0234	0,32
Dissolved Mercury	mg/L	<0,00002	<0,00002	<0,00002	0,0006	0,0006	0,00001	<0,00001
Dissolved Molybdenum	mg/L	0,018	0,0081	0,0069	<0,005	<0,005	0,0166	0,14
Dissolved Nickel	mg/L	0,007	0,005	0,004	0,179	0,171	0,0034	0,001
Dissolved Phosphorus	mg/L	0,16	0,9	0,8				
Dissolved Potassium	mg/L	5,36	6,6	5,8	183	192	2,54	4,4
Dissolved Selenium	mg/L	<0,001	<0,001	<0,001	0,637	0,606	<0,001	0,001
Dissolved Silicon	mg/L	7,98	4,1	3,8				
Dissolved Silver	mg/L	<0,0001	<0,00025	<0,00025	<0,005	<0,005	<0,0001	0,0001
Dissolved Sodium	mg/L	6,29	58,2	55,9	283	338	32	
Dissolved Strontium	mg/L	0,24	0,72	0,76			0,12	
Dissolved Tellurium	mg/L	<0,001	<0,001	<0,001				
Dissolved Thallium	mg/L	<0,0001	<0,0001	<0,0001	<0,01	<0,01	<0,0008	0,002
Dissolved Thorium	mg/L	<0,0005	<0,0005	<0,0005				
Dissolved Tin	mg/L	<0,001	<0,001	<0,001			<0,001	
Dissolved Titanium	mg/L	0,024	<0,001	<0,001			0,01	
Dissolved Uranium	mg/L	0,0077	0,0016	0,0014			0,001	
Dissolved Vanadium	mg/L	<0,001	0,001	0,001			<0,0005	
Dissolved Zinc	mg/L	0,012	<0,005	<0,005	0,02	0,013	0,004	0,004
Dissolved Zirconium	mg/L	<0,001	<0,01	<0,01				
<b>Anions</b>								
Bromide	mg/L						0,05	
Chloride	mg/L	5,4	304	331	10271	9859	4,8	3,3
Fluoride	mg/L	0,35	0,55	0,63	0,55	0,62	1,16	0,3
<b>Nutrients</b>								
Ammonium (N-NH4)	mg/L				0,07	0,27		
Ammonia-Nitrogen (NH3-NH4)	mg/L							
Ammonia (NH3) (non-ionized)	mg/L						<0,01	2
Nitrate and Nitrite	mg/L	<0,05						27
Nitrate	mg/L							
Nitrite	mg/L	0,005	0,005	0,004	<0,01	<0,01	<0,01	1,1
Orthophosphate	mg/L						0,12	
Total Kjeldahl Nitrogen	mg/L		0,6	0,6			0,34	
Total Phosphorus	mg/L	0,145	1,2	1,2			0,06	
<b>Cyanide</b>								
Total Cyanide	mg/L				<0,005		<0,001	
Free Cyanide	mg/L				<0,005			
Weak Acid Dissociable Cyanide	mg/L						<0,001	

APPENDIX B - Analytical Results for Groundw

FIELD PARAMETERS	Unité	East Flat						
		MW-08-03		MW-08-02				
		2008-09-14	2013-09-23	2011-09-21	2011-09-21	2012-07-23	2012-07-23	2009-08-29
Temperature	degC		9,6	8,6		20,5		4,6
pH	-		6,92	8,05		7,94		7,79
Conductivity	µS/cm		644	905		616		616
Oxygen Reduction Potential	mV							
Turbidity	NTU							
<b>LABORATORY ANALYSIS</b>								
<b>General</b>								
Total Alkalinity	mg/L	59	44	76	76	102	100	
Bicarbonate Alkalinity HCO3	mg/L							
Carbonate Alkalinity CO3	mg/L							
Reactive silica	mg/L							
Sulphate (SO4)	mg/L	51	3,4	4	8	5	3	3
Hardness (CaCO3)	mg/L	180	2571	317	305	170	178	240
Dissolved Organic Carbon	mg/L							
Total Organic Carbon	mg/L							
Total Suspended Solids	mg/L	54	3			2	4	
Total Dissolved Solids	mg/L		2408					530
<b>Total Metals</b>								
Total Aluminium	mg/L							
Total Antimony	mg/L							
Total Arsenic	mg/L			0,0023	0,002	<0,0005	<0,0005	
Total Barium	mg/L			0,043	0,037	0,0313	0,0311	
Total Beryllium	mg/L							
Total Bismuth	mg/L							
Total Boron	mg/L							
Total Cadmium	mg/L			<0,00002	<0,00002	<0,00002	<0,00002	
Total Calcium	mg/L			63,1	54,2	35,5	37,4	
Total Chrome	mg/L							
Total Cobalt	mg/L							
Total Copper	mg/L			0,0014	0,0008	<0,0005	<0,0005	
Total Iron	mg/L			1,4	1,4	1,2	1,1	
Total Lead	mg/L			<0,0003	<0,0003	<0,0003	<0,0003	
Total Lithium	mg/L							
Total Magnesium	mg/L			38,9	38	19,8	20,6	
Total Manganese	mg/L			0,1338	0,1213	0,133	0,1362	
Total Mercury	mg/L			0,00009	0,0001	0,00012	0,00016	
Total Molybdenum	mg/L			0,0016	<0,0005	0,0522	0,053	
Total Nickel	mg/L			0,0046	0,0037	0,0017	0,002	
Total Potassium	mg/L			2,1	2	2,5	2,6	
Total Selenium	mg/L			0,005	0,005	0,004	0,006	
Total Silicon	mg/L							
Total Silver	mg/L			<0,0002	<0,0002	<0,0002	<0,0002	
Total Sodium	mg/L			43,3	48,8	26,8	29	
Total Strontium	mg/L							
Total Tellurium	mg/L							
Total Thallium	mg/L			0,005	0,005	<0,005	<0,005	
Total Thorium	mg/L							
Total Tin	mg/L							
Total Titanium	mg/L							
Total Uranium	mg/L							
Total Vanadium	mg/L							
Total Zinc	mg/L			0,01	0,375	0,005	0,004	
Total Zirconium	mg/L							
<b>Dissolved Metals</b>								
Dissolved Aluminium	mg/L							
Dissolved Antimony	mg/L							
Dissolved Arsenic	mg/L	0,001	0,034	<0,005	<0,005	<0,005	<0,005	0,003
Dissolved Barium	mg/L	0,034	0,0579	0,041	0,041	0,025	0,024	0,04
Dissolved Beryllium	mg/L							
Dissolved Bismuth	mg/L							
Dissolved Boron	mg/L							
Dissolved Cadmium	mg/L	0,0002	0,0007	<0,005	<0,005	<0,005	<0,005	<0,001
Dissolved Calcium	mg/L	46		59,9	61	39,1	36,9	51
Dissolved Chrome	mg/L							
Dissolved Cobalt	mg/L							
Dissolved Copper	mg/L	0,0039	0,0287	<0,005	<0,005	<0,005	<0,005	<0,003
Dissolved Iron	mg/L	0,03	<0,01	<0,05	<0,05	<0,05	<0,05	<0,1
Dissolved Lead	mg/L	0,00027	<0,0003	<0,005	<0,005	<0,005	<0,005	<0,001
Dissolved Lithium	mg/L							
Dissolved Magnesium	mg/L	16		35,6	35,5	21,6	20,2	27
Dissolved Manganese	mg/L	0,32		0,107	0,11	0,134	0,128	<0,003
Dissolved Mercury	mg/L	<0,00001	<0,0001	<0,0005	<0,0005	<0,0005	<0,0005	<0,0001
Dissolved Molybdenum	mg/L	0,14	0,0213	<0,005	<0,005	0,046	0,043	0,07
Dissolved Nickel	mg/L	0,0017	0,0563	<0,005	<0,005	<0,005	<0,005	<0,01
Dissolved Phosphorus	mg/L							
Dissolved Potassium	mg/L	4,5		2,3	2,4	2,1	1,9	2
Dissolved Selenium	mg/L	0,001	0,137	0,005	0,005	<0,005	<0,005	<0,001
Dissolved Silicon	mg/L							
Dissolved Silver	mg/L	0,0001		<0,005	<0,005	<0,005	<0,005	<0,0003
Dissolved Sodium	mg/L			44	44,2	25	23,3	36
Dissolved Strontium	mg/L							
Dissolved Tellurium	mg/L							
Dissolved Thallium	mg/L	0,002	<0,005	<0,01	<0,01	<0,01	<0,01	<0,01
Dissolved Thorium	mg/L							
Dissolved Tin	mg/L							
Dissolved Titanium	mg/L							
Dissolved Uranium	mg/L							
Dissolved Vanadium	mg/L							
Dissolved Zinc	mg/L	0,0035	0,513	<0,005	0,013	<0,005	<0,005	0,005
Dissolved Zirconium	mg/L							
<b>Anions</b>								
Bromide	mg/L							
Chloride	mg/L	3,6	2427	169	165	111	109	160
Fluoride	mg/L	0,3	0,11	0,32	0,33	0,42	0,37	0,3
<b>Nutrients</b>								
Ammonium (N-NH4)	mg/L							
Ammonia-Nitrogen (NH3-NH4)	mg/L							
Ammonia (NH3) (non-ionized)	mg/L	2						
Nitrate and Nitrite	mg/L	27		0,01	<0,01			<0,04
Nitrate	mg/L							
Nitrite	mg/L	1,2	0,35	<0,01	<0,01	<0,01	<0,01	<0,02
Orthophosphate	mg/L							
Total Kjeldahl Nitrogen	mg/L							
Total Phosphorus	mg/L							
<b>Cyanide</b>								
Total Cyanide	mg/L		0,005			<0,005	<0,005	
Free Cyanide	mg/L							
Weak Acid Dissociable Cyanide	mg/L							

APPENDIX B - Analytical Results for Groundwater

Site Area		East Flat						
Station ID		MW-08-02						
Sampling Date		2009-08-29	2008-09-08	2008-09-08	2010-09-01	2014-08-20	2015-12-03	2015-12-04
FIELD PARAMETERS	Unité							
Temperature	degC		7,3		9,2			
pH	-		7,05		7,87	8,11	8,09	8,21
Conductivity	µS/cm		808		690	1006	94,8	109,4
Oxygen Reduction Potential	mV							
Turbidity	NTU					14,5	38,1	34,6
<b>LABORATORY ANALYSIS</b>								
<b>General</b>								
Total Alkalinity	mg/L	76	76	76	80	147	33	46
Bicarbonate Alkalinity HCO3	mg/L		76	76			33	46
Carbonate Alkalinity CO3	mg/L		<2	<2			<2	<2
Reactive silica	mg/L						0,3	0,4
Sulphate (SO4)	mg/L	2,9	2,5	2		12,9	5,5	11,5
Hardness (CaCO3)	mg/L	850	240	230	220	299	24	46,5
Dissolved Organic Carbon	mg/L						48,9	35,75
Total Organic Carbon	mg/L						52,1	37,4
Total Suspended Solids	mg/L						7	33
Total Dissolved Solids	mg/L	510	500	520	450	843	39	73,5
<b>Total Metals</b>								
Total Aluminium	mg/L							
Total Antimony	mg/L				<0,006		0,0022	0,0012
Total Arsenic	mg/L				0,003	0,0025	<0,0005	<0,0005
Total Barium	mg/L				0,03		0,0046	0,00765
Total Beryllium	mg/L						<0,0005	<0,0005
Total Bismuth	mg/L							
Total Boron	mg/L						<0,01	<0,01
Total Cadmium	mg/L				<0,001		0,00005	0,000155
Total Calcium	mg/L				45		6,09	11,75
Total Chrome	mg/L				0,03		0,0023	0,0102
Total Cobalt	mg/L				<0,03			
Total Copper	mg/L				<0,003	0,0152	0,004	0,01
Total Iron	mg/L						1,75	4,155
Total Lead	mg/L				<0,001	0,0019	<0,0003	0,00785
Total Lithium	mg/L						<0,005	<0,005
Total Magnesium	mg/L				26		2,15	4,23
Total Manganese	mg/L				0,042		0,2974	0,1808
Total Mercury	mg/L				<0,0001		0,00002	0,00002
Total Molybdenum	mg/L				0,05		0,0027	0,00725
Total Nickel	mg/L				0,01	0,0043	0,0015	0,0118
Total Potassium	mg/L						0,98	1,62
Total Selenium	mg/L				<0,001		<0,001	<0,001
Total Silicon	mg/L							
Total Silver	mg/L				<0,0003			
Total Sodium	mg/L				32		2,01	4,815
Total Strontium	mg/L						0,042	0,0825
Total Tellurium	mg/L							
Total Thallium	mg/L						<0,005	<0,005
Total Thorium	mg/L							
Total Tin	mg/L						<0,001	<0,001
Total Titanium	mg/L						<0,01	0,03
Total Uranium	mg/L						<0,001	<0,001
Total Vanadium	mg/L						<0,0005	<0,0005
Total Zinc	mg/L				0,01	0,045	0,502	0,8555
Total Zirconium	mg/L							
<b>Dissolved Metals</b>								
Dissolved Aluminium	mg/L							
Dissolved Antimony	mg/L						0,0016	0,0005
Dissolved Arsenic	mg/L	<0,002	0,0035	0,0035		0,0026	<0,0005	<0,0005
Dissolved Barium	mg/L	<0,03	0,045	0,043		0,0526	0,0023	0,0062
Dissolved Beryllium	mg/L							
Dissolved Bismuth	mg/L							
Dissolved Boron	mg/L						<0,01	<0,01
Dissolved Cadmium	mg/L	<0,001	0,0002	0,0002		0,00012	0,00005	0,000115
Dissolved Calcium	mg/L	340	50	48				
Dissolved Chrome	mg/L						0,0019	0,00655
Dissolved Cobalt	mg/L							
Dissolved Copper	mg/L	<0,003	0,00056	0,0011		<0,0005	<0,0005	0,0057
Dissolved Iron	mg/L	<0,1	0,03	0,03		0,02	0,03	0,045
Dissolved Lead	mg/L	<0,001	0,0001	0,00027		0,5625	<0,0003	<0,0003
Dissolved Lithium	mg/L						<0,005	<0,005
Dissolved Magnesium	mg/L	<1	27	27				
Dissolved Manganese	mg/L	<0,003	0,03	0,031		0,1526	0,2629	0,1618
Dissolved Mercury	mg/L	<0,0001	<0,00001	<0,00001		<0,0001	<0,00001	<0,00001
Dissolved Molybdenum	mg/L	0,04	0,026	0,025		0,0273	0,0028	0,0068
Dissolved Nickel	mg/L	<0,01	0,019	0,019		0,0045	0,0015	0,00765
Dissolved Phosphorus	mg/L							
Dissolved Potassium	mg/L	1,3	1,8	1,5				
Dissolved Selenium	mg/L	<0,001	0,001	0,001		0,011	<0,001	<0,001
Dissolved Silicon	mg/L							
Dissolved Silver	mg/L	<0,0003	0,0001	0,0001				
Dissolved Sodium	mg/L	24						
Dissolved Strontium	mg/L						0,039	0,074
Dissolved Tellurium	mg/L							
Dissolved Thallium	mg/L	<0,01	0,002	0,002		<0,005	<0,005	<0,005
Dissolved Thorium	mg/L							
Dissolved Tin	mg/L						<0,001	<0,001
Dissolved Titanium	mg/L						<0,01	<0,01
Dissolved Uranium	mg/L						<0,001	<0,001
Dissolved Vanadium	mg/L						<0,005	<0,005
Dissolved Zinc	mg/L	<0,003	0,014	0,014		0,033	0,453	0,206
Dissolved Zirconium	mg/L							
<b>Anions</b>								
Bromide	mg/L							
Chloride	mg/L	160	160	180	160	287	5,7	13,7
Fluoride	mg/L	0,3	0,2	0,2	0,3			
<b>Nutrients</b>								
Ammonium (N-NH4)	mg/L							
Ammonia-Nitrogen (NH3-NH4)	mg/L							
Ammonia (NH3) (non-ionized)	mg/L					<0,01	<0,01	<0,01
Nitrate and Nitrite	mg/L	<0,04	<0,1	<0,1				
Nitrate	mg/L							
Nitrite	mg/L	<0,02	<0,1	<0,1		0,03	0,03	0,02
Orthophosphate	mg/L						0,02	<0,01
Total Kjeldahl Nitrogen	mg/L						0,7	1,57
Total Phosphorus	mg/L						<0,01	<0,015
<b>Cyanide</b>								
Total Cyanide	mg/L					<0,005	<0,005	<0,005
Free Cyanide	mg/L					<0,01	<0,005	<0,005
Weak Acid Dissociable Cyanide	mg/L							





APPENDIX B - Analytical Results for Groundwater

FIELD PARAMETERS	Unité	East Flat						
		Station ID	MW-08-02			ST-8-North		ST-8-South
		Sampling Date	2018-07-17	2018-07-18	2017-09-03	2018-07-19	2017-09-04	2018-07-19
Temperature	degC	3,4	2	1,6	8,1	9,4	7,3	8,8
pH	-	7,33	8	8,08	8,17	8,22	7,73	8,02
Conductivity	µS/cm	41,6	311,3	323,4	90,3	68,9	108,3	86,8
Oxygen Reduction Potential	mV	-9,2	-146,2	-182,5	-17,6	-46	-18,1	-49,4
Turbidity	NTU	54	26,2	13,9	7,35	1,14	4,02	1,45
<b>LABORATORY ANALYSIS</b>								
<b>General</b>								
Total Alkalinity	mg/L	23	181	75	41	29	52	27
Bicarbonate Alkalinity HCO3	mg/L	23	181	75	41	29	52	27
Carbonate Alkalinity CO3	mg/L	<2	<2	<2	<2	<2	<2	<2
Reactive silica	mg/L	0,32	1,4	3,8	1,2	1,3	1,6	2,1
Sulphate (SO4)	mg/L	11,1	5	2,5	8,7	15,2	41,5	25,2
Hardness (CaCO3)	mg/L	25	190	160	38	36	61	41
Dissolved Organic Carbon	mg/L	11,8	47,5	23,6	1,7	1,9	2,5	2,4
Total Organic Carbon	mg/L	11,8	47,5	23,6	2,4	2	2,9	2,4
Total Suspended Solids	mg/L	35	22	10	26	6	23	6
Total Dissolved Solids	mg/L	52	303	380				
<b>Total Metals</b>								
Total Aluminium	mg/L							
Total Antimony	mg/L	0,0077	0,0011	0,0006	<0,0001	0,0001	<0,0001	<0,0001
Total Arsenic	mg/L	<0,0005	<0,0005	<0,0005	<0,0005	<0,0005	0,0022	<0,0005
Total Barium	mg/L	0,0085	0,0223	0,0271	0,0123	0,0101	0,0078	0,0048
Total Beryllium	mg/L	<0,0005	<0,0005	<0,0005	<0,0005	<0,0005	<0,0005	<0,0005
Total Bismuth	mg/L							
Total Boron	mg/L	<0,01	0,12	0,14	<0,01	<0,01	<0,01	<0,01
Total Cadmium	mg/L	0,00012	0,00004	<0,00002	<0,00002	<0,00002	<0,00002	<0,00002
Total Calcium	mg/L	6,15	41,5	33,3	11,5	11,7	16,5	12
Total Chrome	mg/L							
Total Cobalt	mg/L							
Total Copper	mg/L	0,0284	0,0214	0,0028	0,0014	0,0017	0,0011	0,003
Total Iron	mg/L	3,54	2,53	1,4	0,61	0,1	0,17	0,37
Total Lead	mg/L	<0,0003	<0,0003	<0,0003	<0,0003	<0,0003	<0,0003	<0,0003
Total Lithium	mg/L	<0,005	0,006	0,007	<0,005	<0,005	<0,005	<0,005
Total Magnesium	mg/L	2,4	21,1	18,9	2,33	1,72	4,96	2,74
Total Manganese	mg/L	0,1716	0,1057	0,0805	0,0162	0,0015	0,0439	0,0133
Total Mercury	mg/L	0,00004	0,00017	0,00019	<0,00001	0,00003	<0,00001	0,00058
Total Molybdenum	mg/L	0,0028	0,0121	0,0092	0,0008	<0,0005	0,0005	<0,0005
Total Nickel	mg/L	0,0133	0,0052	0,0012	0,0035	<0,0005	0,0085	0,0028
Total Potassium	mg/L	0,95	2,29	1,6	0,99	1,27	1,57	1,61
Total Selenium	mg/L	<0,001	0,004	0,005	<0,001	<0,001	<0,001	<0,001
Total Silicon	mg/L							
Total Silver	mg/L	0,0001	<0,0001	<0,0001	<0,0001	<0,0001	<0,0001	<0,0001
Total Sodium	mg/L	2,28	26,1	23,9	1,21	1,55	1,76	1,77
Total Strontium	mg/L	0,047	0,565	0,473	0,065	0,064	0,088	0,063
Total Tellurium	mg/L							
Total Thallium	mg/L	<0,0008	<0,0008	<0,0008	<0,0008	<0,0008	<0,0008	<0,0008
Total Thorium	mg/L							
Total Tin	mg/L	<0,001	<0,001	<0,001	<0,001	<0,001	<0,001	<0,001
Total Titanium	mg/L	0,01	0,03	0,02	0,03	0,01	0,02	0,01
Total Uranium	mg/L	<0,001	<0,001	<0,001	<0,001	0,001	0,002	0,001
Total Vanadium	mg/L	0,0027	<0,0005	<0,0005	<0,0005	<0,0005	<0,0005	<0,0005
Total Zinc	mg/L	0,215	0,096	0,028	<0,001	0,004	<0,001	0,001
Total Zirconium	mg/L							
<b>Dissolved Metals</b>								
Dissolved Aluminum	mg/L							
Dissolved Antimony	mg/L	0,0041	0,0001	<0,0001	<0,0001	<0,0001	<0,0001	<0,0001
Dissolved Arsenic	mg/L	<0,0005	<0,0005	<0,0005	<0,0005	<0,0005	<0,0005	<0,0005
Dissolved Barium	mg/L	0,004	0,0137	0,0241	0,0068	0,0074	0,0077	0,0053
Dissolved Beryllium	mg/L							
Dissolved Bismuth	mg/L							
Dissolved Boron	mg/L	<0,01	0,07	0,13	<0,01	<0,01	<0,01	<0,01
Dissolved Cadmium	mg/L	<0,00002	0,00003	<0,00002	<0,00002	<0,00002	<0,00002	<0,00002
Dissolved Calcium	mg/L	6,07	27,7	31,4	10,4	11,7	17,7	13,1
Dissolved Chrome	mg/L	<0,005	0,0032	<0,001	<0,0008	<0,0006	<0,0006	<0,0006
Dissolved Cobalt	mg/L							
Dissolved Copper	mg/L	<0,0005	0,002	<0,0005	0,0006	<0,0005	0,001	0,0032
Dissolved Iron	mg/L	<0,01	1,47	0,02	<0,01	0,04	0,02	0,05
Dissolved Lead	mg/L	<0,0003	<0,0003	<0,0003	<0,0003	<0,0003	<0,0003	<0,0003
Dissolved Lithium	mg/L	<0,005	0,006	0,006	<0,005	<0,005	<0,005	<0,005
Dissolved Magnesium	mg/L	2,06	14,6	17,6	1,93	1,89	5,29	3,04
Dissolved Manganese	mg/L	0,1569	0,0662	0,0768	0,0035	0,0016	0,0451	0,0104
Dissolved Mercury	mg/L	<0,00001	0,00015	0,00013	<0,00001	<0,00001	<0,00001	0,00004
Dissolved Molybdenum	mg/L	0,0012	0,0094	0,0091	0,0009	<0,0005	0,0006	0,0005
Dissolved Nickel	mg/L	0,0049	0,0012	0,0009	0,0015	<0,0005	0,0087	0,0033
Dissolved Phosphorus	mg/L							
Dissolved Potassium	mg/L	0,86	1,75	1,41	0,89	1,22	1,74	1,59
Dissolved Selenium	mg/L	<0,001	0,002	0,003	<0,001	<0,001	<0,001	<0,001
Dissolved Silicon	mg/L							
Dissolved Silver	mg/L	<0,0001	<0,0001	<0,0001	<0,0001	<0,0001	<0,0001	<0,0001
Dissolved Sodium	mg/L	2,3	17,5	22,2	1,13	1,61	1,78	2,01
Dissolved Strontium	mg/L	0,05	0,542	0,504	0,067	0,067	0,086	0,085
Dissolved Tellurium	mg/L							
Dissolved Thallium	mg/L	<0,0008	<0,0008	<0,0008	<0,0008	<0,0008	<0,0008	<0,0008
Dissolved Thorium	mg/L							
Dissolved Tin	mg/L	<0,001	<0,001	<0,001	<0,001	<0,001	<0,001	<0,001
Dissolved Titanium	mg/L	<0,01	0,02	0,02	0,01	0,01	0,02	0,01
Dissolved Uranium	mg/L	<0,001	<0,001	<0,001	<0,001	0,001	0,002	0,001
Dissolved Vanadium	mg/L	0,0016	<0,0005	<0,0005	<0,0005	<0,0005	<0,0005	<0,0005
Dissolved Zinc	mg/L	0,14	0,023	0,002	<0,001	0,006	<0,001	0,002
Dissolved Zirconium	mg/L							
<b>Anions</b>								
Bromide	mg/L							
Chloride	mg/L	6,7	100	132	0,9	1	1,6	<0,5
Fluoride	mg/L	0,08	0,31	0,18	0,1	0,05	0,14	0,06
<b>Nutrients</b>								
Ammonium (N-NH4)	mg/L	0,15	0,22	0,12	0,05	<0,05	0,09	<0,05
Ammonia-Nitrogen (NH3-NH4)	mg/L							
Ammonia (NH3) (non-ionized)	mg/L	<0,01	<0,01	<0,01	<0,01	<0,01	<0,01	<0,01
Nitrate and Nitrite	mg/L							
Nitrate	mg/L							
Nitrite	mg/L	0,01	0,01	<0,01	<0,01	<0,01	<0,01	<0,01
Orthophosphate	mg/L	<0,01	<0,01	<0,01	<0,01	<0,01	<0,01	<0,01
Total Kjeldahl Nitrogen	mg/L	0,76	0,66	0,24	<0,05	<0,7	20,6	0,7
Total Phosphorus	mg/L	0,03	0,05	<0,04	0,03	<0,04	0,02	<0,04
<b>Cyanide</b>								
Total Cyanide	mg/L	0,003	<0,001	0,002	0,002	0,003	<0,001	0,005
Free Cyanide	mg/L							
Weak Acid Dissociable Cyanide	mg/L	<0,001	<0,001	0,005	<0,001	0,004	<0,001	0,005

APPENDIX B - Analytical Results for Groundw

Site Area Station ID Sampling Date	Unité	East Flat			South Cell / Central Dike		South Cell / Central Dike	
		MW-IPD-01(S)	MW-IPD-01(D)		BH-10-01		MW-03-04	MW-06-07
		2018-07-08	2018-07-08	2018-11-09	2010-08-27	2010-08-27	2003-09-18	2006-08-30
<b>FIELD PARAMETERS</b>								
Temperature	degC				3,9		3,3	5
pH	-				7,6		7,67	8
Conductivity	µS/cm				910		450	440
Oxygen Reduction Potential	mV							
Turbidity	NTU							
<b>LABORATORY ANALYSIS</b>								
<b>General</b>								
Total Alkalinity	mg/L	41	94	97	110	110		89
Bicarbonate Alkalinity HCO3	mg/L	41	80	97				108
Carbonate Alkalinity CO3	mg/L	<2	14	<2				<0,5
Reactive silica	mg/L	6,5	8,25	6,7				
Sulphate (SO4)	mg/L	34,6	47,1	63,3	210	210	63,8	3,75
Hardness (CaCO3)	mg/L	82	53	64	300	300	53	115
Dissolved Organic Carbon	mg/L			23,2				
Total Organic Carbon	mg/L	2,5	21,4	23,7				
Total Suspended Solids	mg/L	21	29	8				11
Total Dissolved Solids	mg/L	158	283	305	521,5	545,5	154	196
<b>Total Metals</b>								
Total Aluminium	mg/L							
Total Antimony	mg/L	<0,0001	<0,0001	<0,0001				<0,001
Total Arsenic	mg/L	0,0272	0,0063	<0,0005	0,018	0,018		0,001
Total Barium	mg/L	<0,0005	0,0049	0,0147	0,44	0,44		0,11
Total Beryllium	mg/L	<0,0005	<0,0005	<0,0005				<0,001
Total Bismuth	mg/L							<0,001
Total Boron	mg/L	<0,01	0,11	0,18				<0,05
Total Cadmium	mg/L	<0,00002	<0,00002	<0,00002	<0,001	<0,001		<0,0002
Total Calcium	mg/L	19,3	10,4	13,4	71	69		34,9
Total Chrome	mg/L	0,0007	<0,0006	<0,0006				0,006
Total Cobalt	mg/L							0,001
Total Copper	mg/L	0,0005	<0,0005	0,002	<0,003	<0,003		0,011
Total Iron	mg/L	0,11	0,15	0,21	3,1	3,1		1,5
Total Lead	mg/L	<0,0003	<0,0003	<0,0003	<0,001	<0,001		0,001
Total Lithium	mg/L	0,007	0,017	0,014				0,004
Total Magnesium	mg/L	8,31	6,75	7,65	30	30		8,81
Total Manganese	mg/L	0,0609	0,0354	0,1806	0,17	0,17		0,073
Total Mercury	mg/L	<0,00001	<0,00001	<0,00001	<0,0001	<0,0001		<0,00002
Total Molybdenum	mg/L	0,0087	0,0155	0,0351	<0,03	<0,03		0,005
Total Nickel	mg/L	0,0059	0,0219	0,076	0,05	0,04		0,005
Total Potassium	mg/L	3,05	0,8	1,09	7,7	7,7		2,7
Total Selenium	mg/L	<0,001	0,001	0,0027	<0,001	<0,001		<0,001
Total Silicon	mg/L							5,2
Total Silver	mg/L	<0,0001	<0,0001	<0,0001	<0,0003	<0,0003		0,0009
Total Sodium	mg/L	15,5	49,8	78,3	58	58		8,85
Total Strontium	mg/L	0,146	0,243	0,181				0,23
Total Tellurium	mg/L							<0,001
Total Thallium	mg/L	<0,0008	<0,0008	<0,0002	<0,01	0,01		<0,0001
Total Thorium	mg/L							<0,0005
Total Tin	mg/L	<0,001	<0,001	<0,001				<0,001
Total Titanium	mg/L	0,01	<0,01	0,01				0,032
Total Uranium	mg/L	0,008	0,002	<0,001				0,0095
Total Vanadium	mg/L	<0,0005	<0,0005	<0,0005				0,002
Total Zinc	mg/L	0,002	0,002	0,002	<0,003	0,005		0,006
Total Zirconium	mg/L							<0,01
<b>Dissolved Metals</b>								
Dissolved Aluminum	mg/L							
Dissolved Antimony	mg/L	<0,0001	0,0001	<0,0001			0,001	<0,001
Dissolved Arsenic	mg/L	0,0242	0,0103	<0,0005	0,007	0,007	0,007	<0,001
Dissolved Barium	mg/L	<0,0005	<0,0005	0,0093	0,42	0,44	0,03	0,086
Dissolved Beryllium	mg/L							
Dissolved Bismuth	mg/L						<0,001	<0,001
Dissolved Boron	mg/L	<0,01	0,1	0,17			<0,05	<0,05
Dissolved Cadmium	mg/L	<0,00002	<0,00002	0,0001	<0,001	<0,001	<0,0002	<0,0002
Dissolved Calcium	mg/L	15,6	12,9	13,1	68	73	15	31,3
Dissolved Chrome	mg/L	<0,0006	<0,0006	<0,0006			<0,001	<0,001
Dissolved Cobalt	mg/L						0,003	<0,001
Dissolved Copper	mg/L	<0,0005	0,0005	0,0014	<0,003	<0,003	0,006	0,005
Dissolved Iron	mg/L	<0,01	<0,01	0,03	0,2	0,2	0,55	<0,05
Dissolved Lead	mg/L	<0,0003	<0,0003	<0,0003	<0,001	<0,001	0,006	<0,001
Dissolved Lithium	mg/L	0,006	0,016	0,015			0,015	0,002
Dissolved Magnesium	mg/L	6,5	7,69	7,66	30	31	3,81	6,83
Dissolved Manganese	mg/L	0,0588	0,0349	0,1703	0,18	0,18	0,049	0,032
Dissolved Mercury	mg/L	0,00001	0,00002	<0,00001	<0,0001	<0,0001	<0,00002	<0,00002
Dissolved Molybdenum	mg/L	0,0101	0,014	0,0348	<0,03	<0,03	0,024	0,004
Dissolved Nickel	mg/L	0,0059	0,0149	0,0688	0,05	0,05	0,003	0,002
Dissolved Phosphorus	mg/L						5,58	0,3
Dissolved Potassium	mg/L	2,61	1,07	1,18	7,8	8	5,44	2,3
Dissolved Selenium	mg/L	<0,001	0,001	0,0025	<0,001	<0,001	<0,001	<0,001
Dissolved Silicon	mg/L						10,2	2,7
Dissolved Silver	mg/L	<0,0001	<0,0001	<0,0001	<0,0003	<0,0003	<0,0001	<0,00025
Dissolved Sodium	mg/L	12,7	64,5	78,8	59	61	52,9	7,68
Dissolved Strontium	mg/L	0,147	0,234	0,183			0,14	0,19
Dissolved Tellurium	mg/L						<0,001	<0,001
Dissolved Thallium	mg/L	<0,0008	<0,0008	<0,0002	<0,01	<0,01	<0,0001	<0,0001
Dissolved Thorium	mg/L						<0,0005	<0,0005
Dissolved Tin	mg/L	<0,001	<0,001	<0,001			<0,001	<0,001
Dissolved Titanium	mg/L	0,01	0,01	0,01			0,003	<0,001
Dissolved Uranium	mg/L	0,007	0,002	<0,001			0,013	0,0079
Dissolved Vanadium	mg/L	<0,0005	<0,0005	<0,0005			<0,001	<0,001
Dissolved Zinc	mg/L	0,006	0,001	0,001	<0,005	0,012	0,022	<0,005
Dissolved Zirconium	mg/L						<0,001	<0,01
<b>Anions</b>								
Bromide	mg/L	0,17	0,74	0,6				
Chloride	mg/L	10,8	50,2	56,4	17	17	13,4	33,3
Fluoride	mg/L	0,37	0,51	0,56	0,4	0,5	0,34	0,2
<b>Nutrients</b>								
Ammonium (N-NH4)	mg/L			<0,01				
Ammonia-Nitrogen (NH3-NH4)	mg/L							
Ammonia (NH3) (non-ionized)	mg/L	<0,01	<0,01	<0,01				
Nitrate and Nitrite	mg/L				0,57	0,57	<0,05	
Nitrate	mg/L							
Nitrite	mg/L	0,03	0,04	<0,01			0,004	0,003
Orthophosphate	mg/L	0,01	0,02	<0,01				
Total Kjeldahl Nitrogen	mg/L	0,37	0,2	0,25				
Total Phosphorus	mg/L	0,02	0,02	0,0097				0,4
<b>Cyanide</b>								
Total Cyanide	mg/L	<0,001	<0,001	<0,001				
Free Cyanide	mg/L							
Weak Acid Dissociable Cyanide	mg/L	<0,001	<0,001	<0,001	0,1			

APPENDIX B - Analytical Results for Groundwater

FIELD PARAMETERS	Unité	South Cell / Central Dike								
		Station ID	MW-11-02			MW-14-01				
		Sampling Date	2006-08-30	2011-09-26	2011-09-26	2014-10-20	2015-05-31	2015-08-26	2014-10-20	2014-10-20
Temperature	degC	5	8,9							
pH	-	8	8,93		7,9	8,3	8,2	7,9		
Conductivity	µS/cm	440	8,93		5030	1493	2140	5,03		
Oxygen Reduction Potential	mV		8,93							
Turbidity	NTU				16,69	14,8	21,6			
<b>LABORATORY ANALYSIS</b>										
<b>General</b>										
Total Alkalinity	mg/L	89	104	103	182	199	197	182	182	
Bicarbonate Alkalinity HCO3	mg/L	108								
Carbonate Alkalinity CO3	mg/L	<0,5								
Reactive silica	mg/L									
Sulphate (SO4)	mg/L	3,76	42	41	450	507	703	450	470	
Hardness (CaCO3)	mg/L	117,5	167	165	2358	774	657	2358	2361	
Dissolved Organic Carbon	mg/L									
Total Organic Carbon	mg/L									
Total Suspended Solids	mg/L	11								
Total Dissolved Solids	mg/L	191	193	191	3212	1277	1209	3212	3092	
<b>Total Metals</b>										
Total Aluminium	mg/L									
Total Antimony	mg/L	<0,001								
Total Arsenic	mg/L	0,002	<0,0005	<0,0005	0,1521	0,088	0,1185	0,1521	0,1518	
Total Barium	mg/L	0,11	0,2297	0,2097						
Total Beryllium	mg/L	<0,001								
Total Bismuth	mg/L	<0,001								
Total Boron	mg/L	<0,05								
Total Cadmium	mg/L	<0,0002	0,00004	<0,00002						
Total Calcium	mg/L	36,4	49,7	49,2						
Total Chrome	mg/L	0,005								
Total Cobalt	mg/L	0,001								
Total Copper	mg/L	0,011	0,032	0,0247	0,0172	0,0036	0,0017	0,0172	0,0179	
Total Iron	mg/L	1,58	1,9	0,9						
Total Lead	mg/L	0,001	0,003	0,0039	<0,0003	0,0005	0,0074	<0,0003	0,0029	
Total Lithium	mg/L	0,004								
Total Magnesium	mg/L	9,04	10,6	10,4						
Total Manganese	mg/L	0,074	0,2274	0,1853						
Total Mercury	mg/L	<0,00002	0,00058	0,00064						
Total Molybdenum	mg/L	0,0048	<0,0005	<0,0005						
Total Nickel	mg/L	0,005	0,0087	0,0065	0,0415	0,0185	0,0136	0,0415	0,0439	
Total Potassium	mg/L	2,8	1,9	2						
Total Selenium	mg/L	<0,001	<0,001	<0,001						
Total Silicon	mg/L	5								
Total Silver	mg/L	0,0009	0,0006	0,0002						
Total Sodium	mg/L	9,12	10,5	10,3						
Total Strontium	mg/L	0,24								
Total Tellurium	mg/L	<0,001								
Total Thallium	mg/L	<0,0001	<0,005	<0,005						
Total Thorium	mg/L	<0,0005								
Total Tin	mg/L	<0,001								
Total Titanium	mg/L	0,031								
Total Uranium	mg/L	0,0097								
Total Vanadium	mg/L	0,002								
Total Zinc	mg/L	0,006	0,024	0,019	0,049	0,001	0,003	0,049	0,051	
Total Zirconium	mg/L	<0,01								
<b>Dissolved Metals</b>										
Dissolved Aluminum	mg/L									
Dissolved Antimony	mg/L	<0,001								
Dissolved Arsenic	mg/L	0,001	<0,005	<0,005	0,0695	0,0538	0,0868	0,0695	0,1075	
Dissolved Barium	mg/L	0,086	0,16	0,167	0,6186	0,0914	0,0875	0,6186	0,6034	
Dissolved Beryllium	mg/L									
Dissolved Bismuth	mg/L	<0,001								
Dissolved Boron	mg/L	<0,05								
Dissolved Cadmium	mg/L	<0,0002	<0,005	<0,005	0,00003	0,00003	0,00003	0,00003	0,00009	
Dissolved Calcium	mg/L	31,5	42,8	43,4						
Dissolved Chrome	mg/L	<0,001								
Dissolved Cobalt	mg/L	<0,001								
Dissolved Copper	mg/L	0,008	0,008	0,01	0,0161	0,0037	0,0017	0,0161	0,0136	
Dissolved Iron	mg/L	0,05	<0,05	<0,05	0,05	0,01	0,01	0,05	1,1	
Dissolved Lead	mg/L	<0,001	<0,005	<0,005	0,0009	<0,0003	<0,0003	0,0009	<0,0003	
Dissolved Lithium	mg/L	0,002								
Dissolved Magnesium	mg/L	6,92	7,7	8						
Dissolved Manganese	mg/L	0,032	0,145	0,148	1,744	1,867	1,581			
Dissolved Mercury	mg/L	<0,00002	0,0011	0,001	<0,00001	<0,00001	0,00001	<0,0001	0,0003	
Dissolved Molybdenum	mg/L	0,0042	<0,005	<0,005	0,0144	0,0171	0,0156	0,0144	0,0152	
Dissolved Nickel	mg/L	0,002	<0,005	<0,005	0,0386	0,0182	0,0151	0,0386	0,037	
Dissolved Phosphorus	mg/L	0,3								
Dissolved Potassium	mg/L	2,3	1,3	1,4						
Dissolved Selenium	mg/L	<0,001	<0,005	<0,005	0,059	0,006	0,008	0,059	0,055	
Dissolved Silicon	mg/L	2,7								
Dissolved Silver	mg/L	<0,00025	<0,005	<0,005	<0,0001	<0,0001	<0,0001			
Dissolved Sodium	mg/L	7,84	7,6	7,9						
Dissolved Strontium	mg/L	0,2								
Dissolved Tellurium	mg/L	<0,001								
Dissolved Thallium	mg/L	<0,0001	<0,01	<0,01	<0,005	<0,005	<0,005	<0,005	<0,005	
Dissolved Thorium	mg/L	<0,0005								
Dissolved Tin	mg/L	<0,001								
Dissolved Titanium	mg/L	<0,001								
Dissolved Uranium	mg/L	0,008								
Dissolved Vanadium	mg/L	<0,001								
Dissolved Zinc	mg/L	<0,005	<0,005	0,013	0,033	0,002	0,004	0,033	0,054	
Dissolved Zirconium	mg/L	<0,01								
<b>Anions</b>										
Bromide	mg/L									
Chloride	mg/L	33,5	20,9	20,7	1877	272	361	1877	1677	
Fluoride	mg/L	0,11	0,13	0,18	0,4	0,33	0,27	0,4	0,41	
<b>Nutrients</b>										
Ammonium (N-NH4)	mg/L									
Ammonia-Nitrogen (NH3-NH4)	mg/L									
Ammonia (NH3) (non-ionized)	mg/L				0,02		0,02			
Nitrate and Nitrite	mg/L		1,72	1,73						
Nitrate	mg/L									
Nitrite	mg/L	0,003	0,02	0,03	<0,01	<0,01	<0,01			
Orthophosphate	mg/L									
Total Kjeldahl Nitrogen	mg/L									
Total Phosphorus	mg/L	0,4								
<b>Cyanide</b>										
Total Cyanide	mg/L		<0,005		0,191	0,117	0,093	0,191	0,101	
Free Cyanide	mg/L		<0,005			0,04	0,007			
Weak Acid Dissociable Cyanide	mg/L		<0,005							





APPENDIX B - Analytical Results for Groundwater

Site Area Station ID Sampling Date	Unité	Portage Pit E			Portage Pit A		
		Pit-E-Seep-North	Pit-E-Seep-SW	MW-IPD-09	MW-03-03		
		2017-09-05	2017-09-05	2018-07-08	2004-08-09	2004-08-09	2003-09-25
<b>FIELD PARAMETERS</b>							
Temperature	degC	5	8,6		10,3		2,2
pH	-	8,15	8,3		7,77		8,63
Conductivity	µS/cm	1426	438,1		627		350
Oxygen Reduction Potential	mV	-68,3	-82,9		3		79,9
Turbidity	NTU	2,4	1,88				
<b>LABORATORY ANALYSIS</b>							
<b>General</b>							
Total Alkalinity	mg/L	152	94	66	133		93,8
Bicarbonate Alkalinity HCO3	mg/L	152	94	66	162		114
Carbonate Alkalinity CO3	mg/L	<2	<2	<2	<0,5		<0,5
Reactive silica	mg/L	8,5	7,6	11,01			
Sulphate (SO4)	mg/L	702	132	39,2	6,2		26,6
Hardness (CaCO3)	mg/L	1214	324	71	213		140
Dissolved Organic Carbon	mg/L	4,8	4,5				
Total Organic Carbon	mg/L	4,8	4,5	1,6			
Total Suspended Solids	mg/L	<1	<1	43	1		
Total Dissolved Solids	mg/L	1464	404	132	239		254
<b>Total Metals</b>							
Total Aluminium	mg/L						
Total Antimony	mg/L	0,0023	0,0026	0,0004	0,0002		0,002
Total Arsenic	mg/L	0,0296	<0,0005	0,0174	0,015		0,004
Total Barium	mg/L	0,0285	0,1065	<0,0005	0,05		0,02
Total Beryllium	mg/L	<0,0005	<0,0005	<0,0005	<0,0002		<0,001
Total Bismuth	mg/L				<0,0002		<0,001
Total Boron	mg/L	0,23	<0,01	0,03	0,19		0,09
Total Cadmium	mg/L	0,00035	<0,00002	<0,00002	0,00006		<0,0002
Total Calcium	mg/L	257	76,8	16,7	47,7		28
Total Chrome	mg/L			0,0026	0,001		<0,001
Total Cobalt	mg/L				0,0004		<0,001
Total Copper	mg/L	0,0015	<0,0005	0,0016	0,0014		<0,001
Total Iron	mg/L	0,24	0,37	0,91	0,46		<0,05
Total Lead	mg/L	<0,0003	<0,0003	<0,0003	0,0006		0,001
Total Lithium	mg/L	0,008	0,005	<0,005	0,0092		0,007
Total Magnesium	mg/L	139	32,3	7,35	23,5		18
Total Manganese	mg/L	0,2891	0,2214	0,0969	0,131		0,11
Total Mercury	mg/L	<0,00001	0,00002	<0,00001	<0,00002		<0,00002
Total Molybdenum	mg/L	0,1158	0,0163	0,0126	0,093		0,056
Total Nickel	mg/L	0,1993	0,0337	0,018	0,0024		0,003
Total Potassium	mg/L	56,6	11,8	1,77	2,65		3,51
Total Selenium	mg/L	0,001	<0,001	<0,001	<0,0002		<0,001
Total Silicon	mg/L				5,96		3,78
Total Silver	mg/L	<0,0001	<0,0001	<0,0001	0,0001		<0,0001
Total Sodium	mg/L	110	17,4	27,8	33,6		17,6
Total Strontium	mg/L	1,49	0,334	0,126	0,581		0,26
Total Tellurium	mg/L				<0,0002		<0,001
Total Thallium	mg/L	<0,0008	<0,0008	<0,0008	<0,00002		<0,0001
Total Thorium	mg/L				<0,0001		<0,0005
Total Tin	mg/L	<0,001	<0,001	<0,001	<0,0002		<0,001
Total Titanium	mg/L	0,21	0,05	0,01	0,0045		<0,001
Total Uranium	mg/L	0,229	0,028	0,002	0,0088		0,012
Total Vanadium	mg/L	<0,0005	0,0022	<0,0005	0,0002		<0,001
Total Zinc	mg/L	0,001	0,004	0,006	0,006		<0,005
Total Zirconium	mg/L				<0,002		<0,001
<b>Dissolved Metals</b>							
Dissolved Aluminum	mg/L						
Dissolved Antimony	mg/L	0,002	0,0025	0,0008	<0,0002		0,002
Dissolved Arsenic	mg/L	0,023	0,008	0,0124	0,013		0,004
Dissolved Barium	mg/L	0,0254	0,0906	<0,0005	0,048		0,018
Dissolved Beryllium	mg/L						
Dissolved Bismuth	mg/L				<0,0002		<0,001
Dissolved Boron	mg/L	0,26	<0,01	0,01	0,17		0,08
Dissolved Cadmium	mg/L	0,0003	<0,00002	<0,00002	0,00004		<0,0002
Dissolved Calcium	mg/L	217	59,9	12,6	47,1		26,3
Dissolved Chrome	mg/L	<0,0006	<0,0011	<0,0006	0,0003		<0,001
Dissolved Cobalt	mg/L				0,0003		<0,001
Dissolved Copper	mg/L	0,0013	0,0017	<0,0005	0,0002		<0,001
Dissolved Iron	mg/L	0,1	0,01	<0,01	<0,01		<0,05
Dissolved Lead	mg/L	<0,0003	<0,0003	<0,0003	<0,0002		<0,001
Dissolved Lithium	mg/L	0,009	0,005	<0,005	0,0081		0,007
Dissolved Magnesium	mg/L	110	25,1	5,38	22,4		17,1
Dissolved Manganese	mg/L	0,2469	0,1595	0,0786	0,13		0,1
Dissolved Mercury	mg/L	<0,00001	0,00009	<0,00001	<0,02		<0,00002
Dissolved Molybdenum	mg/L	0,1027	0,0149	0,0118	0,09		0,052
Dissolved Nickel	mg/L	0,1699	0,0332	0,0134	0,0018		0,003
Dissolved Phosphorus	mg/L				<0,03		0,07
Dissolved Potassium	mg/L	49,5	11,1	1,46	2,64		3,33
Dissolved Selenium	mg/L	0,002	0,001	<0,001	<0,0002		<0,001
Dissolved Silicon	mg/L				5,7		3,62
Dissolved Silver	mg/L	<0,0001	<0,0001	<0,0001	<0,00005		<0,0001
Dissolved Sodium	mg/L	90,1	13,6	21,1	32		16,5
Dissolved Strontium	mg/L	1,55	0,371	0,121	0,556		0,24
Dissolved Tellurium	mg/L				<0,0002		<0,001
Dissolved Thallium	mg/L	<0,0008	<0,0008	<0,0008	<0,00002		<0,0001
Dissolved Thorium	mg/L				<0,0001		<0,0005
Dissolved Tin	mg/L	<0,001	<0,001	<0,001	<0,0002		<0,001
Dissolved Titanium	mg/L	0,17	0,04	0,01	0,0003		<0,001
Dissolved Uranium	mg/L	0,196	0,024	0,001	0,0087		0,012
Dissolved Vanadium	mg/L	<0,0005	0,0008	<0,0005	<0,0002		<0,001
Dissolved Zinc	mg/L	<0,001	0,002	0,001	0,004		<0,005
Dissolved Zirconium	mg/L				<0,002		<0,001
<b>Anions</b>							
Bromide	mg/L			0,04			
Chloride	mg/L	175	26,8	2,8	121		50,4
Fluoride	mg/L	0,48	0,42	0,91	0,38		0,46
<b>Nutrients</b>							
Ammonium (N-NH4)	mg/L	6,45	0,13				
Ammonia-Nitrogen (NH3-NH4)	mg/L						
Ammonia (NH3) (non-ionized)	mg/L	0,05	<0,01	<0,01			
Nitrate and Nitrite	mg/L				<0,05	<0,01	0,15
Nitrate	mg/L						
Nitrite	mg/L	0,35	0,02	0,04	<0,002		0,003
Orthophosphate	mg/L	0,02	0,01	0,05			
Total Kjeldahl Nitrogen	mg/L	6,5	1,4	0,29	0,2	0,2	
Total Phosphorus	mg/L	<0,04	<0,04	0,01	0,065	0,1	0,07
<b>Cyanide</b>							
Total Cyanide	mg/L	0,044	0,013	<0,001	<0,01	<0,01	
Free Cyanide	mg/L				<0,1	<0,1	
Weak Acid Dissociable Cyanide	mg/L	0,019	0,008	<0,001			